Factors affecting the response to photoperiod stress: light quality and quantity, flowering pathway, and the natural genetic background of *Arabidopsis thaliana*

Inaugural-Dissertation
to obtain the academic degree

Doctor rerum naturalium (Dr. rer. nat.)

submitted to the Department of Biology, Chemistry, Pharmacy
of Freie Universität Berlin

by

Ishita Bajaj

from Delhi, India

2024

This work was conducted under the supervision of

Prof. Dr. Thomas Schmülling and Priv.-Doz. Dr. Anne Cortleven

at Dahlem Centre of Plant Sciences,

Institute of Biology/ Applied Genetics,

Freie Universität Berlin

from August 2018 until March 2024

1st reviewer: Prof. Dr. Thomas Schmülling
2nd reviewer: Prof. Dr. Daniel Schubert

Date of defense: 12.06.2024

Acknowledgments

I wish to express profound gratitude to those whose contributions have been pivotal in the successful completion of this doctoral thesis.

Foremost, my heartfelt appreciation goes to my esteemed supervisors, Prof. Dr. Thomas Schmülling and Dr. Anne Cortleven, for their invaluable guidance, wisdom, and unwavering support throughout this transformative journey. Their expertise not only shaped the trajectory but significantly enhanced the overall quality of this research.

I extend sincere thanks to the second reviewer of my thesis, Prof. Dr. Daniel Schubert, for providing constructive feedback within the dynamic setting of the Applied Genetics seminars.

Special acknowledgment is due to Dr. Bernadette Eichstädt for her meticulous proofreading of my thesis, ensuring its clarity and precision.

My profound appreciation extends to all members of AG Schmülling, AG Johansson, and the former AG Kunze for their scientific insights and the countless moments of joy shared. Your warmth and welcoming spirit truly made me feel at home.

I express deep gratitude to Elsa-Neumann Stiftung, DRS, and Frauenförderung for their financial support, enabling not only the progression of this work but also facilitating my attendance at various conferences.

A heartfelt thank you is reserved for the diligent gardeners who tended to the plants even during holidays, contributing to the vibrant environment in which this research flourished.

This note of appreciation would be incomplete without acknowledging my friends and family in Germany, namely Dr. Michael Hengge, Dr. Harendra Mahato, Johannes Ott, and Maximilian Hessel, who provided unwavering intellectual and emotional support.

Lastly, I thank my parents, Ritu Bajaj and Sanjay Bajaj, for their boundless love, which gave me the strength to turn my dreams into reality.

Declaration of Independence

Herewith I certify that I have prepared and written my thesis independently and that I have not used any sources and aids other than those indicated by me.

Berlin, 13.03.2024 Ishita Bajaj

Contents

List of figures

List of tables

List of abbreviations

3PGA	3-phosphoglycerate
ABA	abscisic acid
ABAR	ABA-binding protein
ACHT4	*Arabidopsis thaliana* atypical cysteine histidine-rich Trxs4
AD	arithmetic division
ADGase	ADP-glucose pyrophosphorylase
ADP	adenosine diphosphate
afb2	*auxin signaling f-box 2*
AGI	Arabidopsis Genome Initiative
AGPase	ADP-glucose pyrophosphorylase
AHK	*ARABIDOPSIS HISTIDINE KINASE*
AHP	ARABIDOPSIS HISTIDINE PHOSPHOTRANSFER PROTEIN
ALA	5-aminolevulinic acid
AMY3	α-amylase 3
ANAC	NAC DOMAIN CONTAINING PROTEIN
ANOVA	analysis of variance
AOX	alternative oxidase
AP1	APETELA 1
ARR	ARABIDOPSIS RESPONSE REGULATOR
ATP	adenosine triphosphate
B:R:Fr	Blue:Red:Far-red
BAM	β-amylases
BAP1	*BON ASSOCIATION PROTEIN 1*
BBX	B-BOX
bHLH	basic helix–loop–helix
bp	base pairs
BZIP63	BASIC LEUCINE ZIPPER
CAB1	Chlorophyll a/b binding protein 1
CAPS	Cleaved Amplified Polymorphic Sequences
CCA1	CIRCADIAN CLOCK ASSOCIATED 1
CCE	C-terminal extension
CDD	CONSTITUTIVE PHOTOMORPHOGENIC 10 (COP10)-DE-ETIOLATED 1 (DET1)-DAMAGED DNA BINDING 1 (DDB1) complex
CDF	CYCLIN DOF FACTOR 1
cDNA	complementary DNA
CEC1	COEXPRESSED WITH CLOCK GENES LHY AND CCA1 1
cGMP	cyclic guanosine monophosphate
CHE	CCA1 HIKING EXPEDITION
CIB1	CRYPTOCHROME-INTERACTING BASIC HELIX–LOOP–HELIX1
CK	cytokinin
CKX	CYTOKININ OXIDASE
CL	continuous light
CO	CONSTANS
COP1	CONSTITUTIVE PHOTOMORPHOGENIC 1

COR	*COLD REGULATED*
CRY	cryptochrome
CTR1	CONSTITUTIVE TRIPLE RESPONSE 1
CYCH;1	CYCLIN H;1
cypDM	*cytochrome P450 monooxygenases-cyp735a1* and *cyp735a2*
DAB	3,3'-diaminobenzidine
DAMP	damage associated molecular pattern
DCMU	3-(3,4-dichlophenyl)1,1-dimethylurea
DDB1	DAMAGED DNA BINDING 1
DELLA	aspartic acid, glutamic acid, leucine, leucine, and alanine
DGIST	Daegu Gyeongbuk Institute of Science and Technology
DMSO	dimethyl sulfoxide
DNA	deoxyribonucleic acid
DREB2A	DEHYDRATION RESPONSIVE ELEMENT BINDING 2A
EDTA	ethylenediaminetetraacetic acid
EIN4	ETHYLENE INSENSITIVE4
ELF4	*EARLY FLOWERING 4*
ELIP1	*EARLY LIGHT INDUCING PROTEIN 1*
ETR1	ETHYLENE RECEPTOR 1
FAD	flavin adenine
FC1	ferrochelatase 1
FCA	*FLOWERING CONTROL LOCUS A*
Fdx	ferredoxin
FHL	FHY1-LIKE
FHY1	FAR-RED ELONGATED HYPOCOTYL 1
FKF1	FLAVIN-BINDING KELCH REPEAT F-BOX 1
FLC	*FLOWERING LOCUS C*
FLD	*FLOWERING LOCUS D*
FLK	*FLOWERING LOCUS K*
FMN	flavin mononucleotide
Fr	Far-red
FRI	*FRIGIDA*
Fru6P	fructose-6-phosphate
FT	*FLOWERING LOCUS T*
FTR	ferredoxin:thioredoxin reductase
FU Berlin	Freie Universität Berlin
FVE/MIS4	*Arabidopsis thaliana* atypical cysteine histidine-rich Trxs4
FW	fresh weight
FY	*FLOWERING LOCUS Y*
G1P	glucose-1-phosphate
GA	gibberellic acid
GABI	German plant genomics research program
GAF	cGMP phosphodiesterase/adenylyl cyclase/FhlA
GARP	Glycoprotein A repetitions predominant

GBSS1	GRANULE BOUND STARCH SYNTHASE 1
GI	GIGANTEA
Glc	glucose
GLK	GOLDEN-2 LIKE
GOI	gene of interest
GUN	GENOME UNCOUPLED
GWAS	genome-wide association studies
GWD	glucan water dikinase 1
HFR1	HYPOCOTYL IN FAR-RED LIGHT 1
HIR	high irradiance response
HK	hexokinase
HKRD	Histidine Kinase-Related Domain
HOS1	HIGH EXPRESSION OF OSMOTICALLY RESPONSIVE GENE 1
HR	hypersensitive
HY5	ELONGATED HYPOCOTYL 5
HYH	HY5 homolog
IAA	indole-3 acetic acid
IPT	ISOPENTENYLTRANSFERASE
JA	jasmonic acid
LD	long day/LUMINIDEPENDENS
LED	light emitting diode
LFR	low fluence response
LFY	LEAFY
LHCB	*LIGHT-HARVESTING CHLOROPHYLL A/B BINDING PROTEIN*
LHCII	light-harvesting chlorophyll-protein complex II
LHY	*LONG HYPOCOTYL*
LKP2	LOV KELCH PROTEIN 2
LNK1/2	LIGHT-INDUCIBLE AND CLOCK REGULATED GENES 1 and 2
LOV	Light-Oxygen-Voltage
LOV1	LONG VEGETATIVE PHASE 1
LSF2	like-starch excess 4, 2
LUX	*LUX ARRHYTHMO*
LWDs	LIGHT REGULATED WDs (tryptophan-aspartic acid)
MAGIC	multiparent advanced generation intercross
MAPK	mitogen activated protein kinase
MDS	mitochondrial dysfunction stimulon
MEcPP	methylerythritol cyclodiphosphate
MED25	PHYTOCHROME AND FLOWERING TIME 1 (PFT1)/MEDIATOR 25
mRNA	messenger ribonucleic acid
MTHF	5,10-methenyltetrahydrofolate
NAD	nicotinamide adenine dinucleotide
NADPH	nicotinamide adenine dinucleotide phosphate hydrogen

NASC	Nottingham Arabidopsis Stock Centre
NCBI	National Center for Biotechnology Information
NILs	near isogenic lines
NTE	N-terminal extension
NTRC	NADP-dependent thioredoxin reductase C
OPM	C-terminal output module
OPP	oxidative pentose phosphate
PAM	pulse amplitude modulated
PAP	SAL1/3′-phosphoadenosine 5′-phosphate
PARP	poly(ADP-ribose) polymerase
PAS	Per/Arnt/Sim
PCD	programmed cell death
PCR	polymerase chain reaction
PFT1	PHYTOCHROME AND FLOWERING TIME 1
PGI	phosphoglucoisomerase
PGM	phosphoglucomutase
phANG	photosynthesis associated nuclear genes
PHOT	phototropin
PHR	photolyase homology related
PHY	phytochrome
PIF	PHYTOCHROME INTERACTING FACTORS
PIF1-OX	PIF1-overexpressor
PLP	prolonged light period
PPIX	protoporphyrin IX
PPKs	PHOTOREGULATORY PROTEIN KINASES
PR1	*PATHOGEN RELATED1*
PRC2	POLYCOMB REPRESSIVE COMPLEX 2
PRR	*PSEUDO-RESPONSE REGULATOR*
PRX	peroxidase
PSII	photosystem II
PSM	photosensory module
PWD	phosphoglucan water dikinase
qRT-PCR	quantitative real time PCR
QTL	quantitative trait loci
RBOHs	respiratory burst oxidase homologs
RCD1	*RADICAL INDUCED CELL DEATH 1*
RILS	recombinant inbred lines
RNA	ribonucleic acid
ROS	reactive oxygen species
RT	room temperature
RVE	REVEILLE
SA	salicylic acid
SAR	systemic acquired resistance

SD	short day
SE	standard error
SEX	STARCH EXCESS
SMZ	SCHLAFMÜTZE
SNP	single nucleotide polymorphism
SnRK1	*SUCROSE non-fermenting RELATED KINASE1*
SnRK2/TOR	Sucrose nonfermenting 1-related kinase 2/Target of Rapamycin
SOC1	*SUPPRESSOR OF OVEREXPRESSION OF CONSTANS 1*
SPA	SUPPRESSOR OF PHYA-105
SPL	SQUAMOSA PROMOTER BINDING PROTEIN-LIKE
SRS5	SHI-RELATED SEQUENCE 5
SWEET	SUGARS WILL EVENTUALLY BE EXPORTED TRANSPORTER
TAE	tris-acetate EDTA
TCA	trichloroacetic acid
TCP22	TEOSINTE BRANCHED1-CYCLOIDEA-PCF 22
TF	transcription factor
tir1	*transport inhibitor resistant 1*
TOC1	*TIMING OF CAB EXPRESSION 1*
TOE1	*TARGET OF EARLY ACTIVATION TAGGED 1*
TPL	TOPLESS
TPSI	TREHALOSE 6-PHOSPHATE SYNTHASE I
Trx	thioredoxin
TSF	*TWIN SISTER OF FT*
*t*Z	*trans*-zeatin
*tz*R	tZ-ribosides
UDP	uridine diphosphate
UDPGlc	UDP-glucose
UV-A	ultraviolet
UVR8	UV RESISTANCE LOCUS8
VASC	Versailles Arabidopsis Stock Center
VDE	*Violaxanthin de-epoxidase*
VLFR	very low fluence response
WT	wild type
yuc1D	*yucca 1D*
ZAT12	*ZINC FINGER OF ARABIDOPSIS THALIANA 12*
ZTL	ZEITLUPE

Summary

Prolongation of the light period causes photoperiod stress in plants. During the night following the prolonged light treatment, stress marker gene expression is induced, and stress hormones and ROS accumulate. The next day, the experienced strong photoperiod stress leads to the formation of water-soaked lesions in leaves and eventually programmed cell death ensues.

In this study, the impact of light intensity and light quality on the photoperiod stress response has been investigated. A threshold light intensity of about 50 µmol m^{-2} s^{-1} was found to be necessary for the induction of photoperiod stress, hinting at the involvement of chloroplasts. Lower photoperiod stress symptoms in *gun4, gun5, rcd1,* and *glk1 glk2* mutants revealed a possible role of retrograde signaling in photoperiod stress and corroborated the involvement of chloroplasts. Furthermore, starch and sugar content were higher in photoperiod stressed plants and starch biosynthesis mutants developed less photoperiod stress symptoms. This indicated that the starch and sugar metabolism might be affecting a plants' response to photoperiod stress, strengthening the argument for the importance of chloroplast in photoperiod stress.

Both monochromatic red and blue light caused a photoperiod stress response, but the response provoked by red light was stronger. Mutant analysis revealed the photoreceptors phyB and CRY2 as probable sensors of photoperiod stress. Among the downstream light signaling components, HY5 and PIF1 have demonstrated potential for involvement in sensing photoperiod stress.

Although *cry2* mutation did not rescue the strong photoperiod stress phenotype of *cca1 lhy*, some clock genes were differentially regulated in *cry2.* This indicates a possible involvement of CRY2 in photoperiod stress through its role in regulating the circadian rhythm.

Overall, these results support that both plastid-dependent and photoreceptor-dependent signaling pathways are involved in sensing light conditions causing photoperiod stress and governing the response to it.

Since *co* and *ft tsf* mutants demonstrated less photoperiod stress symptoms, participation of the photoperiodic flowering pathway in sensing and responding to photoperiod stress has been considered a possibility.

Most ecotypes other than Columbia showed low sensitivity to photoperiod stress, suggesting that photoperiod stress sensitivity might be a rare trait in nature. The low photoperiod stress sensitivity of the F1 generation of crosses between Col-0 and some of the ecotypes that show low photoperiod stress sensitivity is evidence of the recessive nature of the photoperiod stress sensitivity trait.

Zusammenfassung

Eine Verlängerung der Lichtperiode führt zu photoperiodischem Stress in Pflanzen. In der Nacht nach einer verlängerten Lichtbehandlung wird die Expression von Stressmarker-Genen induziert und Stresshormone sowie ROS (reaktive Sauerstoffspezies) akkumulieren. Am nächsten Tag kann starker photoperiodischer Stress zur Bildung von wassergefüllten Läsionen auf den Blättern und eventuell zum Zelltod führen.

Im Zuge dieser Arbeit wurde der Einfluss von Lichtintensität und Lichtqualität auf die Antwort einer Pflanze auf photoperiodischen Stress untersucht. Eine minimale Lichtintensität von etwa 50 µmol m^{-2} s^{-1} als Schwellenwert ist notwendig, um photoperiodischen Stress zu induzieren, was auf die Beteiligung von Chloroplasten hinweist. Schwächere Symptome in Reaktion auf photoperiodischen Stress bei den Mutanten *gun4*, *gun5*, *rcd1* und *glk1 glk2* deuteten auf eine mögliche Rolle der retrograden Signalübertragung bei photoperiodischem Stress hin und bestätigten eine Involvierung der Chloroplasten. Darüber hinaus waren Stärke- und Zuckergehalt in photoperiodisch gestressten Pflanzen höher, und Mutanten mit verminderter Stärkebiosynthese entwickelten schwächere Symptome in Reaktion auf photoperiodischen Stress. Dies deutete auf eine Rolle des Stärke- und Zuckermetabolismus bei photoperiodischem Stress hin und stärkte das Argument für die Bedeutung von Chloroplasten in der Wahrnehmung von und der Antwort auf photoperiodischen Stress. Sowohl monochromatisches rotes als auch blaues Licht verursachten eine photoperiodische Stressreaktion, wobei die Reaktion auf rotes Licht stärker war. Mutantenanalysen zeigten, dass die Photorezeptoren phyB und CRY2 vermutlich die Rolle von photoperiodischen Stresssensoren spielen. Unter den nachgeschalteten Lichtsignalkomponenten haben HY5 und PIF1 gezeigt, dass sie möglicherweise an der Erkennung von photoperiodischem Stress beteiligt sind. Obwohl die *cry2* Mutation den starken Phänotyp von *cca1 lhy* in Reaktion auf photoperiodischen Stress nicht verbesserte, wurden einige Gene der zirkadianen Uhr in *cry2* differentiell reguliert. Dies deutete auf eine mögliche Rolle von CRY2 in photoperiodischem Stress durch seine Funktion bei der Regulation der zirkadianen Uhr hin. Insgesamt zeigten diese Ergebnisse, dass sowohl plastidabhängige als auch photorezeptorabhängige Signalwege an der Erkennung von Lichtbedingungen beteiligt sind, die photoperiodischen Stress verursachen, und die Reaktion darauf beeinflussen.

Da *co* und *ft tsf* Mutanten geringfügigere Symptome in Reaktion auf photoperiodischen Stress zeigten, ist eine Beteiligung des photoperiodischen Signalwegs der Blühinduktion am photoperiodischen Stress möglich.

Die meisten Ökotypen außer Columbia zeigten eine geringere Empfindlichkeit gegenüber photoperiodischem Stress, was darauf hindeutet, dass Sensibilität gegenüber photoperiodischem Stress in der Natur eine seltene Eigenschaft sein könnte. Die geringe Empfindlichkeit gegenüber photoperiodischem Stress der F1-Generation aus Kreuzungen einiger der Ökotypen, die eine geringere Empfindlichkeit gegenüber photoperiodischem Stress zeigen, mit Col-0, ist ein Hinweis auf die rezessive Natur dieser Eigenschaft.

1 Introduction

1.1 Photoperiod stress

Light is one of the most important elements for the survival of plants. It orchestrates important life processes in plants such as growth and development, metabolism, photosynthesis, and entrainment of the circadian clock. However both excess and insufficient light levels can lead to abiotic stresses such as high light stress, fluctuating light stress, and shade stress (Gao et al., 2020; Shi et al., 2022). Nitschke et al. (2016, 2017) defined a novel abiotic stress called photoperiod stress. Photoperiod stress is caused by the disruption of alternate light and dark cycles by a prolonged light period (PLP) in short day (SD)-grown *Arabidopsis thaliana* plants. The photoperiod stress symptoms are characterized by an increased expression of cell death stress marker genes *ZINC FINGER OF ARABIDOPSIS THALIANA 12* (*ZAT12*) and *BON ASSOCIATION PROTEIN BB1* (*BAP1*) and an accumulation of reactive oxygen species (ROS).

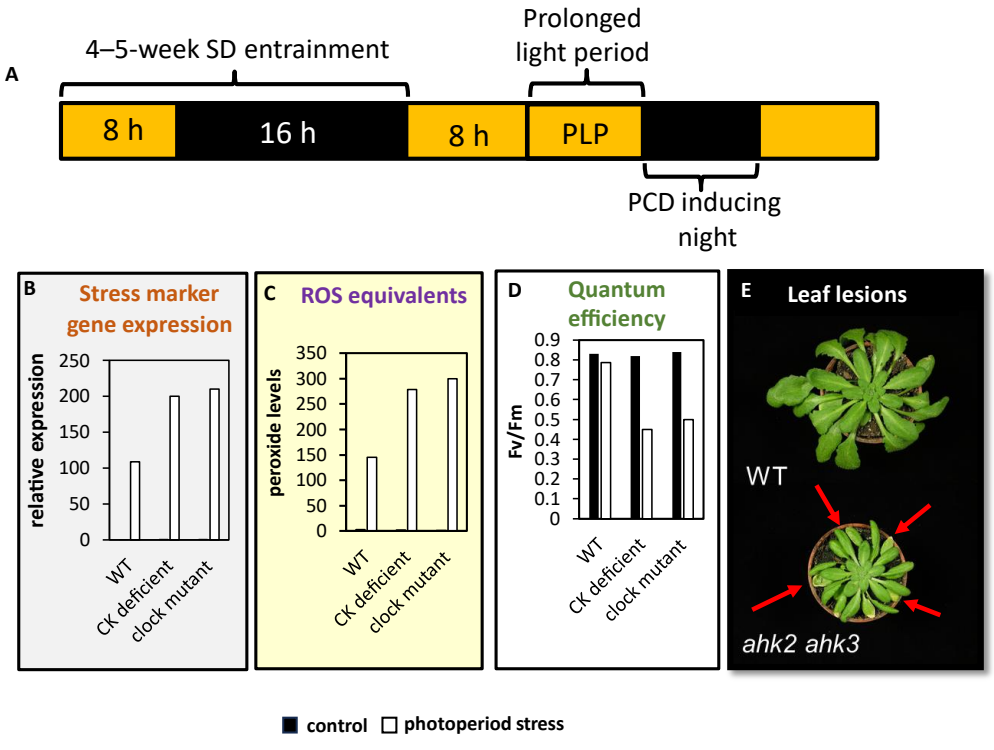

Figure 1.1: Prolonged light treatment and the hallmark photoperiod stress symptoms. (A) Schematic representation of photoperiod stress treatment. After 4-5 weeks of short day (SD) entrainment, plants are exposed to a prolonged light period (PLP), followed by programmed cell death (PCD) inducing night. This ultimately leads to photoperiod stress. At the end of the PCD-inducing night, (B) higher expression of stress marker genes and (C) an increased accumulation of ROS equivalents can be observed. During the following day, (D) quantum efficiency of the leaves of photoperiod stressed plants reduces and (E) water-soaked lesions can be observed on these leaves. All these stress symptoms are more pronounced in cytokinin (CK) deficient mutants such as *ahk2 ahk3* (CK-receptor mutants) and clock mutants such as *cca1 lhy*. Figure adapted from Nitschke et al. (2017).

These symptoms are accompanied by increased levels of hormones, jasmonic acid (JA) and salicylic acid (SA). The stress symptoms appear during the night following the PLP (Nitschke et al., 2016, 2017; Abuelsoud et al., 2020). The next day the photosynthetic capacity of the plant is decreased and lesions on leaves may form on stress-sensitive plants, eventually leading to programmed cell death (PCD) (Figure 1.1) (Nitschke et al., 2016). Plants with reduced cytokinin (CK) status such as *arabidopsis histidine kinase 2/3 (ahk2 ahk3)* CK receptor mutant and certain clock mutants such as *circadian clock associated 1 long hypocotyl (cca1 lhy)* were strongly sensitive to photoperiod stress. In fact, during the night following the PLP, the *CCA1* and *LHY* expression, the two key components of circadian clock morning loop genes, was reduced in wild type (WT) and even more drastically reduced in the CK deficient mutants, indicating the importance of the circadian clock and CK in coping with photoperiod stress (Nitschke et al., 2016).

The photoperiod stress syndrome was first observed in CK deficient plants (Nitschke et al., 2017). Therefore, the role of CK in the photoperiod stress syndrome has been investigated in detail. The proteins ISOPENTENNYL TRANSFERASE 3 (IPT3), IPT5/7, AHK2/3, ARABIDOPSIS RESPONSE REGULATOR 2 (ARR2), ARR10/12, and CYTOKININ OXIDASEs (CKXs) were found to be the key players in this context (Nitschke et al., 2016). Frank et al. (2020) further elaborated and reported an increase in CK-free bases, CK ribosides, and CK nucleotides in response to photoperiod stress. Root-derived *trans*-zeatin (*t*Z) CK, requiring the action of ARABIDOPSIS HISTIDINE PHOSPHOTRANSFER PROTEIN 2 (AHP2), AHP3, and AHP5, plays a protective role in the photoperiod stress response. This was corroborated by the observation that the *t*Z biosynthesis mutant *cytochrome P450 monooxygenases-cyp735a1* and *cyp735a2* (*cypDM)* and the *t*Z transport mutant *ATP-binding cassette containing subfamily G-14* (*abcg14)* showed strong photoperiod stress symptoms. In addition, spraying the *cypDM* mutants with *t*Z and *t*Z-ribosides (*t*ZR) led to the rescue of the photoperiod stress symptoms (Frank et al., 2020).

It was observed that under photoperiod stress, plants with a reduced CK status had increased levels of JA synthesis and signaling genes (Nitschke et al., 2016). JA derivatives such as JA-isoleucine accumulated in these plants upon photoperiod stress and the loss of JA-isoleucine synthesis genes in CK mutant background rescued the photoperiod stress symptoms (Nitschke et al., 2016). In addition to JA, SA and camalexin were induced upon photoperiod stress (Cortleven et al., 2022). SA and camalexin are known signaling molecules in the pathogen defense response of plants (Cheval et al., 2017). A possible connection between photoperiod stress and pathogen defense in plants has been further investigated (Venja Röber-Terstegen, doctoral thesis in preparation).

Besides CK and JA, the role of auxin and ethylene in the photoperiod stress response has also been investigated. The role of auxin in growth and development is often antagonistic to that of CK. Auxin was found to promote the response to photoperiod stress, which stands in contrast to the protective

role of CK in this context (Frank et al., 2022). An increase in the concentration of indole-3-acetic acid (IAA), IAA-Glc, and IAA-Asp was noted upon exposure to photoperiod stress in both WT and CK mutants. In the CK mutants, the increase was stronger. A higher concentration of IAA in *yucca 1D (yuc1D)* increased its sensitivity to photoperiod stress, while a decrease in auxin sensitivity in auxin receptor mutants such as *transport-inhibitor-resistant 1 (tir1), auxin signaling f-box 2 (afb2) and afb3* contributed to their lower photoperiod stress response (Frank et al., 2022).

In response to photoperiod stress, the abundance of ethylene synthesis genes increased during the night following the PLP (Frank, 2019). A constitutively active ethylene signaling due to loss of CONSTITUTIVE TRIPLE RESPONSE 1 (CTR1), or three of the five ethylene receptors ETHYLENE RECEPTOR1 (ETR1), ETR2, ETHYLENE INSENSITIVE4 (EIN4), led to a decreased photoperiod stress sensitivity. This suggested that ethylene is a positive regulator of photoperiod stress resistance (Frank, 2019). Gibberellic acid (GA) status, on the other hand, had little effect on the photoperiod stress sensitivity (Frank, 2019).

Besides the hormonal responses to photoperiod stress, the cellular redox status forms a key component of the photoperiod stress response. As mentioned earlier, an increased ROS production during the night following the PLP is one of the characteristic symptoms of photoperiod stress (Abuelsoud et al., 2020). This is accompanied by an increased apoplastic peroxidase (PRX) activity and higher expression of *PRX* genes (Abuelsoud et al., 2020). Catalase activity and ascorbic acid redox status in leaves are also lowered (Abuelsoud et al., 2020). Consistently, genes related to oxidative stress were differentially expressed in response to photoperiod stress in more sensitive genotypes (Cortleven et al., 2022).

The strength of the photoperiod stress symptoms depends on several factors. The length of the photoperiod before the PLP (that is, the entrainment) is inversely proportional to the strength of the photoperiod stress symptoms (Nitschke et al., 2016). SD-entrained plants were more sensitive compared to long-day (LD)-entrained plants to the photoperiod stress conditions. Also, the length of the PLP and the dark period following the PLP are positively correlated to the strength of the symptoms. Nitschke et al. (2016) used 16 h PLP (in total a period of 32 h continuous light) followed by 16 h dark (D) as the standard photoperiod stress treatment. It was later revealed that a PLP of 1 h is enough to cause photoperiod stress in SD grown plants, but the magnitude of the symptoms declines with the decrease in the length of the PLP (Abuelsoud et al., 2020). Visible symptoms such as water-soaked lesions are not easily observed with shorter PLP (Dr. Anne Cortleven, personal communication). Altogether, the length of the light period before and during the PLP is an important deciding factor for the strength of photoperiod stress. Since light is one of the most important Zeitgeber for the circadian clock, these observations once again highlight the importance of the circadian clock in photoperiod

stress. Further adding to the importance of the clock is the fact that reduction of temperature, an important regulator of the circadian clock, during the night following PLP alleviated the photoperiod stress symptoms (Nitschke et al., 2016).

In addition, the photoperiod stress response depends on plant age and different tissues have a diverse sensitivity towards photoperiod stress. It was indicated by Nitschke et al. (2016) that mature fully expanded leaves are more prone to photoperiod stress symptoms. In line with this, a more detailed analysis revealed that the oldest but non-senescent leaves were the most affected by photoperiod stress (Frank, 2019). Also, in general, 4-to 5-weeks-old plants were more sensitive to photoperiod stress compared to 3-weeks-old plants. According to *ZAT12* and *BAP1* expression, it became clear that leaves are more sensitive to photoperiod stress compared to the roots, at least in terms of oxidative stress (Frank, 2019).

1.2 Effect of light quantity and quality on plants

Since in this work the effect of light quantity and quality on photoperiod stress has been explored, it is important to briefly review the existing literature on the significance of different light quality and quantity on general plant physiology. Light quality and quantity serve as the key environmental cues for the plants providing information about weather conditions, time of the day, and cover by the canopy. In crop plants and tree species, a direct impact of light intensity on morphology and physiology has been described by Wittmann et al. (2001) and Feng et al. (2019). At low light intensities, a decrease in plant dry matter and physiological processes such as photosynthetic rate, transpiration, and stomatal conductance have been reported in soybean (Yang et al., 2014, 2017). The effect of light intensity also contributes to the concentration of phytohormones as described by Mengel et al. (1985). Under lower light intensity, the concentration of gibberellin increased, while at higher light intensity the level of abscisic acid rose in *Triticum aetivum* (Mengel et al., 1985). In addition, metabolic processes are also influenced by light intensity. An increase in light intensity led to an increase in starch production in duckweed, a valuable feedstock for bioethanol production (Yin et al., 2015), and glutathione content in wheat (Toldi et al., 2019).

Along with light intensity, light quality is a major effector of vital physiological processes such as photosynthesis and morphological adaptations in plants. In 2021, Yavari et al., studied the impact of monochromatic LED light on *A. thaliana* leaves in a 24-hour photoperiod. They reported that red light significantly increased the leaf area and biomass and promoted the net photosynthetic rate, while blue light increased leaf area growth, carotenoid, and anthocyanin content (Yavari et al., 2021). On the other hand, in ornamental plant species *Cordyline australis*, *Ficus benjamiana,* and *Sinngia speciosa,* a

16 h photoperiod under blue light resulted in higher quantum yield and quantum efficiency compared to red light (Zheng and Van Labeke, 2017). Red and blue light also have an impact on the circadian rhythm. Treatment with red and blue light was shown to alter the period length of leaf movement rhythm (Halaban, 1969). A low red and far-red light ratio is a warning signal for shade and encroaching vegetation and initiates the shade avoidance syndrome (SAS) in plants to enable them to avoid or tolerate shade conditions (Morgan and Smith, 1978; Smith, 1982; Smith and Whitelam, 1997). However, SAS has been suggested to compromise the plant defense mechanism against pathogens and herbivores (Pierik and Ballaré, 2021).

1.3 Retrograde signaling

In order to explore the role of chloroplasts in sensing photoperiod stress, the effect of photoperiod stress in retrograde signaling mutants has been investigated. Therefore, retrograde signaling and the corresponding genes that have been studied in this work are here briefly introduced.

Retrograde signals in plants originate from cell organelles such as chloroplasts, mitochondria, and peroxisomes to regulate nuclear gene expression (Mielecki et al., 2020). Two main types of retrograde signals from chloroplasts can be distinguished in plants: 'biogenic control' and 'operational control'. Biogenic control signals occur during the early stages of chloroplast biogenesis and seed germination (Wu and Bock, 2021). Operational retrograde signals, on the other hand, act as environmental cues from mature chloroplasts for example during abiotic stress (Wu and Bock, 2021). This complex retrograde signaling between chloroplasts and the nucleus can be conducted by a variety of signaling molecules such as ROS, RNA, proteins, tetrapyrrole biosynthesis intermediates, and other metabolites (Mielecki et al., 2020; Wu and Bock, 2021). The expression of some of the prominent photosynthesis associated nuclear genes (phANGs) such as *LIGHT-HARVESTING CHLOROPHYLL A/B BINDING PROTEIN (LHCB)* and the small subunit of the central carbon-fixing enzyme *Rubisco (RBCS)* is controlled by retrograde signals (Mielecki et al., 2020).

As an example of operational control, retrograde signaling based response to wounding, drought, and high light stress have been reviewed by Crawford et al. (2018). In a nutshell, the aforementioned stresses cause ROS production leading to a disturbed redox status of the chloroplasts. This causes inhibition of certain enzyme activities and accumulation of intermediates such as 3'-phosphoadenosine 5'-phosphate (PAP), methylerythritol cyclodiphosphate (MEcPP), and Mg-protoporphyrin IX (Mg-PPIX) (Crawford et al., 2018). These intermediates are exported from the chloroplast to the nucleus and influence the expression of stress responsive genes in a direct or indirect manner (Crawford et al., 2018). ROS can also act as secondary messengers for retrograde signaling

during abiotic stress (Sachdev et al., 2021). Since H_2O_2 is known to be generated as a part of the response to photoperiod stress (Abuelsoud et al., 2020), it is of interest, how it acts as a signaling molecule. In chloroplasts, H_2O_2 is generated by photosystem II (PSII) (reviewed by Li & Kim, 2022). H_2O_2 can cross the membrane from its production site via peroxoporins, a specific type of aquaporin channel (Henzler and Steudle, 2000). Known targets of H_2O_2 in the nucleus are the transcription factors (TFs) ZAT12, DEHYDRATION RESPONSIVE ELEMENT BINDING 2A (DREB2A), members of the WRKY family, and immune response genes such as *cytochromeP450* (Crawford et al., 2018). H_2O_2 is also known to activate members of mitogen activated protein kinase (MAPK) family to induce PCD (Neill, 2002). Key components of the chloroplast retrograde signaling pathway are *GUN* (*GENOME UNCOUPLED*) genes, *GLK* (*GOLDEN-2 LIKE*) genes, and *RCD1* (*RADICAL INDUCED CELL DEATH1*).

gun mutants are well studied retrograde signaling mutants (Richter et al., 2023). These were isolated as mutants that had a derepressed expression of *LHCB* genes despite the absence of fully developed chloroplasts due to norflurazon treatment (Susek et al., 1993). GUN1 is a pentatricopeptide containing protein, localized in plastids (Koussevitzky et al., 2007). It accumulates during active chloroplast biogenesis shortly after seed germination or during the development of the basal part of newly emerging true leaves (Wu et al., 2019; Wu and Bock, 2021) and interacts with components of the tetrapyrrole biosynthesis pathway leading to the formation of chlorophyll (Colombo et al., 2016). GUN1 inactivation or overexpression in adult plants leads to delayed flowering or early flowering, respectively (Richter et al., 2023). Also, it was observed that *gun1* mutants experienced more oxidative damage due to water stress (Cheng et al. 2011).

GUN2/3/4/5 have a direct role in tetrapyrrole biosynthesis and encode components participating in the chlorophyll biosynthesis pathway and the mutants for these genes are pale green (Crawford et al., 2018; Wu and Bock, 2021). GUN4, like GUN1, is also most abundant in young green tissue (Peter and Grimm, 2009). GUN4 stimulates the activity of Mg-chelatase by binding to its Chlorophyll H (ChlH) subunit encoded by GUN5 (Mochizuki et al., 2001; Peter and Grimm, 2009; Adhikari et al., 2011). Mg-chelatase catalyzes the insertion of Mg^{2+} into protoporphyrin IX (PPIX) to form Mg-PPIX, the first dedicated step in the biosynthesis of chlorophyll *a* (Jensen et al., 1996). GUN4 is also involved in posttranslational regulation of the synthesis of 5-aminolevulinic acid (ALA) (Peter and Grimm, 2009), whose application improves plant growth under various abiotic stresses (reviewed by Wu et al., 2019). GUN5, also known as ABAR (ABA-binding protein), is a receptor for the phytohormone abscisic acid, that is responsible for plant adaptations to several environmental stresses (Shen et al., 2006). Lower freezing tolerance and higher oxidative damage due to water stress were reported in *gun5* mutants probably due to lower accumulation of Mg-PPIX (Kindgren et al., 2015;

Cheng et al., 2011). *gun2* and *gun3* are alleles of *hy1* and *hy2* required for phytochromobilin synthesis from heme (Mochizuki et al., 2001).

GUN6 encodes for ferrochelatase 1 (FC1), an enzyme responsible for inserting Fe^{2+} into PPIX for the heme biosynthesis pathway (Woodson et al., 2011). The mutant *gun6* is an overexpressor of FC1 and retains phANG expression upon norflourazon application (Woodson et al., 2011). In this study, *gun1, gun4, gun5,* and *gun6* mutants have been investigated under photoperiod stress.

GOLDEN-2 LIKE 1 (GLK1) and GLK2 are nuclear-localized members of the GARP family of Myb transcription factors (reviewed by Chen et al., 2016). They are known to directly impact the expression of phANGs and are primarily involved in chloroplast development (Langdale and Kidner, 1994; Waters et al., 2009). Consequently, *glk1 glk2* mutants have pale-green leaves because of the reduced amount of synthesized mature chloroplasts (Fitter et al., 2002). *GLKs* are overexpressed in *gun* mutants (Leister and Kleine, 2016). Conversely, overexpression of *GLK1* leads to a *gun* phenotype, and this *GLK1-overexpressor* is also known as *GUN7* (Leister and Kleine, 2016; Martín et al., 2016). Individually, *GLK1* expression is found to occur mainly in the leaves, while that of *GLK2* occurs mainly in the fruit (Chen et al., 2016). Several studies indicate the role of GLKs in plant defense against pathogens (Chen et al., 2016). Overexpression of *GLK1* resulted in significant upregulation of defense and SA signaling genes, but downregulation of *PATHOGEN RELATED 1 (PR1)*, a marker for activation of systemic acquired resistance (SAR) (Savitch et al., 2007). Additionally, GLKs participate in abiotic stress response (Savitch et al., 2005; Wang et al., 2022). *GLK1* silencing in cotton leads to more damage by drought and cold stress (Li et al., 2021). Correspondingly, RNA-seq data analysis by Wang et al. (2022) demonstrated that *GLKs* were differentially regulated by cold, drought, and salt stress in tomatoes.

RADICAL INDUCED CELL DEATH1 (RCD1) encodes a putative poly-(ADP-ribose) polymerase (PARP). PARPs transfer the ADP-ribose subunit from NAD^+ to proteins as a posttranslational modification. RCD1 is discussed to be a common regulator of chloroplastic and mitochondrial retrograde signaling via SAL1/PAP pathway (reviewed by Wang et al. 2020). RCD1 negatively regulates the expression of Arabidopsis *NAC DOMAIN CONTAINING PROTEIN 013 (ANAC013)* and *ANAC017* TFs (Shapiguzov et al., 2019). These TFs have been described to mediate ROS-related retrograde signals from mitochondrial complex III and regulate mitochondrial dysfunction stimulon (MDS) genes that impact the redox status of the chloroplast (Shapiguzov et al., 2019). Especially ANAC017 is mentioned in the literature as the master regulator of alternative oxidase (AOX), the major indicator of mitochondrial retrograde signaling (Wang et al., 2020). The *rcd1* mutant is methylviologen and UV-B resistant as well as ozone hypersensitive (Fujibe et al., 2004; Overmyer et al., 2000). It has general morphology defects and is sensitive to oxidative and salt stress (Katiyar-Agarwal et al., 2006).

1.4 Starch

A previous study has shown that the starch concentration was higher at the end of the night following PLP in the photoperiod stressed plants (Nitschke, 2015). Since a large part of starch metabolism takes place in the chloroplast, to further explore the role of chloroplast in photoperiod stress sensing, starch metabolism during photoperiod stress has been investigated in this work and is here briefly introduced.

Intricate mechanisms for carbon sensing, storage, and transport allow plants to direct carbon into processes such as growth and respiration. Carbon metabolism in plants is often defined in terms of the 'source' and 'sink' relationship (Dong and Beckles, 2019). Autotrophic leaves act as a source, while tissues such as roots and seeds act as sink (Dong and Beckles, 2019). Carbon partitioning refers to the process of distributing the photosynthetic assimilates throughout the plant body (Braun and Slewinski, 2009). Starch and sucrose are the two main forms of carbohydrates that are the components of carbon partitioning (MacNeill et al., 2017). Carbohydrate is stored in plants mainly as starch and transported in the form of sucrose (MacNeill et al., 2017). There are two main types of starch in higher plants: storage starch and transient starch (Lloyd and Kossmann, 2015). Storage starch is produced in the amyloplast for long-term storage, while transient starch is metabolized in the chloroplast and is subjected to the diurnal cycle (MacNeill et al., 2017).

1.4.1 Starch biosynthesis

During the light period, starch synthesis starts with fructose-6-phosphate (Fru6P), a Calvin cycle intermediate, that is first converted to glucose-6-phosphate (Glc6P) by phosphoglucoisomerase (PGI) and subsequently to glucose-1-phosphate (Glc1P) by phosphoglucomutase (PGM) (Zeeman et al., 2007b). Two isoforms of PGM are localized either in the plastid or in the cytosol (Herbert et al., 1979; Gottlieb, 1982). *pgm1* mutants completely lack the activity of the plastidic isoform of PGM and were shown to be starchless (Caspar et al., 1985). Although *pgm1* mutants have severe growth defects under SD, under continuous light, their growth is equal to WT (Caspar et al., 1985). Conversion of Glc1P to ADP-glucose (ADPGlc) is catalyzed by ADP-glucose pyrophosphorylase (AGPase/ADGase). This is the first committed step for starch biosynthesis (Iglesias and Preiss, 1992). AGPase is a heterodimer comprised of two large regulatory subunits and two small catalytic subunits. *ADG2* codes for the large subunit of the enzyme, while *ADG1* encodes the small subunit of AGPase (Wang et al., 1997; Wang et al., 1998). The production of starch granules has been reviewed in detail by Zeeman et al. (2007a, 2007b). To transfer the glucosyl moiety of ADPGlc to an existing glucan chain via α-1,4-linkage, starch

synthase is required, which eventually leads to the production of amylopectin. The starch granule finally forms in between the thylakoid membranes (MacNeill et al., 2017).

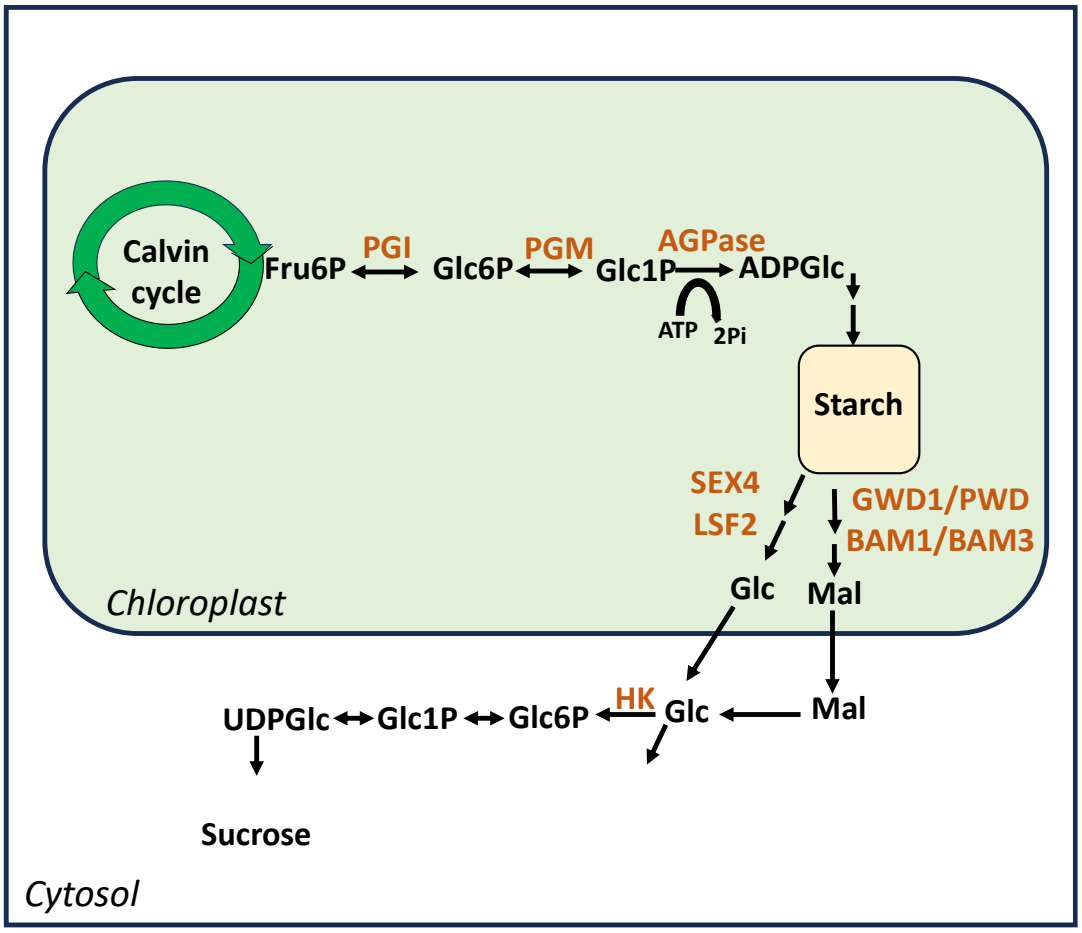

Figure 1.2: Simplified scheme of starch metabolism. Transit starch is synthesized during the day from the products of the Calvin cycle and is broken down to simple sugars like maltose. Maltose is exported to the cytosol where it is converted into sucrose. F6P, fructose-6-phosphate; G6P, glucose-6-phosphate; G1P, glucose-1-phosphate; ADPGlc, ADP-glucose; Mal, maltose; Glc, glucose, UDPGlc, UDP-glucose; SucroseP, sucrose-phosphate; PGI, phosphoglucose isomerase; PGM, phosphoglucomutase; AGPase, ADP-glucose pyrophosphorylase; GWD1, glucan water dikinase 1; PWD, phosphoglucan water dikinase; SEX4, starch excess 4; LSF2, like-starch excess 4, 2; BAM, β-amylase; HK, hexokinase. Figure adapted from Zeeman et al. (2007b) and Skryhan et al. (2018).

1.4.2 Starch breakdown

Transient starch synthesized during the day is broken down during the night. In order to be accessible to degradation enzymes, double helices of α-glucan chains are loosened by reversible phosphorylation by glucan water dikinase (GWD) and phosphoglucan water dikinase (PWD) (MacNeill et al., 2017). In 1998, Lorberth et al. demonstrated that antisense repression of GWD leads to a reduction in starch bound phosphate and thus accumulation of starch in leaves. *starch excess 1 (sex1)* mutant lacks GWD

and has starch levels 4-6-fold higher than WT at the end of the day (Yu et al., 2001). This is probably because *sex1* mutants lack the ability to transport glucose produced by starch hydrolysis out of chloroplast (Trethewey and Ap Rees, 1994). The added phosphate groups are removed by glucan phosphatases SEX4 and LIKE STARCH EXCESS 4-2 (LSF2) (MacNeill et al., 2017). Hydrolytic enzymes ß-amylases (BAM1 and BAM3) cleave the α-1,4-glycosidic bond and debranching enzyme, isoamylase cleaves α-1,6-linkages of these linear dephosphorylated chains, ultimately releasing maltose, leading to sucrose synthesis (Smith and Zeeman, 2020) (Figure 1.2). A simplified scheme of starch breakdown and synthesis is given in Figure 1.2.

1.4.3 Regulation of starch metabolism

Regulation of starch synthesis and breakdown is influenced by several overlapping factors. Some of them are described here.

1. ***Diurnal regulation***

   Transient starch in leaves accumulates during the day and degrades during the night. This diurnal regulation calls for the perception of the length of the photoperiod alongside the coordination of biosynthesis and starch degradation (MacNeill et al., 2017). Low levels of starch stored during the day, or a too high rate of starch breakdown during the night, might lead to carbon starvation accompanied by the catabolism of protein and lipids and is deleterious to plant health (Smith and Stitt, 2007; Sulpice et al., 2009; Graf and Smith, 2011). Under SD, several plant species partition more of their carbon assimilate into starch compared to the plants grown under LD conditions (Chatterton and Silvius, 1981). The rate of starch breakdown during the night is constant and complementary to the rate of starch synthesis during the light period. Therefore, the rate of starch breakdown is slower under SD compared to LD (Zeeman et al., 2007b). The rate of starch degradation is resistant to disturbances such as interruptions of by dark period in between a light period or an early dusk (Graf et al., 2010). *GRANULE BOUND STARCH SYNTHASE1 (GBSS1)*, responsible for amylose synthesis, is circadian clock regulated and is a dawn marker gene (Martin and Smith, 1995). A model by Seki et al. (2017) suggested that starch degradation is circadian clock regulated as well, thus impacting the sucrose profile. Feedback from sucrose in turn then adjusts the phase of the circadian clock by regulation of *PSEUDO-RESPONSE REGULATOR 7 (PRR7)* that in turn regulates the expression of *CCA1* (Seki et al., 2017). *PRR7* is regulated by the transcription factor basic leucine zipper 63 (bZIP63), which is regulated by *SUCROSE non-fermenting RELATED KINASE1 (SnRK1)* (Viana et al., 2021). This model is referred to as the retrograde metabolic signaling (RMS) model in the

literature (Moraes et al., 2019). A competing model known as the arithmetic division (AD) model for the regulation of starch metabolism by the clock, emphasizes the convergence of the clock and metabolic signals (Moraes et al., 2019). This model suggests that the amount of starch and time of dawn determine the rate of starch degradation (Moraes et al., 2019).

2. Regulation by light

To ensure maximum plant growth and avoid carbon starvation, the rate of starch metabolism should match the rate of photosynthesis, and photosynthesis is dependent on light (MacNeill et al., 2017). In 2019, Moraes et al. reported a decreased rate of starch accumulation under lower light intensity compared to the control. Furthermore, AGPase, a key enzyme for starch biosynthesis is subjected to transcriptional, posttranslational, and allosteric regulation, especially in response to light (Geigenberger, 2011). Thioredoxin (Trx) which is indirectly regulated by light, activates AGPase by reduction of regulatory disulfide. Upon light activation, ferredoxin (Fdx) is reduced by photosynthetic electron transport. These reducing equivalents are transferred to Trx by ferredoxin:thioredoxin reductase (FTR), allowing Trx to activate AGPase. Additionally, NADP-dependent thioredoxin reductase C (NTRC), which is linked to Fdx during the light, also mediates AGPase activation through reduction by NADPH (reviewed by Geigenberger 2011). Furthermore, AGPase is activated through allosteric regulation by 3-phosphoglycerate (3PGA), the first fixation product of the Calvin-Benson cycle, which occurs during the light (Hendriks et al., 2003). *A. thaliana* atypical cysteine histidine-rich Trxs4 (ACHT4) has a role in quenching AGPase activity through an oxidative signal by reacting with the small subunit of AGPase. It is responsible for the dynamic regulation of AGPase under changing light intensity (Eliyahu et al., 2015). Taken together, this indicates an important role of light in starch regulation.

3. Abiotic stress

The response to abiotic stress requires the synthesis of osmoprotectants and cryoprotectants such as proline in order to maintain osmotic balance and stabilize proteins. For this purpose, carbon is reallocated from starch (Yoshiba et al., 1997; Ribeiro et al., 2022). To assist proline production under osmotic stress, BAM1 and α-amylase 3 (AMY3) facilitate the degradation of starch during the daytime (Zanella et al., 2016). Moreover, starch degradation allows the maintenance of carbon flux during stress conditions such as water deficit to prevent major changes in the primary metabolism (Hummel et al., 2010). Transitory starch content was reported to decline under salt, drought, and cold stress (Thalmann and Santelia, 2017; Dong

and Beckles, 2019; Ribeiro et al., 2022). A decline in the rate of starch synthesis during water and temperature stress due to lower rates of photosynthesis was also reported by Zrenner and Stitt (1991) and Thitisaksakul et al. (2012). The abscisic acid (ABA)-mediated closure of stomata during these stresses leads to lower CO_2 levels and consequently a lower rate of photosynthesis (Movahedi et al., 2021). This lower rate of photosynthesis can further trigger carbon starvation that leads to differential regulation of several circadian clock genes due to the accumulation of REVEILLEs (RVEs) (Moraes et al., 2019). *PRR7* is upregulated and *EARLY FLOWERING 4 (ELF4)* is downregulated under such conditions (Moraes et al., 2019).

The starch degradation to facilitate carbon reallocation, as enumerated in the instances given above, mostly occurs in response to strong stress conditions (Ribeiro et al., 2022). However, under mild drought and salinity stress, starch accumulates probably because although the growth is inhibited, photosynthesis is not (Ribeiro et al., 2022). Therefore, starch metabolism is an integral part of the abiotic stress response.

1.5 Photoreceptors

In plants, light information is perceived by photoreceptors, which are specific for a particular spectrum of solar radiation. The red and far-red range of wavelengths are perceived by phytochromes and blue and UV-A by cryptochromes, phototropins, and Zeitlupe family members (Paik and Huq, 2019).

1.5.1 Phytochromes

A. thaliana has five types of phytochromes, phyA-phyE. The N-terminal photosensory module (PSM) and C-terminal output module (OPM), the two major modules of phytochrome, are connected by a flexible hinge region (Rockwell et al., 2006; Burgie et al., 2014). The components of PSM include N-terminal extension (NTE), a Per/Arnt/Sim (PAS) domain, a cyclic guanosine monophosphate (cGMP) phosphodiesterase/adenylyl cyclase/FhlA (GAF) domain which binds a bilin chromophore (a linear tetrapyrrole prosthetic group), and a phytochrome-specific PHY domain responsible for the stability of the Pfr form of phytochrome (Rockwell et al., 2006; Burgie et al., 2014). OPM is required for phytochrome dimerization and consists of two PAS-related domains (PAS-A, PAS-B) and a Histidine Kinase Related Domain (HKRD) (Nagatani, 2010; Qiu et al., 2017). PhyA is a light-labile phytochrome, while phyB-E are light-stable phytochromes (Sharrock and Quail, 1989).

Phytochromes are synthesized in the red light absorbing (Pr) form in the cytosol and are converted to the active Pfr upon red light exposure and translocated to the nucleus (Chen et al., 2005; Hiltbrunner et al., 2005). While phyB translocates to the nucleus on its own upon exposure to

continuous red light in a slow process, fast import of phyA into the nucleus is mediated by two proteins, FAR-RED ELONGATED HYPOCOTYL 1 (FHY1) and FHY1-LIKE (FHL), upon exposure to even a brief pulse of blue, red and far-red light (Hiltbrunner et al., 2005; 2006; Chen et al., 2005; Li et al., 2011). Pfr reverts to the Pr form upon absorption of far-red light or spontaneously in the absence of light by a temperature-dependent process known as 'thermal reversion' or 'dark reversion' or the phytochrome is just degraded (Klose et al., 2020).

Although different phytochromes have different roles in photomorphogenesis, they also have overlapping roles. The role of phyA and phyB have been studied in detail (Whitelam and Devlin, 1997). phyA is responsible for mediating the far-red high irradiance response, while phyB is more responsible for the effects of prolonged red light (Whitelam and Devlin, 1997). The mode of action of phytochromes has been divided into three responses, namely, very low fluence response (VLFR), low fluence response (LFR), and high irradiance response (HIR). The expression of *LHCB* is an example of VLFR, while seed germination, chloroplast rotation, and leaf movement are examples of LFR (Li et al., 2011b). HIR includes seedling de-etiolation (Li et al., 2011b).

Phytochromes also regulate the shade avoidance response, flowering time, entrainment of the circadian clock, and gravitropism (Paik and Huq, 2019).

The light signaling pathway downstream of phytochromes is described in section 1.6 (Figure 1.3).

1.5.2 Cryptochromes

Cryptochromes are blue light photoreceptors with structural similarity to the DNA repair enzyme photolyase (Lin 2002). *CRY1* and *CRY2* are the cryptochrome genes in Arabidopsis (Ahmad and Cashmore, 1993; Hoffman et al., 1996). Additionally, a newly identified cryptochrome, called CRY-DASH has been identified and is also known as *AtCRY3* (Brudler et al., 2003).

Most plant cryptochromes are 70-80 kDa proteins (Lin, 2002) with an N-terminal domain, called photolyase homology related (PHR) domain that harbors two chromophores, flavin adenine dinucleotide (FAD) as catalytic chromophore (Lin et al., 1995; Malhotra et al., 1995; Banerjee et al., 2007; Bouly et al., 2007) and 5,10-methenyltetrahydrofolate (MTHF) as light harvesting chromophore (Malhotra et al., 1995; Selby and Sancar, 2006; Song et al., 2006). The C-terminal domain consists of the cryptochrome C-terminal extension (CCE), which is a highly variable signaling domain (Mishra and Khurana, 2017). Cryptochromes exist as monomers in darkness. Upon photoexcitation and photoactivation of the FAD domain, they homodimerize with the help of the PHR domains which causes disengagement of the PHR and CCE domains (Liu et al., 2011; Wang and Lin, 2020). This is accompanied by the release of a small magnitude of ROS (El-Esawi et al., 2017). The stability of CRY1

is unaffected by light, while CRY2 is degraded when exposed to 20-30 µmol m^{-2} s^{-1} of blue light (Ahmad et al., 1998; Lin et al., 1998)

Although CRY1 and CRY2 are nuclear proteins, CRY1 might be imported to the nucleus in the dark and exported to the cytosol in the light, or just remain in the cytosol in response to light, while CRY2 appears to be constitutively imported into the nucleus (Lin and Shalitin, 2003).

Light responses are regulated by CRYs by at least two different mechanisms. First, the transcriptional regulation of CRY2 by the CRYPTOCHROME-INTERACTING BASIC HELIX–LOOP–HELIX1 (CIB1) (Liu et al., 2008). Secondly, through the light-dependent modulation of transcription through the same pathway as phytochromes, which is explained in section 1.6 (Figure 1.3). Additionally, it has been demonstrated that the BLUE LIGHT INHIBITOR OF CRYPTOCHROME 1 (BIC1) inhibits CRY signaling by preventing the homodimerization of CRY2 (Wang et al., 2016).

CRY1 and CRY2 mediate several blue light-dependent morphogenic responses such as flowering time, temperature sensing, gravitropism, inhibition of hypocotyl elongation, inhibition of seed germination, and regulation of the shade avoidance response (Wang and Lin, 2020). An important function of the CRYs is the entrainment of the circadian clock. It has been shown that *cry1* mutants have a longer period of circadian rhythms at both high and low fluence rates while *cry2* mutants have a shorter period of circadian rhythms at lower fluence rates of blue light (Yu et al., 2010). However, cryptochromes are not an intrinsic part of the circadian oscillator as *cry1 cry2* double mutants retain the rhythmicity of the circadian clock (Yu et al., 2010).

1.5.3 Phototropins

Phototropins (PHOT1 and PHOT2) are blue/ UV-A light activated serine/threonin kinases (Christie et al., 2002). Phototropins consist of two light-oxygen-voltage (LOV) domains that bind to flavin mononucleotide (FMN) non-covalently in a 1:1 ratio (Gallagher et al., 1988; Christie, 2007; Suetsugu and Wada, 2013). LOV2 undergoes light-dependent autophosphorylation and is the predominant light-sensing domain of PHOT1 (Christie 2002). It was seen that LOV2 alone was sufficient to induce hypocotyl phototropism (Christie et al., 2002). PHOT1 and PHOT2 are localized at the plasma membrane and upon blue light induction, PHOT1 re-localizes to the cytoplasm (Suetsugu and Wada, 2013). Similar to PHOT1, PHOT2 is also internalized, but a fraction of PHOT2 associates with the Golgi apparatus (Suetsugu and Wada, 2013).

PHOT1 and PHOT2 have partially overlapping functions such as phototropism, stomatal opening, palisade cell elongation, leaf flattening, and chloroplast relocation. However, PHOT1 and PHOT2 also regulate some of these functions independently (Briggs and Christie, 2002; Celaya and

Liscum, 2005; Dou and Niu, 2020). For instance, both PHOT1 and PHOT2 regulate the accumulation of chloroplast to the upper cell surface to improve photosynthesis under low light. However, under high light conditions, only PHOT2 mediates the relocation of chloroplasts away from the radiation to protect them from damage (Christie, 2007). These studies indicate a difference in the blue light sensitivity of PHOT1 and PHOT2. While PHOT1 is sensitive to all blue light fluences, PHOT2 is sensitive to only higher fluence of blue light (Suetsugu and Wada, 2013). Besides blue light, PHOT1 and PHOT2 play a role in responding to photo-oxidative stress induced by UV-C. Both PHOT1 and PHOT2 inhibit foliar cell death induced by UV-C, but at the same time also contribute to the maintenance of higher foliar H_2O_2 levels. Phototropins are also engaged in the maintenance of optimal photochemical reactions and non-photochemical reactions upon UV-C exposure (Rusaczonek et al., 2021). Chloroplast accumulation in response to UV-B is also controlled by phototropins especially PHOT1 (Hermanowicz et al., 2019).

1.5.4 ZEITLUPE

Besides phototropins, there exist several other LOV domain photoreceptors in Arabidopsis such as members of the ZEITLUPE (ZTL) family. They include ZEITLUPE (ZTL), FLAVIN-BINDING KELCH REPEAT F-BOX 1 (FKF1), and LOV KELCH PROTEIN 2 (LKP2) (Ito et al., 2012; Suetsugu and Wada, 2013). ZTL family members localize in the nucleus or cytosol (Takase et al., 2011). The photosensory LOV domain of ZTL/FKF1/LKP2 is present at the N-terminal, followed by an F-box and six Kelch repeats at the C-terminus (Suetsugu and Wada, 2013). F-Box associates with Skp Cullin F-box (SCF)-type E3 ubiquitin ligases responsible for proteasome degradation, while six kelch repeats mediate interactions between proteins (Takase et al., 2011; Ito et al., 2012).

ZTL family members have a role in controlling the stability and degradation of circadian clock components and the photoperiod control of flowering (Takase et al., 2011; Christie et al., 2015). ZTL is stabilized by GIGANTEA (GI) in blue light and together with FKF1 plays a role in stabilizing CONSTANS (CO) protein, which is a key flowering regulator (Corbesier and Coupland, 2006). Further details on the function of CO can be found in section 1.8.1.

1.5.5 UVR8

Most of the UV-B radiation (280 to 315 nm) from the sun is filtered out by ozone; only wavelengths above ~295 nm reach the earth's surface (Jenkins, 2014). UV-B radiation is potentially damaging to all life forms, as it can damage DNA. However, low doses of UV-B affect photomorphogenesis, plant growth, and biochemical content (Jenkins, 2014). These photomorphogenic responses were found to

be controlled by a different pathway than the UV-B damage responses such as DNA damage signaling, ROS signaling, and defense signaling (Jenkins, 2014).

UV RESISTANCE LOCUS8 (UVR8) was identified as the photomorphogenic receptor of UV-B (Kliebenstein et al., 2002). UVR8 is a 'beta-propeller' and exists as a dimer in its inactive state in the cytoplasm (Christie et al., 2012; Di Wu et al., 2012). The two monomers are held together by salt bridges (Jenkins, 2014). Specific tryptophan residues form the chromophore, and these tryptophan residues interact with the nearby arginine residues. Upon absorption of UV-B light, these bonds break, triggering the monomerization of UVR8 dimers (Rizzini et al., 2011). In the dark, UVR8 re-dimerizes and gets inactivated by the activity of REPRESSOR OF UV-B PHOTOMORPHOGENESIS 1 (RUP1) and RUP2 (Tilbrook et al., 2013).

Functions of UVR8 encompass UV-B acclimation by the accumulation of UV-B absorbing compounds such as flavonol glycosides, hypocotyl length elongation, and the entrainment of circadian rhythm (Tilbrook et al., 2013; Jenkins, 2014). Additionally, UV-B was shown to improve the resistance of Arabidopsis plants to *Botrytis cinerea* (Demkura and Ballaré, 2012).

1.6 Light signaling

Light perceived by phytochromes, cryptochromes, and UVR8 triggers a common downstream light signaling pathway. Some of the major components of this pathway are explained here briefly and are illustrated in Figure 1.3.

1.6.1 COP1/SPA-HY5 module

This module is central to the light signaling pathway and is directly dependent on interaction with the photoreceptors. The mechanism of this module is described further in this section.

ELONGATED HYPOCOTYL 5 (HY5) is a bZIP transcription factor that acts as a master regulator of several physiological processes such as photomorphogenesis, root growth, flavonoid biosynthesis and accumulation, and abiotic stress responses (Roeber et al., 2021; Xiao et al., 2022). HY5 interacts with B-BOX (BBX) proteins, which are rate-limiting cofactors for the induction of numerous downstream target genes (Bursch et al., 2020; Xiao et al., 2022). BBX20, BBX21, and BBX22 were identified as essential for hypocotyl elongation and anthocyanin production (Bursch et al., 2020). Besides BBX proteins, other transcription factors such as TEOSINITE BRANCHED 1/CYCLOIDEA/PROLIFERATING CELL FACTOR (TCP2) and SHI-RELATED SEQUENCE 5 (SRS5) modulate HY5 activity and thus play a role in light signal transduction (Xiao et al., 2022).

CONSTITUTIVE PHOTOMORPHOGENIC 1 (COP1) is an E3 ubiquitin ligase that acts as a negative regulator of light signaling by mediating the proteasomal degradation of the positive regulators of light signaling (Hoecker, 2017). COP1 was identified in a genetic screen as a member of CONSTITUTIVE PHOTOMORPHOGENIC/DE-ETIOLATED/FUSCA (COP/DET/FUS) proteins, which are chief negative regulators of photomorphogenesis (Li et al., 2011b; Yadav et al., 2020).

SUPPRESSOR OF PHYA-105 1(SPA1) to SPA4 is a family of WD-repeat proteins (Laubinger et al., 2004). Although they all interact with COP1 to suppress photomorphogenesis, minor differences exist in their function. SPA1 and SPA2 are active in dark-grown seedlings and SPA3 and SPA4 inhibit photomorphogenesis in light (Laubinger and Hoecker, 2003; Laubinger et al., 2004).

Under dark conditions, COP1 is present in the nucleus, and the COP1-SPA complex degrades HY5 (Yadav et al., 2020). COP1 also suppresses HY5 homolog (HYH) by direct interaction (Holm et al., 2002). In the presence of light, COP1 interacts with phytochromes and cryptochromes, that sequester COP1 (Yadav et al., 2020). This allows HY5 accumulation and derepression, promoting photomorphogenesis (Yadav et al., 2020). Subsequently, phyA, phyB, and CRY2 are targeted for degradation by COP1/SPA under far-red, red, and blue light (Ponnu and Hoecker, 2021) (Figure 1.3).

COP1 positively regulates UVR8 signaling, which is in contrast to phytochrome and cryptochrome signaling as discussed above. COP1 is required for the nuclear accumulation of UVR8 (Yin et al., 2016). In the nucleus, UVR8 sequesters COP1, allowing HY5 stabilization (Yin et al., 2016). WRKY36 and BRI1-EMS-SUPPRESSOR 1(BIM1)/BES1-INTERACTING MYC-LIKE 1 (BES1) also participate in the UVR8 signaling pathway (Liang et al., 2018; Yang et al., 2018). WRKY36 represses *HY5* by binding to its promoter. However, under UV-B light, UVR8 binds to WRKY36 and prevents it from suppressing *HY5* transcription (Yang et al., 2018) (Figure 1.3).

1.6.2 PIFs

PHYTOCHROME INTERACTING FACTORS (PIFs) are basic helix–loop–helix (bHLH) transcription factors that are crucial to the photomorphogenic pathway. PIFs were described as signal integrators of phytochromes. Until now, PIF1/3/4/5/6/7 have been identified in Arabidopsis (Li et al., 2011b).

As described in the previous section, under darkness, in their inactive Pr form, phytochrome remains in the cytoplasm. This allows PIFs to accumulate in the nucleus and orchestrate skotomorphogenesis (Leivar and Monte, 2014). In the presence of light, the active Pfr form of the phytochromes interacts with PIFs, resulting in PIFs' phosphorylation and degradation (Li et al., 2011b; Leivar and Monte, 2014). All PIFs are known to interact with the Pfr form of phyB, but only PIF1 and

PIF3 show binding to phyA (Li et al., 2011b). PIFs are also regulated by COP1 via HECTASE (Kathare et al., 2020).

The PIF quadruple mutant *pif1 pif3 pif4 pif5 (pifQ)* showed a constitutive photomorphogenic phenotype (Leivar et al., 2008). PIF1 has been shown to regulate seed germination by ABA and GA signaling pathways, along with transcriptional regulation of auxin, CK, JA, and brassinosteroid genes (Oh et al., 2009). Additionally, PIF1 acts as a DNA helicase and is involved in DNA resection (Jimeno et al., 2018). PIFs integrate diverse signals such as temperature, hormones, and circadian clock to modulate growth (Leivar and Monte, 2014). The COP1/SPA-HY5 module and PIFs regulate plant responses to several abiotic stresses such as cold acclimation, thermotolerance, shade avoidance, and drought tolerance (Jia et al., 2020; Roeber et al., 2021).

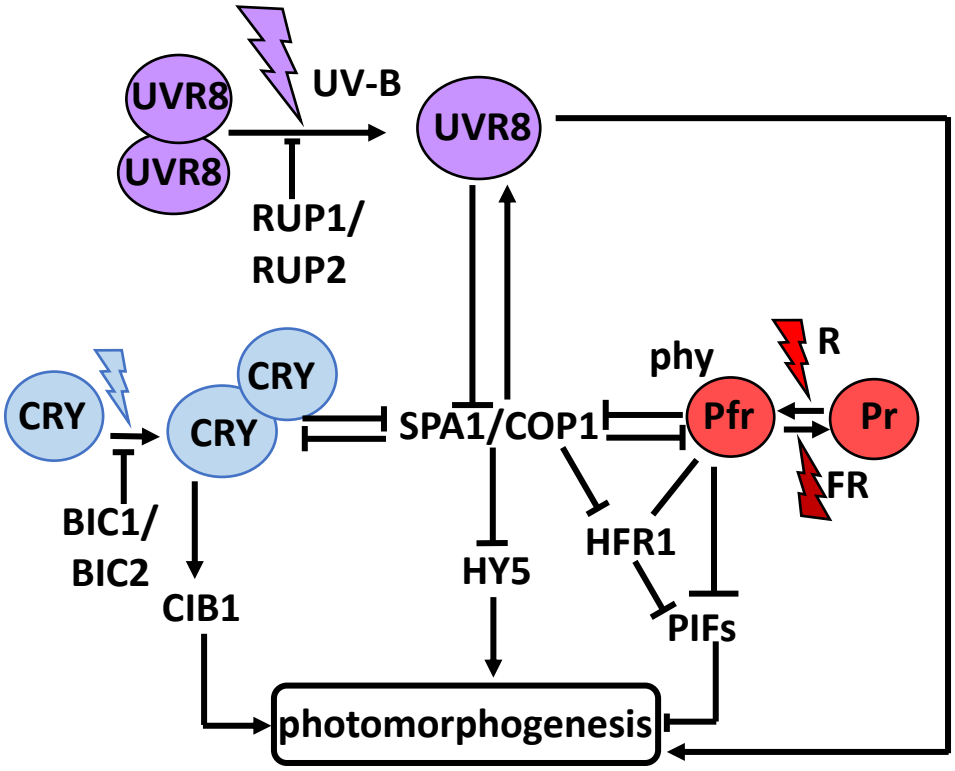

Figure 1.3: Simplified scheme of major light signaling pathways. Upon activation by light, phytochromes in their active Pfr form sequester SPA1/COP1 that allows HY5 activation. HY5 promotes photomorphogenesis by acting as a transcriptional activator of several genes responsible for photomorphogenic responses. In their Pfr form, phytochromes also repress PIFs independently or through their interaction with HFR1. PIFs also suppress photomorphogenesis. HFR1 is also targeted for degradation by COP1. CRYs also regulate light response similar to phytochrome through SPA1/COP1 dependent proteolysis. Additionally, CRYs regulate light responses by regulating the transcription of CIB1. BIC1/BIC2 prevent homodimerization of CRYs, thereby inhibiting light signaling by CRYs. Both phytochromes and CRYs are targeted for degradation by SPA1/COP1. In the presence of UV-B light UVR8 monomerizes and accumulates in the nucleus which requires the action of COP1. In the nucleus, UVR8 sequesters COP1, stabilizing HY5. In the dark, UVR8 re-dimerizes and gets deactivated by RUP1/RUP2. Abbreviations: B, blue light; phy, phytochromes; UV-B, ultraviolet light; R, red light; FR, far-red light. Figure adapted from Roeber et al. (2021).

1.6.3 HFR1

LONG HYPOCOTYL IN FAR-RED LIGHT 1 (HFR1) is a positive regulator of cryptochrome and phytochrome signaling. HFR1 forms homo- and heterodimers with PIF3 that can preferentially bind to the Pfr form of phyA and phyB (Fairchild, Schumaker & Quail 2000). HFR1 forms heterodimers with PIF4 and PIF5 to prevent exaggerated shade avoidance response (Li et al., 2011b). Several publications suggest that HFR1 inhibits PIF activity by sequestering PIFs in a PIF-HFR1 complex (Li et al., 2011b; Paulišić et al., 2021). During phyA signaling, HFR1 is also targeted for degradation by COP1 (Jang et al., 2005).

Besides playing an essential role in photomorphogenesis, the light signaling pathway plays an important role in the abiotic and biotic stress responses. For instance, to stimulate excess light tolerance, UVR8 and CRY1 mediate suppression of COP1, which derepresses HY5. This allows the activity of genes that enable the D1 repair cycle and ROS scavenging (Roeber et al., 2021). The role of photoreceptors and light signaling pathways in other abiotic stress responses such as cold and thermotolerance has been extensively reviewed by Roeber et al. (2021).

1.7 Circadian clock

As light is one of the Zeitgeber for the circadian oscillator, one of the important functions of photoreceptors and light signaling pathways is to entrain the circadian clock. Light of different intensities and wavelengths affects the period length of the clock. According to Aschoff's rule - with an increase in the intensity of light, the period length decreases. This phenomenon is known as parametric entrainment (Oakenfull and Davis, 2017; Ronald and Davis, 2017) Besides light, photosynthesis and sugar production also entrain the circadian clock (Haydon 2013).

A simplified summary of the molecular mechanism of the Arabidopsis circadian clock is presented below (see Figure 1.4).

Arabidopsis circadian clock consists of multiple feedback loops that are here referred to as morning-phased genes, day genes, evening-phased genes, and night-phased genes. The morning-phased genes operate at dawn and consist of *CCA1* and *LHY*. The day genes mainly include several *PRR* genes such as *PRR9* and *PRR7* (Shim and Imaizumi, 2015). *LUX ARRHYTHMO (LUX)*, *ELF4, ELF3,* and *PRR5* are some of the main evening-phased genes, and *TIMING OF CAB EXPRESSION 1 (TOC1)* is a night-phased gene (Shim and Imaizumi, 2015).

At dawn, CCA1 and LHY activate the expression of *PRR9* and *PRR7* (Farré et al., 2005). Secondly, by forming a complex with CONSTITUTIVE PHOTOMORPHOGENIC 10 (COP10)−DE-ETIOLATED 1 (DET1)−DAMAGED DNA BINDING 1 (DDB1) (CDD complex), they suppress the expression of evening-

phased genes and *TOC1* (Lau et al., 2011). Eventually, CCA1 and LHY also suppress their own expression in a negative feedback loop (Shim 2015). In the early afternoon, PRR7 and PRR9 proteins suppress the *CCA1* and *LHY* expression through direct interaction with TOPLESS (TPL) (Wang et al., 2013). This downregulation of *CCA1* and *LHY* derepresses the evening-phased genes (Shim and Imaizumi, 2015). REVEILLE 8 (RVE8) and NIGHT LIGHT-INDUCIBLE AND CLOCK REGULATED GENES 1 and 2 (LNK1/2) act as coactivators of evening-phased genes such as *LUX* and *ELF4*, and *TOC1* (Rawat et al., 2011; Xie et al., 2014). The evening complex (EC) comprising ELF3-ELF4-LUX, represses *PRR9* and *PRR7* expression possibly by establishing repressive chromatin domains (Tong et al., 2020). Later during the night, TOC1 further suppresses the expression of morning genes *CCA1* and *LHY* either on its own or by interaction with CCA1 HIKING EXPEDITION (CHE) (Alabadí et al., 2001; Pruneda-Paz et al., 2009). TOC1 also suppresses the evening-phased genes, *PRR9, PRR7,* and *GI*. Eventually, PRR7 and PRR9 also repress their own and each other's gene expression (Shim and Imaizumi, 2015).

During the day, ZTL activity is restricted by the GI-ZTL complex (Jose and Bánfalvi, 2019). However, in the dark, ZTL is released from this complex and degrades TOC1, allowing the EC to suppress the *PRR9* expression (Jose and Bánfalvi, 2019). This allows the induction of *CCA* and *LHY* expression, thereby completing the cycle (Shim and Imaizumi, 2015).

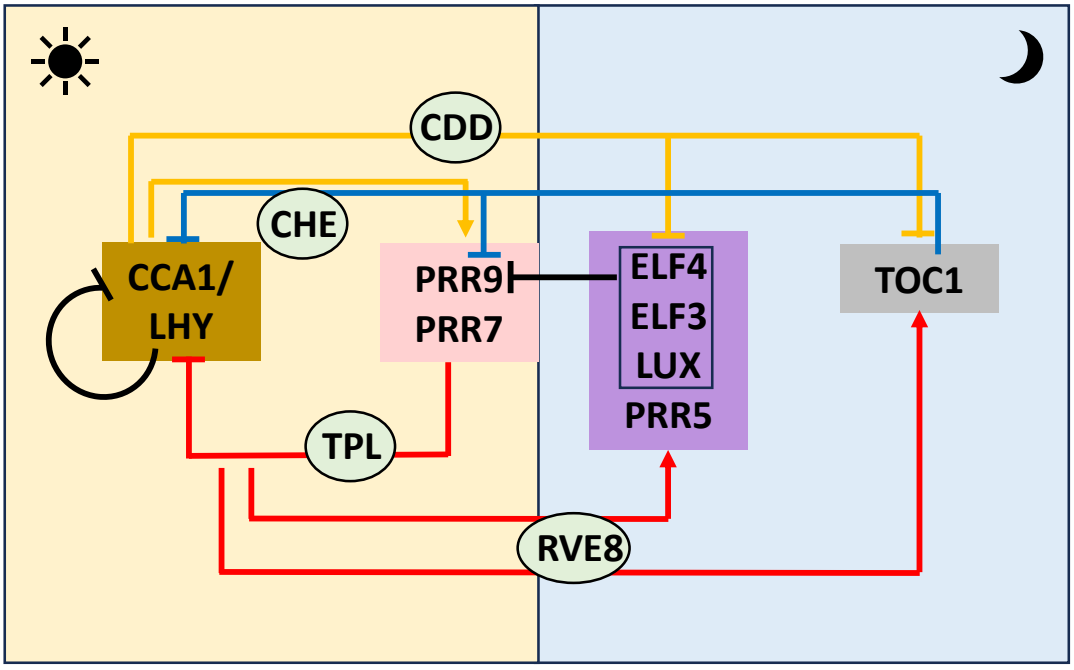

Figure 1.4: Schematic representation of the circadian rhythm in plants. At dawn, *CCA1/LHY*, the morning-phased genes (golden box) promote the expression of day genes (pink box) and repress the expression of the evening-phased genes (lilac box) and *TOC1* by forming a complex with CDD. The day genes repress *CCA1/LHY* expression with the help of TPL as a corepressor. Repression of *CCA1/LHY* leads to derepression of evening phased genes and *TOC1,* and RVE8 acts as their coactivator. During the night, TOC1 represses the expression of *ELF4* and *LUX*. Additionally, TOC1 suppresses *CCA1/LHY* expression on its own or with the help of CHE. The evening complex (ELF4-ELF3-LUX) represses *PRR9* expression, thus allowing *CCA1/LHY* expression and completing the cycle. Figure adapted from Shim and Imaizumi (2015).

Circadian clock components are not only regulated by light at transcriptional, translational, and post-translational levels via signaling cascades but also by direct interaction of photoreceptors with circadian clock components. For instance, phyB interacts with ELF3 and CCA1 (Yeom et al., 2014). phyA is important for low fluence red and blue light input to the circadian clock, and phyB/D/E for high intensity red light (Somers et al., 1998; Devlin and Kay). CRY1 and CRY2 act in blue light input to the circadian clock oscillator (Devlin & Kay 2000). It was recently shown that at dawn, phytochrome and cryptochrome mutations lead to a transcriptional delay of several photomorphogenesis-related genes and a complete elimination of the burst of *HY5* and *BBX* gene expression (Balcerowicz et al., 2021). The expression of *PHYA-E* and *CRY* genes also follow a diurnal rhythm, with maximum expression in the light phase (Tóth et al., 2001). This rhythm is maintained under constant light and constant dark (Tóth et al., 2001). Furthermore, UV-B light input into the circadian oscillator through UVR8 also entrains the circadian clock (Oakenfull and Davis, 2017).

1.8 Flowering pathway

Floral transition is an important phase during the life cycle of a plant to ensure its reproductive success. Temperature, together with intensity and duration of light exposure, are key environmental cues that determine flowering time (Srikanth and Schmid, 2011). Internal flowering cues include age, carbohydrate assimilate status, and hormonal status of the plant (Srikanth and Schmid, 2011). These external and internal cues encompass at least five major flowering pathways: photoperiod, autonomous, gibberellin, age, and vernalization pathways (Teotia and Tang, 2015). Since the photoperiodic flowering pathway directly responds to the photoperiod in nature, the possibility of its involvement in photoperiod stress has been explored in this work and is thus described here in more detail.

All the above-mentioned flowering pathways converge at floral integrator genes *FLOWERING LOCUS T (FT)* and *SUPPRESSOR OF OVEREXPRESSION OF CONSTANS 1 (SOC1)* (Corbesier and Coupland, 2006). FT translocates through the phloem to the shoot apex where it forms a complex with the bZIP protein FD (Abe et al., 2005). This FT-FD complex promotes *SOC1* expression, which is a key regulator of APETALA1 (AP1) and LEAFY (LFY). AP1 and LFY are the primary regulators of floral morphogenesis (Corbesier and Coupland, 2006).

1.8.1 Photoperiod flowering pathway

Photoperiodic flowering involves the crosstalk between the circadian clock, light signaling, and flowering regulation genes. *GI* and *CO* are the key components of the photoperiod flowering pathway (Corbesier and Coupland, 2006). The CO protein is responsible for the induction of gene expression of *FLOWERING LOCUS T (FT)* by directly binding to its proximal promoter region (Kim, 2020). The homolog of *FT*, *TWIN SISTER OF FT (TSF)*, is regulated in a similar way as *FT* by CO and shows a similar pattern of diurnal expression (Yamaguchi et al., 2005). Although FT and TSF have partially overlapping functions, they seem to act independently (Michaels et al., 2005). The effect of *tsf* mutation alone is not so prominent because the *tsf* mutant flowered at a similar time point as WT under LD and SD, however, under SD, *ft tsf* double mutation caused late flowering (Michaels et al., 2005).

CYCLIN DOF FACTOR 1 (CDF1), CDF2/3/5 represses *CO* expression by binding to the *CO* promoter (Sawa et al., 2007). They also directly negatively regulate *FT* expression (Imaizumi et al., 2005; Fornara et al., 2009). As also briefly mentioned in the section describing the circadian clock (see section 1.7), the *GI* transcript as well as the GI protein are regulated by the circadian clock and blue light (Mishra and Panigrahi, 2015). During the day (in the presence of light), facilitated by ELF4, GI is sequestered into nuclear bodies (Yu et al., 2008). In the LD afternoon, GI and FKF1 form a complex and degrade CDF1 via physical interaction (Sawa et al., 2007). Thus the GI-FKF1 complex derepresses *CO* and *FT* (Turck et al., 2008). Additionally, during the afternoon, *CDF1* is negatively regulated by PRR9, PRR7, and PRR5, but at dawn positively regulated by CCA1 and LHY (Shim and Imaizumi, 2015). *CO* expression is also regulated by several other factors such as RED AND FAR-RED INSENSITIVE 2 (RFI2), LONG VEGETATIVE PHASE 1 (LOV1), COEXPRESSED WITH CLOCK GENES LHY AND CCA1 1 (CEC1) (also known as LNK2), and members of chromatin remodeling complex (reviewed by Shim & Imaizumi 2015). *CO* mRNA reaches a peak at the end of the day and remains at a high level even in the dark both under LD and SD (Turck et al., 2008). However, CO protein reaches a peak at the end of the day but falls rapidly during the dark in LD due to posttranscriptional regulation. Under SD, the CO protein level remains constantly low (Turck et al., 2008).

CO protein is posttranscriptionally regulated by the light signaling pathway as well. CO is a BBX protein stabilized by light. Suppression of the COP1/SPA pathway by CRY1, CRY2, and phyA also leads to the stabilization of CO (Kim, 2020). However, phyB destabilizes the CO protein by promoting its ubiquitination by the RING-finger-containing E3-ligase protein HIGH EXPRESSION OF OSMOTICALLY RESPONSIVE GENE 1 (HOS1) (Lazaro 2015 from Kim 2020). phyB also negatively regulates *FT* expression by facilitating posttranslational suppression of the positive *FT* regulator PHYTOCHROME AND FLOWERING TIME 1 (PFT1)/MEDIATOR 25 (MED25) (Iñigo et al., 2012). This is corroborated by the fact

that *cry2* and *phyA* mutants are late flowering and *phyB* mutants are early flowering under LD (Guo et al., 1998; Valverde et al., 2004; Jang et al., 2008).

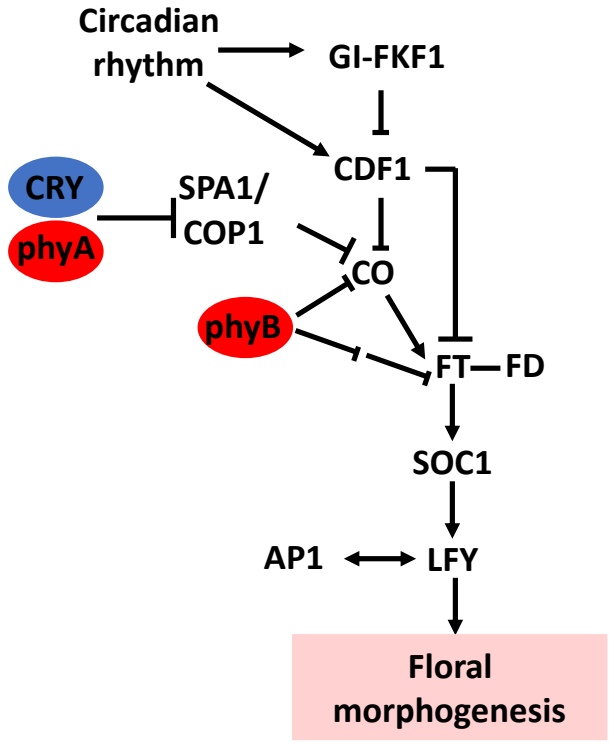

Figure 1.5: Schematic representation of the photoperiodic flowering pathway. The circadian rhythm regulates GI-FKF1 complex formation. In LD afternoon, GI-FKF1 degrades CDF1 by forming a complex, thus releasing *CO* and *FT* from suppression. CDF1 is also directly regulated by other components of the circadian clock (see section 1.8.1). CO promotes the expression of *FT*. FT forms a complex with FD as it gets transported from the phloem to the shoot apex. The FT-FD complex promotes *SOC1*, which upregulates *AP1* and *LFY*. AP1 and LFY activate each other and are the key regulators of floral morphogenesis. Besides CDF1, *CO* is also regulated by the light signaling pathway involving SPA/COP1. However, unlike phyA and CRY, phyB negatively regulates *CO* and *FT*. Figure adapted from Corbesier and Coupland (2006) and Kim (2020).

1.8.2 Age pathway

As the name suggests, this pathway encompasses internal cues on plant age for flowering initiation. *FT* expression is negatively regulated by SCHLAFMÜTZE (SMZ) by directly binding to the *FT* promoter. *SMZ* expression is controlled by microRNA miR172, which mainly controls flowering in an age-dependent manner (Shim and Imaizumi, 2015). miR156 is expressed primarily during the early developmental stages and suppresses SQUAMOSA PROMOTER BINDING PROTEIN-LIKE (SPL) TFs. As the plant ages, the expression of miR156 decreases, allowing SPL9 and SPL10 to activate miR172 expression. miR172 suppresses the expression of *FT* repressors, AP2-type transcription factors *TARGET OF EARLY ACTIVATION TAGGED 1 (TOE1)* and *TOE2* which allows induction of flowering (Shim and Imaizumi, 2015; Kim, 2020).

1.8.3 Autonomous pathway

The autonomous pathway (AP) is known for controlling floral initiation independent of the environment (Amasino and Michaels, 2010). AP mutants display a delayed flowering phenotype both under LD and SD (Kim 2020). *LUMINIDEPENDENS (LD), FLOWERING CONTROL LOCUS A (FCA), FLOWERING LOCUS Y (FY), FLOWERING LOCUS D (FLD), MULTICOPY SUPPRESSOR OF IRA1 4 (FVE/MIS4), FLOWERING LOCUS K (FLK)*, and *RELATIVE OF EARLY FLOWERING 6 (REF6)* are some of the genes identified as AP genes (Kim 2020). The floral repressor, *FLOWERING LOCUS C (FLC)*, is a common target of several AP proteins (Sheldon et al., 1999; Michaels and Amasino, 2001). FLC suppresses *FT* and *SOC1* expression, which suppresses flowering (Searle et al., 2006). Chromatin modifying complex, POLYCOMB REPRESSIVE COMPLEX 2 (PRC2) acts alongside FVE to catalyze the tri-methylation of histone H3-lysine 27 (H3K27me3). The PRC2 complex silences the expression of *FLC* (reviewed by Kim 2020).

1.8.4 Vernalization

Through exposure to long-term cold temperatures, plants acquire the ability to flower the next spring. This process is called vernalization (Kim et al., 2009). According to their vernalization requirement, Arabidopsis ecotypes have been grouped into winter and summer annuals (Amasino, 2004; Amasino, 2018). *FLC* and *FRIGIDA (FRI)* have been identified as important genes in the vernalization pathway in winter annuals (Henderson et al., 2003). FRI positively regulates *FLC* expression thus causing delayed flowering in winter annuals; however, *FRI* has a genomic deletion in summer annuals, that ultimately results in their early flowering phenotype (Sheldon et al., 1999; Johanson et al., 2000; Michaels and Amasino, 2001; Amasino, 2005). Prolonged cold exposure eventually represses *FLC* expression and this repressed state of *FLC* is maintained during the mitotic division throughout the warmer temperatures of the following spring (Bastow et al. 2004; De Lucia et al. 2008).

1.8.5 GA signaling pathway

Gibberellin treatment can cause floral induction in several plant species including Arabidopsis (Kim, 2020). GA biosynthesis mutant *ga1-3* showed no flowering phenotype under SD and delayed flowering under LD (Mutasa-Gottgens and Hedden, 2009). In a DELLA-dependent manner, GA promotes the expression of *LFY* and *SOC1*, thus promoting flowering (Moon et al., 2003; Achard et al., 2004).

1.9 Ecotypes

So far, photoperiod stress has only been shown to occur in *A. thaliana* Col-0. However, there are many more ecotypes available, and this work has explored whether photoperiod stress also occurs in different ecotypes.

According to biogeography studies, Arabidopsis is native to western Eurasia but is also found in Africa, South America, and Australia (Shindo, 2006). Natural ecotypes of *A. thaliana* have been collected from around the world and these can be obtained from the Arabidopsis Biological Resource Center (ABRC), Nottingham Arabidopsis Stock Center (NASC), and Versailles Arabidopsis Stock Centre.

According to Hufford & Mazer (2003), ecotypes are "distinct genotypes (or populations) within a species, resulting from adaptation to local environmental conditions; capable of interbreeding with other ecotypes of the same species". Natural variation within a species such as different ecotypes is considered to be the main resource for adaptation to their local climatic conditions (Shindo et al., 2007). Variations in response to day length, vernalization, and dormancy are the most common variations among the natural ecotypes of Arabidopsis (Koncz et al., 1992). These variations can be attributed to one or more allelic variations within the ecotypes. An example is the variation in the flowering time of Arabidopsis ecotypes due to allelic variation in the *FRI* gene. Late flowering ecotypes such as Bli-7 carry a fully functional *FRI* allele, while the allele in early flowering ecotype Col-0 has a 16-bp deletion that leads to a premature stop codon (Schmalenbach et al., 2014).

In the last decades, several studies have been published to explore this variation between the ecotypes or accession to identify genes underlying a specific phenotype or discover new genes. These studies used techniques such as quantitative trait loci (QTL) mapping in recombinant inbred lines (RILS) and multiparent advanced generation inter-cross (MAGIC) lines for fine-mapping the traits (Kover et al., 2009; Pollard, 2012). Numerous traits including flowering time (Schwartz et al., 2009) and photomorphogenesis (Matsusaka et al., 2021) have been studied through this approach.

In 2016, thanks to the 1001 whole genome project, global polymorphism pattern in 1135 naturally inbred lines of *Arabidopsis thaliana* were mapped (1001 Genomes Consortium, 2016). This study opened up the possibility for Genome-Wide Association Studies (GWAS) for different phenotypes in *A. thaliana.* A catalog of these studies can be found in the AraGWAS catalog of the 1001 whole genome website (https://aragwas.1001genomes.org/#/studies).

The effect of photoperiod stress was studied in the ecotypes listed in Table 2.2. These ecotypes selected based on their similarity to Col-0 (1001 Genomes Consortium, 2016), geographical location of their natural habitat (Weigel, 2012) , and a general collection of ecotypes from Versailles Arabidopsis Stock Center (VASC) .

Ten Ecotypes with similarity index 0.95 were chosen for analysis. The genetic similarity to Col-0 was calculated by 1001 Genomes Consortium, (2016) on the basis of single nucleotide polymorphism (SNP) in the whole genome. Furthermore, seven Col ecotypes besides Col-0 were also studied under photoperiod stress.

Sixteen ecotypes were chosen with consideration to their geographical locations from Detlef Weigel collection to ensure a diverse representation of various regions across different latitudes (Weigel, 2012). It was hypothesized that ecotypes from various latitudes, each accustomed to different natural photoperiods, would exhibit varying sensitivities to photoperiod stress.

A general collection of sixteen ecotypes from Versailles Arabidopsis Stock Center (VASC) was also analyzed to increase the diversity ecotypes analyzed for their response to photoperiod stress.

1.10 Research Aims

Photoperiod stress was first defined and characterized by Nitschke et al. (2016; 2017). In the following publications, the role of redox status in leaves and phytohormones status, especially that of CK in different plant tissue of varying age during photoperiod stress was further elaborated (Abuelsoud et al., 2020; Frank et al., 2020; Frank et al., 2022). This work aims to broaden the understanding of photoperiod stress by exploring three main objectives.

Primary aim of this work was to elucidate the light quantity and quality required to cause photoperiod stress. Therefore, the effect of different light intensities during the PLP was studied on photoperiod stress. Since a certain minimum light intensity was found to be necessary for causing photoperiod stress, a role of the chloroplasts in photoperiod stress was concluded. To explore this further, the effect of retrograde signaling pathway and starch metabolism was explored in photoperiod stress. Some retrograde signaling and starch metabolism mutants were tested under photoperiod stress in this regard. The metabolism of starch and sugar was also monitored. Additionally, plants were sprayed with DMSO, which inhibits photosynthesis by blocking electron flow, to gain further evidence on how chloroplasts could be involved in photoperiod stress.

Until now, photoperiod stress had only been studied under white light, prompting questions about which component of white light during the PLP is pivotal in causing photoperiod stress. Since red and blue light are known to influence several biological processes including photomorphogenesis in plants, monochromatic red and blue lights, or their combinations with far-red light were applied in different ratios during the PLP to investigate their impact on photoperiod stress symptoms. Next, the role of red and blue light photoreceptors in photoperiod stress was investigated by studying the effect of photoperiod stress in photoreceptor mutants. Some of these photoreceptor mutations were

introgressed into CK receptor mutants and clock mutants, to see if the photoreceptor mutation could rescue their strong photoperiod stress phenotype. To further ascertain the mode of action of photoreceptors, light signaling mutants were also tested under photoperiod stress.

The second aim was to test the possible involvement of the photoperiodic flowering pathway in photoperiod stress. The effect of photoperiod stress on selected flowering pathway mutants was analyzed in this regard.

Most of the work done on photoperiod stress has been performed with the Col-0 ecotype as the wild type. The third aim of this work was to investigate photoperiod stress in different ecotypes of *A. thaliana*. Several different ecotypes of *A. thaliana*, selected based on their geographical distribution and genetic similarity to Col-0, were tested under photoperiod stress. Some of these ecotypes were crossed with Col-0 and their F1 and F2 generation were also examined under photoperiod stress to get a first information of the inheritance pattern of photoperiod stress sensitivity.

2 Materials and methods

2.1 Plant growth conditions

A. thaliana accession Columbia-0 (Col-0) was used as wild type (WT) in this study. Table 2.1 lists all the *A. thaliana* mutants used in this study. Different ecotypes of *A. thaliana* used are mentioned in Table 2.2. For conducting experiments, *A. thaliana* plants were grown in soil under SD conditions (8 h light/16 h dark) in a phytochamber at 22 °C and 60 % relative humidity with a white light of intensity 120 µmol m^{-2} s^{-1} generated using a combination of Philips Son-T Agros 400 W and Philips Master HPI-T Plus, 400 W/645 lamps. 'Sowing soil' (2:2:1, Soil Type P: Soil Type T: Sand) (Einheitserde, H. Nitsch & Sohn GmbH & Co. KG, Kreuztal, Germany, Article: 540203) was used at all stages for these plants. Seeds of each genotype were sown in a single pot and stratified at 4 °C for two days before transferring to the phytochamber. In order to ensure sufficient humidity, seedlings were cultivated in plastic hoods for the first few days. After approximately one-and-a-half weeks, the plants were singled out into individual pots.

For the purpose of genotyping, propagation, crossing, and segregation analysis, plants were grown under LD conditions (16 h light/8 h dark) with a temperature cycle of 22 °C during light and 18 °C during the dark in a greenhouse. The seeds of a single genotype were sown in a single pot in 'sowing soil' and kept under a hood to ensure sufficient humidity. After about two weeks, the seedlings were singled out into individual pots with soil containing Perligran G instead of sand.

Table 2.1: Mutant and transgenic Arabidopsis plants used in this study.

Mutant name[1)]	**Background**	**Publication**	**Seed donor**
cytokinin mutant			
ahk2-5 (ahk2) ahk3-7 (ahk3)	Col-0	Riefler et al. (2005)	Dr. Anne Cortleven, FU Berlin
clock mutant			
cca1-1 (cca1) lhy-20 (lhy)	Col-0	Nitschke et al. (2016)	Dr. Anne Cortleven, FU Berlin
photoreceptor mutants			
phyA-211 (phyA)	Col-0	Reed et al. (1994)	Dr. Daniela Pezzetta, FU Berlin
phyB-9 (phyB)	Col-0		
phyB-GABI_652F05	Col-0	Lim et al. (2018)	Prof. Songhyun Hong, DGIST, Republic of Korea
phyA phyB	Col-0	Lascève et al. (1999)	Prof. Andreas Hiltbrunner, Albert-Ludwigs-Universität Freiburg
phyA ahk2 ahk3	Col-0	Pezzetta (2019)	Dr. Daniela Pezzetta, FU Berlin
phyB ahk2 ahk3	Col-0	Generated in this study	

Mutant name[1)]	Background	Publication	Seed donor
phyB cca1 lhy	Col-0	Generated in this study	
phot1-5 (phot1)	Col *gl-1*	Huala et al. (1997)	Prof. Atsushi Takemiya, Yamaguchi University, Japan
phot2-1 (phot2)	Col *gl-1*	Kagawa et al. (2001)	
phot1 phot2	Col *gl-1*		
ztl-105, SALK_069091 (ztl)[2)]	Col-0	Martin-Tryon et al. (2007)	N569091
cry1 hy4-B104 (cry1)	Col	Bruggemann et al. (1998)	Prof. Alfred Batschauer, Philipps Universität Marburg
cry2-1 (cry2)	Col-4	Guo et al. (1998)	Dr. Anne Cortleven, FU Berlin
cry1 cry2	Col	Lascève et al. (1999)	Prof. Alfred Batschauer, Philipps Universität Marburg
cry2-2	Col	Guo et al. (1998)	Prof. Chentao Lin, UCLA, USA
cry1 ahk2 ahk3	Col-0	Generated in this study	
cry2 ahk2 ahk3	Col-0		
cry1 cca1 lhy	Col-0		
cry2 cca1 lhy	Col-0		
uvr8-6 (uvr8)	Col	Favory et al. (2009)	Prof. Roman Ulm, University of Geneva, Switzerland
uvr8-7	Ws		
uvr8 ahk2 ahk3	Col-0	Generated in this study	
uvr8 cca1 lhy	Col-0		
Light signaling mutants			
hy5-215 (hy5)	Col-0	Cluis et al. (2004)	Dr. Katharina Bursch, FU Berlin
cop1-4 (cop1)	Col-0	McNellis et al. (1994)	
spa1-100 (spa1) spa2-2 (spa2)	Col-0	Fackendahl (2012)	Dr. Henrik Johansson, FU Berlin
spa3-1 (spa3) spa4-3 (spa4)	Col-0		
rup1-1 rup2-1	Col-0	Ren et al. (2019)	Dr. Henrik Johansson, FU Berlin
pifQ	Col-0	Leivar et al. (2008)	Dr. Anne Cortleven, FU Berlin
som-1 (som)	Col-0	Kim et al. (2008)	Dr. Daniela Pezzetta, FU Berlin
hfr1-1 (hfr1)	Col-0	Fairchild et al. (2000)	Dr. Daniela Pezzetta, FU Berlin
PIF1 overexpressor (PIF1-OX)	Col-0	Oh et al. (2009)	Dr. Daniela Pezzetta, FU Berlin
Starch metabolism mutants			
adg1-1 (adg1)	Col	Wang et al. (1998)	Prof. Margarete Baier, FU Berlin
adg2-1 (adg2)	Col	Wang et al. (1997)	
pgm1	Col	Egli et al. (2010)	Dr. John Lunn, Max Planck Institute of Molecular Plant Physiology
sex1-8 (sex1)	Col	Ritte et al. (2006)	Prof. Jörg Fettke, Universität Potsdam
Retrograde signaling mutants			
rcd1-1 (rcd1)	Col-0	Overmyer et al. (2000)	Dr. Anne Cortleven, FU Berlin
gun1	Col	Mochizuki et al. (2001)	Prof. Bernhard Grimm, Institut für Biologie, HU Berlin
gun4-1 (gun4)	Col	Larkin et al. (2003)	
gun5-1 (gun5)	Col	Mochizuki et al. (2001)	
gun6	Col	Woodson et al. (2011)	
glk1 glk2	Col	Fitter et al. (2002)	Prof. Bernhard Grimm, Institut für Biologie, HU Berlin

Mutant name[1)]	Background	Publication	Seed donor
Flowering mutants			
fkf1	Col *gl1-1*	Nelson et al. (2000)	Prof. Takato Imaizumi, University of Washington, USA
co-1 (co)	L*er*	Putterill et al. (1995)	Dr. Isabel Bartrina, Universität Graz, Austria
gi-201 (gi)	Col	Martin-Tryon et al. (2007)	Dr. Anne Cortleven, FU-Berlin
ft-10 (ft)	Col	Michaels et al. (2005)	Dr. Isabel Bartrina, Universität Graz, Austria
tsf	Col		
ft-1 tsf (ft tsf)	Col		

1) Written in parentheses are the names used throughout this study.
2) NASC ID if ordered from the stock center or seeds kindly provided by the indicated researcher.

Table 2.2: Ecotypes of *A. thaliana* used in this study.

Ecotype	Latitude	Longitude	Location	Country	NASC ID[1)]	Versailles accession number	similarity to Col-0
Col ecotypes[2)]							
Col-0					N1092		
Col-1					N3176		
Col-2					N907		
Col-3					N908		
Col-4					N28172		
Col-5[3)]					N1644		
Col-7					N28173		
gl-1							
Ecotypes based on similarity to Col-0							
TÄL 07					N77339		0.980027
UKSE06-500	51.1	0.6	Sissinghurst garden	UK	N78805		0.960666
Gd-1	53.5	10.5	Gudow	DE	N1184		0.955622
Altenb-2					N76353		0.955541
En-2	50	8.5	Enkheim/Frankfurt	DE	N6696		0.954645
Boot-1	54.4	-3.26			N76452		0.952792
Bran-1	45.57	25.41	Bran	RO	N76722		0.951661
Epidauros	37.6	23.08	Epidauros	GR	N76844		0.950961
CSHL-5			New York	USA	N76779		0.950783
BRR107	40.83	-87.73		USA	N78948		0.950454
Ecotypes from VASC collection							
Jea	43.68	7.33	Jea	FR	N1305	25AV	
Mh-1	50.95	7.5	Muhlen /Ostpr	PO	N1368	215AV	
Edi-0	55.94	-3.16	Edinburgh	UK	N1122	83AV	0.936916
Gre-0	43.17	-85.23	Greenville, MI	USA	N1210	200AV	0.940326

Ecotype	Latitude	Longitude	Location	Country	NASC ID[1)]	Versailles accession number	similarity to Col-0
N13	61.36	34.15	Konchezero	RU	CS22491	266AV	
Oy-0	60.38	6.19	Oystese	NO	N1436	224AV	0.938544
St-0	59	18	Stockholm	SE	N1534	62AV	0.94199
Kn-0	54	23	Kaunas	LT	N1286	70AV	0.936427
Blh-1	48	19	Bulhary	CZ	N1030	180AV	
Sakata				JP		257AV	
Akita				JP		252AV	
Ita-0			Ibel Tazekka	MA	N1244	157AV	
Shahdara			Pamiro-Alay	TJ	N929	236AV	
Mt-0	32.34	22.46	Martuba/Cyrenaika	LY	N1380	94AV	
Ct-1	37.3	15	Catania	IT	N1094	162AV	
Tsu-0	34.3	136.31	Tsushima	JP		91AV	0.939763
Ecotypes based on geographical location							
Tanz-2	2.5	0.36	Tanzania	TZ	N75925		
Pa-3	38	14	Palermo	IT	N6827		
Cvi-0	16	23	Cape Verde Islands	CP	N22682		0.914382
La-1	53	15.16	Landsberg/Warthe	DE	N6767		
Ka-0	47	15	Karnten	AT	N6752		
Elmonte	42.1167	12.4833	Belmonte	IT	N77625		
L*er*-0	47.984	10.8719	Landsberg/Warthe	DE	N97814		0.935341
Hen	65.25	15.6		SE	N77670		
Ber-0	55	12	Copenhagen	DK	N28066		
H55	49	15	Relichova	CZ	N76897		0.975069
Pigna-1	41.18	14.18	Pignataro Maggiore	IT	N77177		0.940646
Lag1	58.1834	15.0062	Lagnebrunne	SE	N78675		0.931233
Mr-0	44	44.478	Monte/Tosso	IT	N76553		
Can-0	28	15	Canary Islands	ES	N28130		0.921109
Ting-1	56.5	15	Tingsryd	SE	N22549		0.936763
Ws-1	52	30	Wassilewskija	RU	N2223		

1) All ecotypes were ordered from NASC except the ones where the Versailles accession number is mentioned. These were a part of the Versailles ecotype collection and were ordered from VASC.
2) Discrepancy exists about the original habitat of Col. Although according to NASC the original habitat is the USA, other sources (Koncz et al., 1992) mention that they originally came from Europe.
3) Col-5 is reported as *gl-1* by NASC.

2.2 Genetic crosses

Genetic crosses were performed on plants growing under LD conditions in the greenhouse. Newly bolted plants with a single stem with inflorescence were preferred as 'mother plant' due to the ease of performing a cross. All the leaves, open flowers, and siliques were removed from the stem. Flower buds that were slightly larger but not ready to open were chosen for crossing and all the other buds were removed. Using precision tweezers, the gynoecia of the selected flower buds were prepared by

removing the sepals, petals, and all six stamens. After making sure that the gynoecia were intact, the stigma was brushed with anthers of freshly opened flowers. The pollinated mother plant was kept under a plastic hood for a day and pollinated again the next day. Upon successful crossing, elongation of siliques could be observed after two to three days.

2.3 Genotyping of *A. thaliana* mutants

2.3.1 Genotyping strategies

Mutant seeds were genotyped to confirm the mutation. Genotyping was also performed to find the homozygous mutants in a segregating F2 population. The T-DNA insertion mutations were confirmed by PCR with one primer flanking the insertion and a gene specific primer. Alongside, PCR was also performed with gene specific primers for the wild-type control. Deletion mutations were confirmed by PCR with gene specific primer pairs and the absence of a band was used as confirmation of mutation. SNP mutations were confirmed by sequencing the band obtained from PCR with gene specific primers or genotyped using Cleaved Amplified Polymorphic Sequences (CAPS) primers (section 2.3.4). Table 2.3 to Table 2.6 gives the primers and genotyping techniques used for confirming mutants used in this study.

Table 2.3: Sequence of primers used to genotype insertional mutants and size of amplified DNA fragment.

Mutant	Wild-type allele		Mutant allele	
	Primers (5'-3')	**size [bp]***	**Primers (5'-3')**	**size [bp]**
ahk2-5	F-GCAAGAGGCTTTAGCTCCAA R-TTGCCCGTAAGATGTTTTCA	672	F + SAIL	650
ahk3-7	F-CCTTGTTGCCTCTCGAACTC R-CGCAAGCTATGGAGAAGAGG	558	R + GABI	450
cca1-1	F-TGTCCAGATAAGAAGTCACGCTCAGAAA R-TTTATTCATGGAGGATGCAGCAGAGA	914	F + GATGCACTCGAAATCAGCCAATTTTAGAC	250
lhy-20	F-GAGAGCGATGGACTGAGGA R-TTTTCGGGGTAGAGATGATAGAG	795	R + SALK	ca. 500
phyB-GABI	F-GGTAATTTGCTAAAATCGCCACACA R-TAGACTGAGTTAGCCTATCGTCCT	137	F+ ATATTGACCATCATACTCATTGC	ca. 600
phot1-5	F-AGTTCAGCTCATCAACTACACC R-AACGAGTTCCACTAGATGCAC		F + ATGTAGAACACCGGAATATTCG	ca. 600
ztl-105	F-GGACCGTTTGCTAAAAGAAGG R-GTGTCACTTAGAAGAACGCCG	1013	F + SALK	ca. 600
uvr8-6	F-AGGAGTGATATGCATTC	1026	F + LBa1	670

Mutant	Wild-type allele		Mutant allele	
	R-TCCCAAACTAGACAGACG			
hy5-215	F-TAAGAAAAATGCAGGAAC	340	F + CTCATCGCTTTCAATTCT	340
	R-CTCATCGCTTTCAATTCC			
spa1-00	F-CTGACCACTGCTGTAATTGAAC	539	F + TAGCATCTGAATTTCATAACCA	ca. 600
	R-CATTCATAATACTATTCTCACCAGC			
spa2-2	F-GGGAAAATGTCTTTGCCTGA	355	F + CTGGGAATGGCGAAATCAAG	ca. 400
	R-AGCACGGCAAACCATCATA			
spa3-1	F-TTCGGACTCTGGCTCTGATTCCTTG	580	F + SAIL	ca. 600
	R-GTCCTCATTGATGGTCGACAAGTT			
spa4-3	F-GGTCAAGAAGCTTCCTCGTG	378	F + CTGGGAATGGCGAAATCAAG	ca. 400
	R-TCATCATCAAGTCCTCCCAAG			
pif1-1	F-CGAGATAACCGGTACATCGTCATC	920	F + TAGCATCTGAATTTCATAACCAATCTCGATACAC	ca. 200
	R-CATGTGAGTTTGTGTAGGCAAAGGTC			
pif3-3	F-AGAAGCAATTTGGTCACCATGCTC	461	F'-GGTGTGTATGTGAGAAGGTACATCCATCG	800
	R-TGCATACAAATAGTCGATCGTATG		R'-AAGCTTAGCTTTGGTGAGCCTGAAAAGCTC	
pif4-2	F-ACCTCCTCAAGTCATGGTTAAGCCTAAGGC	1380	R + TAGCATCTGAATTTCATAACCAATCTCGATACAC	ca. 400
	R-TCCAAACGAGAACCGTCGGT			
pif5-3	F-GCTTTATTAAATCATTTCCTCCTAGATTGTTG	1150	F + Lba1	ca. 600
	R-TGTATACCTTTCTGAGAGATTATGAACTT			
hfr1-1	F-GAGAACCGAAACCTTGTCCG	212	R + SALK	ca. 400
	R-GCTACAGCAACTCGTACCT			
rup1-1	F-CGGGATCCATTTAAATCTCTCTCTTTCCGCCG	400	R + Lba1	710
	R-GGTCTAGAGGCGCGCCCACATTTGAACCGTTCC			
rup2-1	F-CCGGCGAAACTTAGTAGTC	1100	F + LBa1	690
	R-CTTGAAGAAAGTCATTCCCA			
som-1	F-ATGGATGTCGTTTGTACGGAACATCAA	1182	R + SALK	146
	R-TCAAGTCAAGAGATCATTGACCCATCC			
sex1-8	F-GCATCGGTCAGTTTTATGCTCA	440	F + SALK	ca. 200
	R-GTGGACAGAGTCTAAACTTC			
gi-201	F-GCAAGAGTAGAGATAACCAACCAA	872	R + SALK	ca. 200
	R-CGGATGATGAAGGACAAACA			

Sequence of T-DNA insertion-specific primers	
IT-LB1 (SAIL)	GCCTTTTCAGAAATGGATAAATAGCCTTGCTTCC
SALK LBb1.3 (SALK)	ATTTTGCCGATTTCGGAAC
LBa1	TGGTTCACGTAGTGGGCCATCG

*bp-base pairs

Table 2.4: Sequence of primers used to genotype deletion mutants and size of the amplified DNA fragment.

Mutant	Primers (5'-3')	size [bp]
phyA-211	F-TTATCCACAGGGTTACAGGG	1136
	R-GCATTCTCCTTGCATCATCC	
cry1(hy4-B104)	F-CGCAGAAAAGCCGATAGTGC	740
	R-TGAAGCCGTGCTTTTGCTTC	
cry2-1 /cry2-2	F-CATGGAACAACTTGGTTAGAGTGTGGA	400
	R-ACGTGATCGCATCAACCTCAGTTGCAC	

Table 2.5: Sequence of CAPS primers and enzymes used for genotyping SNP mutants.

Mutant	Primers (5'-3')	Enzyme	size after digestion [bp]	Reference
phyB-9	F-CAATGTAGCTAGTGGAAGAAGCTCGATGTGG	MnlI	100 + 20	Ward et al. (2005)
	R-ACATAACAGTGTCTGCGTTCTCAAAACGC			
phot2-1	TATTCTGACAGTCTCCTTTGTG	HinfI	100 + 20	Prof. Atsushi Takemiya, personal communication
	TGGACACATGCAATGTTGTAC			
pgm	AGGCTTCCGAGCAACTCAATATC	BspCNI	1295 + 243	Egli et al. (2010)
	CTGACCACTGCTGTAATTGAAC			

Table 2.6: Sequence of primers used for genotyping SNP mutants by sequencing.

Mutant	Primers	size [bp]	Point mutation	Reference
uvr8-7	F-GCTTATTCACAATCAGGCA	560	Gln-124 to stop	Favory et al. (2009)
	R-GAAAACAAGACAAGACAGAC			
gun4-1	F-CAACCTCTGTGTCAAGAAG	436	Leu-88 to Phe	Larkin et al. (2003)
	R-CTTTCCCTCAAACAACC			
gun5-1	F-CAAGCTTACCTCGCTTCTT	468	Ala-990 to Val	Mochizuki et al. (2001)
	R-GTATCAGCAATTGGTCTCAC			
adg1	F-GCAATTGGAGTTCTCAAGGTA	419	Gly-92 to Arg	Wang et al. (1998)
	R-TTCGCTCTCTTCTTCGTAAGT			
adg2	F-CTAACTTCTCTCAGAAGAG	511	Gly-118 to Gln	Wang et al. (1997)
	R-CATTGGAGTTGTAAGCAC			

2.3.2 Genomic DNA extraction

A small piece of leaf tissue was used for genomic DNA extraction in either an 8X stripe or a 1.5 ml microcentrifuge tube containing two metal balls. After homogenization in a Retsch Mixer Mill MM2000 (Retsch, Haan, Germany), 400 µl of extraction buffer (0.2 M Tris/HCl pH 7.5, 0.25 M NaCl,

0.025M EDTA, 0.5 % (w/v) SDS) was added to each sample and centrifuged for 15 minutes (3 minutes for 1.5 ml microcentrifuge tubes) at maximum speed. 300 µl supernatant from each sample was transferred to fresh 8X stripe or microcentrifuge tubes and 300 µl isopropanol was added. After vortexing, the mixture was left undisturbed for 5-7 minutes. The 8X stripes were centrifuged at maximum speed for 1 h. The microcentrifuge tubes were centrifuged for 5 minutes at 10,000 rpm. The supernatant was discarded, and the pellet was washed with 70 % ethanol, followed by centrifugation for 15 minutes at maximum speed for 8X stripes (for microcentrifuge tubes – centrifugation at 10,000 rpm for 5 minutes). The pellet was dried at 60 °C and resolved in double distilled water at 4 °C for at least 1 h.

2.3.3 PCR analysis

Genomic DNA extracts were used for PCR analysis. The reaction mix used for the PCR is given in Table 2.7. For the PCR, a thermocycler (Biometra, Göttingen, Germany) was used using the conditions described in Table 2.8.

Table 2.7: Reaction mix for PCR.

Components	Stock concentration	Final concentration	Volume [µL]
Buffer	10 X	1 X	2
dNTP	5 mM	200 µM	0.8
Taq-Polymerase	---	---	0.5
Forward primer	50 µM	625 nM	0.25
Reverse primer	50 µM	625 nM	0.25
Water	---	---	18
Template	---	---	2

Table 2.8: Temperature cycle for PCR.

Step	Temperature	Time	
Initial denaturation	95 °C	5 minutes	
Denaturation	95 °C	15 seconds	X 35
Annealing	57 °C	30 seconds	
Elongation	72 °C	1 kb min^{-1}	
Final elongation	72 °C	5 minutes	

2.3.4 Restriction digestion

For genotyping using CAPS markers (Table 2.5), restriction enzymes from New England BioLabs were used. For a typical reaction, 5 µl PCR product, 5-10 U of the restriction enzyme, and 1X of the recommended reaction buffer were mixed and water was added to a final volume of 10 µl. This reaction mix was incubated at the temperature specific to the restriction enzyme for at least an hour. Afterward, the restriction enzyme was deactivated at the temperature specified in the manual for 20 minutes.

2.3.5 Agarose gel electrophoresis

DNA fragments from PCR or restriction digestion were separated according to size by agarose gel electrophoresis. 6X loading dye (30 % glycerol, 0.25 % bromophenol blue, 0.25 % xylene cyanol FF), was added to the PCR product or restriction digest product to obtain a final loading dye concentration of 1X. A 1 % or 2 % agarose gel in 1X TAE (40 mM Tris, 20 mM acetic acid, and 1 mM EDTA, pH 8) was prepared and ethidium bromide (0.75 µl/ml gel) was added. The DNA band size was determined with the help of a 1000 bp DNA ladder (Thermo Scientific™, Vilnius, Lithuania, Article: Hyperladder I,) or pBR322 Hae III (MBBL, Bielefeld, Germany, Article: P-205). The prepared samples were loaded in the agarose gel for electrophoresis and were visualized through a UV-transilluminator (Genoplex, VWR International GmbH, Darmstadt, Germany) using GenoCapture software (VWR, Germany).

2.3.6 PCR product purification

The PCR products were purified by gel extraction before being sent for sequencing using the NucleoSpin® Gel and PCR-clean-up kit (Machery-Nagel, Düren, Germany, Cat. No. 740609.250) by following the manufacturer's protocol.

2.4 Photoperiod stress treatment

For stress treatment, 4-weeks- or 5-weeks-old plants were treated with a PLP of 4, 8, or 16 hours. A schematic overview of the used experimental setup is mentioned individually in the results section. Stress treatments were given in plant cabinets (CLF Plant Climatics, Wertingen, Germany, Model: AR-41L2,) (4 or 8 h) or in a walk-in growth chamber (16 h). Monochromatic light conditions and their ratios were generated by LEDs present in the afore mentioned plant cabinets. The used light qualities and light intensities are given in Table 2.9. The light quality was measured by SKL 904 SpectroSense2 with

one 4-channel sensor SKR 1850D/SS2 42262 (Skye Instruments Ltd, Llandrindod Wells LD1 6DF, United Kingdom).

Table 2.9: Used intensity of different light wavelengths.

	Intensity during the light treatment [µmol m^{-2} s^{-1}]					
Wavelength	**White light**	**Red light**	**Blue light**	**R:FR (1:1)**	**B:R:FR (1:2:1)**	**Shade**
PAR	127.6	117.6	212.9	74.3	100.7	118.1
Blue	3	0	75	0.13	14.65	9.8
Red	10.9	75.1	0.06	41.39	33.4	6.66
Far-red	5.4	0.02	0.05	39.74	13.78	13.3

The light intensity is given in µmol m^{-2} s^{-1}. Central wavelengths were 472.7 nm for blue light, 668.6 nm for red light, and 748.5 nm for far-red light. The PAR of all the treatments is comparable because similar strength of photoperiod stress symptoms is induced at light intensities (PAR) ranging from 50-300 µmol m^{-2} s^{-1} (see section 3.1). PAR, photosynthetic active radiation; R:FR, red:far-red; B:R:FR, blue:red:far-red.

2.5 Sampling of leaf material

Plant leaf material was harvested at the time points indicated in the experimental setup. Sampling in the dark was performed under green light. Distal ends of leaves number 8-11 were sampled in 2 ml Eppendorf safelock tubes with two stainless-steel beads (2 mm diameter) and flash-frozen in liquid nitrogen. The frozen leaf samples were homogenized by a Retsch Mixer Mill MM2000 (Retsch, Haan, Germany) for 3 min at 30 Hz.

2.6 Peroxide determination

Peroxide levels were determined as described in Abuelsoud et al. (2020) by using the Pierce™ Quantitative Peroxide Assay Kit (Thermo Scientific, Rockford, USA, Cat. No. 23280). For determination of peroxide levels ca. 100 mg of leaf material was harvested per sample in the dark as described in section 2.5. 700 µl of 0.1 % TCA was added to the homogenized leaf samples and kept on ice. The samples were vortexed thrice at an interval of 5 minutes and subsequently centrifuged at 16,000 *g* at 4 °C for 15 minutes. 300 µl of the sample supernatant was transferred to fresh 1.5 ml microcentrifuge tubes and further used for analysis. Meanwhile, to obtain a standard curve for H_2O_2 level determination, a dilution series consisting of 100 µM, 80 µM, 60 µM, and 20 µM H_2O_2 (Emsure®, Darmstadt, Germany, Cat. No. K48386109648) was prepared and water served as the blank for H_2O_2. A working solution of the reagent was prepared by mixing in a ratio of 1:100 solution A (clear) and solution B (yellow) from the Pierce™ Quantitative Peroxide Assay Kit. 20 µl of the sample/ each H_2O_2

dilution/ blank (0.1 % TCA) was mixed with 200 µl of the working solution in a 96-well plate. After an incubation of 10 minutes, absorption was measured with Synergy™ 2 Multi-Detection Microplate Reader (Biotek®, Winooski, Vermont, USA) at a wavelength of 595 nm using Gen5™ Reader Control and Data Analysis Software. Absorption of a second plate with sample/ each H_2O_2 dilution/ blank (0.1 % TCA) in similar wells mixed with 200 µl of water instead of the reagent was also measured as plate control. For determining the H_2O_2 level, the absorption of TCA blank was subtracted from all other values, and the linear function y = mx + c (m = slope, c = 0) was calculated from the dilution series. The value of the slope was used to calculate the peroxide levels in the samples by the following equation: peroxide levels [nmol H_2O_2 equivalents g^{-1} fresh weight (FW)] = [absorption 595 nm * ml TCA solution added / fresh weight (g)] * m.

2.7 Total RNA extraction and qRT-PCR

2.7.1 Total RNA extraction

Total RNA was extracted from the leaf samples that were prepared as described in section 2.5 using the NucleoSpin® RNA plant kit (Machery and Nagel, Düren, Germany, REF 740949.50). Mostly the steps were followed as described in the user manual with a few changes. 700 µl or 350 µl of lysis buffer RAP was added to the grounded sample from 5-weeks- or 4-weeks-old plants and vortexed rigorously. This was centrifuged at 16,000 g for 5 minutes. The lysate was filtered through the NucleoSpin® filter by centrifuging at 11,000 *g* to reduce the viscosity. In order to adjust the RNA binding conditions of the lysate, the filtrate collected in the collection tube was mixed with 70 % ethanol in a 1:1 ratio in a 1.5 ml Eppendorf tube and vortexed rigorously. Next, 700 µl of the lysate-ethanol mixture was added to the NucleoSpin® RNA Plant Column placed in a collection tube and centrifuged for 30 s at 11,000 *g* for binding the RNA to the silica membrane of the column. The filtrate was discarded. 350 µl of the membrane desalting buffer (MDB) was added to this column and centrifuged at 11,000 *g* for 1 minute. After this, the membrane was washed. For the 1st wash, 200 µl of wash buffer RAW2 was added and centrifuged at 11,000 *g* for 1 minute. For the 2nd wash, the column was placed in a new collection tube and 600 µl wash buffer RA3 was added to it (wash buffer RA3 was prepared by adding 100 ml of 100 % ethanol to its supplied concentrate) and centrifuged at 11,000 *g* for 30 s. The flowthrough was discarded and 250 µl of the RA3 buffer was added to the column for the 3rd wash and centrifuged at 11,000 *g* for 2 minutes to completely dry off the membrane. The column was placed on 1.5 ml microcentrifuge tubes and the RNA was eluted in 20-30 µl of water by letting it incubate on the membrane for ca. 2 minutes before centrifuging at 11,000 *g* for 1 minute.

The quality and the quantity of the RNA were measured photometrically with a NanoDrop ND-1000 spectrophotometer (Thermo Fisher Scientific, Wilmington, USA) at 260, 280, and 230 nm.

2.7.2 DNase I treatment

3000 ng of total RNA in 16 µl of water was treated with 4 µl of 1:1 DNase I (Thermo Fisher, Vilnius, Lithuania, Cat. No. EN0521) and DNase buffer mix by incubating at 37 °C for 30 minutes. The activity of the DNase I was inhibited by adding 2 µl of 2.5 mM EDTA followed by 10 minutes of incubation at 65 °C.

2.7.3 First-strand cDNA synthesis

Table 2.10: Reaction mix for cDNA synthesis per sample.

Components	Stock concentration	Working concentration	Volume [µl]
Mix 1			
Oligo-dT_{25}	50 µM	2.5 µM	0.85
Random primers (N_9)	50 µM	4.5 µM	1.53
dNTPs	5 mM	500 µM	1.7
Mix 2			
First-strand buffer	5 X	1 X	3.4
DTT	0.1 M	5 mM	0.85
Reverse transcriptase	100 U μl^{-1}	50 U μl^{-1}	0.47

7.7 µl of the 1000 ng or 500 ng of the DNase I treated total RNA was used for cDNA synthesis using SuperScript™ III Reverse Transcriptase (Invitrogen/ Thermo Scientific, Carlsbad, USA, Cat. No. 18080093). The concentration of the RNA was adjusted by adding RNase-free water. 4.08 µl of mix 1 (Table 2.10) was added to each RNA sample and incubated at 65 °C. After cooling down, 4.67 µl of mix 2 (Table 2.10) was added to each sample and finally incubated for the first-strand cDNA synthesis at the temperature cycle as mentioned in Table 2.11 in a thermocycler.

Table 2.11: Temperature cycle for cDNA synthesis.

Temperature	Time
25 °C	5 minutes
50 °C	60 minutes
70 °C	15 minutes
16 °C	pause

The cDNA was stored at -20 °C until use.

2.7.4 Quantitative real-time PCR (qRT-PCR)

For qRT-PCR, the cDNA was diluted 1:10 or 1:5 if 1000 ng or 500 ng total RNA was used for cDNA synthesis, respectively. qRT-PCR was performed with CFX96^{TM} Real-Time Touch System (Bio-Rad Laboratories GmbH; Feldkirchen, Germany) with the reaction mix given in Table 2.12 and the PCR cycles in Table 2.13. 18 µl of this master mix including Immolase (Meridian Bioscience, Ohio, USA, Cat. No. BIO-21047) was added to 2 µl of the template cDNA or water (for negative control) of each sample in a single well of a 96-well plate. A dissociation curve was generated by the Bio-Rad CFX Manager after the PCR, which was checked to ensure amplification specificity. All primers used in this study are listed in Table 2.14. The expression of the gene of interest (GOI) was normalized against the reference genes *TRANSCRIPTION FACTOR IID (TFIID)* and *UBIQUITIN-CONJUGATING ENZYME 21 (UBC21)* or *ACTIN* according to (Vandesompele et al., 2002).

Table 2.12: Reaction mix for qRT-PCR per sample.

Components	Stock concentration	Final concentration	Volume [µL]
Buffer	10 X	1 X	2
$MgCl_2$	50 µM	2 µM	0.8
dNTP	5 mM	100 µM	0.4
SYBR Green I	10 X	0.1 X	0.2
Water	---	---	14.32
Immolase	5 U/µl	0.01 U/µl	0.04
Forward primer	50 µM	300 nM	0.12
Reverse primer	50 µM	300 nM	0.12

Table 2.13: Temperature cycle for qRT-PCR.

Step	Temperature	Time	
Heat inactivation of the Immolase Taq Polymerase	95 °C	15 minutes	
Denaturation	95 °C	5 seconds	
Annealing	55 °C	15 seconds	X 40
Elongation	72 °C	10 seconds	

Table 2.14: Sequence of primers used for qRT-PCR.

Gene	AGI number[1)]	Forward primer (5'-3')	Reverse Primer (5'-3')
ACT2	AT3G18780	CCGATCCAGACACTGTACTTCCTT	CCATTAGATCTTGTCTCTCTGCT
BAP1	AT3G61190	CCAGAGATTACGGCGCGTGTT	TACAGACCCCAAACCGGAACTCC
TFIID	AT1G17440	GAATCACGGCCAACAATC	ACTCTTAGCCAAGTAGTGCTCC
UBC21	AT5G25760	CTCTTAACTGCGACTCAGGGAATC	TGCCATTGAATTGAACCCTCTCAC

ZAT12	AT5G59820	CGCTTTGTCGTCTGGATTG	AGCAGCCCCACTCTCGTT
ELIP1	AT3G22840	GTTGGCGTTCACTGAGTTC	CACACAGTAGGCCTAACACAGA
LHCBI	AT1G29910.1	GTGACAATGGCTTGAACGAA	GGCTACAGAGTCGCAGGAAA
CHE	AT5G08330	GAAGACGACCACGAACCAC	ACCCTAAAACCCTAATCAAACAAG
CCA1	AT2G46830	TGAGGCGGATGCATCAGAAAG	AAGGCAATTCGACCCTCGTC
LHY	AT1G01060	CAACGAAACAGGTAAGTGGCGACA	TGCGTGGAAATGCCAAGGGT
TOC1	AT5G61380	TTGGTCACCGGCAGGAAATCC	ACTGACCCTTAACGCGGGGT

1) AGI, Arabidopsis Genome Initiative

2.8 Lesion quantification

Lesions were quantified in the 5-weeks-old 16 h PLP treated plants (Figure 3.6 A), during the day three to four hours after the stress-inducing night. From the total number of leaves (excluding leaves number 1 and 2, and cotyledons), the leaves that were limp or were only limp on the edges were counted as lesioned leaves. The percentage of the lesions was calculated by dividing the number of leaves with lesions by the total number of analyzed leaves.

2.9 Chlorophyll fluorometry (Fv/Fm ratio)

The quantum efficiency of the photosystem II (PSII) was measured as an indication of stress and cell death (Baker, 2008). The F_v/F_m ratio was measured in 5-weeks-old 16 h PLP treated plants, during the day four to five hours following the stress-inducing night (Figure 3.6 A). 8^{th}, 9^{th}, 10^{th}, and 11^{th} leaves were detached from a single plant and floated in a petri-dish with water with the abaxial side of the leaf facing the water. These were incubated in the dark for 20 minutes before the pulse-amplitude-modulated (PAM) measurement was performed by the chlorophyll fluorometer. Closed FluorCam (Photon Systems Instrument, Drásov, Czech Republic). The minimum fluorescence signal (F_0) was first recorded. A saturating pulse of 1500 µmol m^{-2} s^{-1} was given to induce the maximum fluorescence yield, Fm. The variable fluorescence was calculated as $Fv = Fm-F_0$. Therefore, the complete equation is $Fv / Fm = (Fm-F_0)/ Fm$.

2.10 DCMU treatment

4-weeks-old plants were treated with 3-(3,4-dichlophenyl)1,1-dimethylurea (DCMU) at time points shown in Figure 3.7. The plants were first sprayed with 0.2 % Tween® followed by spraying with 100 µM DCMU.

2.11 Carbohydrate quantification

2.11.1 Preparation of enzymes for a single reaction of starch and sugar quantification

The concentration of all enzymes and chemicals used for starch (2.11.2) and sugar quantification (2.11.3) were prepared as follows.

- 1 U Amyloglucosidase (AMG) and 2 U α-amylase (α-AMY) mix: 1 mg AMG (Sigma-Aldrich, Cat. No. 10113) was dissolved in 1 ml of 50 mM Na-acetate buffer (pH 4.75) to reach a concentration of 120 U ml^{-1}. 8.3 µl of this U ml^{-1} AMG was mixed with 0.2 µl of α-AMY (Roche, Cat No. 10102814001) and 41.5 µl of 50 mM Na-acetate buffer.
- 1.4 U Glucose-6-phosphate dehydrogenase (G6PDH) mix: 2 µl of the G6PDH suspension (Roche, Cat. No. 10127671001) was centrifuged at 14,000 *g* at 4 °C for 10 minutes. To G6PDH pellet 1 µl of 200 mM ATP (Roche, Cat. No. 10127523001) solution, 1 µl of 120 mM NADP (Roche, Cat. No. 10128040001) solution, and 138 µl of 100 mM imidazole buffer at pH 6.9 with HCl (containing 1.5 mM $MgCl_2$) was added. ATP and NADP solutions were also prepared with imidazole buffer as mentioned before.
- 1.2 U HK mix: 0.8 µl of the HK suspension (Roche, Cat. No. 11426362001) was centrifuged at 14,000 *g* at 4 °C for 10 minutes. 5 µl of the imidazole buffer was added to the pellet.
- 1.7 U PGI: 0.486 µl of PGI (Roche, Cat. No. 10128139001) was centrifuged similarly to HK and resuspended in the 5 µl of the 100 mM imidazole buffer.
- 125 U Invertase: 0.417 mg of invertase (Merck, Cat. No. I4504) was dissolved in 5 µl of the imidazole buffer.

2.11.2 Starch quantification

Starch quantification was performed according to Smith & Zeeman (2006) with slight modifications. Ca. 50 mg of leaf material was harvested as described in section 2.5. 775 µl of 0.2 M KOH was added to the grounded leaf material and vortexed. This was transferred to 1.5 ml-microcentrifuge screw-capped tubes (Sarstedt, Nümbrecht, Germany, Cat. No. 72.607.772 [tubes], 65.716 [caps]) and incubated at 95 °C for 1 h in a thermomixer (Eppendorf, Wesseling-Berzdorf, Germany) with continuous agitation. Following the incubation, the samples were cooled down to room temperature (RT), which required ca. 5-7 minutes, and centrifuged at 16,000 *g* for 10 minutes. 300 µl of the supernatant was transferred to a fresh 1.5 ml microcentrifuge tube. In order to acidify the sample to a pH between 5 and 6, 100 µl of 1 M of acetic acid was added to it. Next, in 1.5 mL-microcentrifuge screw-capped tubes, 50 µl of this neutralized starch solution was digested with 50 µl of an enzyme mix of 1 U AMG and 2 U α-AMY. For activation of α-AMY, this reaction mixture was incubated at 37 °C for 1 h, followed by overnight incubation at 55 °C for activation of AMG. This reaction was stopped by heat treatment of 95 °C for 5 minutes. This was centrifuged at 16,000 *g* for 10 minutes and 5 µl of the

supernatant and glucose standards (6, 4, 2, 0.4, 0.1 mM) mixed with 15 µl of water were used for enzymatic optical glucose determination assay. The sample and the standards were added to a 96-well plate in duplicates (20 µl sample/ standard in each well) and 140 µl of G6PDH-mix was added to each well to digest any Glu6P. A_{start} was measured at 340 nm wavelength using the Synergy™ 2 Multi-Detection Microplate Reader (Biotek®, Winooski, Vermont, USA) until a plateau was reached (ca. 5-7 minutes). To measure the amount of glucose in the samples, 5 µl HK mix was added and the absorbance was measured again at 340 nm until a second plateau was reached after ca. 40-50 minutes (A_{end}). The absorbance (ΔA) was determined by subtracting A_{start} from A_{end}. The concentration of the starch in µmol g^{-1} FW was calculated using the slope generated from the standard curve and multiplying with a dilution factor of 10.66 (calculated by accounting the dilution of the sample concentration at each step).

2.11.3 Sugar quantification

Sugar quantification was performed as described in Orzechowski et al. (2021) with a few modifications. 1 ml of 80 % ethanol was added to ca. 50 mg grounded leaf tissue (see section 2.5) and vortexed. This was transferred to heat resistant 1.5 mL-microcentrifuge screw-capped tubes and heated at 80 °C for 30 min with shaking in the thermomixer. The samples were cooled down and centrifuged for 10 min at 4 °C at 16,000 g. 20 µl of the sample supernatant or glucose standard (6, 4, 2, 0.4, 0.1 mM in 80 % ethanol) was added to a 96-well plate in duplicates and mixed with 140 µl G6PDH mix. The absorbance was measured at 340 nm wavelength until a plateau was reached (ca. 5 minutes). To this 5 µl of HK mix was added and the absorbance was measured at 340 nm until a plateau was reached (ca. 30-40 minutes) to measure the concentration of glucose. 5 µl of PGI mix was added in each well and the absorbance was measured at the same wavelength as above until a plateau was reached (ca. 20 minutes) to measure the concentration of fructose. 5 µl of 125 U invertase was added until a plateau was attained (ca. 20 minutes) to measure the concentration of sucrose. The equation obtained from the glucose standard curve from the change in absorbance after the addition of HK was used for calculation. The change in absorbance after the addition of each enzyme was applied in this equation for calculating the concentration of glucose, fructose, and sucrose in µmol g^{-1}.

2.12 Statistical analysis

Statistical analysis was performed with SAS® OnDemand for Academics (https://welcome.oda.sas.com/home). Normality and homoscedasticity were tested by a Shapiro-Wilk

test and Levene's test. For comparison between multiple groups, ANOVA followed by Tukey post-hoc test was performed. If assumptions were not met, log transformations were done followed by ANOVA. In case a non-parametric test had to be used, a Kruskal-Wallis-Test followed by a Wilcoxon rank-sum test was done. For comparison between two groups, Student´s t-test was performed and if a non-parametric test had to be done, the Wilcoxon rank-sum test was performed.

2.13 Databases and software

The databases and software used in this study are listed in Table 2.15.

Table 2.15: Databases and software used in this study.

Name	Company, reference, or internet link	Purpose of use
NCBI	The National Center for Biotechnology Information (http://www.ncbi.nlm.nih.gov/)	Literature (PubMed)
Excel	Microsoft Office	Calculations and graph design
PowerPoint	Microsoft Office	Figure preparation
Photoshop	Adobe®	Figure design
Inkscape	The Inkscape Project	Figure design
NEBcutter	New England BioLabs Inc. (http://tools.neb.com/NEcutter2/)	Search for restriction sites
Bio-Rad CFX Manager	Bio-Rad®	Quantitative real time-PCR (qRT- PCR)
NASC	The European Arabidopsis Stock Centre (http://arabidopsis.info/)	Ordering Arabidopsis seeds
1001 Genomes	1001 Genome Consortium 2016 (https://1001genomes.org/index.html)	Information on Arabidopsis ecotypes
TAIR	Phoenix Bioinformatics (https://www.arabidopsis.org/)	Arabidopsis gene information search
SIGnAL T-DNA Express	Salk Institute Genomic Analysis Laboratory, Alonso et al., 2003 (http://signal.salk.edu/cgi-bin/tdnaexpress)	Searching for Arabidopsis T-DNA insertion mutants
SIGnAL T-DNA Primer Design	Salk Institute Genomic Analysis Laboratory (http://signal.salk.edu/tdnaprimers.2.html)	Primer design for T-DNA insertional mutants
Gen5™ Reader Control and Data Analysis Software B	Biotek®, Winooski, Vermont, U.S.A.	Controlling of Synergy™ 2 Multi-Detection Microplate Reader for ROS, starch, and soluble sugar measurements
GenoCapture	Synoptics Ltd., Cambridge, UK	Agarose gel documentation
FlourCam 7	Photon Systems Instruments	Chlorophyll fluorescence (Fv/Fm) measurement

3 Results

3.1 Light intensity of at least 50 µmol m^{-2} s^{-1} is necessary for the induction of photoperiod stress

In order to investigate whether there is a certain threshold light intensity required for the induction of photoperiod stress, the effect of different light intensities was investigated in WT plants. 4-weeks-old SD-grown WT (grown at 120 µmol m^{-2} s^{-1}) plants were subjected to 4 h PLP at light intensities ranging from 30 µmol m^{-2} s^{-1} to 120 µmol m^{-2} s^{-1} (Figure 3.1 A). No significant ROS induction could be observed at light intensities of 40 µmol m^{-2} s^{-1} and below. A significant 2.5-fold increase in ROS production was first observed at light intensities of 50-70 µmol m^{-2} s^{-1} (Figure 3.1 B, Supplementary Figure 1 A). A ~12-fold increase in the expression of stress marker genes *ZAT12* and *BAP1* was also observed first at light intensities of 50-70 µmol m^{-2} s^{-1} (Figure 3.1 C-D, Supplementary Figure 1 B-C). The expression of *EARLY LIGHT INDUCING PROTEIN 1* (*ELIP1)* was ~50 % higher at 50-70 µmol m^{-2} s^{-1} than at 40 µmol m^{-2} s^{-1} light intensity (Figure 3.1 F, Supplementary Figure 1 D). On the other hand, at light intensity of 70 µmol m^{-2} s^{-1}, *LHCB1* expression tended to be lower by ~50 % compared to its expression at a lower light intensity of 40 µmol m^{-2} s^{-1} (Supplementary Figure 1 E) The change in expression of *ELIP1* and *LHCB1* in response to photoperiod stress treatment at different light intensities was more gradual than observed for the stress marker gene expression.

Similarly, a threshold light intensity of 70 µmol m^{-2} s^{-1} during the PLP was required for the induction of the photoperiod stress symptoms in the photoperiod stress sensitive *ahk2 ahk3* mutants (Figure 3.2). A 9-fold increase in ROS equivalents and a 10- and 9-fold increase in the expression of stress marker genes *ZAT12* and *BAP1* was seen for the PLP under 70 µmol m^{-2} s^{-1} compared to PLP under 40 µmol m^{-2} s^{-1} in *ahk2 ahk3* (Figure 3.2 A-C). Similar to WT (Figure 3.1), in *ahk2 ahk3*, with increasing light intensity, the *ELIP1* expression increased, while the expression of *LHCB1* decreased (Figure 3.2 D-E).

Therefore, it can be concluded from these experiments that a threshold light intensity of 50-70 µmol m^{-2} s^{-1} during the PLP is necessary for the induction of photoperiod stress for plants grown in SD at a light intensity of 120 µmol m^{-2} s^{-1}.

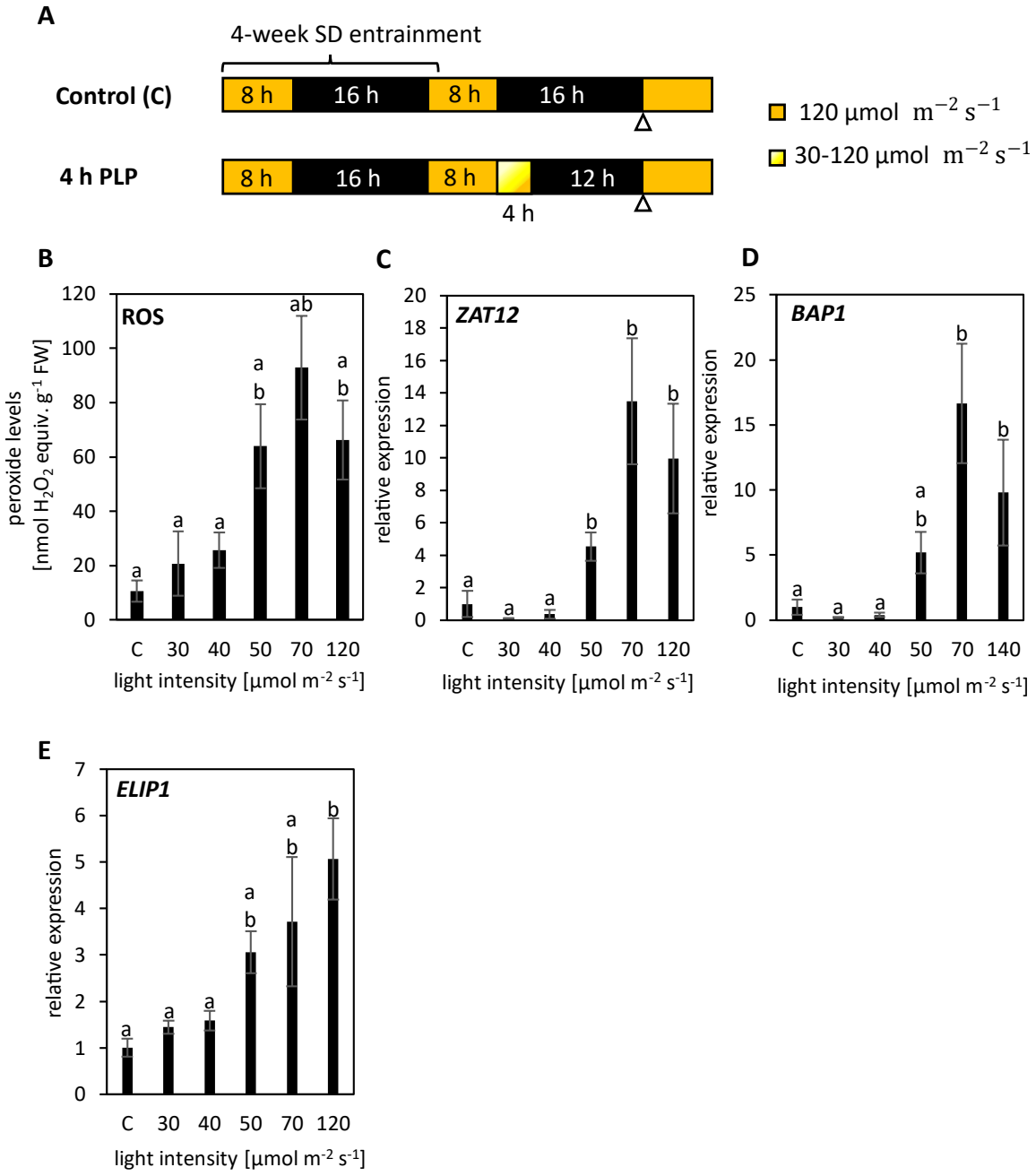

Figure 3.1: The strength of the photoperiod stress symptoms is light intensity-dependent in WT. (A) Schematic representation of the experimental setup. 4-weeks-old SD grown WT plants were treated with 4 h of PLP with light intensities ranging from 30-120 µmol m^{-2} s^{-1}. Leaf samples were harvested at time points indicated by the arrow heads. (B) ROS equivalents. Error bars represent SE (n ≥ 3). (C-E) Relative expression of *ZAT12*, *BAP1*, and *ELIP1*. Error bars represent SE (n ≥ 3). Expression was normalized to WT control which was set to 1. Letters indicate significant differences between groups as determined by ANOVA followed by a Tukey post-hoc test ($p < 0.05$). C, control; PLP, prolonged light period. Two similar experiments were performed with a light intensity range of 10-120 µmol m^{-2} s^{-1}, but the stress response at 50 µmol m^{-2} s^{-1} was not measured in these experiments and 70 µmol m^{-2} s^{-1} was the minimum light intensity at which photoperiod stress was induced (Supplementary Figure 1).

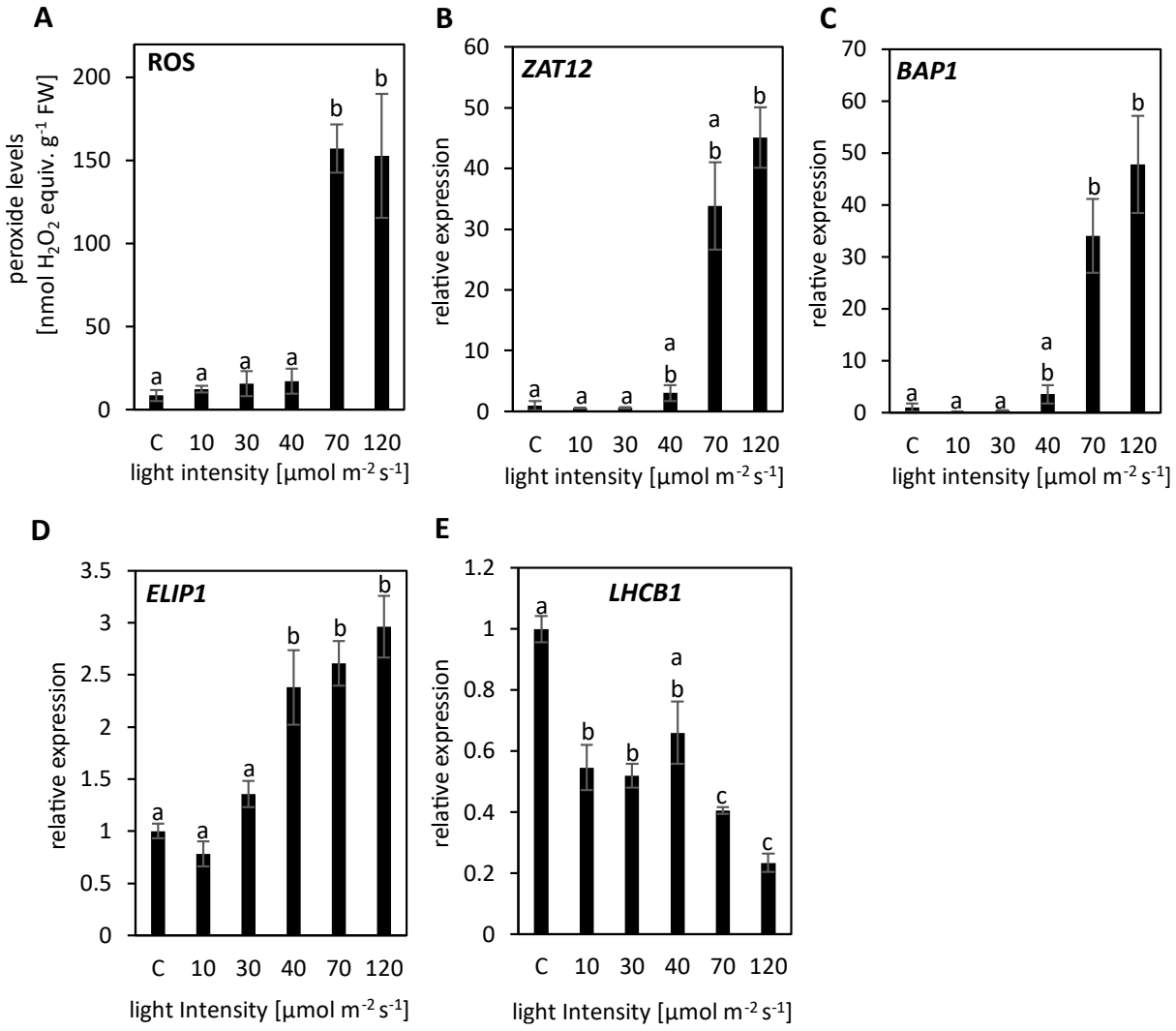

Figure 3.2: The strength of the photoperiod stress symptoms is light intensity-dependent in *ahk2 ahk3* mutants. 4-weeks-old SD grown *ahk2 ahk3* plants were treated with 4 h of PLP with light intensities between 10-120 µmol m^{-2} s^{-1} (see experimental setup in Figure 3.1 A). (A) ROS equivalents. Error bars represent SE (n ≥ 3). (B-E) Relative expression of *ZAT12, BAP1, ELIP1* and *LHCB1*. Error bars represent SE (n ≥ 3). Expression was normalized to WT control which was set to 1. Letters indicate significant differences between groups as determined by ANOVA followed by Tukey post-hoc test ($p < 0.05$). C, control; PLP, prolonged light period. This experiment was conducted two times with similar results.

Next, it was tested if a higher light intensity than 120 µmol m^{-2} s^{-1} during the PLP would lead to stronger photoperiod stress symptoms. The expression of stress marker genes *ZAT12* and *BAP1,* and *ELIP1* were similar under the PLP with light intensities of 120 µmol m^{-2} s^{-1} and 300 µmol m^{-2} s^{-1} (Figure 3.3 A-C). However, in plants subjected to PLP at 300 µmol m^{-2} s^{-1}, the expression of *LHCB1* was lower compared to those subjected to PLP at 120 µmol m^{-2} s^{-1} (Figure 3.3 D). Together these results indicate that a light intensity of 300 µmol m^{-2} s^{-1} during the PLP did not lead to stronger photoperiod stress in WT plants (Figure 3.3).

Since light intensity in the range that causes a change in photoperiod stress is sensed by chloroplasts, these results hint towards the possible involvement of chloroplasts in photoperiod stress.

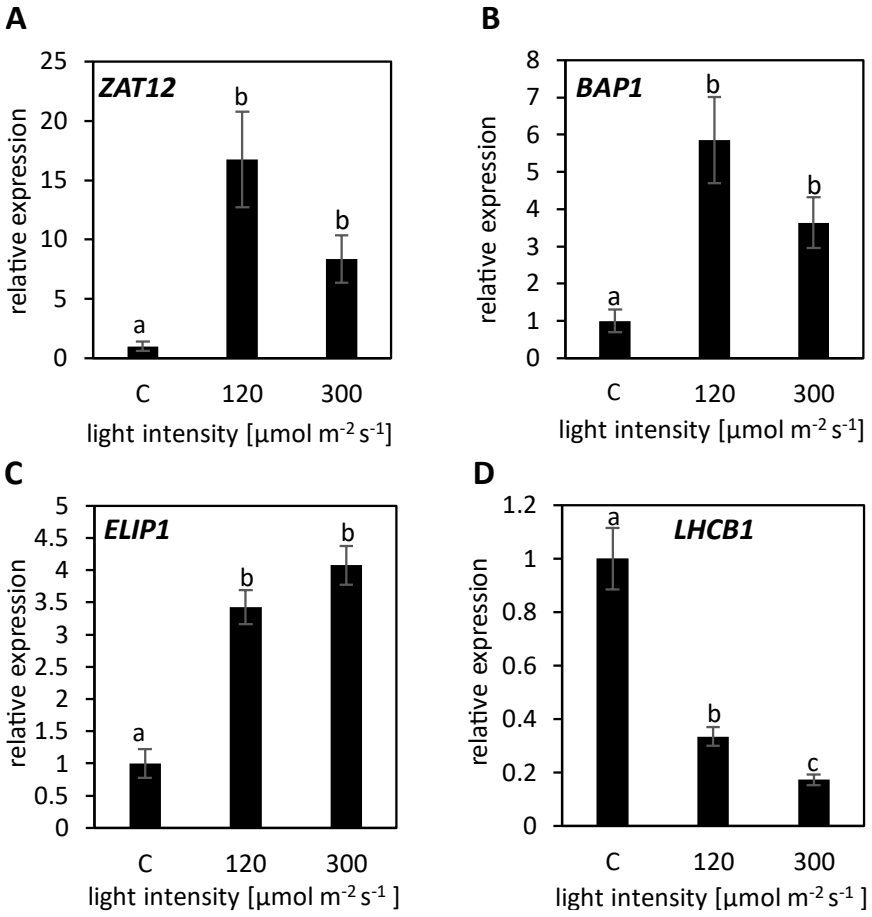

Figure 3.3: A light intensity higher than 120 µmol m^{-2} s^{-1} does not cause an increase in photoperiod stress symptoms. The experimental setup is displayed in Figure 3.1 A. 4-weeks-old SD grown WT plants were treated with a 4 h PLP with a light intensity of 120 µmol m^{-2} s^{-1} or 300 µmol m^{-2} s^{-1}. (A - D) Relative expression of *ZAT12*, *BAP1*, *ELIP1* and *LHCB1*. Error bars represent SE (n ≥ 3). Expression was normalized relative to WT control which was set to 1. Letters represent significant differences between groups as determined by ANOVA followed by a Tukey post-hoc test ($p < 0.05$). C, control; PLP, prolonged light period. This experiment was conducted two times with similar results.

3.2 A prolonged light period followed by dark is requisite for photoperiod stress

Since a threshold light intensity of 50-70 µmol m^{-2} s^{-1} is required to cause photoperiod stress (see section 3.1), it was examined whether only a change in light intensity without a PLP would cause photoperiod stress. 2-weeks-old WT and *ahk2 ahk3* plants gown in SD at a light intensity of 120 µmol m^{-2} s^{-1} (control), were transferred to SD with 100 µmol m^{-2} s^{-1} (LL) for 2 weeks or stayed under control conditions. After two weeks under 100 µmol m^{-2} s^{-1}, these 4-weeks-old plants were transferred to 300 µmol m^{-2} s^{-1} during the light period of the SD conditions for 1 day (LH) or stayed at 100 µmol m^{-2} s^{-1} (Figure 3.4 A). Plants were not exposed to any PLP in this experiment. In both WT and *ahk2 ahk3* plants, no increase in ROS equivalents and upregulation of stress marker genes *ZAT12* and *BAP1* could be observed when they were transferred from 100 µmol m^{-2} s^{-1} to 300 µmol m^{-2} s^{-1} in the

absence of a PLP (Figure 3.4 B-D). Also, the expression of *ELIP1* did not change upon the transfer of plants from a lower light intensity of 100 µmol m^{-2} s^{-1} to a higher light intensity of 300 µmol m^{-2} s^{-1} (Figure 3.4 E). *LHCB1* expression increased by 1.5- and 1.9-fold in WT and *ahk2 ahk3*, which were moved from 120 µmol m^{-2} s^{-1} to a lower light intensity of 100 µmol m^{-2} s^{-1}. However, no significant change in *LHCB1* expression was observed when the plants were moved from a lower light intensity of 100 µmol m^{-2} s^{-1} to a higher light intensity of 300 µmol m^{-2} s^{-1} without a PLP (Figure 3.4 F). This result shows that only a change in light intensity without PLP does not lead to photoperiod stress.

Since PLP is important for photoperiod stress, it was investigated whether continuous light (CL) would lead to photoperiod stress in the absence of a regular light and dark rhythm. 3-weeks-old WT plants were grown under SD (control) or in CL without any dark period. After 3 weeks, the plants grown in CL were given 16 h D (CL + dark) or continued to grow under CL (Figure 3.5 A). ROS equivalents did not show a spike under either of the conditions and were similar to the control (SD) (Figure 3.5 B). Therefore, only continuous light and a single dark period in the absence of the regular light-dark rhythm do not lead to photoperiod stress.

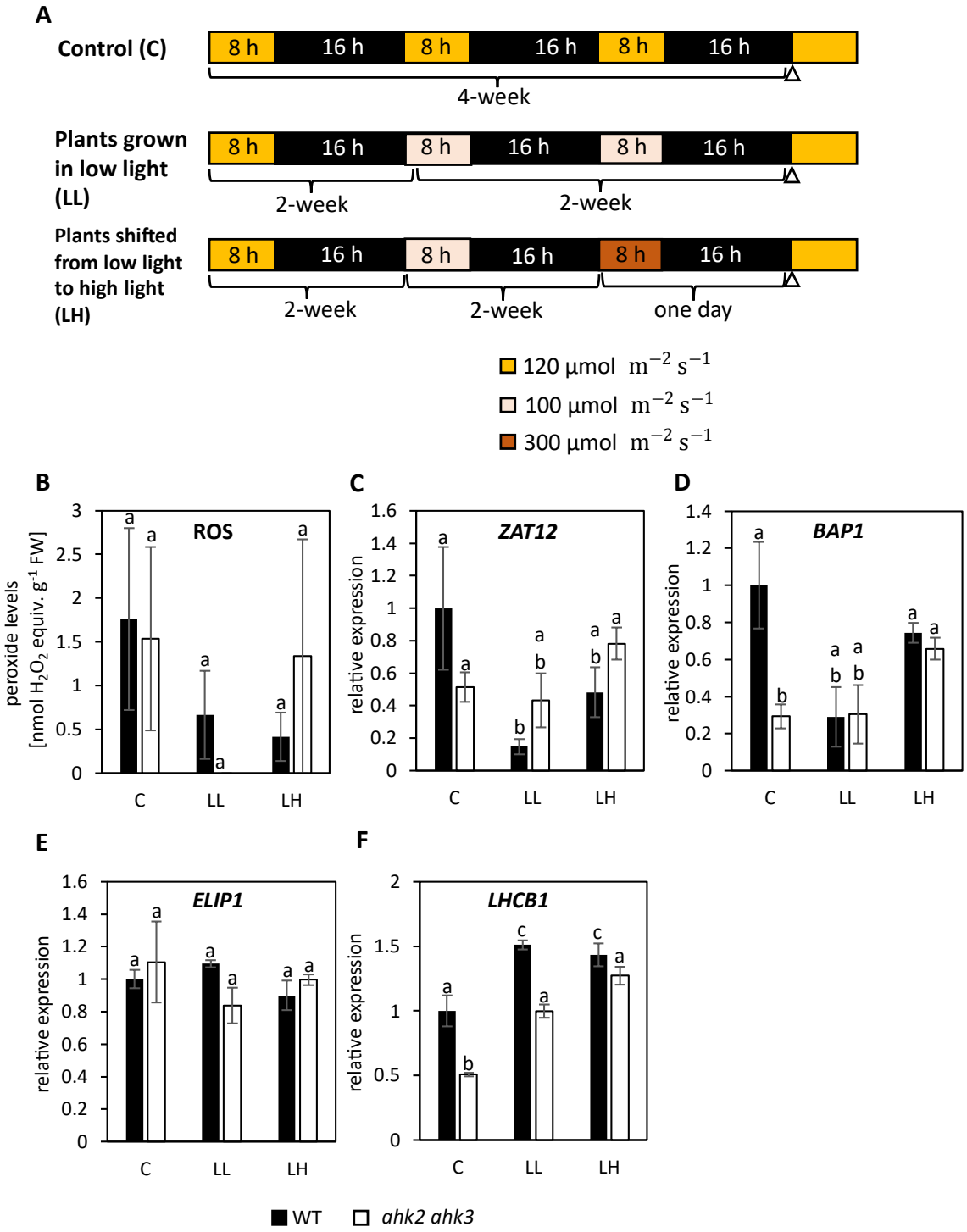

Figure 3.4: Change in the light intensity without prolongation of the light period does not cause photoperiod stress. (A) Schematic representation of the experimental setup. WT and *ahk2 ahk3* plants were grown under SD for 2 weeks at 120 µmol m^{-2} s^{-1} (control, C). These plants were transferred to SD with a lower light intensity of 100 µmol m^{-2} s^{-1} for the next 2 weeks (LL) or stayed under control conditions. After 2 weeks under SD with 100 µmol m^{-2} s^{-1}, these 4-weeks-old plants were shifted to SD with a high light intensity of 300 µmol m^{-2} s^{-1} for 1 day (LH) or stayed at 100 µmol m^{-2} s^{-1}. Leaf samples were harvested at time points indicated by the arrow heads. (B) ROS equivalents. Error bars represent SE (n ≥ 3). (C-F) Relative expression of *ZAT12, BAP1, ELIP1* and *LHCB1*. Error bars represent SE (n ≥ 3). Expression was normalized relative to WT control samples which were set to 1. Letters indicate significant differences between groups as determined by ANOVA followed by a Tukey post-hoc test (C, E, F) and Kruskal-Wallis test followed by Wilcoxon-rank test (D), ($p < 0.05$). This experiment was conducted once.

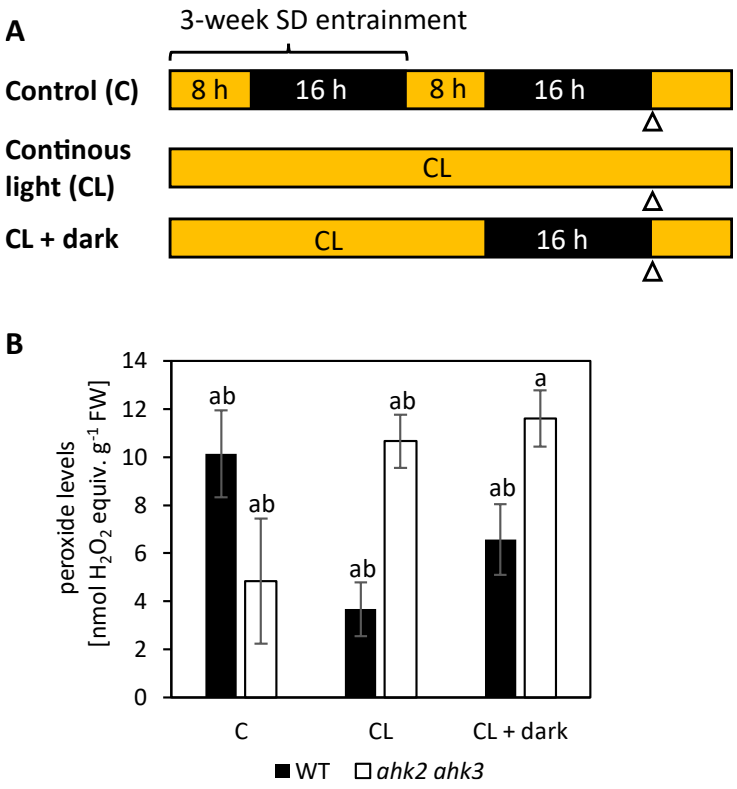

Figure 3.5: Continuous light without regular dark and light cycle does not lead to photoperiod stress. (A) Schematic representation of the experimental setup. WT and *ahk2 ahk3* plants were grown for 3 weeks under SD (control) or continuous light (CL). The plants grown under CL were given a single dark period of 16 h (CL + dark) or continued to grow under CL. Leaf samples were harvested at time points indicated by the arrow heads. (B) ROS equivalents. Error bars represent SE ($n \geq 3$). Letters indicate significant difference between groups as determined by ANOVA followed by a Tukey post-hoc test ($p < 0.05$). C, control; CL, continuous light. This experiment was conducted once.

3.3 Relevance of retrograde signaling in photoperiod stress

In order to further understand the role of chloroplast in sensing photoperiod stress, the role of retrograde signaling was investigated. The response of the retrograde signaling mutants *gun1, gun4, gun5*, *gun6* (*FC1* overexpressor), *rcd1*, and *glk1 glk2* to photoperiod stress caused by a 16 h PLP was examined (Figure 3.6 A).

Amongst the *gun* mutants, *gun1* displayed similar ROS levels and *ZAT12* and *BAP1* expression as WT in response to photoperiod stress, and thus has no role in sensing or responding to photoperiod stress (Figure 3.6 B-D). However, *gun4* and *gun5* showed ROS accumulation ~40 % and ~31 % of WT in response to photoperiod stress (Figure 3.6 B), although under control conditions, *gun4* and *gun5* have higher ROS levels compared to the WT (Supplementary Figure 6A). *gun4* and *gun5* also showed *ZAT12* induction ~3 % and ~10 % of WT and *BAP1* induction ~12 % of WT upon photoperiod stress (Figure 3.6 C-D). Thus, *gun4* and *gun5* are less responsive to photoperiod stress and could be involved in instigating photoperiod stress response. In contrast, after photoperiod stress treatment

gun6 had 2.5-fold higher ROS levels and 1.8-fold higher *BAP1* expression (Figure 3.6B, D), but a similar *ZAT12* expression as WT (Figure 3.6 D).

Although under control conditions *rcd1* had higher ROS levels than WT (Supplementary Figure 6 A), it accumulated ROS ~3 % of WT and displayed *ZAT12* and *BAP1* expression ~2 % and ~3 % of WT in response to photoperiod stress (Figure 3.6 B-D). *glk1 glk2* also displayed lower sensitivity to photoperiod stress compared to WT (Figure 3.6 B-D)

Under photoperiod stress, *chlorophyll a/b binding protein 1* (*CAB1)* expression is downregulated (Frank et al., 2020). But *gun1, gun4, gun5, glk1 glk2,* and *rcd1* maintained a similar *LHCB1* expression under control and in response to photoperiod stress treatment (Figure 3.6 E). In contrast, in *gun6* the *LHCB1* expression decreased strongly after photoperiod stress (Figure 3.6 E).

Since *gun4, gun5, rcd1,* and *glk1 glk2* mutants, which are deficient in retrograde signaling, are nearly insensitive to photoperiod stress, it can be concluded that retrograde signaling plays a role in the response to photoperiod stress, corroborating the role of chloroplasts in this kind of stress.

In order to find additional evidence for the role of chloroplasts in photoperiod stress, 4-weeks-old SD-grown WT plants were exposed to a 4 h PLP or continued to grow under SD conditions. Both the non-PLP exposed and 4 h PLP exposed plants were treated with either only Tween® or DCMU (see section 2.10) 4 h before the respective dark period began. Sampling was performed before dark to see if there is any direct effect of the Tween® or DCMU without the PLP and after dark to observe their impact on photoperiod stress symptoms. Non-PLP exposed plants treated with Tween® were considered as control, and the sampling point before dark in these plants was set as 1 for normalization of stress marker gene expression (see Figure 3.7 A for experimental setup). It was observed that PLP exposed DCMU treated plants showed 1.84- and 1.73-fold lower expression of *ZAT12* and *BAP1* after the stress-inducing night compared to PLP exposed Tween® treated plants. (Figure 3.7 B-C) However, *LHCB1* expression decreased in both DCMU and Tween® treated plants in response to photoperiod stress to a similar extent compared to their non-PLP exposed counterparts (Figure 3.7 D). Since the stress marker gene expression is lower in PLP exposed plants that have been treated with DCMU compared to those treated with Tween®, it can be inferred that DCMU treatment decreases the photoperiod stress symptoms. Since DCMU inhibits photosynthesis by blocking the electron flow from photosystem II to plastoquinone, this result possibly adds to the evidence for the role of chloroplasts in photoperiod stress.

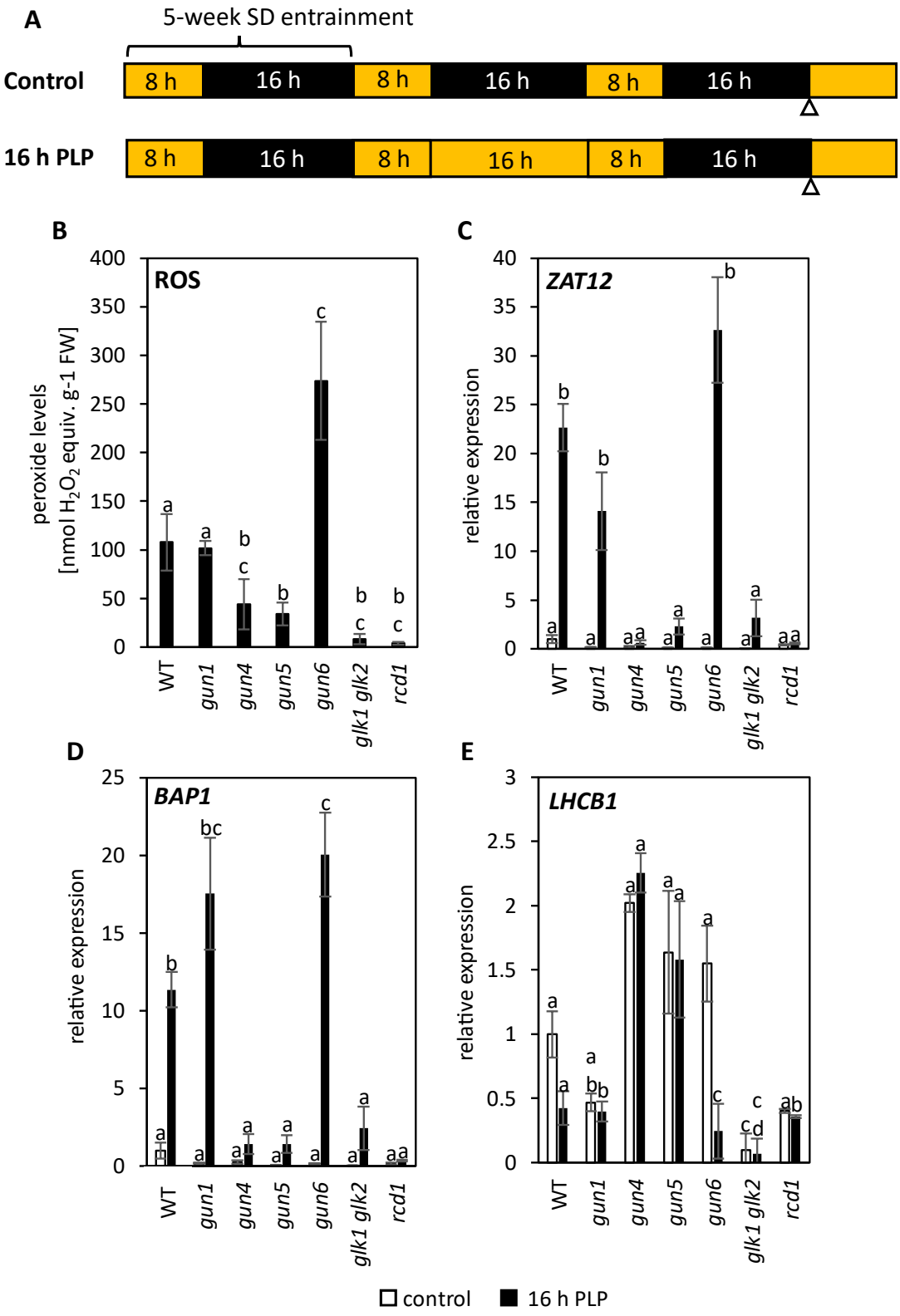

Figure 3.6: The photoperiod stress response in retrograde signaling mutants. (A) Schematic representation of the photoperiod stress treatment. 5-weeks-old SD-grown plants were treated with a 16 h PLP. Leaf samples were harvested at time points indicated by arrow heads. (B) ROS equivalents. Error bars represent SE (n ≥ 3). (C-E) Relative expression of *ZAT12, BAP1* and *LHCB1*. Error bars represent SE (n ≥ 3). Expression was normalized relative to WT control which was set to 1. Letters indicate significant difference between groups as determined by Kruskal-Wallis-Test followed by a Wilcoxon rank-sum test ($p < 0.05$). PLP, prolonged light period. This experiment was conducted two times with similar results.

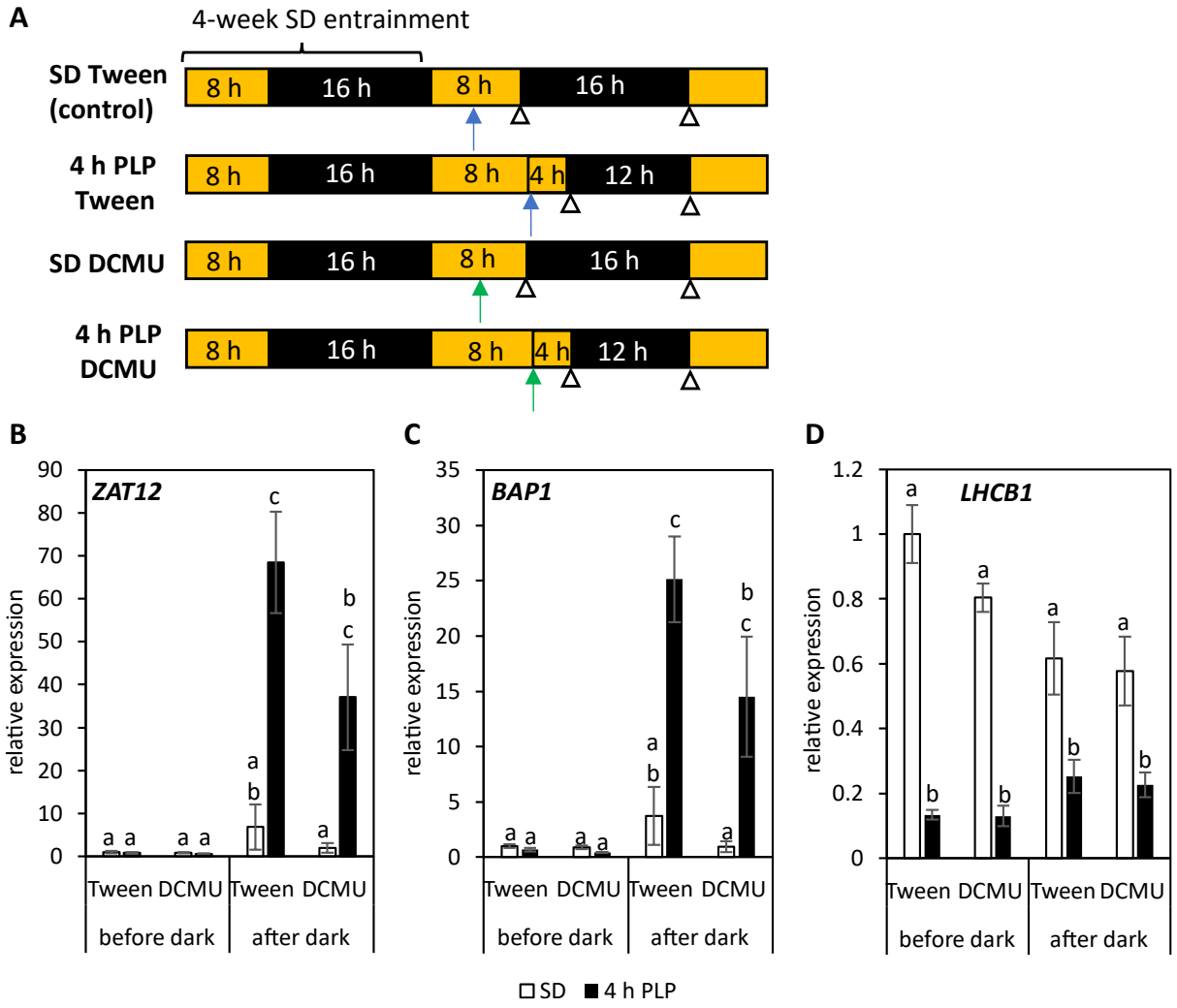

Figure 3.7: DCMU treatment reduces the strength of photoperiod stress symptoms. (A) Schematic representation of the experimental setup. 4-weeks-old SD-grown WT plants were treated with Tween® (control) or DCMU (see section 2.10) 4 h before the respective dark. These plants were exposed to 4 h PLP or continued to grow under SD. Blue and green arrows represent time points of Tween® and DCMU treatment. (B-D) Relative expression of *ZAT12, BAP1* and *LHCB1*. Error bars represent SE (n ≥ 3). Expression was normalized relative to WT control samples (non-PLP exposed Tween® before dark) which were set to 1. Letters indicate significant difference between groups as determined by Kruskal-Wallis-Test followed by a Wilcoxon rank-sum test ($p < 0.05$). C, control; PLP, prolonged light period. This experiment was conducted two times with similar results.

3.4 Starch accumulation in response to photoperiod stress

Transient starch in the form of starch granules is synthesized during the light phase in the chloroplast and hydrolyzed to release sugars in the dark (Ribeiro et al., 2022). Nitschke (2015) observed that the starch content was higher in photoperiod-stressed plants at the end of the night following the PLP compared to the control. To observe and confirm the impact of the photoperiod stress on starch and sugar accumulation, 5-weeks-old SD-grown WT plants were exposed to photoperiod stress caused by a 16 h PLP, and leaves were sampled at the time points indicated in Figure 3.8 A. The starch level in photoperiod stressed plants was much higher during the day following the PLP and at the end of the

following night compared to the control plants (Figure 3.8 B). Amongst the sugars, the level of glucose was ~9-fold higher than the control at the end of the night following PLP (time point 4) (Figure 3.8 C). Although the level of fructose and sucrose was ~2-fold and ~7-fold higher compared to their respective controls at time point 3, that is the end of the PLP; at the end of the following night, their levels were comparable to the control (Figure 3.8 D-E). The absolute values of sugars under control conditions in this analysis are higher than those in the previously published studies, but the diel pattern is similar (Lu et al., 2005). The difference in absolute values could be due to some differences in the sugar measurement method and used equipment for the same.

Since starch accumulation was so noticeably high during the photoperiod stress treatment, we wondered if starch accumulation plays a role in photoperiod stress. For this purpose, starch synthesis mutants *adg1, adg2, pgm,* and the starch accumulation mutant *sex1* (Zeeman et al., 2007a) were tested under 16 h PLP stress conditions (Figure 3.9). Starch biosynthesis mutants *adg1* and *pgm* accumulated only minute amounts of ROS, which was in the range ~1 % of WT in response to photoperiod stress inducing conditions (Figure 3.9 A). The *ZAT12* and *BAP1* expression in *adg1* was ~3 % and ~15 % of that in WT, while in *pgm*, their expression was ~9 % and 25 % of WT (Figure 3.9 B-C). However, *adg2* showed similar peroxide levels and *ZAT12* and *BAP1* expression as WT (Figure 3.9 A-C). Starch accumulation mutant *sex1* also showed lower photoperiod stress symptoms compared to WT (Figure 3.9 A-C).

These results indicate that the starch breakdown and glucose accumulation could impact the strength of the photoperiod stress symptoms.

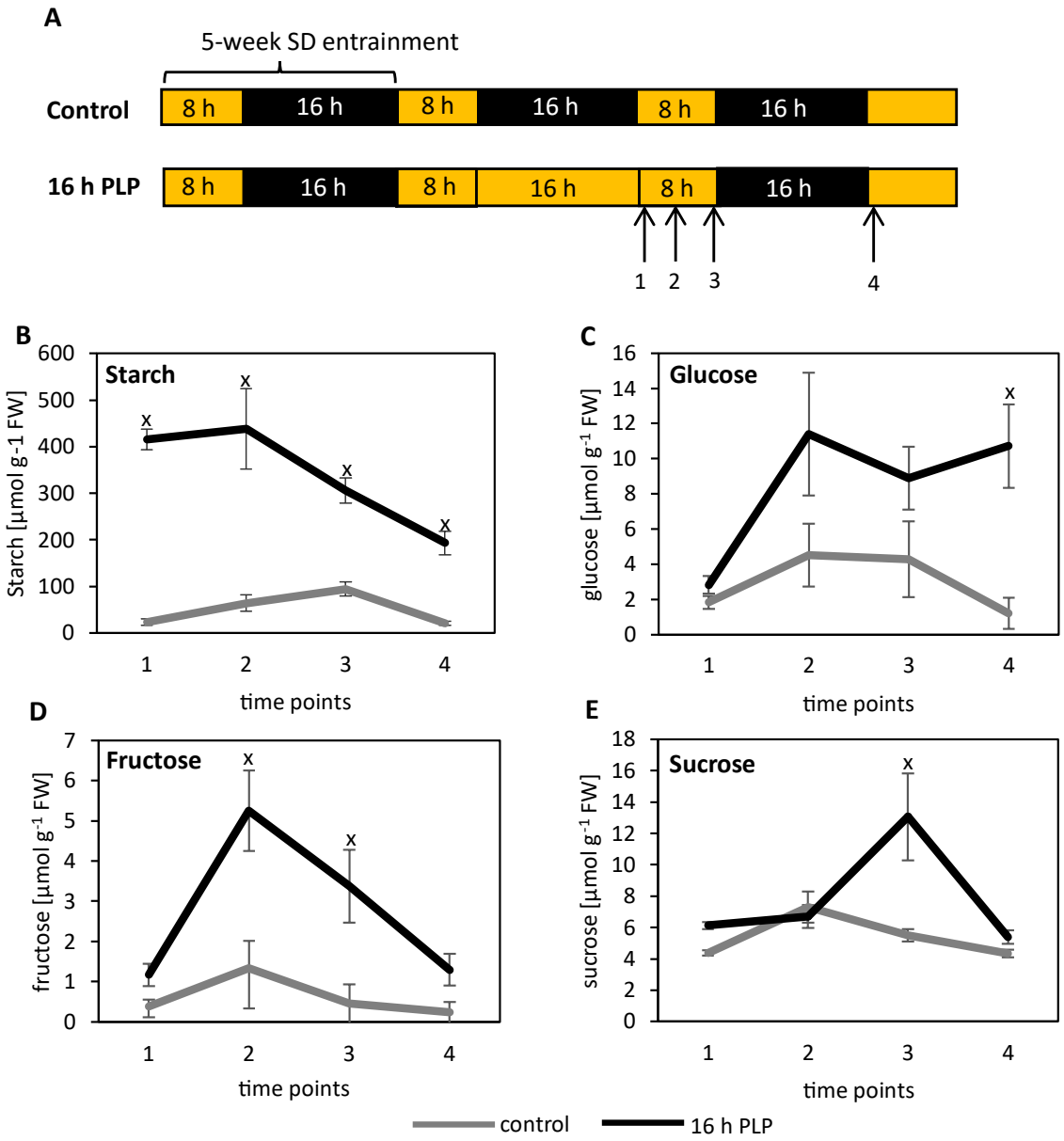

Figure 3.8: Starch and soluble sugar accumulation in response to photoperiod stress. (A) Schematic representation of the photoperiod stress treatment. 5-weeks-old SD-grown plants were treated with 16 h PLP. Leaf samples were harvested at time points indicated by arrow heads. (B) Starch content. (C) Glucose content. (D) Fructose content. (E) Sucrose content. Error bars represent SE ($n \geq 3$). Statistical significance is denoted by (x), highlighting differences between the control group and plants treated with 16 h PLP at the corresponding time point. This determination was made through a Student's t-test ($p < 0.05$). PLP, prolonged light period. This experiment was conducted once.

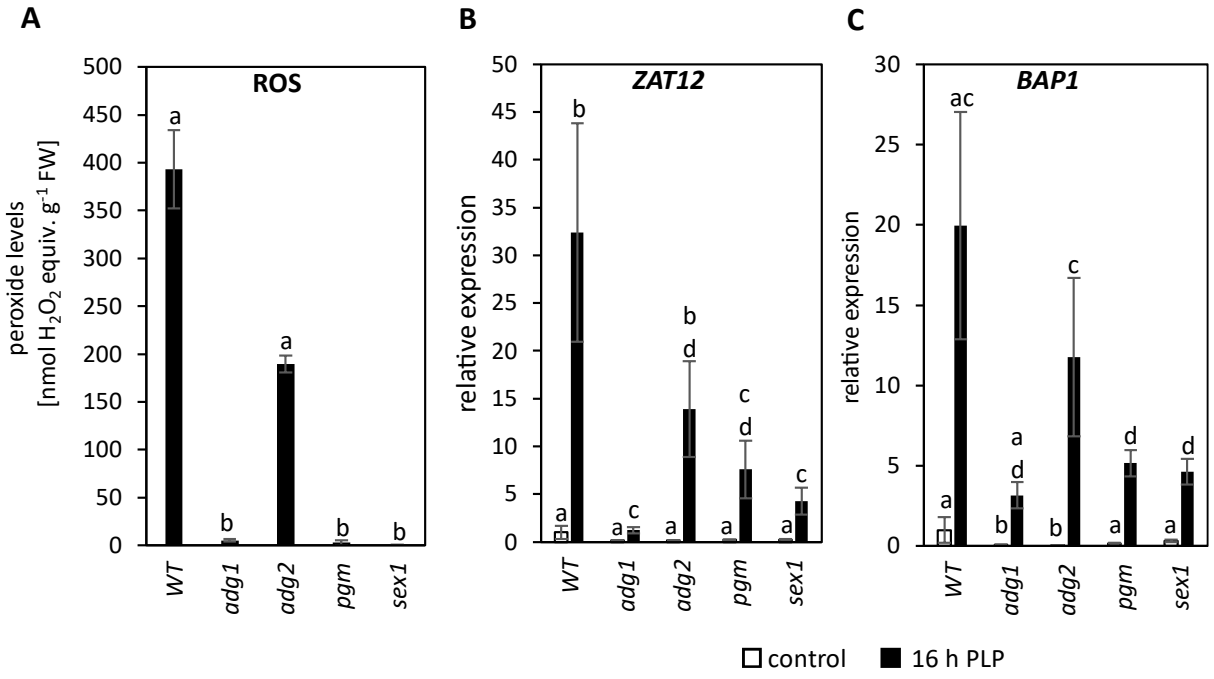

Figure 3.9: The photoperiod stress response in starch metabolism mutants. 5-weeks-old SD-grown plants were treated with 16 h PLP. Experimental setup can be found in Figure 3.6 A. (A) ROS equivalents. Error bars represent SE (n ≥ 3). (B-C) Relative expression of *ZAT12* and *BAP1*. Error bars represent SE (n ≥ 3). Expression was normalized relative to WT control samples which were set to 1. Letters indicate significant difference between groups as determined by Kruskal-Wallis-Test followed by a Wilcoxon rank-sum test ($p < 0.05$). PLP, prolonged light period. This experiment was conducted two times with similar results.

3.5 Effect of monochromatic wavelengths of light and their ratio on photoperiod stress

Next, in order to find out whether light of different wavelength would cause differences in the photoperiod stress response, we investigated the impact of light of specific wavelengths on the photoperiod stress response in WT and also in photoreceptor mutants *phyB* and *cry2*. As described in more detail in section 3.6, *phyB,* and *cry2,* the red and blue light photoreceptor mutants show a lower photoperiod stress response under white light compared to the WT (Figure 3.14, Figure 3.15). 4-weeks-old SD-grown plants were exposed to an 8 h PLP. The light treatment during the PLP consisted of white light (positive control treatment) or monochromatic red or blue light (Figure 3.10 A). The PAR of the monochromatic lights was comparable to that of the white light in this experiment (see Table 2.9). Red light provoked a photoperiod stress response in WT plants as strong as white light according to the peroxide levels (Figure 3.10 B). However, *ZAT12* and *BAP1* expression reached only half the level induced by white light (Figure 3.10 C-D). In response to blue light, the peroxide levels in WT were similar to those under control conditions indicating a low stress level (Figure 3.10 B). However, the expression of *ZAT12* and *BAP1* in response to blue light was induced as robustly as in response to red light (Figure 3.10 C-D).

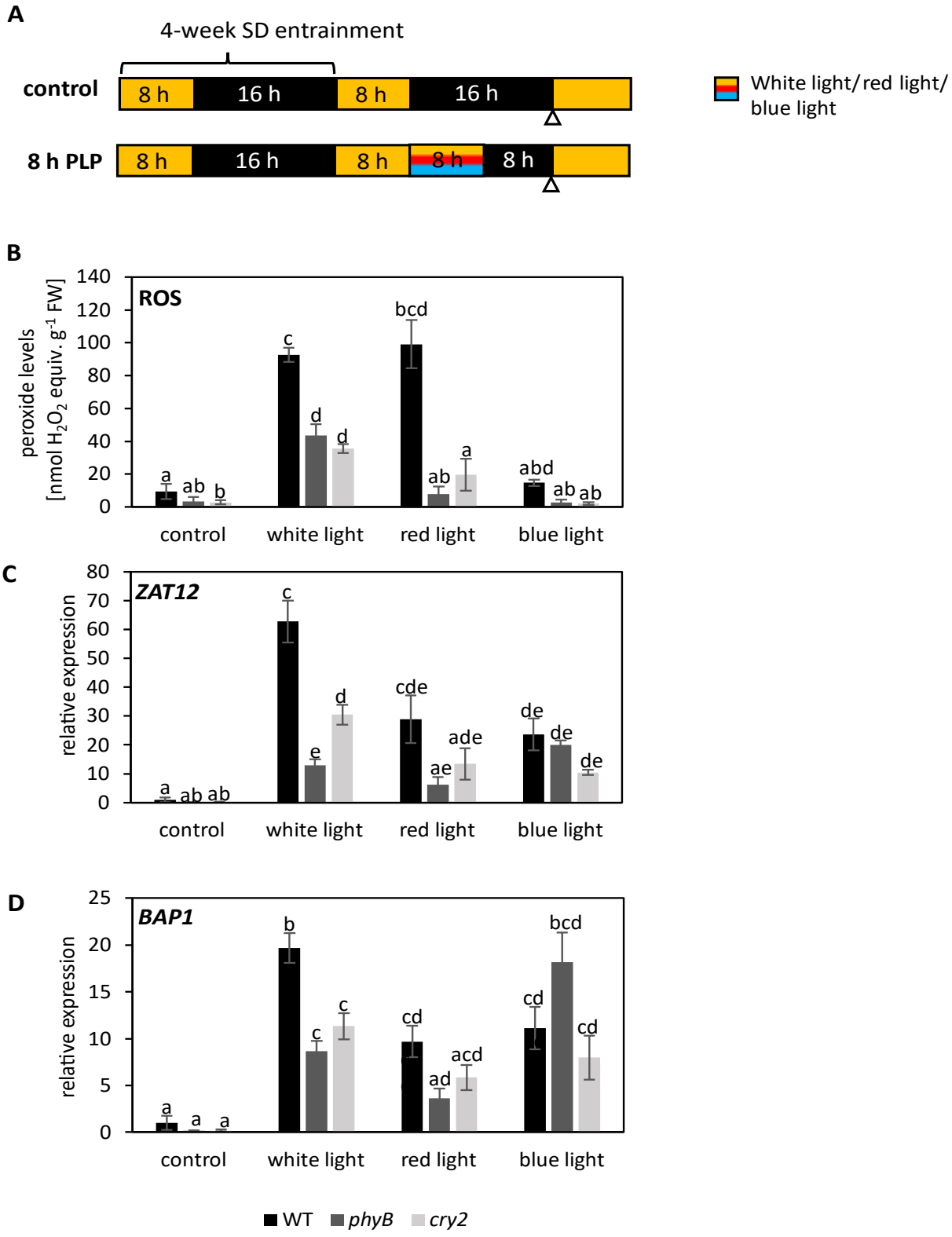

Figure 3.10: Effect of monochromatic light on photoperiod stress. (A) Schematic representation of the photoperiod stress treatment. 4-weeks-old SD-grown WT, *cry2,* and *phyB* plants were treated with an 8 h PLP under white light, and monochromatic red or blue light (see Table 2.9 for light intensities). Leaf samples were harvested at time points indicated by the arrow heads. (B) ROS equivalents. Error bars represent SE ($n \geq 3$). (C-D) Relative expression of *ZAT12* and *BAP1*. Error bars represent SE ($n \geq 3$). Expression was normalized relative to WT control samples which were set to 1. Letters represent significant difference between groups as determined by Kruskal-Wallis-Test followed by Wilcoxon rank-sum test ($p < 0.05$). PLP, prolonged light period. This experiment was conducted three times with similar results.

The photoreceptor mutants *phyB* and *cry2* showed a reduced response to photoperiod stress under white light in comparison to WT (Figure 3.10 B-D). Under red light, *phyB,* a red light photoreceptor mutant, showed as expected, the lowest level of photoperiod stress in comparison to WT and *cry2*. (Figure 3.10 B-D).

Under blue light, peroxide production was low in WT and the mutants, with the lowest levels found in the latter (Figure 3.10 B). *ZAT12* and *BAP1* expression in WT, *phyB*, and *cry2* were similar, with a spike in *BAP1* expression in *phyB* mutants under blue light (Figures 3.10 C-D).

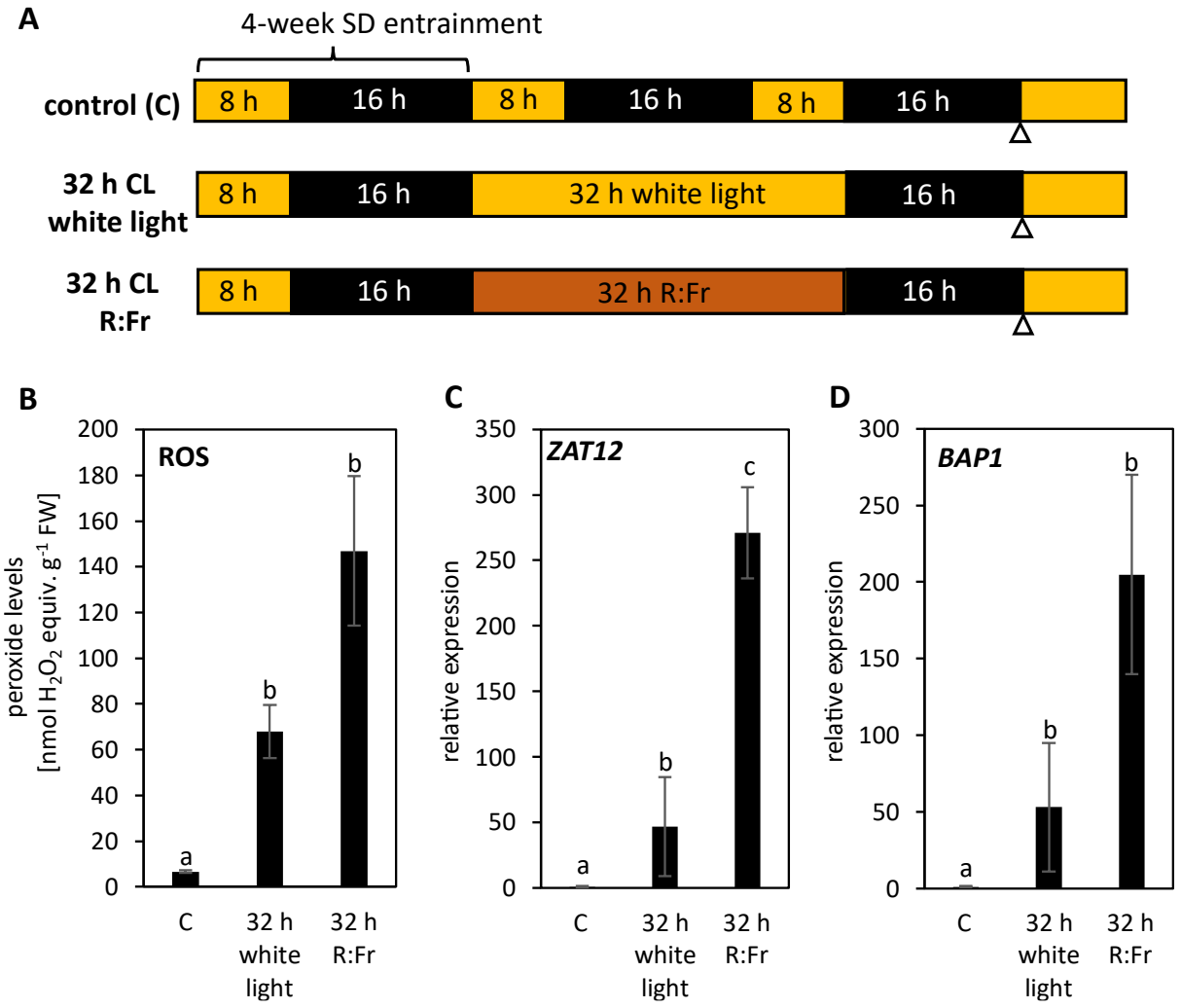

Figure 3.11: Effect of 32 CL with 1:1 R:Fr on photoperiod stress. (A) Schematic representation of photoperiod stress treatment. 4-weeks-old SD-grown WT plants were treated with 32 h continuous white light or 1:1 of monochromatic Red:Far-red (R:Fr) light (see Table 2.9 for light intensities). Leaf samples were harvested at time points indicated by arrow heads. (B) ROS equivalents. Error bars represent SE (n ≥ 3). (C-D) Relative expression of *ZAT12* and *BAP1*. Error bars represent SE (n ≥ 3). Expression was normalized relative to WT control samples which were set to 1. Letters indicate significant differences between groups as determined by Kruskal-Wallis test followed by a Wilcoxon rank-sum test ($p < 0.05$). CL, continuous light This experiment was conducted two times with similar results.

To sum up, although red light induced a stronger response to photoperiod stress than blue light as measured by peroxide levels, according to *ZAT12* and *BAP1* expression, both monochromatic red and blue light induced similar levels of photoperiod stress which is less than the photoperiod stress induced by white light. Therefore, from this experiment, it can be concluded that both monochromatic red and blue light can cause photoperiod stress.

Next, the effect of 1:1 ratio of monochromatic Red:Far-red (R:Fr) light and a 1:2:1 ratio of monochromatic Blue:Red:Far-red (B:R:Fr) light on photoperiod stress response was tested (Figure 3.11, 3.12). 4-weeks-old SD-grown plants were treated with a 32 h CL under white light (positive control treatment) or 1:1 R:Fr or 1:2:1 B:R:Fr (Figure 3.11, Figure 3.12). 1:1 R:Fr led to both higher peroxide levels (by 2.8-fold), and *ZAT12* and *BAP1* expression (by 3.9- and 5.8-fold) than white light (Figure 3.11 B-D). On the other hand, 1:2:1 B:R:Fr led to a similar peroxide level and *ZAT12* and *BAP1* expression as white light (Figure 3.12 A-C). These results indicate that R:FR is a strong inducer of photoperiod stress and that a prolonged light treatment with a composition of B:R:FR of 1:2:1 resembles the white light treatment. 1:2:1 B:R:Fr is similar to the ratio of blue, red, and far-red light in the white light of the climate chamber used (Table 2.9), which would explain their similar effects on photoperiod stress.

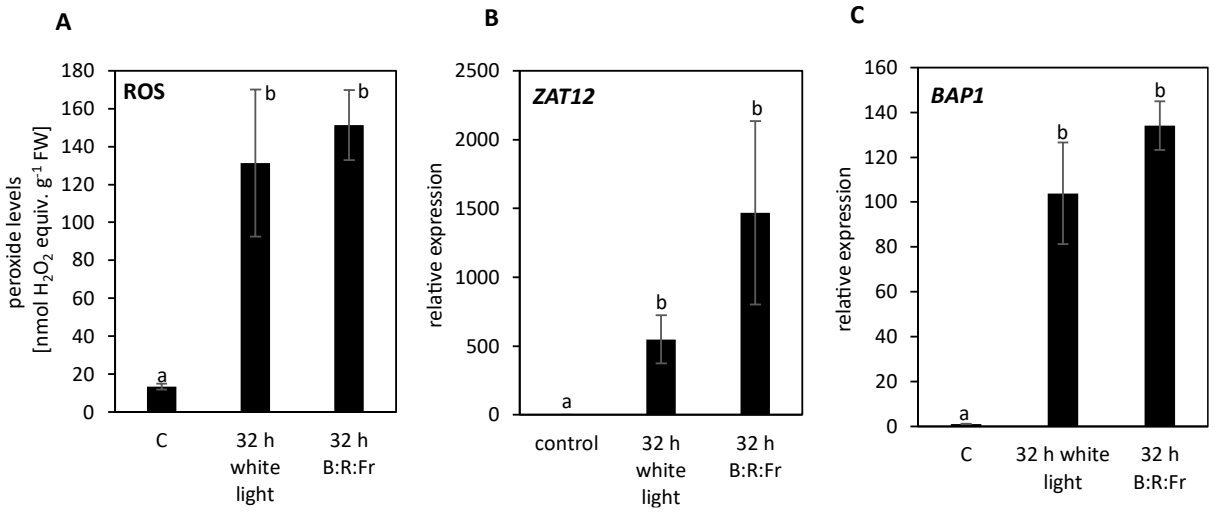

Figure 3.12: Effect of 32 h CL with 1:2:1 B:R:Fr on photoperiod stress. The experimental setup can be found in Figure 3.11 A. 4-weeks-old SD-grown WT plants were treated with 32 h continuous white light or 1:2:1 of monochromatic Blue:Red:Far-red (B:R:Fr) light. (A) ROS equivalents. Error bars represent SE ($n \geq 3$). (B-C) Relative expression of *ZAT12* and *BAP1*. Error bars represent SE ($n \geq 3$). Expression was normalized relative to WT control samples which were set to 1. Letters indicate significant difference between groups as determined by ANOVA followed by Tukey post-hoc test ($p < 0.05$). (A) was conducted twice with similar results and (B-C) was conducted once.

In addition to the above-mentioned wavelength combinations, the effect of shade light conditions on the occurrence of photoperiod stress was also investigated. A higher ratio of far-red light in addition to white light was supplied during the 16 h of CL (see Table 2.9 for light conditions, Figure 3.13 A for experimental setup). It was observed that shade conditions did not lead to photoperiod stress symptoms as the peroxide levels under shade and control were similar and consequently much lower than those under white light (Figure 3.13).

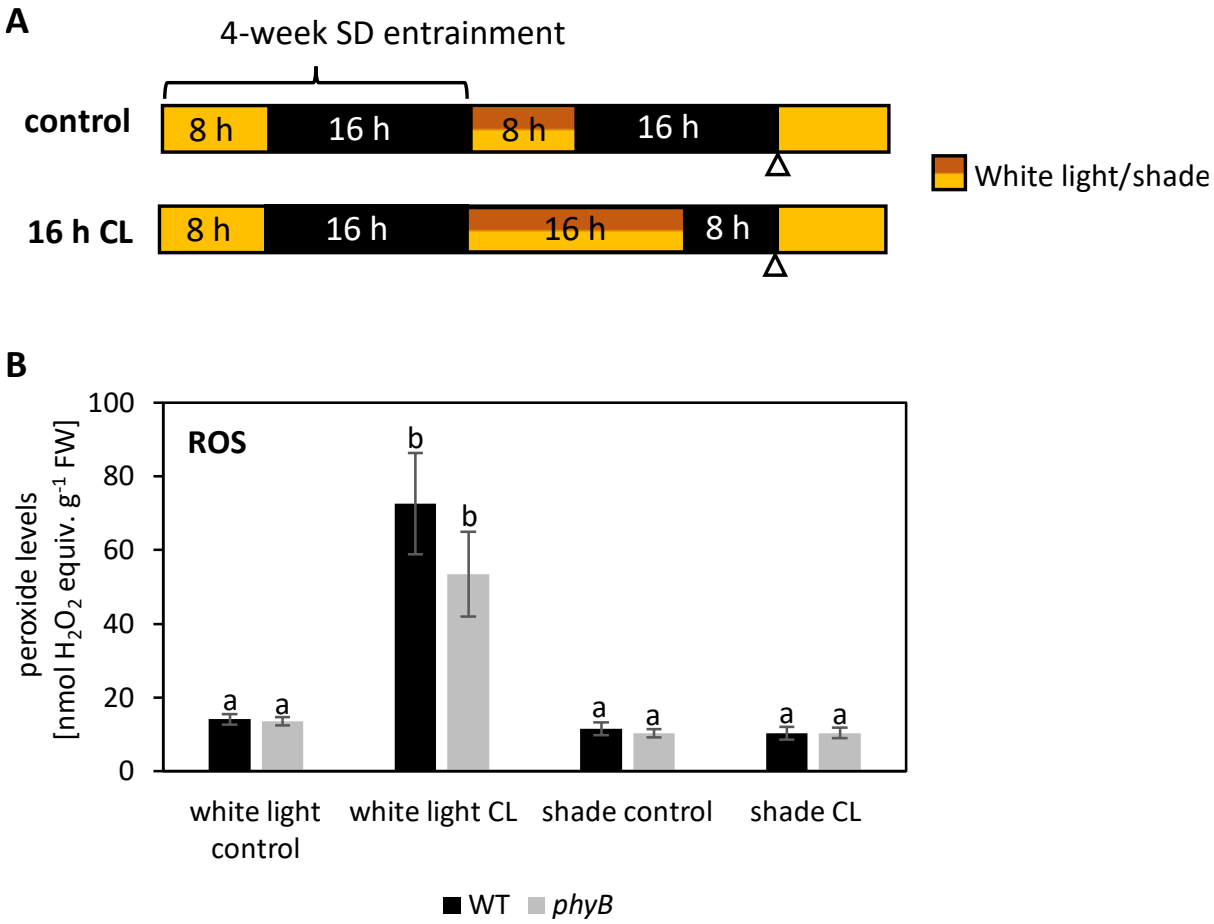

Figure 3.13: The effect of shade on photoperiod stress. (A) 4-weeks-old SD-grown plants were treated with 16 h of continuous white light or shade (see Table 2.9). Leaf samples were harvested at time points indicated by arrow heads. (B) ROS equivalents. Error bars represent SE (n ≥ 3). Letters represent significant difference between groups as determined by Kruskal-Wallis-Test followed by Wilcoxon rank-sum test ($p < 0.05$). CL, continuous light. This experiment was conducted once.

3.6 Effect of photoperiod stress in photoreceptor mutants

In order to investigate the role of photoreceptors in sensing photoperiod stress, the response of photoreceptor mutants to photoperiod stress was studied. Red and far-red light receptor mutants *phyA, phyB, phyA phyB* (phytochromes – Figure 3.14, Supplementary Figure 2); blue light receptor mutants *cry1, cry2, cry1 cry2* (cryptochromes – Figure 3.15, Supplementary Figure 3), *phot1, phot2,*

phot1 phot2 (phototropins – Figure 3.16), *ztl* (zeitlupe – Figure 3.17); and UV-B receptor mutant *uvr8* (Figure 3.18) were exposed to strong photoperiod stress (16 h PLP) (experimental setup in Figure 3.6 A). Additionally, in order to further investigate whether the mutation of the photoreceptors would alter the strong photoperiod stress response of *ahk2 ahk3* (CK receptor mutant), *phyA, phyB, cry1, cry2,* and *uvr8* mutations were introgressed into this photoperiod stress-sensitive background.

phyA mutation altered the photoperiod stress sensitivity of neither WT nor *ahk2 ahk3* in terms of peroxide level and stress marker gene expression (Figure 3.14 A-C). Lesion formation and quantum efficiency of *phyA* were also similar to WT, but that of *phyA ahk2 ahk3* was intermediate between WT and *ahk2 ahk3* (Figure 3.14 D-E). Additionally, *phyA phyB* double mutants showed peroxide levels similar to WT in response to photoperiod stress (Supplementary Figure 2). *phyA phyB* mutant displayed growth defects and had to be germinated and cultivated for 3 weeks in LD. Perhaps these general growth defects contributed to the photoperiod stress sensitivity of *phyA phyB* double mutants. In *phyB,* peroxide levels were ~10.3 % (Figure 3.14 A), and expression of *ZAT12* and *BAP1,* ~13.7 % and ~23.5 % (Figure 3.14 B-C) of that in WT in response to photoperiod stress treatment. From these results, it can be inferred that *phyB* has lower photoperiod stress sensitivity than WT and could thus be involved in photoperiod stress response. The difference between the response of *phyB* and WT to photoperiod stress, however, was not so clearly visible in lesion formation and quantum efficiency, that were measured during the day following the PLP (Figure 3.14 D-E). Also, *phyB ahk2 ahk3* showed a photoperiod stress sensitivity as high as *ahk2 ahk3* (Figure 3.14 A-C).

Peroxide levels and relative expression of stress marker genes in *cry1* were similar to WT. In accordance, the introgression of *cry1* mutation into *ahk2 ahk3* did not alter the photoperiod stress level of the photoperiod-sensitive background (Figure 3.15 A-C). On the other hand*, cry2* and *cry2 ahk2 ahk3* mutants showed strongly reduced photoperiod stressed symptoms (Figure 3.15 A-C). Peroxide levels in *cry2* and *cry2 ahk2 ahk3* were ~12 % and ~25 % (Figure 3.15 A), *ZAT12* expression ~10 % and ~25 % and *BAP1* expression ~16 % and ~40 % of that in WT in response to photoperiod stress treatment (Figure 3.15 B-C). At the phenotypic level, *cry1* and *cry2* developed a higher and a similar number of lesions as WT respectively (Figure 3.15 D). Both *cry1* and *cry2* had similar quantum efficiency as WT after the photoperiod stress treatment (Figure 3.15 E).

cry1 cry2 mutant also showed lower photoperiod stress symptoms in terms of peroxide levels and stress marker gene expression compared to WT (Supplementary Figure 3 A-C). However, the number of lesions and quantum efficiency were similar to WT (Supplementary Figure 3 D-E). Together these results depict an important role for CRY2 in photoperiod stress response.

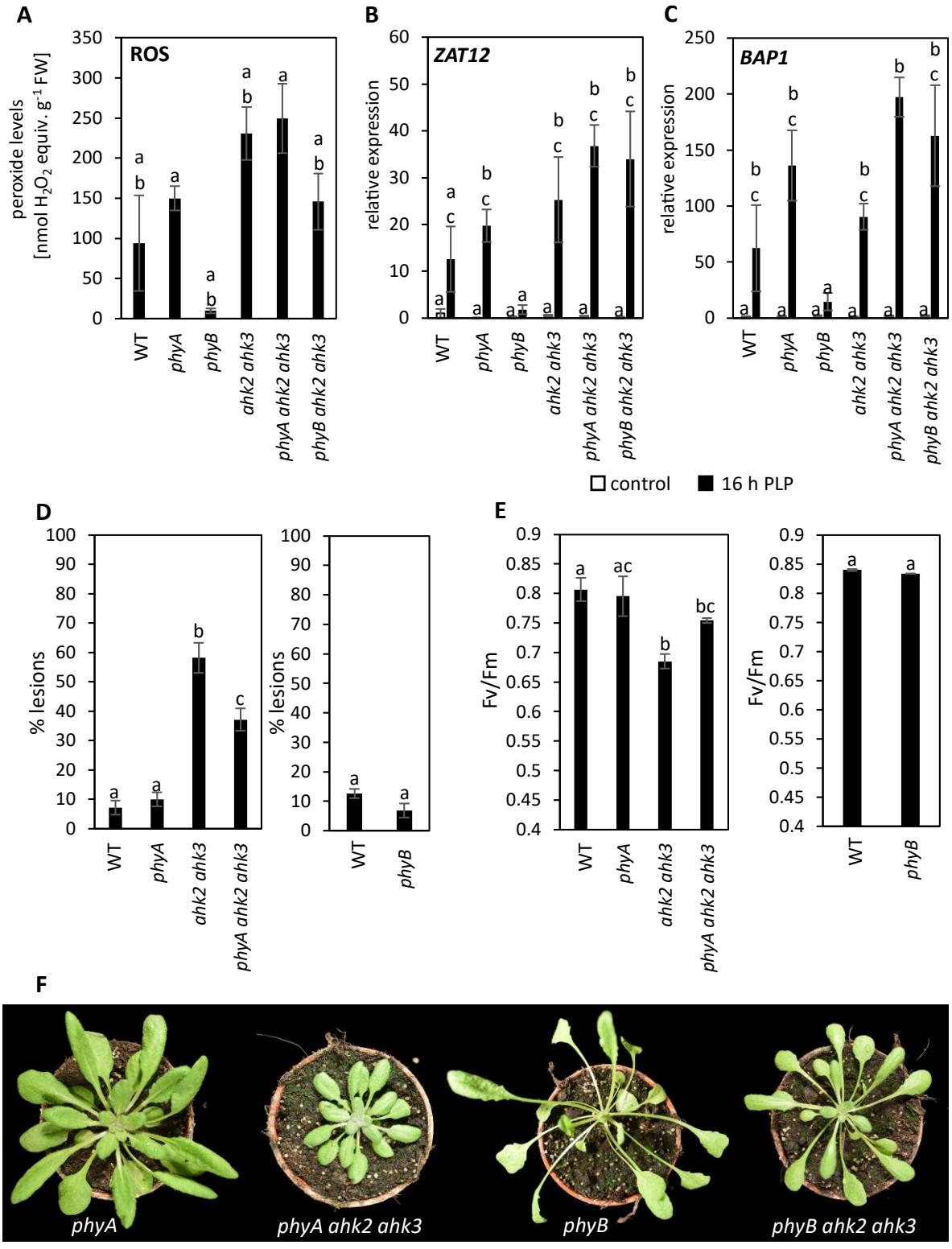

Figure 3.14: The photoperiod stress response in phytochrome mutants. The experimental setup can be found in Figure 3.6 A. 5-weeks-old SD-grown plants were treated with a 16 h PLP. (A) ROS equivalents. Error bars represent SE (n ≥ 3). (B-C) Relative expression of *ZAT12* and *BAP1*. Error bars represent SE (n ≥ 3). Expression was normalized relative to WT control samples which were set to 1. (D) Lesion formation after photoperiod stress (n ≥ 10). (E) Quantum efficiency (Fv/Fm) after photoperiod stress (n ≥ 8). (F) Pictures of photoperiod-stressed *phyA*, *phyA ahk2 ahk3*, *phyB*, and *phyB ahk2 ahk3* mutants taken during the day following the stress-inducing night. Letters represent significant differences between groups as determined by Kruskal-Wallis-Test followed by Wilcoxon rank-sum test ($p < 0.05$). PLP, prolonged light period. This experiment was conducted two times with similar results.

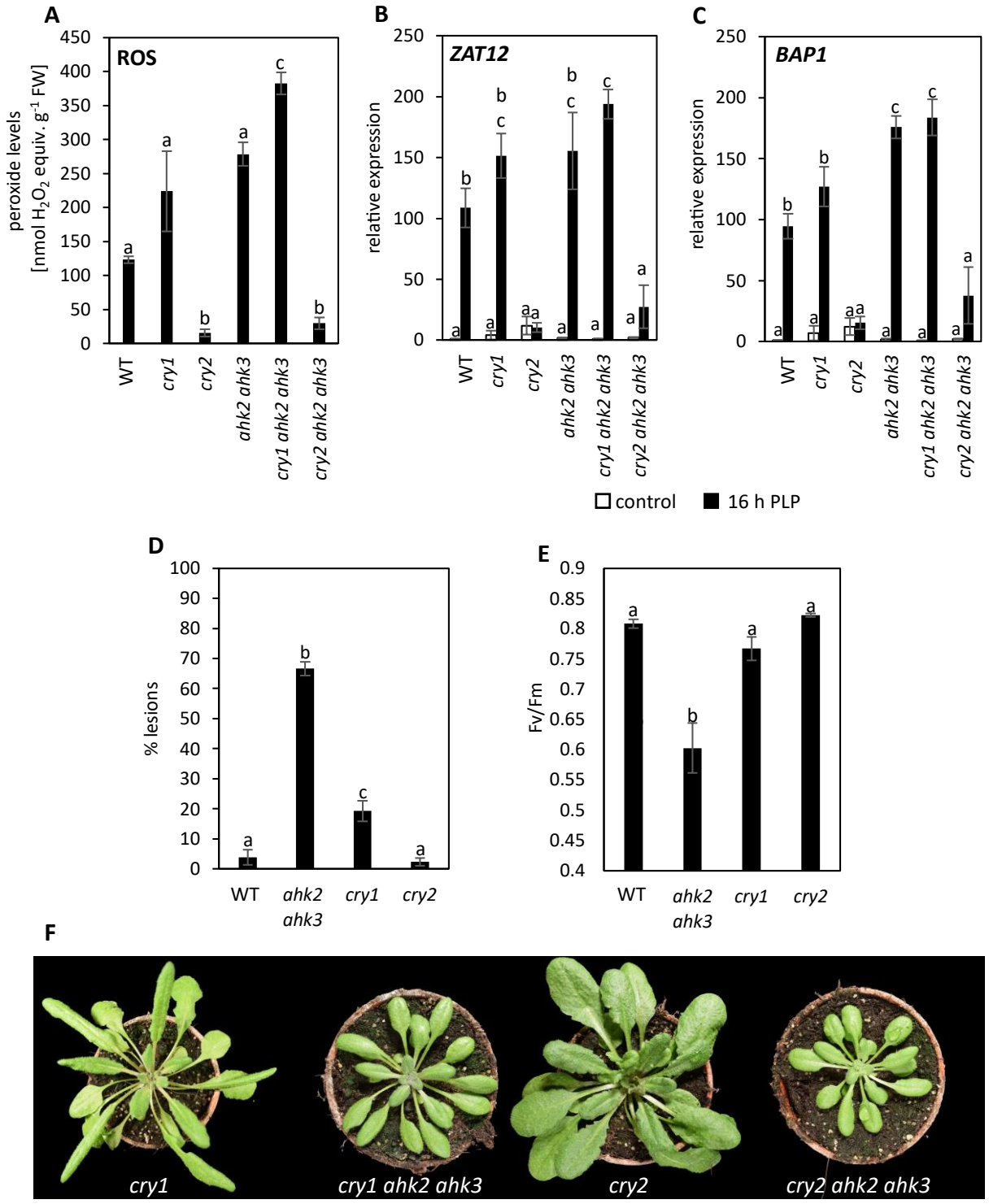

Figure 3.15: The photoperiod stress response in cryptochrome mutants. 5-weeks-old SD-grown plants were treated with 16 h PLP. Experimental setup can be found in Figure 3.6 A. (A) ROS equivalents. Error bars represent SE (n ≥ 3). (B-C) Relative expression of *ZAT12* and *BAP1*. Error bars represent SE (n ≥ 3). Expression was normalized relative to WT control samples which were set to 1. (D) Lesion formation after photoperiod stress (n ≥ 10). (E) Quantum efficiency (Fv/Fm) after photoperiod stress (n ≥ 8). (F) Pictures of photoperiod stressed *cry1, cry1 ahk2 ahk3, cry2,* and *cry2 ahk2 ahk3* mutants taken during the day following the stress-inducing night. Letters represent significant difference between groups as determined by Kruskal-Wallis-Test followed by Wilcoxon rank-sum test ($p < 0.05$). PLP, prolonged light period. This experiment was conducted two times with similar results.

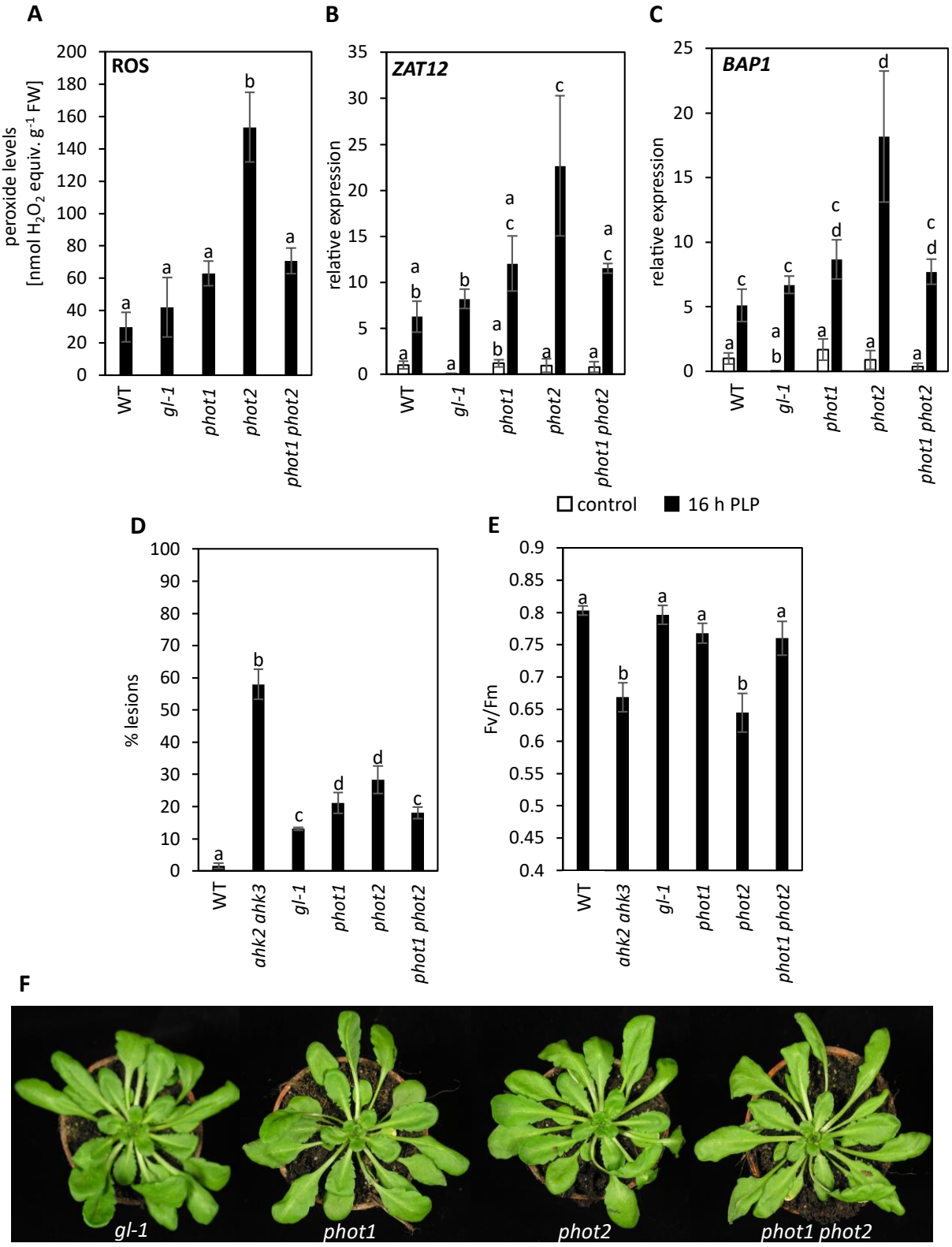

Figure 3.16: The photoperiod stress response in phototropin mutants. 5-weeks-old SD-grown plants were treated with 16 h PLP. Experimental setup can be found in Figure 3.6 A. (A) ROS equivalents. Error bars represent SE (n ≥ 3). (B-C) Relative expression of *ZAT12* and *BAP1*. Error bars represent SE (n ≥ 3). Expression was normalized relative to WT control samples which were set to 1. (D) Lesions formation after photoperiod stress (n ≥ 10). (E) Quantum efficiency (Fv/Fm) after photoperiod stress (n ≥ 8). (F) Pictures of photoperiod stressed *gl-1, phot1, phot2,* and *phot1 phot2* mutants taken during the day following the stress-inducing night. Letters represent significant difference between the groups as determined by Kruskal-Wallis-Test followed by Wilcoxon rank-sum test ($p < 0.05$). PLP, prolonged light period. These experiments were conducted two times with similar results.

A similar response as WT (Col-0) to photoperiod stress in terms of peroxide level (ROS), *ZAT12* and *BAP1* expression, and quantum efficiency was observed in *gl-1*, *phot1,* and *phot1 phot2* (Figure 3.16 A-C, E). In *phot2*, the peroxide levels were 5.1-fold higher than WT, and the *ZAT12* and *BAP1* expression were 3-fold higher than in WT (Figure 3.16 A-C). The quantum efficiency in *phot2* was lower than WT and was similar to *ahk2 ahk3* (Figure 3.16 D). The lesion formation in *gl-1*, *phot1, phot2*, *phot1 phot2* mutants was higher than WT (Col-0). Moreover, lesion formation in *phot1* and *phot2* was even higher than in *gl-1* (Figure 3.16 E). Overall, these results indicate that a lack of only PHOT2 makes plants more susceptible to photoperiod stress.

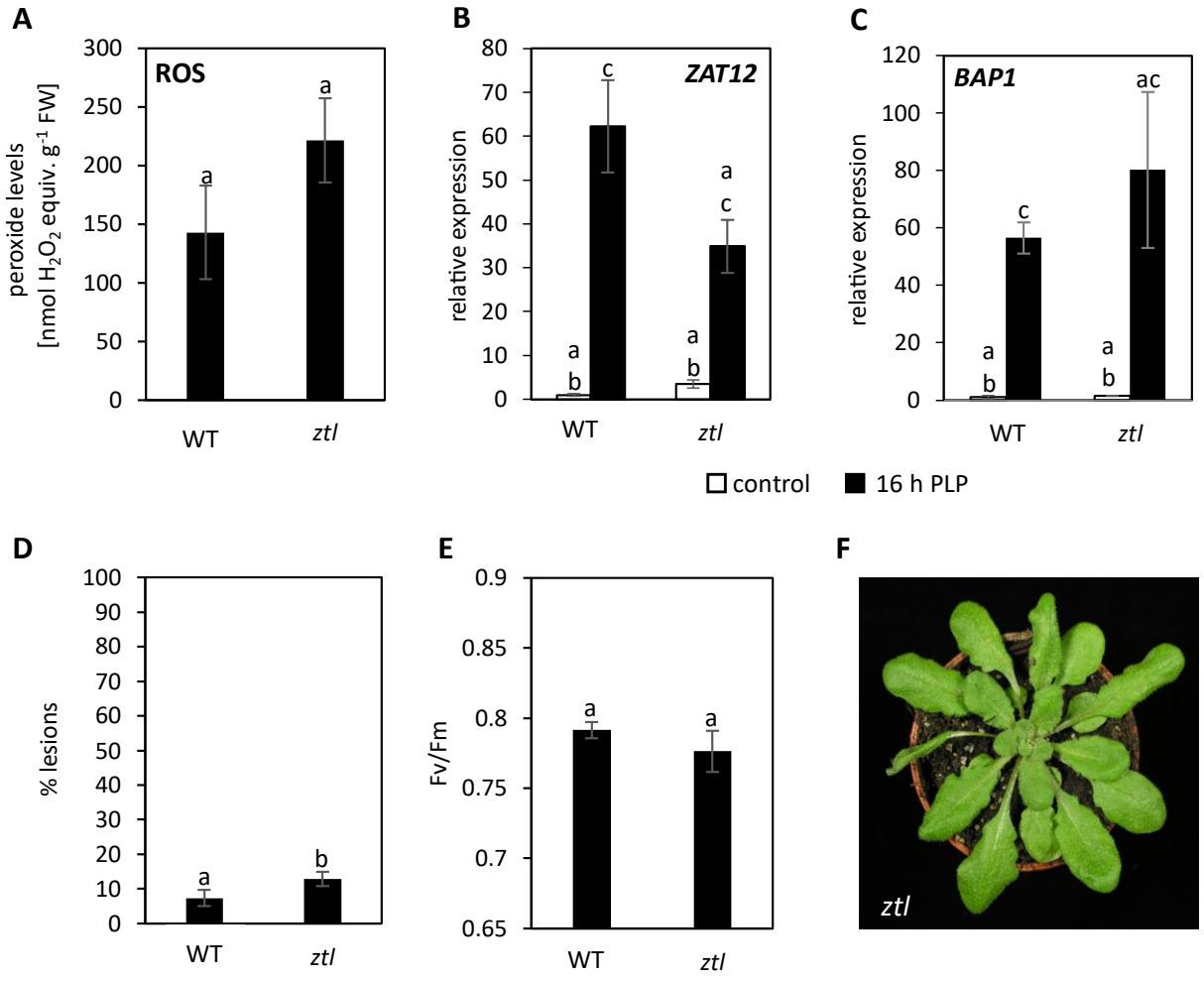

Figure 3.17: The photoperiod stress response in *ztl* mutants. 5-weeks-old SD-grown plants were treated with 16 h PLP. Experimental setup can be found in Figure 3.6 A. (A) ROS equivalents. Error bars represent SE (n ≥ 3). (B-C) Relative expression of *ZAT12* and *BAP1*. Error bars represent SE (n ≥ 3). Expression was normalized relative to WT control samples which were set to 1. (D) Lesion formation after photoperiod stress (n ≥ 10). (E) Quantum efficiency (Fv/Fm) after photoperiod stress (n ≥ 8). (F) Pictures of photoperiod stressed *ztl* mutant taken during the day following the stress-inducing night. Letters represent significant difference between the groups as determined by Kruskal-Wallis-Test followed by Wilcoxon rank-sum test ($p < 0.05$). PLP, prolonged light period. These experiments were conducted two times with similar results.

ztl mutants had similar peroxide levels, *ZAT12* and *BAP1* expression, and quantum efficiency as WT in response to photoperiod stress (Figure 3.17 A-C, E), but slightly higher lesion formation than WT (Figure 3.17 D). Overall, *ztl* mutants showed similar photoperiod stress symptoms as WT, therefore, ZTL is not important for the photoperiod stress response.

The UV-B photoreceptor mutant, *uvr8* also displayed a very low photoperiod stress response compared to WT (Figure 3.18 A-C). From these results, it can be inferred that UVR8 is involved in photoperiod stress response. However, *uvr8 ahk2 ahk3* mutants had photoperiod stress levels as high as *ahk2 ahk3* (Figure 3.18 A-C). Since UV-B light was not present in the growth chambers, the precise role of UVR8 in photoperiod stress remains to be further investigated.

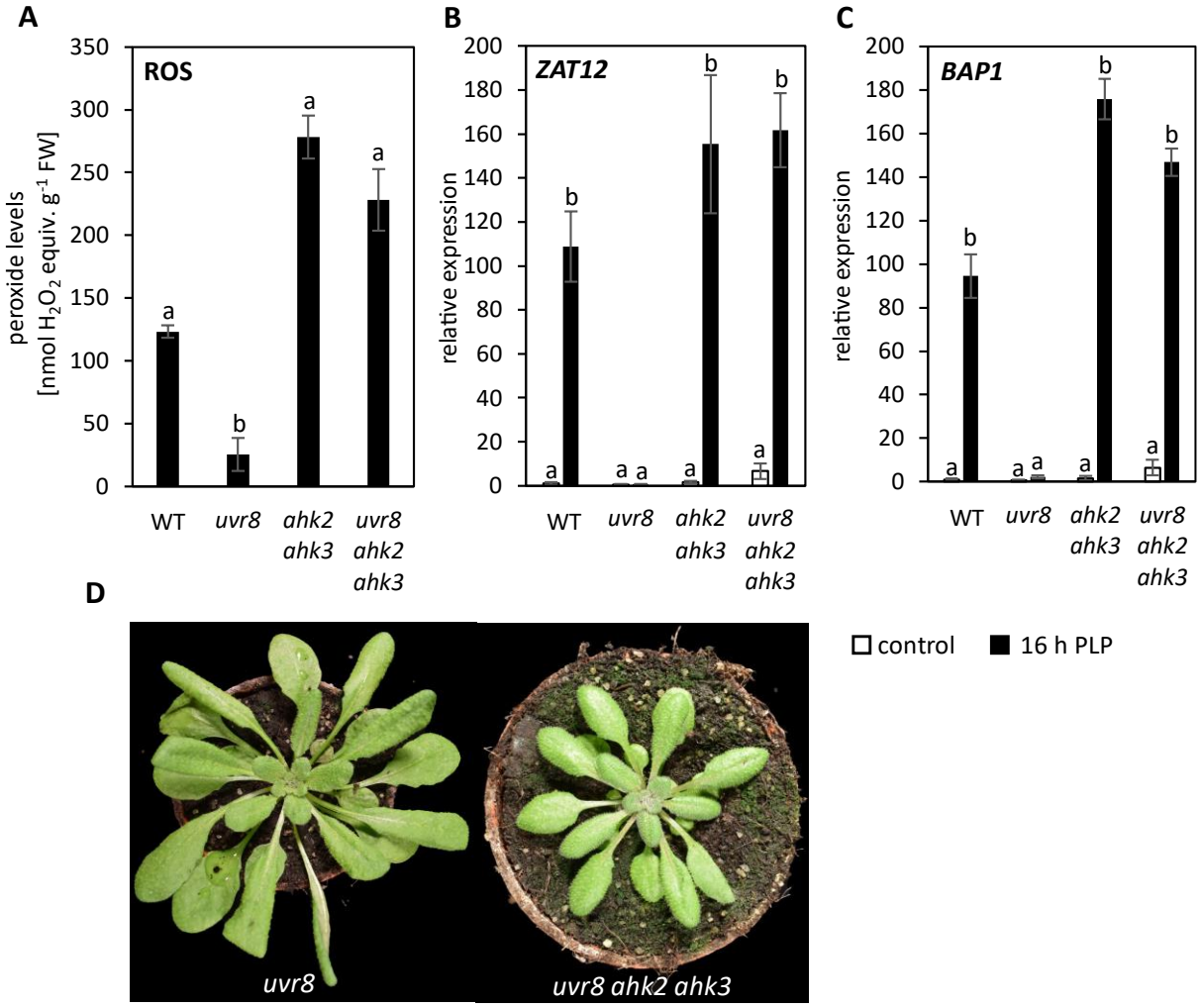

Figure 3.18: The photoperiod stress response in *uvr8* mutants. 5-weeks-old SD-grown plants were treated with 16 h PLP. Experimental setup can be found in Figure 3.6 A. (A) ROS equivalents. Error bars represent SE (n ≥ 3). (B-C) Relative expression of *ZAT12* and *BAP1*. Error bars represent SE (n ≥ 3). Expression was normalized relative to WT control samples which were set to 1. (D) Pictures of photoperiod stressed *uvr8* and *uvr8 ahk2 ahk3* mutants taken during the day following the stress-inducing night. PLP, prolonged light period. Letters represent significant difference between groups as determined by Kruskal-Wallis-Test followed by Wilcoxon rank-sum test ($p < 0.05$). This experiment was conducted two times with similar results.

To confirm the results obtained from the different photoreceptor mutants**,** second mutant alleles of *phyB (GABI), cry2-2, and uvr8-7* were also tested under 16 h PLP photoperiod stress. Results indicate that they also showed lower photoperiod stress symptoms than WT (Supplementary Figure 4) confirming that the response of these photoreceptor mutants is not just allele specific.

3.7 Involvement of light signaling pathway components in the photoperiod stress response

Since photoreceptors such as CRY2 and phyB play an important role in the response to photoperiod stress (section 3.6), the role of downstream light signaling components in photoperiod stress was also investigated. 5-weeks-old SD-grown light signaling mutants *cop1, spa1 spa2, spa3 spa4, hy5, pifQ,* and *PIF1-OX* were exposed to 16 h PLP (Figure 3.19). 3.9-, 6.3-, and 2.8-fold higher peroxide levels than WT were measured in *spa3 spa4, spa1 spa2,* and *pifQ*, respectively. According to *ZAT12* and *BAP1* expression, the stress levels in these mutants were similar to WT (Figure 3.19 A-C). *cop1* had similar peroxide levels and *ZAT12* and *BAP1* expression as WT (Figure 3.19 A-C). Although the peroxide levels in *hy5* were similar, both the *ZAT12* and *BAP1* expression reached only half of the WT level (Figure 3.19 A-C). Peroxide levels in PIF1-OX were similar to WT, but the *ZAT12* and *BAP1* expression were ~7 % and ~11 % of that in WT in response to photoperiod stress treatment (Figure 3.19 A-C). In addition, *hfr1, rup1 rup2,* and *som* also showed photoperiod stress symptoms similar to WT (Supplementary Figure 5). These results indicate that higher expression of *PIF1* might play a protective role against photoperiod stress. Additionally, HY5 might participate in responding to photoperiod stress.

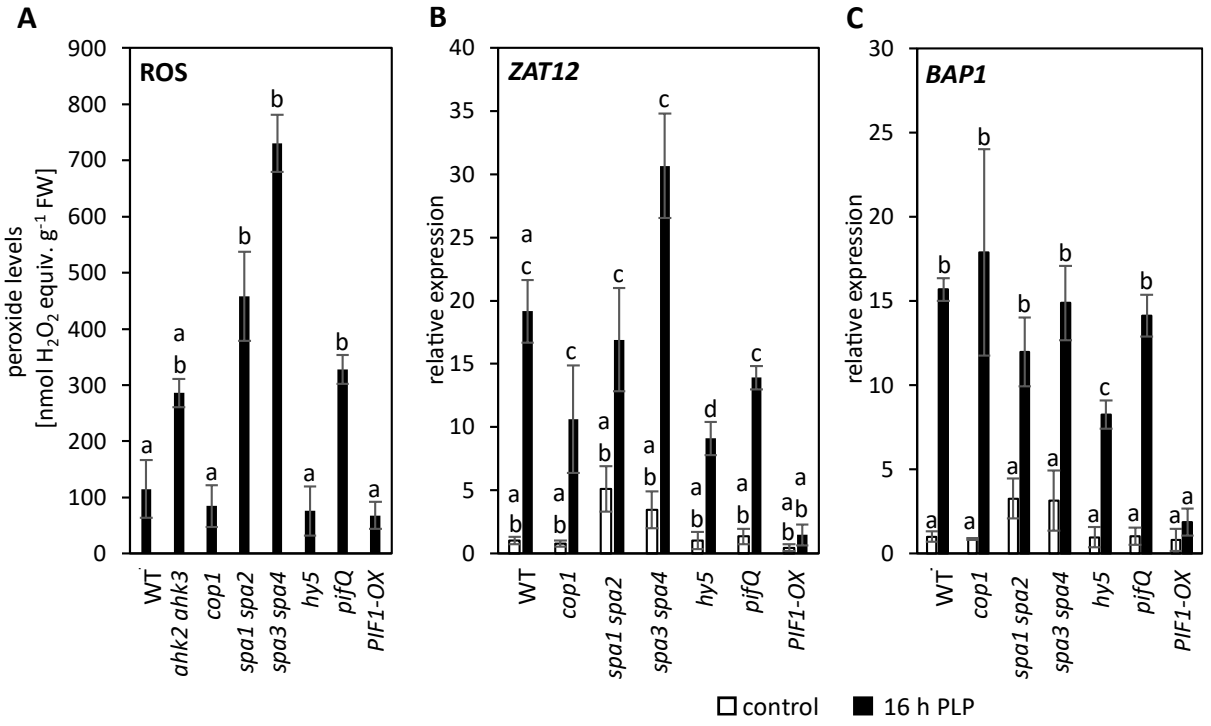

Figure 3.19: The photoperiod stress response in light signaling mutants. 5-weeks-old SD-grown plants were treated with 16 h PLP. Experimental setup can be found in Figure 3.6 A. (A) ROS equivalents. Error bars represent SE (n ≥ 3). (B-C) Relative expression of *ZAT12* and *BAP1*. Error bars represent SE (n ≥ 3). Expression was normalized relative to WT control samples which were set to 1. PLP, prolonged light period. Letters represent significant difference between groups as determined by Kruskal-Wallis-Test followed by Wilcoxon rank-sum test ($p < 0.05$). This experiment was conducted three times with similar results.

3.8 Possibility of cooperation between photoreceptors and circadian clock components in sensing photoperiod stress

Previously, it was shown that the circadian clock is involved in the response to photoperiod stress (Nitschke et al., 2016, 2017). Photoreceptors are responsible for light input to the clock (Devlin and Kay 2000). Therefore, the role of photoreceptors in the perception of photoperiod stress was investigated in circadian clock mutant *cca1 lhy*. The *cca1 lhy* is particularly photoperiod stress sensitive (Nitschke et al., 2016). The photoreceptor mutants *phyB, cry1, cry2*, and *uvr8* were introgressed into the *cca1 lhy* clock mutants, and these 5-weeks-old SD-grown homozygous triple mutants were exposed to a 16 h PLP (Figure 3.20). Peroxide levels and stress marker gene expression (*ZAT12, BAP1*) in *cry1 cca1 lhy, cry2 cca1 lhy, phyB cca1,* and *uvr8 cca1 lhy* were similar to *cca1 lhy* (Figure 3.20 A-C). This result indicates that mutations in *CRY2, PHYB,* and *UVR8* are not able to rescue the photoperiod stress symptoms in the absence of a fully functional circadian clock.

CRY2 was revealed to play an important role in photoperiod stress (section 3.6). To investigate if CRY2 and CRY1 blue light photoreceptors are important for the circadian clock regulation during photoperiod stress, the expression of clock genes, *CCA1, LHY, TOC1,* and *CHE* was studied in

the *cry* mutants (Figure 3.21). It was observed that under photoperiod stress, the expression of *CCA1* and *LHY* was lower in all genotypes compared to the control (Figure 3.21 A-B). No difference in *CCA1* expression could be observed between the genotypes after photoperiod stress, except in *ahk2 ahk3*, which had a higher *CCA1* expression than the other tested genotypes (Figure 3.21 A). *LHY* expression was lower in *ahk2 ahk3* and *cry1* compared to WT in response to photoperiod stress, while *cry1 ahk2 ahk3, cry2*, and *cry2 ahk2 ahk3* had *LHY* expression similar to WT (Figure 3.21 B). In response to photoperiod stress, even though *TOC1* expression exhibited an elevation in all genotypes when compared to their corresponding controls, elevation in *cry2* was lower. *TOC1* expression in *cry2* was 60 % of WT in response to photoperiod stress (Figure 3.20 C). *CHE* expression remained the same as the respective control in response to photoperiod stress in WT, *cry1,* and *cry2 ahk2 ahk3,* but increased in *cry2* (Figure 3.21 D). In fact, *CHE* expression in *cry2* was ~3-fold higher than WT in response to photoperiod stress (Figure 3.20 D). The expression of *CHE* in *ahk2 ahk3* and *cry1 ahk2 ahk3* decreased drastically in response to photoperiod stress (Figure 3.21 D). This result points towards a possible role of CRY2 in responding to the photoperiod stress through the circadian clock. The expression of *CCA1, LHY, TOC1,* and *CHE* in response to photoperiod stress in WT and CK deficient mutants were also studied by Nitschke (2015). The outcomes of this investigation have been compared with those of the Nitschke (2015) in section 4.2.4 alongside further discussion. However, since the expression of clock genes in *cry* mutants was measured only once, the results of this experiment need to be further confirmed through repetition before drawing a strong conclusion.

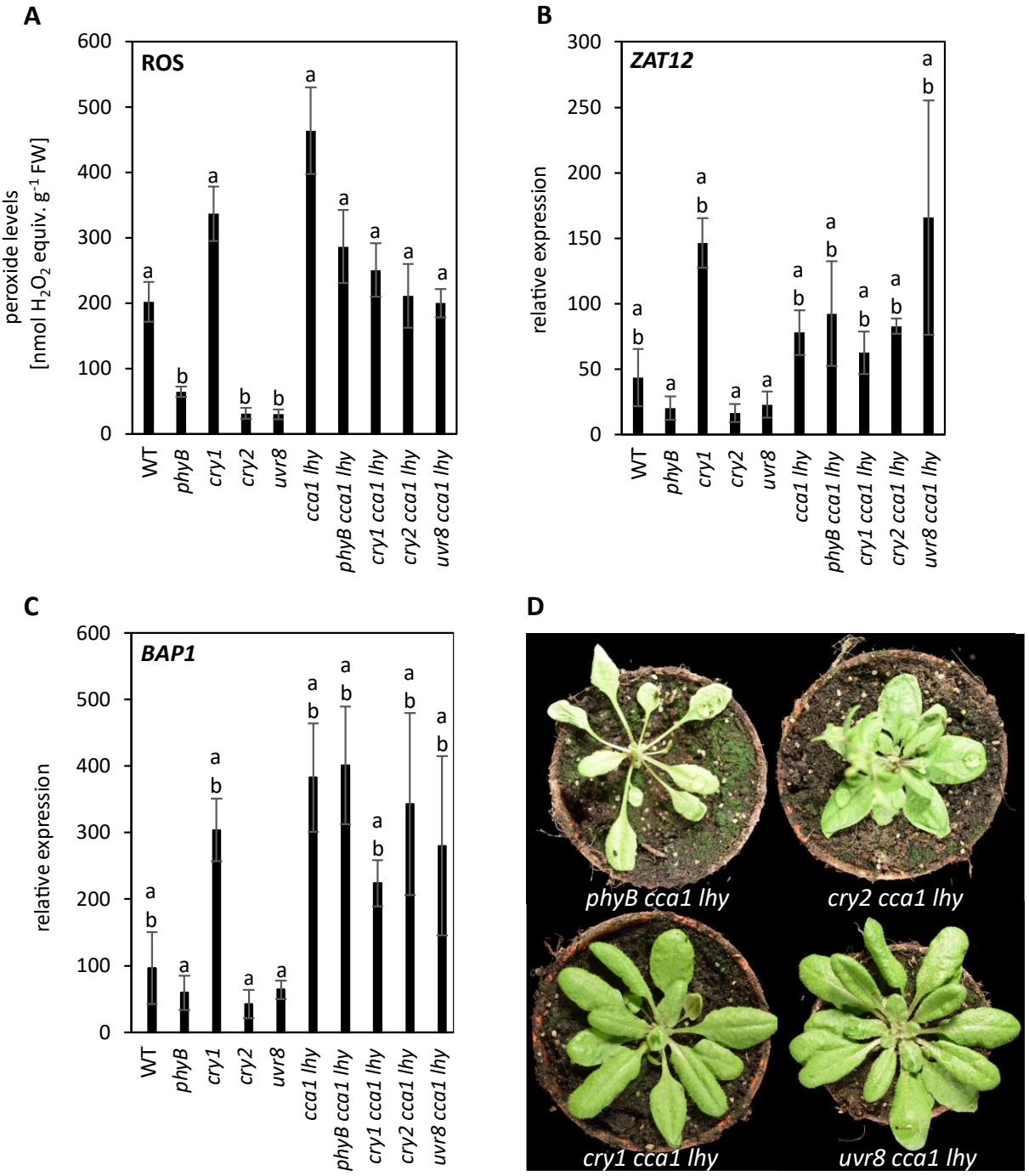

Figure 3.20: The photoperiod stress response in photoreceptor mutants in the *cca1 lhy* background. 5-weeks-old SD-grown plants were treated with a 16 h PLP. Experimental setup can be found in Figure 3.6 A. (A) ROS equivalents. Error bars represent SE (n ≥ 3). (B-C) Relative expression of *ZAT12* and *BAP1*. Error bars represent SE (n ≥ 3). Expression was normalized relative to WT control samples which were set to 1. (D) Pictures of photoperiod stressed *phyB cca1 lhy*, *cry2 cca1 lhy, uvr8 cca1 lhy,* and *cry1 cca1 lhy* mutants (clockwise) taken during the day following the stress-inducing night. Letters represent significant difference between groups as determined by ANOVA followed by a Tukey post-hoc test (A, C) or a Kruskal-Wallis-Test followed by a Wilcoxon rank-sum test (B) ($p < 0.05$). PLP, prolonged light period. This experiment was conducted two times with similar results.

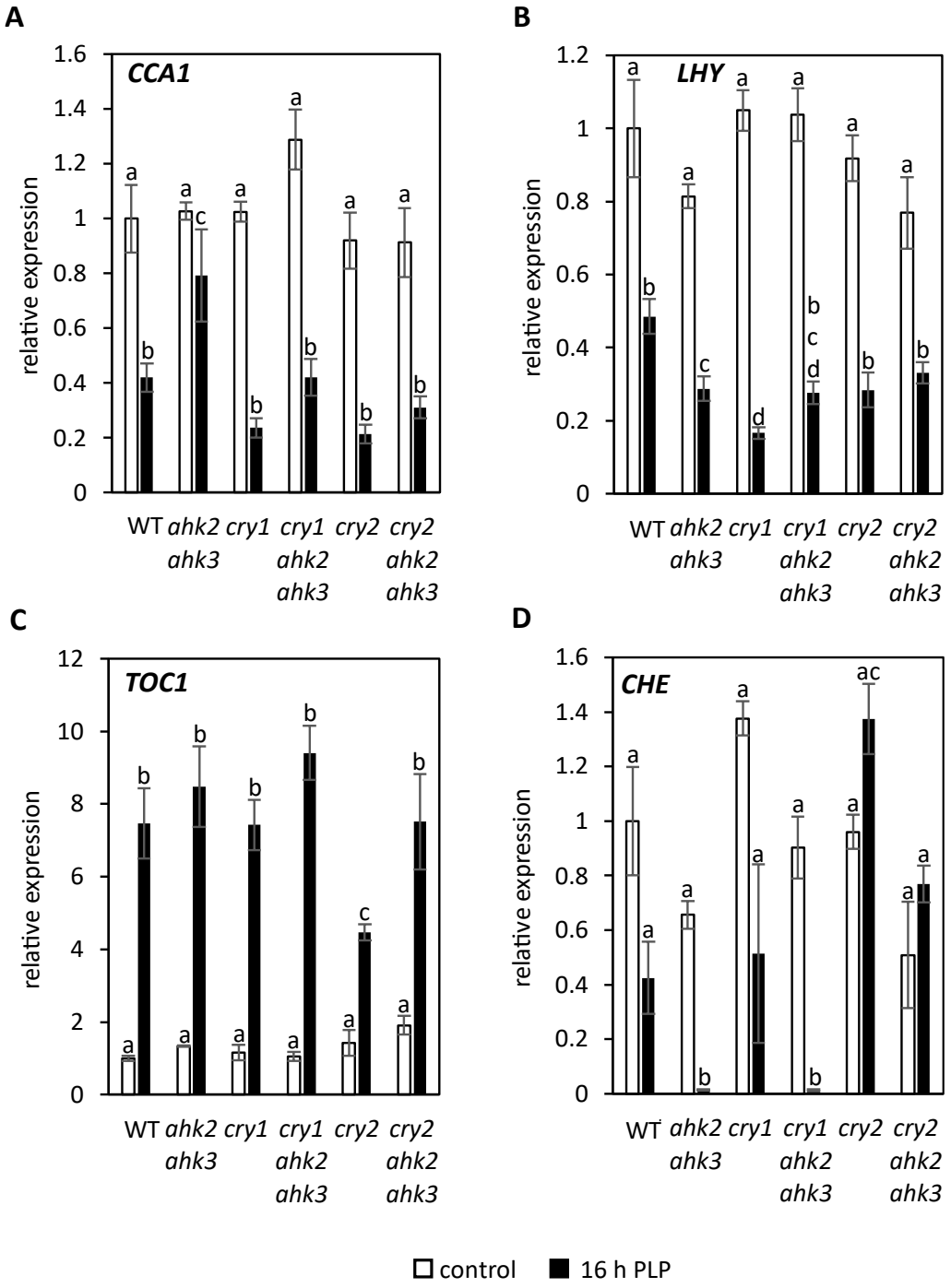

Figure 3.21: Expression of clock genes in cryptochrome mutants in response to photoperiod stress. 5-weeks-old SD-grown plants were treated with a 16 h PLP. Experimental setup can be found in Figure 3.6 A. (A-D) Relative expression of *CCA1*, *LHY*, *TOC1*, and *CHE*. Error bars represent SE (n ≥ 3). Expression was normalized relative to WT control samples which were set to 1. Letters represent significant difference between groups as determined by ANOVA followed by a Tukey post-hoc test (A, C) or a Kruskal-Wallis-Test followed by a Wilcoxon rank-sum test (B, D) ($p < 0.05$). PLP, prolonged light period. This experiment was conducted once.

3.9 Effect of photoperiod stress in flowering pathway mutants.

A well-studied pathway for measuring the photoperiod in plants is the photoperiodic flowering pathway. In order to investigate the possible role of the flowering pathway in photoperiod stress, 5-weeks-old flowering mutants *fkf1, gi, co, ft, tsf,* and *ft tsf,* were studied under photoperiod stress with a 16 h PLP (Figure 3.22).

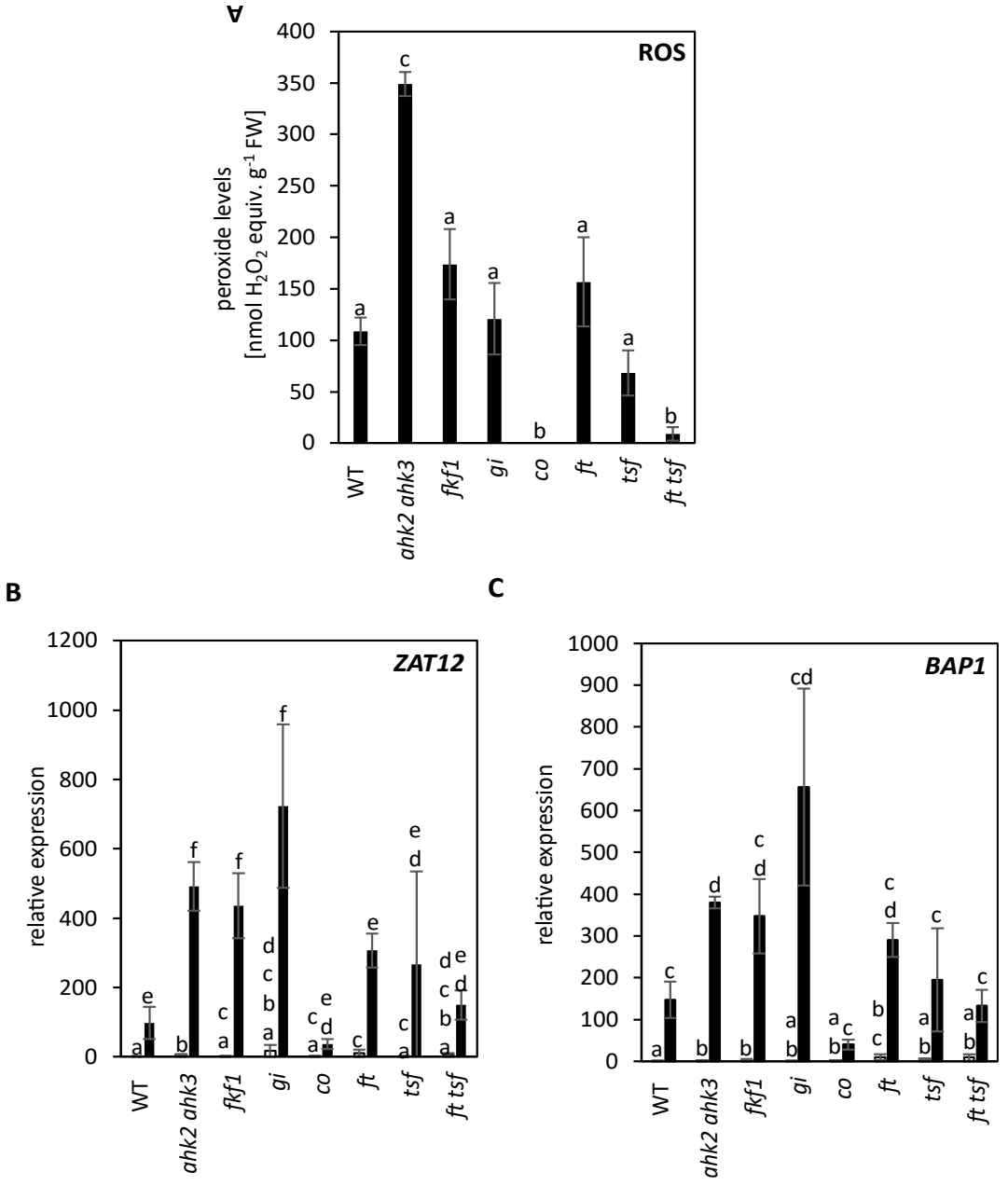

Figure 3.22: The photoperiod stress response in flowering pathway mutants. 5-weeks-old SD-grown plants were treated with a 16 h PLP. Experimental setup can be found in Figure 3.6 A. (A) ROS equivalents. Error bars represent SE (n ≥ 3). (B-C) Relative expression of *ZAT12* and *BAP1*. Error bars represent SE (n ≥ 3). Expression was normalized relative to WT control samples which were set to 1. Letters represent significant difference between groups as determined by ANOVA followed by a Tukey post-hoc test (A) or a Kruskal-Wallis-Test followed by Wilcoxon rank-sum test (B, C) ($p < 0.05$). PLP, prolonged light period. This experiment was conducted two times with similar results. *ZAT12*, *BAP1* expression for *tsf*, *ft tsf* was measured only once.

In response to photoperiod stress treatment, the peroxide levels in *fkf1* and *gi* were as strong as WT, while the expression of *ZAT12* and *BAP1* was higher than in WT (Figure 3.22 A-C). In contrast, *co* and *ft tsf* encountered peroxide levels ~1 % and ~ 8 % of WT (Figure 3.22 B). The *ZAT12* expression in *co* was 3.4-fold lower than WT, but the *BAP1* expression was similar to the WT in response to photoperiod stress (Figure 3.22 B-C). The *ZAT12* and *BAP1* expression in *ft tsf* was similar to WT (Figure 3.22 B-C). According to both peroxide levels and stress marker gene expression, *ft* and *tsf* developed similar photoperiod stress symptoms as WT (Figure 3.21 A-C). This result indicates a possible involvement of CO in regulating the photoperiod stress symptoms.

3.10 Response of different ecotypes of *Arabidopsis thaliana* to photoperiod stress.

In all the above experiments the ecotype Col-0 of *A. thaliana* has been used as WT. In order to see if other ecotypes besides Col-0 also show a photoperiod stress response, several other SD-grown 4-weeks-old ecotypes of *A. thaliana* were exposed to 16 h PLP photoperiod stress (experimental setup similar to Figure 3.6 A). The peroxide levels and stress marker gene expression upon photoperiod stress in the ecotypes in comparison to Col-0 have been summarized in Table 3.1. Stress marker gene expression was not measured for all of the selected ecotypes.

Ten Col ecotypes besides Col-0 were exposed to photoperiod stress to see if other Col ecotypes are equally sensitive to photoperiod stress as Col-0. It was observed that all the Col accessions tested showed a photoperiod stress response similar to Col-0 (Figure 3.23), indicating high photoperiod stress sensitivity of the Col ecotypes.

Ten ecotypes selected based on their high similarity index to Col-0 (> 0.95) as calculated by 1001 Genomes Consortium (2016) were exposed to photoperiod stress. Amongst these, only UKSE06-500 (according to both peroxide levels and *ZAT12* and *BAP1* expression) and En-2 (according to peroxide levels and *BAP1* expression) showed similar photoperiod stress susceptibility as Col-0. All other 8 ecotypes selected on the aforementioned basis showed lower susceptibility to photoperiod stress than Col-0 (Figure 3.24, see Table 3.1). This result indicates that similarity in sequence to Col-0 is not a significant criterion for sensitivity to photoperiod stress.

Sixteen ecotypes from a general VASC ecotype collection that represent high genomic diversity were also examined under photoperiod stress. The ecotypes from the Versailles collection showed different photoperiod stress sensitivity according to peroxide levels and stress marker gene expression (Figure 3.25). All the ecotypes from this collection accumulated lower peroxide levels than Col-0 in response to photoperiod stress. However, amongst the ecotypes from this collection that were also tested for the stress marker gene expression in response to photoperiod stress, only Jea and N13 displayed statistically lower stress marker gene expression than Col-0 (Figure 3.25 A-C, see

Table 3.1 for exact difference). For example, in Ita where peroxide levels were almost nil in response to photoperiod stress, *ZAT12* and *BAP1* expression was similar to Col-0 (Figure 3.25 D-F).

Sixteen ecotypes from the Detlef Weigel collection (Weigel, 2012) were selected so that their natural habitats represent regions at different latitudes ranging from 2.5 N to 65 N, and consequently different natural photoperiods. However, in this group as well, only Elmonte showed stress marker gene expression comparable to Col-0, but the peroxide levels in Elmonte were lower than Col-0 (Figure 3.26 A-C). However, the high *ZAT12* expression was not reproduced in a later experiment (Figure 3.29 A). All other ecotypes from this collection developed lower photoperiod stress symptoms than Col-0 (Figure 3.26). These results indicate that the latitude of the natural habitat of the ecotype is also not an important factor influencing photoperiod stress sensitivity.

Together, these results indicate that photoperiod stress susceptibility is a rare trait in nature, and more complex factors than similarity to Col-0 and geographical location might be contributing to its occurrence.

Table 3.1: Peroxide levels and stress marker gene expression in the ecotypes of *A. thaliana* in response to photoperiod stress.

Ecotypes	**Figure Number**	**ROS**		***ZAT12* expression**		***BAP1* expression**	
		fold difference to Col-0 (%)	**SE**	**fold difference to Col-0 (%)**	**SE**	**fold difference to Col-0 (%)**	**SE**
Col family							
Col-1	Figure 3.23 A-C	77.8	24.4	104.5	33.0	92.9	19.9
Col-2	Figure 3.23 A-C	68.7	26.3	183.4	28.5	135.0	20.1
Col-3	Figure 3.23 A-C	51.7	14.3	95.4	15.0	98.9	14.6
Col-4	Figure 3.23 D	95.7	22.3				
Col-5	Figure 3.23 D	106.6	25.7				
Col-7	Figure 3.23 D	80.2	8.7				
gl-1	Figure 3.23 D	13.9	0.6				
Ecotypes based on similarity to Col-0							
TÄL 07	Figure 3.24 A-C	17.8	10.2	19.8	12.5	13.2	6.4
UKSE06-500	Figure 3.24 A-C	61.4	15.1	22.8	11.4	23.6	19.6
Gd-1	Figure 3.24 A-C	43.9	2.1	1.8	0.3	3.7	2.1
Altenb-2	Figure 3.24 D-F	5.1	0.7				
En-2	Figure 3.24 A-C	47.8	7.9	8.6	7.2	1.5	0.4
Boot-1	Figure 3.24 D-F	10.9	1.6	0.9	0.2	5.7	0.8
Bran-1	Figure 3.24 A-C	29.1	11.0	16.9	9.6	23.6	21.8
Epidauros	Figure 3.24 A-C	40.4	4.9	7.2	5.7	14.2	11.5
CSHL-5	Figure 3.24 D-F	18.5	1.3	2.0	0.6	10.0	3.0
BRR107	Figure 3.24 A-C	15.2	1.1	11.5	10.7	11.1	4.6

Ecotypes	Figure Number	ROS		*ZA12* expression		*BAP1* expression	
		fold difference to Col-0 (%)	SE	fold difference to Col-0 (%)	SE	fold difference to Col-0 (%)	SE
Ecotypes from VASC collection							
Jea	Figure 3.25 A-C	8.5	0.5	0.4	0.21	3.4	1.2
Mh-1	Figure 3.25 A-C	15.2	5.3	10.9	3.1	29.8	2.9
Edi-0	Figure 3.25 A-C	9.8	1.4	19.5	12.4	44.9	22.5
Gre-0	Figure 3.25 A-C	8.3	1.3	8.8	2.9	28.2	7.1
N13	Figure 3.25 A-C	8.1	0.8	1.5	0.5	2.8	0.97
Oy-0	Figure 3.25 A-C	11.6	2.3	13.6	6.4	20.9	11.0
St-0	Figure 3.25 A-C	9.3	1.2	41.3	15.2	71.5	28.4
Kn-0	Figure 3.25 D	28.9	2.1				
Blh-1	Figure 3.25 D	22.2	2.1				
Sakata	Figure 3.25 D	0.0	0.0				
Akita	Figure 3.25 D	0.0	0.0				
Ita-0	Figure 3.25 D-F	0.0	0.0	66.3	27.6	332.1	82.7
Shahdara	Figure 3.25 D	11.3	2.3				
Mt-0	Figure 3.25 D	8.1	2.1				
Ct-1	Figure 3.25 G	13.3	0.9				
Tsu-0	Figure 3.25 G	15.2	3.2				
Ecotypes based on geographical location							
Tanz-2	Figure 3.26 A-C	23.4	2.3	2.6	2.3	14.2	8.8
Pa-3	Figure 3.26 A-C	11.4	1.2	0.3	0.1	2.3	0.9
Cvi-0	Figure 3.26 A-C	17.5	5.0	0.8	0.1	5.0	2.2
La-1	Figure 3.26 A-C	39.8	1.0	0.4	0.1	2.2	0.2
Ka-0	Figure 3.26 A-C	49.7	10.5	0.3	0.2	2.8	1.0
Elmonte	Figure 3.26 A-C	10.1	0.6	21.7	9.7	199.4	41.5
L*er*-0	Figure 3.26 A-C	27.2	9.2	11.6	6.2	11.2	6.2
Hen	Figure 3.26 A-C	13.1	3.0	5.1	4.8	0.4	0.2
Ber-0	Figure 3.26 A-C	5.2	0.4	2.0	1.0	3.5	1.6
H55	Figure 3.26 D-F	2.1	0.7	4.6	2.0	13.8	4.5
Pigna-1	Figure 3.26 D-F	14.0	3.2	0.7	0.2	11.4	4.6
Lag1	Figure 3.26 D-F	2.2	0.2	0.4	0.1	1.6	0.3
Mr-0	Figure 3.26 D-F	11.6	1.6	0.2	0.0	1.1	0.3
Can-0	Figure 3.26 G	0.0	0.0	0.0	0.0	0.0	0.0
Ting-1	Figure 3.26 G	0.0	0.0	0.0	0.0	0.0	0.0
Ws-1	Figure 3.26 H	69.0	11.9	0.9	0.1	4.6	0.8

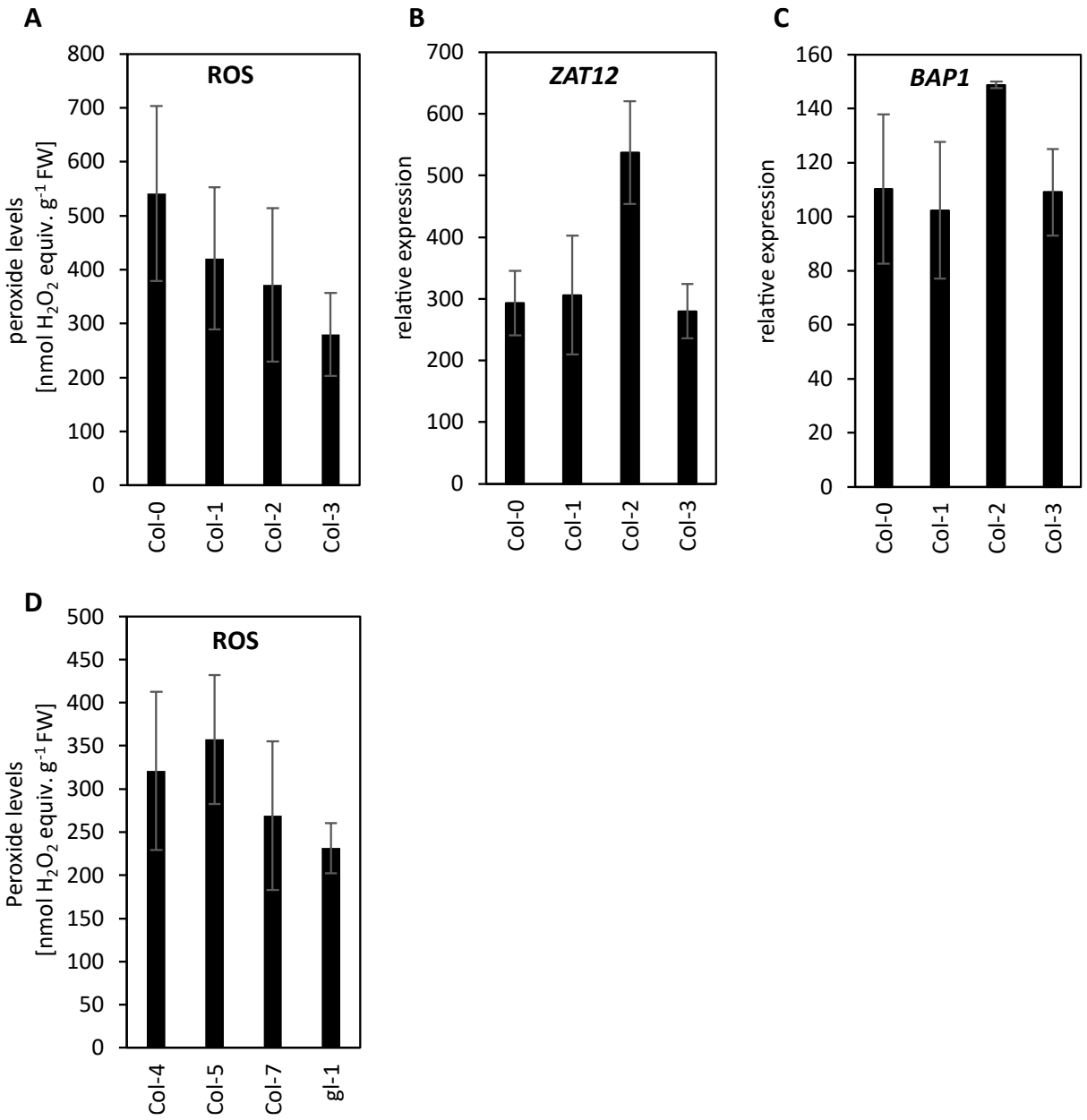

Figure 3.23: The photoperiod stress response in Col accessions of *A. thaliana*. 4-weeks-old SD-grown plants were treated with a 16 h PLP. Experimental setup can be found in Figure 3.6 A. (A, D) ROS equivalents. Error bars represent SE (n ≥ 3). (B-C) Relative expression of *ZAT12* and *BAP1*. Error bars represent SE (n ≥ 3). Expression was normalized relative to Col-0 control samples which were set to 1. PLP, prolonged light period. There was no significant difference between the individual ecotype groups and Col-0 according to Student's t-test. This experiment was conducted once.

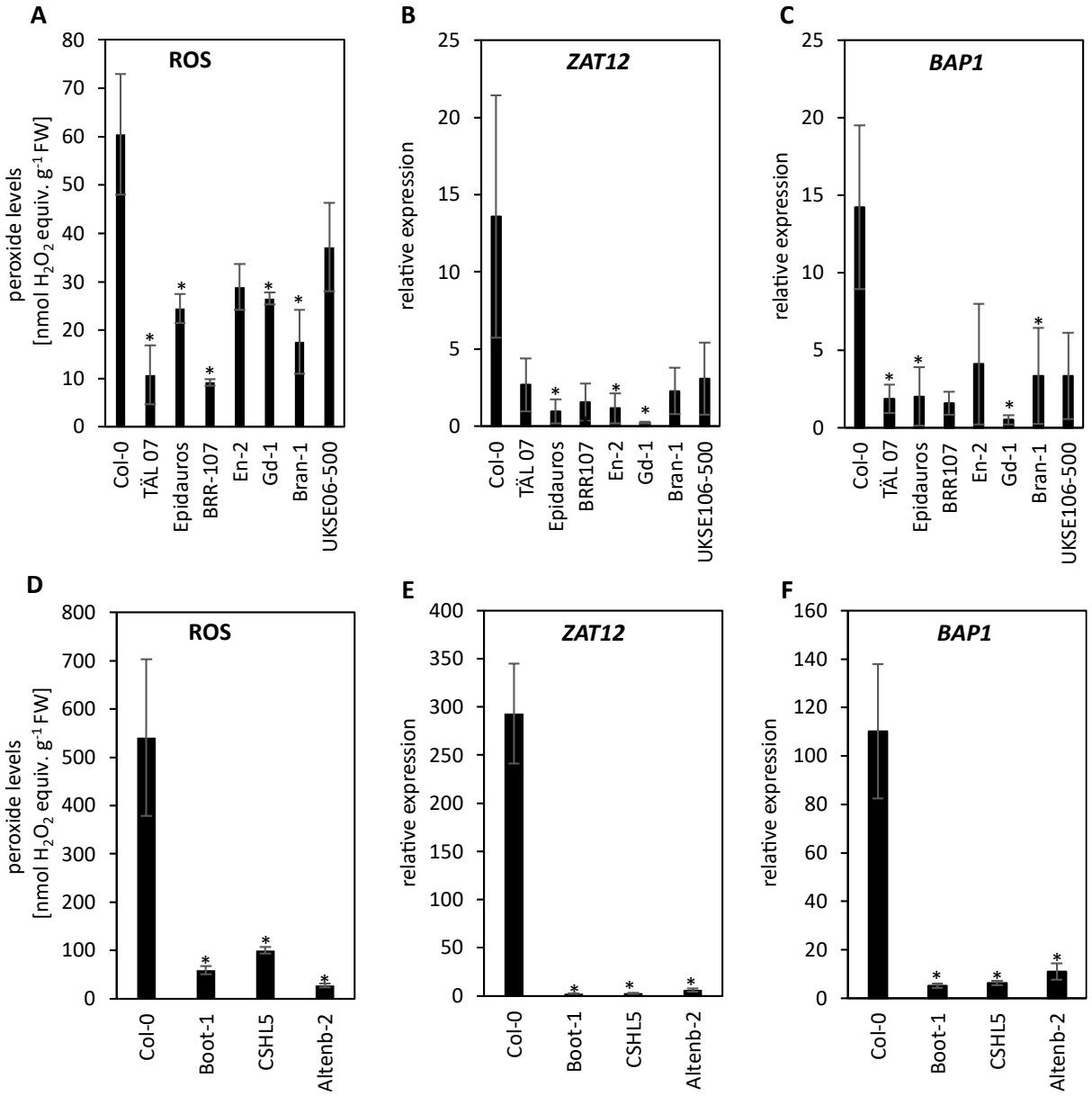

Figure 3.24: The photoperiod stress response in ecotypes of *A. thaliana* selected based on genetic similarity to Col-0. 4-weeks-old SD-grown plants were treated with a 16 h PLP. Experimental setup can be found in Figure 3.6 A. (A, D) ROS equivalents. Error bars represent SE (n ≥ 3). (B, E) Relative expression of *ZAT12*. Error bars represent SE (n ≥ 3). (C, F) Relative expression of *BAP1*. Error bars represent SE (n ≥ 3). Expression was normalized relative to Col-0 control samples which were set to 1. Asterisks represent significant difference from Col-0 as determined by Wilcoxon rank-sum test. PLP, prolonged light period. This experiment was conducted once.

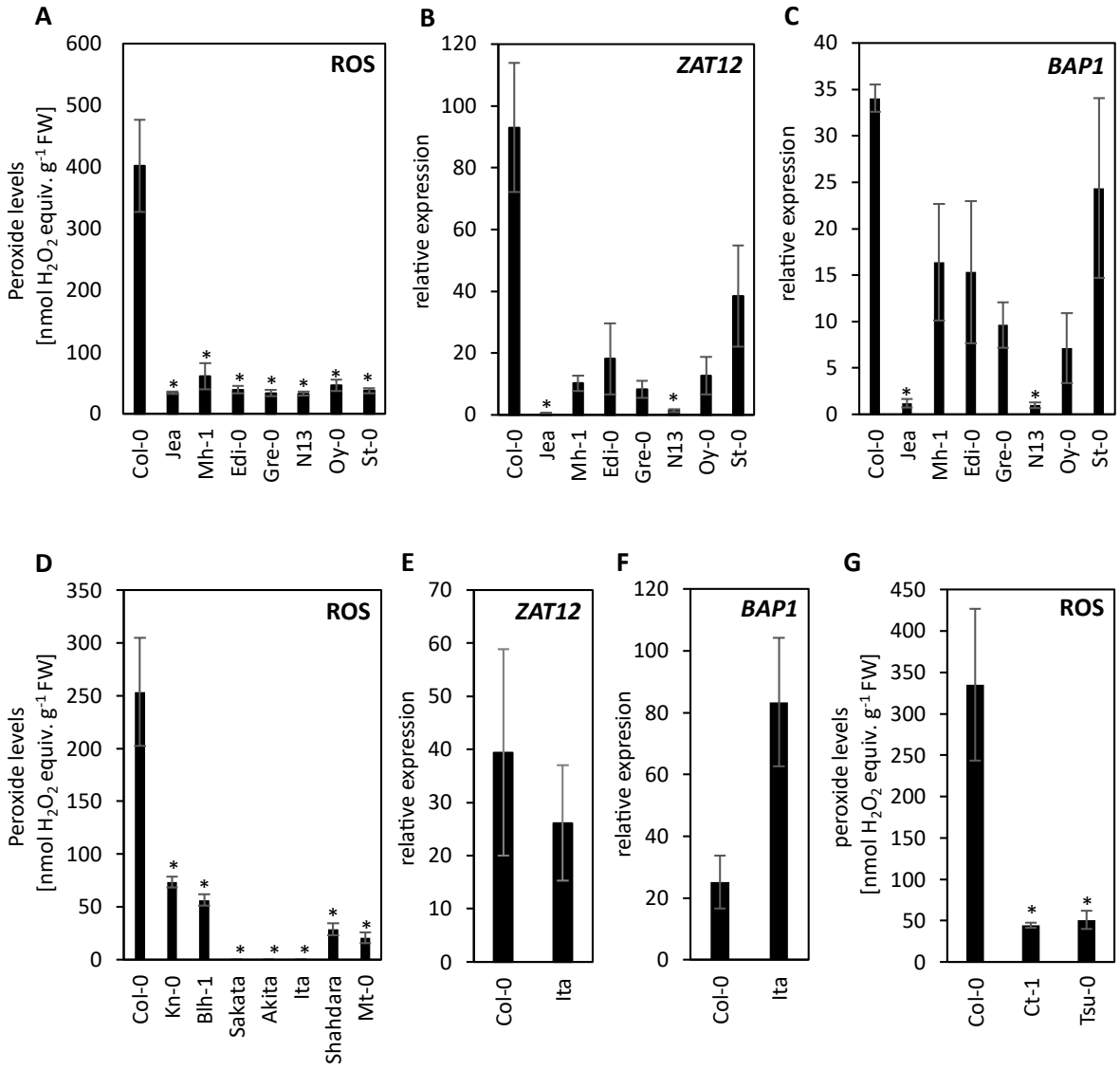

Figure 3.25: The photoperiod stress response in the ecotypes of *A. thaliana* from the VASC collection. 4-weeks-old SD-grown plants were treated with a 16 h PLP. Experimental setup can be found in Figure 3.6 A. (A, D, G) ROS equivalents. Error bars represent SE (n ≥ 3). (B, E) Relative expression of *ZAT12*. Error bars represent SE (n ≥ 3). (C, F) Relative expression of *BAP1*. Error bars represent SE (n ≥ 3). Expression was normalized relative to Col-0 control samples which were set to 1. Asterisks represent significant difference from Col-0 as determined by Wilcoxon rank-sum test. PLP, prolonged light period. This experiment was conducted once.

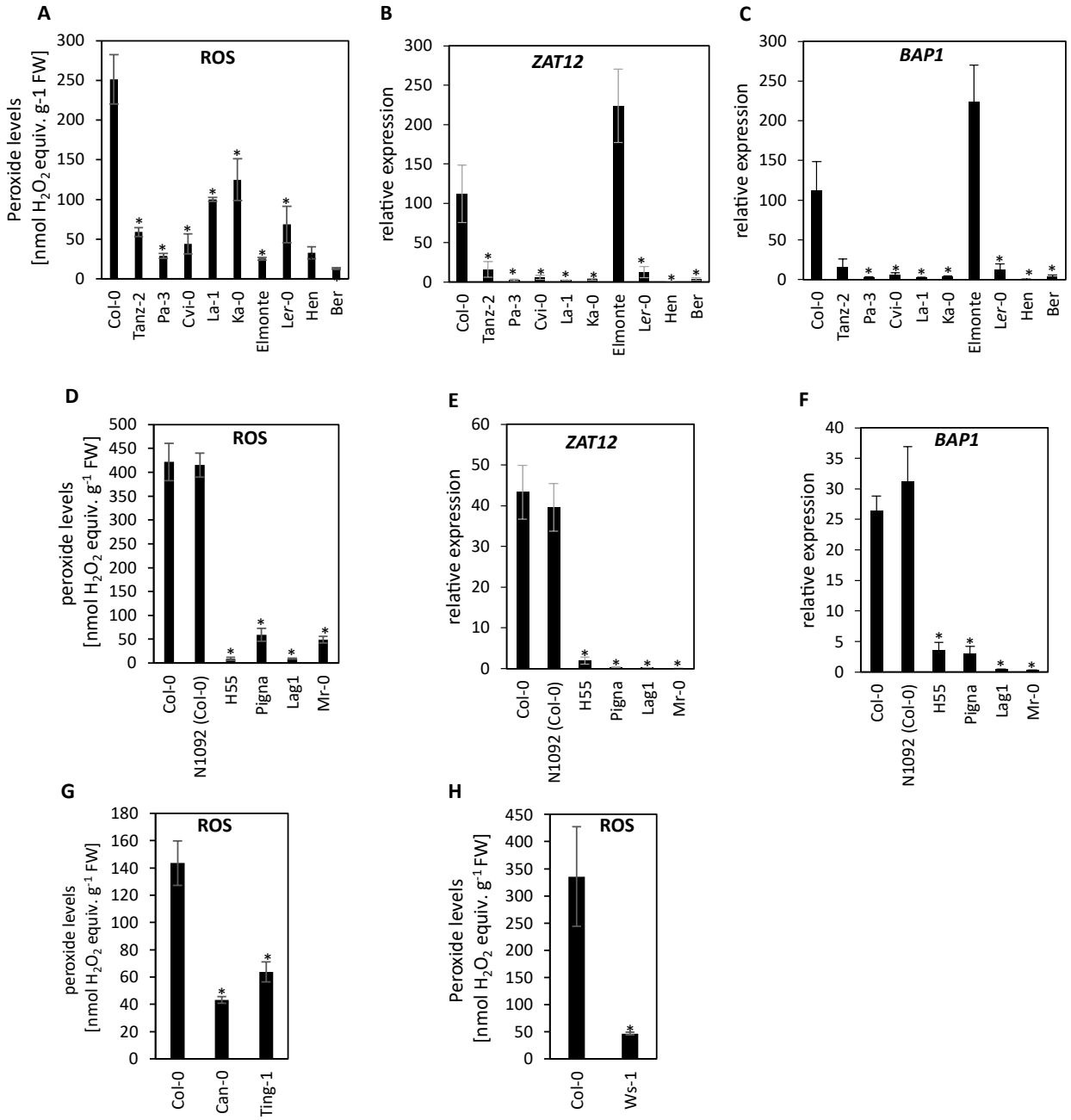

Figure 3.26: The photoperiod stress response in ecotypes of *A. thaliana* selected based on the latitude. 4-weeks-old SD-grown plants were treated with a 16 h PLP. Experimental setup can be found in Figure 3.6 A. (A, D, G, H) ROS equivalents. Error bars represent SE (n ≥ 3). (B, E) Relative expression of *ZAT12*. Error bars represent SE (n ≥ 3). (C, F) Relative expression of *BAP1*. Error bars represent SE (n ≥ 3). Expression was normalized relative to Col-0 control samples which were set to 1. PLP, prolonged light period. Asterisks represent significant difference from Col-0 as determined by Wilcoxon rank-sum test. A-C was repeated two times with similar results, and D-H was conducted once.

3.11 Tracing the inheritance pattern of photoperiod stress susceptibility trait

Since most of the ecotypes showed much lower photoperiod stress symptoms compared to Col-0, it prompted the question of whether the photoperiod stress susceptibility of Col-0 is a recessive or dominant trait. To test this hypothesis, F1 and F2 crosses of Col-0 with selected ecotypes were examined under photoperiod stress conditions. Initially, Col-0 was crossed with L*er*-0, Pa-3, La-1, Ber-0, H55, and Elmonte. Except for Elmonte, which was specifically chosen, the ecotypes selected for crossing with Col-0 were characterized by their low susceptibility to photoperiod stress (see section 3.10, Figure 3.26). Elmonte was deliberately included to investigate whether the combination of two photoperiod stress-sensitive backgrounds would result in progeny with heightened sensitivity to photoperiod stress. The crossing was performed for L*er*-0, Pa-3, La-1, and Tanz-2 in both directions, that is Col-0 as the maternal and the L*er*-0, Pa-3, La-1, and Tanz-2 as the paternal donor and vice versa (Figure 3.27-Figure 3.28). For example, between L*er*-0 and Col-0, two crosses were generated, Col-0 X L*er*-0 and L*er*-0 X Col-0. The crosses were named conventionally: the maternal plant is written first followed by the paternal plant. For the crosses with Elmonte, H55, and Ber-0, the ecotype Col-0 only acted as the paternal donor (Figure 3.29-Figure 3.30). 4-weeks-old plants of the F1 generation were subjected to photoperiod stress conditions with a 16 h PLP (experimental setup similar to Figure 3.6 A). It was observed that L*er*-0 X Col-0 and Col-0 X L*er*-0, Pa-3 X Col-0 and Col-0 x Pa-3, La-1 X Col-0 and Col-0 X La-1, Elmonte X Col-0, H55 X Col-0, and Ber-0 X Col-0 showed lower *ZAT12* and *BAP1* expression than Col-0 upon photoperiod stress (Figure 3.27, Figure 3.28 A-C, Figure 3.29, Figure 3.30). All these F1 generations had a photoperiod stress response similar to their other respective parent. It's worth noting that while Elmonte exhibited stress marker gene expression similar to Col-0 in response to photoperiod stress in a previously described experiment (Figure 3.26 B-C), in this instance, the expression of *ZAT12* in Elmonte was only ~12 % of Col-0 (Figure 3.29 A). Taken together, these results indicate that photoperiod stress susceptibility is a recessive trait. However, as a notable exception, in F1 plants of Tanz-2 X Col-0, photoperiod stress symptoms were as strong as in Col-0. In contrast, F1 plants of Col-0 X Tanz-2 had photoperiod stress symptoms as low as Tanz-2 (Figure 3.28 D-F). The variation in photoperiod stress response between the reciprocal crosses could stem from the genetic composition of Tanz-2. Additional experimental inquiries are required to gain a deeper insight into the underlying cause of this phenomenon. Another notable observation is the larger size of F1 progenies across all mentioned crosses compared to either parent, suggesting the possibility of heterosis.

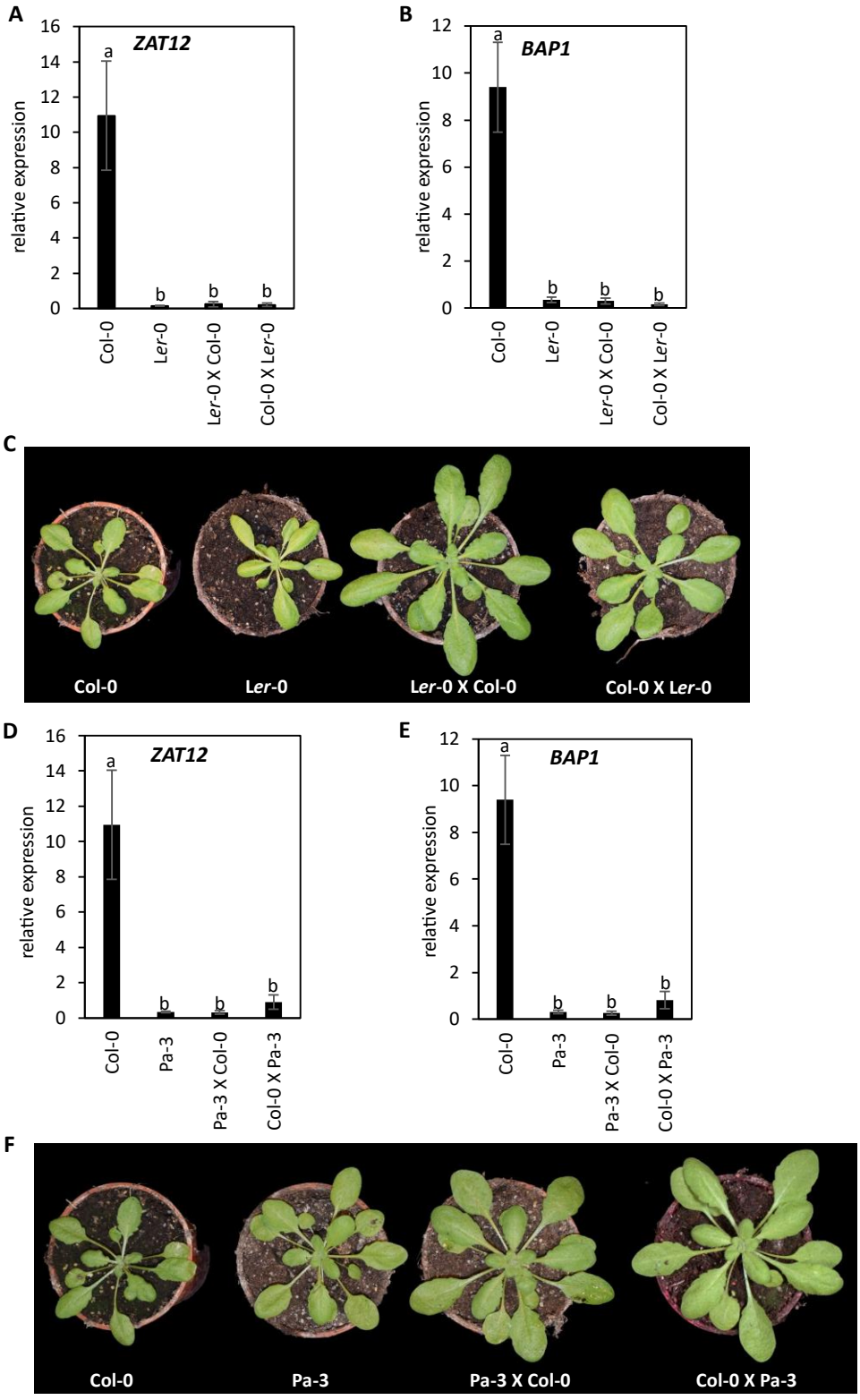

Figure 3.27: The photoperiod stress response in F1 crosses of L*er*-0 and Pa-3 with Col-0. 4-weeks-old SD-grown plants were treated with 16 h PLP. Experimental setup can be found in Figure 3.6 A. (A, D) Relative expression of *ZAT12*. Error bars represent SE (n ≥ 3). (B, E) Relative expression of *BAP1*. Error bars represent SE (n ≥ 3). Expression was normalized relative to Col-0 control samples which were set to 1. (C, F) Pictures of F1 crosses of Col-0 with L*er*-0 and Pa-3 under control conditions. Letters represent significant difference between groups as determined by Kruskal-Wallis-Test followed by Wilcoxon rank-sum test ($p < 0.05$). PLP, prolonged light period. This experiment was conducted once.

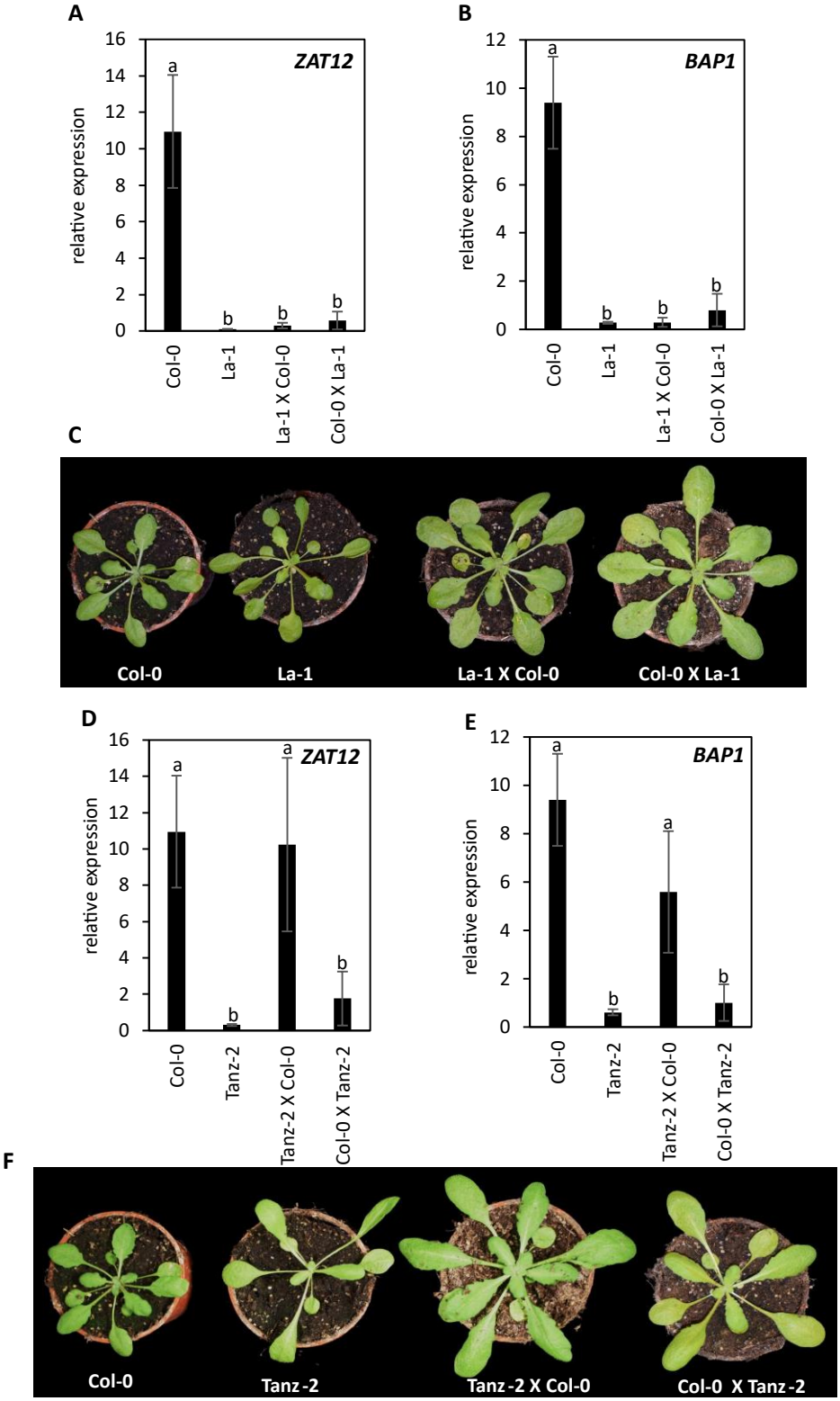

Figure 3.28: The photoperiod stress response in F1 crosses of La-1 and Tanz-2 with Col-0. 4-weeks-old SD-grown plants were treated with a 16 h PLP. Experimental setup can be found in Figure 3.6 A. (A, D) Relative expression of *ZAT12*. Error bars represent SE (n ≥ 3). (B, E) Relative expression of *BAP1*. Error bars represent SE (n ≥ 3). Expression was normalized relative to Col-0 control samples which were set to 1. (C, F) Pictures of F1 crosses of Col-0 with La-1 and Tanz-2 under control conditions. Letters represent significant difference between groups as determined by Kruskal-Wallis-Test followed by Wilcoxon rank-sum test ($p < 0.05$). PLP, prolonged light period. This experiment was conducted once.

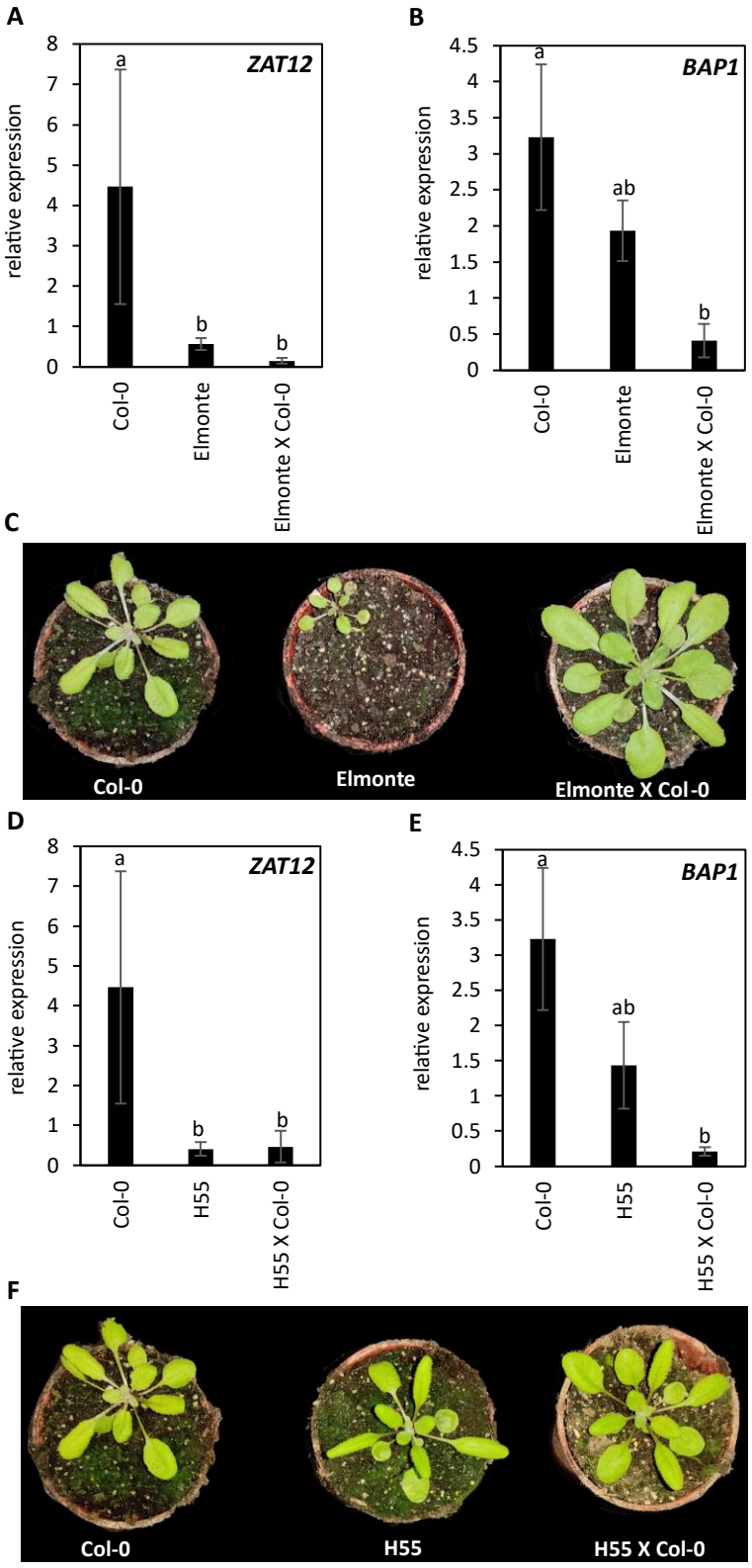

Figure 3.29: The photoperiod stress response in F1 crosses of Elmonte and H55 with Col-0. 4-weeks-old SD-grown plants were treated with 16 h PLP. Experimental setup can be found in Figure 3.6 A. (A, D) Relative expression of *ZAT12*. Error bars represent SE (n ≥ 3). (B, E) Relative expression of *BAP1*. Error bars represent SE (n ≥ 3). Expression was normalized relative to Col-0 control samples which were set to 1. (C, F) Pictures of F1 crosses of Col-0 with Elmonte and H55 under control conditions. Letters represent significant difference between groups as determined by Kruskal-Wallis-Test followed by Wilcoxon rank-sum test ($p < 0.05$). PLP, prolonged light period. This experiment was conducted once.

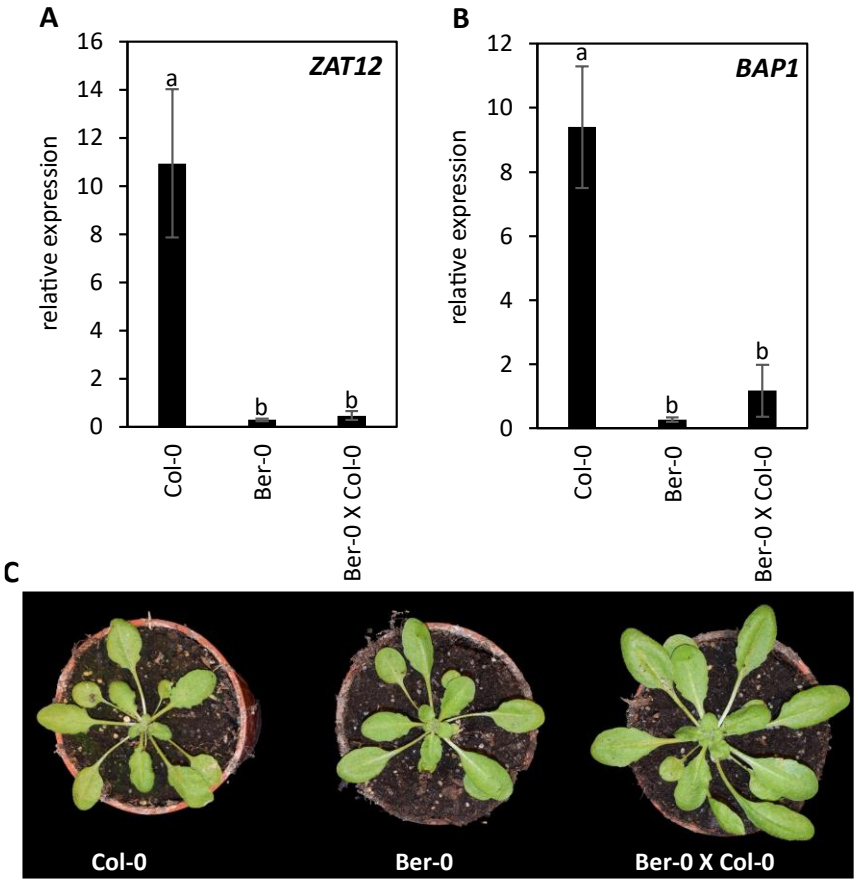

Figure 3.30: The photoperiod stress response in F1 cross of Ber-0 with Col-0. 4-weeks-old SD-grown plants were treated with a 16 h PLP. Experimental setup can be found in Figure 3.6 A. (A-B) Relative expression of *ZAT12* and *BAP1*. Error bars represent SE (n ≥ 3). Expression was normalized relative to Col-0 control samples which were set to 1. (C) Pictures of F1 cross of Col-0 with Ber-0 under control conditions. Letters represent significant difference between groups as determined by Kruskal-Wallis-Test followed by Wilcoxon rank-sum test ($p < 0.05$). PLP, prolonged light period. This experiment was conducted once.

To gather some more initial information about the inheritance pattern of the trait, the F2 progeny of Col-0 X La-1 was tested under photoperiod stress. In total, 50 individuals from the F2 progeny (numbered 1-50) alongside their parental donors, Col-0 and La-1 were analyzed under 16 h PLP photoperiod stress when they were 4 weeks old, and the stress response was measured through relative expression of *ZAT12* and *BAP1* (Figure 3.31). Upon photoperiod stress, the relative expression of *ZAT12* and *BAP1* in La-1 ranged from 0.3-1.04 and 0.7-6.4, while in Col-0, the expression ranges for *ZAT12* and *BAP1* were 10.0-88.4 and 13.2-44.3. These expression of values of all the samples in this experiment were normalized relative to the average value of Col-0 control. *UBC21* and *TFIID* were used as reference genes in this experiment. Based on *ZAT12* and *BAP1* expression, the F2 progenies were ordered from the lowest to the highest expression for the respective genes (Figure 3.31 A-B). Based on the observation of the relative expression of the stress marker genes in the parent ecotypes, a cut-off was defined to categorize the F2 progeny phenotype as similar to either parent, intermediate, or higher. The cutoff was set to include all F2 progenies with stress marker gene expression equal to

or lower than the highest La-1 sample in the "similar to La-1" category. Progenies with stress marker gene expression higher than the highest La-1 sample but lower than the lowest Col-0 sample were categorized as "intermediate." Those falling within the expression range of Col-0 were labeled "similar to Col-0," while progenies with expression exceeding the highest Col-0 sample were designated as "higher." Only those F2 plants that fell into the same category according to both *ZAT12* and *BAP1* expression were taken into final consideration for the analysis of the result; the F2 plants that fell into different categories according to *ZAT12* and *BAP1* were left out of the analysis. Out of these 35 plants from the F2 progeny of Col-0 X La-1, nine plants showed a low photoperiod stress response similar to La-1, twenty plants similar to Col-0, two plants showed intermediate stress response and four plants higher than Col-0. The susceptibility to the photoperiod stress in the F2 generation follows a continuous distribution and does not show a pattern expected for one or few loci following Mendelian segregation (1:3 for a single locus or 9:3:3:1 for two loci). This indicates that photoperiod stress susceptibility is a quantitative trait, with probably one locus that leads to a major difference.

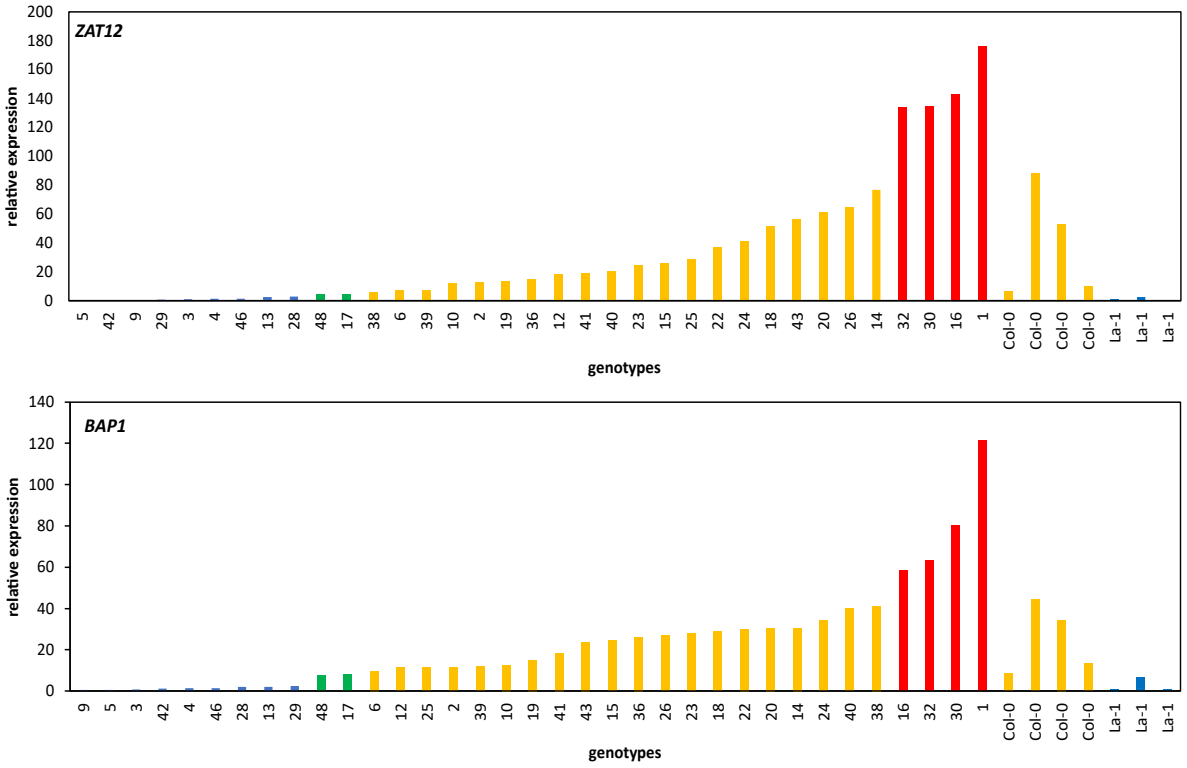

Figure 3.31: The photoperiod stress response in Col-0 X La-1 F2 generation. 4-weeks-old SD-grown plants were treated with 16 h PLP. Experimental setup can be found in Figure 3.6 A. (A-B) Relative expression of *ZAT12* and *BAP1*. Expression was normalized relative to Col-0 control samples which were set to 1. The values from only the stressed plants are shown in the graphs and not from the control plants. PLP, prolonged light period. F2 progenies are assigned numbers from 1 to 50. Those depicted with blue bars exhibit a photoperiod stress response 'similar to La-1', while those with green bars display an 'intermediate' phenotype between La-1 and Col-0. Progenies marked with yellow bars show photoperiod stress response 'similar to Col-0', and those with red bars denote a 'higher' photoperiod stress response. The criteria for categorizing the phenotype of the F2 generation is based on the range of stress marker gene expression in La-1 and Col-0 samples (also see section 3.11). This experiment was conducted once.

4 Discussion

4.1 The chloroplast is a sensor for photoperiod stress.

4.1.1 A minimum light intensity of 50 µmol m^{-2} s^{-1} is necessary during the PLP to cause photoperiod stress

Since photoperiod stress is caused by a prolongation of the light period (Nitschke et al., 2016), the question arose what is the minimum intensity of light during this PLP that is necessary to cause photoperiod stress. Therefore, plants were treated with light intensities ranging between 30-120 µmol m^{-2} s^{-1} during the PLP. The peroxide and stress marker gene expression showed that in the plants grown at 120 µmol m^{-2} s^{-1}, photoperiod stress symptoms such as an increase in peroxide levels and stress marker gene expression only occur when a light intensity of at least ~50 µmol m^{-2} s^{-1} is present during the PLP (Figure 3.1).

Light is perceived in plants by photoreceptors and chloroplasts, but the light intensities at which they operate are different. Numerous responses dependent on light perception by photoreceptors require much lower light intensities. For example, significant phototropic responses occur with fluence rates around or below 1 µmol m^{-2} s^{-1} (Iino, 2001). Similarly, hypocotyl elongation and cotyledon opening mediated by CRY2 responds to fluence rates of ~1 µmol m^{-2} s^{-1} (Lin et al., 1998; Ahmad et al., 2002) and phyA-dependent seed germination responds to even lower light fluence (Shinomura et al., 1996). In contrast, photosynthesis, which is the main function of chloroplasts requires higher light intensity and reaches at 50 µmol m^{-2} s^{-1} about ~20 % of its maximum value (Kaiser et al., 2016). Since photoperiod stress requires a minimum light intensity in the range of 50-70 µmol m^{-2} s^{-1}, a role of the chloroplasts has been concluded in sensing photoperiod stress.

The expression of *ELIP1* increased statistically due to photoperiod stress under a light intensity above 50 µmol m^{-2} s^{-1} (Figure 3.1 E). An increase in *ELIP1* expression has been characterized as a response to photoinhibitory conditions in the thylakoid (Casazza et al., 2005). *LHCB1* expression decreased statistically in response to PLP under a light intensity above 70 µmol m^{-2} s^{-1} (Supplementary Figure 1 E). *LHCB1* codes for light-harvesting chlorophyll-protein complex II (LHCII) and is known to be down-regulated by high light stress (Jansson et al., 1992; Floris et al., 2013). Therefore, the change in expression level of *ELIP1* and *LHCB1* in response to photoperiod stress under different light intensities, adds to the evidence for a role of chloroplasts in photoperiod stress.

Although *ahk2 ahk3* is more sensitive to photoperiod stress (Nitschke et al., 2016), the threshold light intensity to induce photoperiod stress was still between 40-70 µmol m^{-2} s^{-1} similar to WT (Figure 3.2). This reinforces the fact that the minimum threshold intensity of ~50 µmol m^{-2} s^{-1}

during the PLP is quintessential for photoperiod stress to occur even in a more photoperiod stress sensitive background. The necessity for a comparable minimum light intensity in both WT and *ahk2 ahk3* adheres to a consistent pattern, mirroring the requirement for a uniform dark period of 5-7.5 hours for the induction of photoperiod stress in both WT and *ahk2 ahk3* (Nitschke et al., 2016).

Furthermore, it was also shown that a light intensity exceeding 120 µmol m^{-2} s^{-1} did not lead to stronger photoperiod stress symptoms (Figure 3.3). Besides, it appears that the lower threshold light intensity leads to a full photoperiod stress response (Figure 3.1, Supplementary Figure 1). This observation distinguishes the photoperiod stress response from the response to high light stress. Unlike high light stress response, which escalates with greater light intensity (Essemine et al., 2012), the photoperiod stress response remains unaffected by an increase in light intensity beyond the minimum light intensity required to induce the photoperiod stress.

Light intensity exerts a pivotal influence on the modulation of responses to various abiotic stresses, including drought. In apples experiencing progressive drought, elevated light intensities corresponded to a higher loss of relative water content. However, at a higher light intensity, reduction in net photosynthesis rate and stomatal conductance were slower, while concurrently showcasing heightened activities of antioxidant enzymes, such as ascorbate and peroxidase (Ma et al., 2015). In the case of rice, escalating light intensity and water stress both contributed to an increase in protein content. Notably, malondialdehyde content rose specifically under heightened water stress conditions in the presence of higher light intensity (Chatterjee et al., 2021). Beyond its impact on abiotic stress, light intensity plays a crucial role in SAR. Avirulent bacterial infection in the dark failed to induce SAR. However, at a light intensity of 70 µmol m^{-2} s^{-1}, SAR was triggered, accompanied by SA accumulation. Interestingly, at a higher light intensity of 500 µmol m^{-2} s^{-1}, SAR developed without a concurrent increase in SA levels (Zeier et al., 2004). Additionally, there is speculation that chloroplastic ROS may contribute to hypersensitive response-mediated cell death (Lukan and Coll, 2022). These examples emphasize that the different light intensities can have different effects on other abiotic stresses as well, just like they have an effect on photoperiod stress. However, these examples do not truly mirror the light intensity dependence of photoperiod stress because it is a novel abiotic stress, who's main cause is differential light treatment, while in other abiotic stresses stated here, light intensity is a secondary factor.

4.1.2 A regular light and dark rhythm followed by a prolonged light period is necessary for the induction of photoperiod stress

Since a threshold light intensity of ~50 µmol m^{-2} s^{-1} is necessary to cause photoperiod stress, it was questioned whether only a change in light intensity without a PLP would also lead to photoperiod

stress. The results suggest that a change in light intensity from 100 µmol m^{-2} s^{-1} to 300 µmol m^{-2} s^{-1} without a PLP does not lead to photoperiod stress (Figure 3.4). This result reinforces the fact that a PLP is essential for photoperiod stress. It was also previously shown by Abuelsoud et al. (2020), that a PLP of at least 1 h is necessary for the induction of photoperiod stress.

Since PLP is essential for the induction of photoperiod stress, the question arose whether photoperiod stress symptoms would also appear in plants grown in CL or in CL with a single dark period. According to the ROS measurements, these plants did not show any photoperiod stress (Figure 3.5). Therefore, it can be concluded that an entrainment through a regular light and dark rhythm which is later disturbed by a PLP is crucial for causing photoperiod stress. This was also shown by Nitschke et al. (2016) in a similar experiment, where leaf necrosis was used as a read-out for photoperiod stress. Since, light signals are important Zeitgeber for the circadian clock (McClung, 2006), this result additionally indicates an important role of the circadian clock in photoperiod stress which will be discussed in later sections.

4.1.3 Retrograde signaling may participate in photoperiod stress

Retrograde signals originate in cell organelles such as chloroplasts and mitochondria in response to environmental cues and regulate nuclear gene expression, both for the development and for stress responses (Mielecki et al., 2020). Several mutants of retrograde signaling which are also involved in chloroplast development showed only a weak response to photoperiod stress (Figure 3.6).

Amongst the *gun* mutants, which are well-known retrograde signaling mutants. *gun4* and *gun5* mutants showed a lower photoperiod stress phenotype than WT, indicating their involvement in photoperiod stress sensing (Figure 3.6). GUN4 regulates the Mg-chelatase enzyme, whose chlH subunit is coded by GUN5 (Mochizuki et al., 2001; Peter and Grimm, 2009). Mg-chelatase catalyzes the conversion of PPIX to Mg-PPIX chlorophyll intermediates (Mochizuki et al., 2001). Mutation of either of these genes reduces Mg-chelatase activity resulting in low levels of chlorophyll biosynthesis intermediates, Mg-PPIX and protochlorophyllide which are candidates for plastid-derived signaling molecules functioning in stress signaling (Strand et al., 2003; Ankele et al., 2007). If Mg-PPIX would act as a retrograde signal in photoperiod stress sensing, it might explain the low photoperiod stress phenotype of *gun4* and *gun5*. However, the claim for Mg-PPIX as a potential retrograde signaling molecule has been challenged and instead, heme has been argued as the more probable retrograde signal (Mochizuki et al., 2008; Moulin et al., 2008). As an example of their role in abiotic stress, recently, GUN4 and GUN5 were identified as interactors of EXECUTER1 (EX1) and EX2 in plastids resulting in the suppression of PIF activity in the response to high light stress and thus impacting nuclear gene

expression (Li et al., 2023). This indicates that these proteins are involved in specific functions distinct from other GUN proteins. Interestingly, under control conditions, *gun4* and *gun5* showed higher peroxide levels than WT (Supplementary Figure 6 A). Li et al. (2021) also observed a higher ROS in rice *gun4* mutant grown at 100 µmol m^{-2} s^{-1}. However, for *gun5* most studies show similar ROS levels as WT under a control state (Voigt et al., 2010; Cheng et al., 2010) Nonetheless, it should be kept in mind that these studies used visual methods such as 3,3'-diaminobenzidine (DAB) staining, which quantifies ROS differently compared to the method used in this work (Daudi and O'Brien, 2012; Abuelsoud et al., 2020) (also see section 2.6).

gun6, which is an overexpression mutant of heme producing ferrochelatase I (FCI) enzyme (Woodson 2011), showed a higher ROS level and *BAP1* expression than WT (Figure 3.6 B, D). In the last years, heme has garnered recognition as a positive retrograde signal (Woodson et al., 2011; Richter et al., 2023). It could be that higher retrograde signaling through heme in *gun6* could have contributed to its slightly stronger photoperiod stress response.

gun1 mutants have a similar photoperiod stress level as WT, which indicates no direct involvement of GUN1 in photoperiod stress sensing and/or signaling (Figure 3.6). It was reported that *gun1* was insensitive to Mg-PPIX accumulation (Koussevitzky et al., 2007). Also, although GUN1 interacts with the proteins involved in the chlorophyll biosynthesis pathway, its direct involvement in this pathway has not yet been reported (Shimizu and Masuda, 2021). The role of retrograde signaling molecules in photoperiod stress deserves further investigation.

glk1 glk2 double mutants also showed lower photoperiod stress symptoms than WT indicating their requirement in generating photoperiod stress response (Figure 3.6). GLKs are also involved in chlorophyll biosynthesis and chloroplast development (Langdale and Kidner, 1994; Waters et al., 2009). In *glk1 glk2* mutants, *GUN4 and CHLH (GUN5)* expression was downregulated, and the level of Pchlide, which forms downstream of Mg-PPIX was lower (Waters et al., 2009). Therefore, perhaps GLKs act in the same pathway as GUN4 and GUN5 in responding to photoperiod stress.

rcd1 also showed lower photoperiod stress symptoms than WT, indicating a role for RCD1 in photoperiod stress (Figure 3.6). *rcd1* is known to develop cellular $O_2^{\cdot -}$ and transient spreading lesions in response to ozone (O_3) and extracellular $O_2^{\cdot -}$, but not H_2O_2 (Overmyer et al., 2000). In response to oxidative stress, *rcd1* was reported to show lesions that resemble the hypersensitive response that is caused by a compatible host-pathogen interaction (Overmyer et al., 2000). Despite being sensitive to a certain kind of oxidative stress, *rcd1* is resistant to chloroplast ROS caused by paraquat (Sipari et al., 2022). Furthermore, several antioxidants including tocopherol were reported to be elevated in *rcd1* (Sipari et al., 2022). Perhaps, the *rcd1* mutant shows less sensitivity to photoperiod stress due to elevated antioxidant levels. It might be interesting to measure the antioxidant levels in *rcd1* before and

after photoperiod stress provocation. Shapiguzov et al. (2019) reported that RCD1 interacts with and suppresses the activity of TFs ANAC013 and ANAC017, which mediate a ROS-related retrograde signal originating from mitochondrial complex III. The exact function of RCD1 in enhanced ROS signaling caused by photoperiod stress and whether mitochondrial processes are involved remains to be determined.

CAB2 (LHCB1.1) expression is decreased due to photoperiod stress (Frank et al., 2020). *LHCB1* expression showed a tendency to be lowered in WT by photoperiod stress and is strongly decreased in *gun6* in response to photoperiod stress (Figure 3.6 E). Both WT and *gun6* are sensitive to photoperiod stress (Figure 3.6 B-D). On the other hand, *gun4, gun5, glk1 glk2,* and *rcd1,* the retrograde signaling mutants that have low photoperiod stress sensitivity, had similar *LHCB1* expression under control and photoperiod stress conditions (Figure 3.6 B-E). This adds to the argument that retrograde signaling could be involved in causing photoperiod stress.

Retrograde signaling is also known to be involved in several other abiotic stresses such as heat stress, drought, and salinity that lead to oxidative stress in several plant species such as *Arabidopsis, Nicotiana*, and tomato (Sun and Guo, 2016; Crawford et al., 2018).

DCMU is an inhibitor of photosystem II (PSII) and drastically reduces its efficiency (Khandelwal et al., 2008). On the reducing side of the PSII to plastoquinone (PQ) pool, DCMU blocks the electron flow from the primary quinone electron acceptor (Q_A) to the secondary quinone electron acceptor (Q_B). This reduces the amount of O_2 generation by splitting the water molecule (Metz et al., 1986; Pansook et al., 2019). Additionally, in vitro DCMU has been reported to decrease the photodamage and degradation of D1 protein (Krieger-Liszkay, 2004). Several redox-regulated genes were differentially regulated upon DCMU application, out of which 232 genes were directly regulated by photosynthetic electron transport (Fey et al., 2005). Application of DCMU 4 h before the beginning of the dark period in the plants reduced the photoperiod stress symptoms (Figure 3.7 A-C). This is, therefore, an additional indication of the role of chloroplasts in sensing photoperiod stress.

4.1.4 Accumulation of starch and sugars at the end of photoperiod stress

According to the results presented in this study, during the day following PLP and in the early morning following the night after PLP, a notable increase in starch content was observed compared to control conditions (Figure 3.8 B). In a similar experiment conducted by Lu et al. (2005), where plants originally grown under SD conditions were transferred to LD, an accelerated rate of starch degradation was observed during the shorter night, and by the end of the night, leaf starch concentration was notably

higher compared to control plants that remained under SD conditions. These findings from Lu et al. (2005) align with the results obtained in this study.

Furthermore, although glucose concentrations were similar to the control during the day following a 16 h PLP, they were higher than the control early next morning (Figure 3.8 C). Lu et al. (2005) also had previously reported a higher glucose level towards the end of the night in plants shifted from SD to LD conditions. Perhaps, the likely higher rate of starch degradation during the photoperiod stress-inducing night would have resulted in higher glucose levels the following morning.

Lu et al. (2005) had also reported a significant increase in sucrose concentration during and at the end of the night following the extended light period which is in contrast to the results presented in this study. Sucrose and fructose concentrations were elevated at the end of the day following the PLP but returned to control levels in the early morning following the night (Figure 3.8 D-E).

More conclusive insights could have been drawn from the present study if sampling had also been conducted during the 16 h PLP and the photoperiod stress-inducing night (see Figure 3.8 A for the experimental setup). Besides Arabidopsis, continuous light treatment in tomato and rocket plants led to a higher starch and sugar accumulation as well (Haque et al., 2015; Proietti et al., 2021).

It is noteworthy that CK signaling mutants that display increased sensitivity to photoperiod stress are hypersensitive to sugars (Franco-Zorrilla et al., 2005). However, although Nitschke (2015), also observed a higher starch concentration in all photoperiod-stressed plants, no difference in starch levels between WT and CK deficient mutants was reported. Probably higher stress sensitivity of CK deficient mutants is not associated with higher starch accumulation during photoperiod stress.

The fact that starch synthesis mutants such as *adg1, adg2,* and *pgm*, showed lower photoperiod stress symptoms compared to WT (Figure 3.9), supports a relevant role of the starch metabolism in photoperiod stress. Alongside, a starch accumulating mutant, *sex1* also showed a lower photoperiod stress sensitivity than WT (Figure 3.9). During the dark period, *adg1* and *sex1* mutants accumulate lower sucrose and glucose levels than the WT (Matsoukas et al., 2013). Lower sugar levels in these mutants during the dark period could be a possible reason for their lower photoperiod stress response. Therefore, correspondingly higher sugar levels in WT during the photoperiod stress treatment might cause the stress symptoms. Additional work needs to be done to support this possibility.

Whether or not starch or sugar accumulation may be (partly) causative for the symptoms of the photoperiod stress response is unclear. In the upcoming sections, I will delve into the mechanisms by which elevated sugar levels might impact the response to photoperiod stress.

There are several links between sugars and ROS generation. ROS (high peroxide level) is induced by photoperiod stress and made responsible for at least part of its consequences (Abuelsoud

et al., 2020). Sugars have a dual role concerning ROS by either being involved in ROS producing metabolic pathways or acting as ROS scavengers (Couée et al., 2006). Both low and high sugar levels have been reported to trigger ROS production (Keunen et al., 2013). Glucose is the main carbon precursor for ascorbate and carotenoid (Fanciullino et al., 2014), which act in defense against oxidative stress (Stahl and Sies, 2003; Akram et al., 2017). Moreover, soluble sugars such as glucose can feed into NADPH producing pathways such as the oxidative pentose phosphate (OPP) pathway, which aids in ROS scavenging (Couée et al., 2006). On the flip side, it has been reported that high glucose concentration can activate NADPH oxidase in animal cells (Bonnefont-Rousselot, 2002). NADPH oxidases, also known as respiratory burst oxidase homologs (RBOHs) are major ROS synthesizing enzymes in the apoplast (Qi et al., 2017; Hu et al., 2020).

Another interesting link between sugars and photoperiod stress comes from the known role of sugars in the entrainment of the circadian clock (Müller et al., 2014). Under red and blue light and darkness, sucrose was found to stabilize the circadian period (Philippou et al., 2019). SnRK1, which regulates starch biosynthesis and carbohydrate metabolism, also regulates the activity of TF bZIP63 (Wang 2017, Frank 2018 from Philippou 2019). bZIP63 subsequently promotes *PRR7* expression in response to low sugar levels (Haydon et al., 2013; Mair et al., 2015). Furthermore, a mutation in *TREHALOSE 6-PHOSPHATE SYNTHASE I (TPSI)*, which synthesizes sugar signaling molecule trehalose-6-phosphate, leads to the insensitivity of the circadian oscillator to sucrose (Frank et al., 2018). The circadian clock has been identified as an important player in the development of photoperiod stress. Therefore, it might be that higher sugar levels cause photoperiod stress symptoms through a disturbed circadian rhythm. However, GI has also been identified as a signaling component required for clock regulation by sucrose (Dalchau et al., 2011), but *gi* mutants tested in this study are similarly photoperiod stress sensitive as WT (Figure 3.22). Therefore, the possibility that higher sugar levels cause photoperiod stress symptoms through disturbed circadian rhythm is not entirely clear and requires further investigation.

Another possible link between the sugar concentration in plant cell and a plant's stress response is autophagy (Rensburg and Ende, 2018). Autophagy is a major pathway responsible for the recycling of cellular components in response to both stress and non-stress conditions (Rensburg and Ende, 2018). UDP-glucose has been proposed as a signaling molecule for autophagy (Rensburg et al., 2019). Indeed, higher glucose leading to a disturbance in ROS homeostasis has been cited as the reason for root tissue damage via autophagy (Huang et al., 2019). Also, UDP-glucose accumulating rice mutant seedlings developed a spontaneous PCD phenotype (Xiao et al., 2018). It has been proposed that extracellular glucose could be interpreted in plants as damage associated molecular pattern (DAMP) (Versluys et al., 2017). DAMPS are danger signals emitted by both plants and animal cells when faced

with stress (Hou et al., 2019). The sugar sensing Sucrose nonfermenting 1-related kinase 2/Target of Rapamycin (SnRK2/TOR) nexus has been suggested to be triggered in response to excess sugar and stimulate autophagy (Rensburg et al., 2019). In a yet to be published data, Roeber et al. showed that *snRK2.8* mutants were more susceptible to photoperiod stress than WT, indicating a possible involvement of this pathway in sensing and/or responding to photoperiod stress (V. Roeber, personal communication).

Other reports document the protective role of sugars in different species under different stress conditions. Unlike under photoperiod stress, under other abiotic stress conditions such as salt and drought stress, starch is depleted and hydrolyzed to form sugar derivatives that support a plant cell in maintaining the osmotic balance of the cell and protect membranes and proteins from damage (Krasensky and Jonak, 2012). During the early stages of cold acclimation, *sex1* mutants accumulated lower levels of glucose and other sugar derivatives, which resulted in their higher stress sensitivity (Yano et al., 2005). Similarly, in Jatropha seedlings, chilling stress caused hydrolysis of starch and accumulation of sugars, which was important for developing resistance to the chilling stress (Wang et al., 2018).

Taken together, results from this study indicate that starch metabolism plays a role in photoperiod stress. It has been speculated in this section that higher sugar levels during the PLP and at the end of the stress-inducing night could contribute to the development of photoperiod stress symptoms. It could contribute to photoperiod stress symptoms development through various pathways such as ROS signaling, circadian rhythm, and autophagy as described above.

4.2 Photoreceptors are sensors of photoperiod stress

4.2.1 Both monochromatic red and blue wavelengths can induce photoperiod stress

Chlorophyll, the predominant pigment responsible for light absorption in plants, exhibits absorption peaks within the red and blue wavelength range. Photoreceptors also absorb light of these specific wavelengths. Red and blue wavelengths are known to influence several physiological and morphological processes in plants such as germination, photosynthesis and regulation of circadian rhythm (Devlin and Kay, 2000; Liu and Van Iersel, 2021; Wei et al., 2023) Consequently, an investigation was conducted to determine whether exposure to monochromatic red and blue light induces photoperiod stress (see section 3.5). Both monochromatic red and blue light during the PLP could induce photoperiod stress (Figure 3.10). However, the output of each tested photoperiod stress symptom differs quantitatively. Despite having equivalent Photosynthetically Active Radiation (PAR)

levels (refer to Table 2.9), monochromatic red and blue wavelengths generally induced lower photoperiod stress symptoms compared to white light. This suggests that a blend of diverse wavelengths contributes to more pronounced photoperiod stress symptoms. White light encompasses all wavelengths within the 400-700 nm range, encompassing both red and blue wavelengths, among others. It is plausible that the combined effect of red and blue wavelength ranges, along with others present in white light, exerts a more significant impact, ultimately leading to heightened photoperiod stress symptoms. This was partly confirmed by results in Figure 3.12, which shows that the level of photoperiod stress symptoms caused by 1:2:1 B:R:Fr are comparable to those caused by white light. This has also been discussed later in this section.

Red light had tended to cause stronger photoperiod stress symptoms than blue light, especially according to peroxide levels (Figure 3.10 B). Blue light is known to increase antioxidant content in several plant species (Piovene et al., 2015). This could be a possible explanation for the low peroxide levels under photoperiod stress induced by blue light.

Red and blue light photoreceptors *phyB* and *cry2* mutants that showed lower photoperiod stress symptoms than WT under 16 h white light PLP (Figure 3.14-Figure 3.15) were also tested under 8 h PLP in white light, monochromatic red light, and monochromatic blue light. Very low stress symptoms were observed in *phyB* in response to red light treatment, which suits the expectations from a red-light receptor mutant that is assumed to not perceive the monochromatic red light during PLP. Therefore, this experiment confirmed the relevance of phyB and red light in photoperiod stress.

Under blue light, the ROS levels in WT and the mutants *phyB* and *cry2* were minute and similar to each other and in general lower than in red light as also mentioned above (Figure 3.10 B). Although the stress marker gene expression in WT under blue light was as high as under red light, it was expected that the stress marker gene expression in *cry2* under blue light would be lower than WT. However, the *ZAT12* and *BAP1* expression under blue light was similar in WT and *cry2.* This can be ascribed to the existence of a fully functional copy of CRY1, a cryptochrome known for its greater stability at higher intensity blue light, within the *cry2* mutants (Lin et al., 1998). This intact CRY1 copy may still possess the capability to perceive blue light and decode the corresponding signal leading to photoperiod stress symptoms. However, the exact reason for this anomaly is difficult to explain since the stress marker gene expression in *cry2* was much lower than WT in response to photoperiod stress due to 16 h PLP in white light (Figure 3.15 B). Surprisingly, *BAP1* expression in *phyB* under PLP in blue light was higher than WT. This could be due to an experimental variation because this was not observed in the repetition of the experiment. In order to obtain further evidence for the role of monochromatic red and blue light and corresponding photoreceptors in photoperiod stress, *phyB cry1 cry2* triple mutants could also be tested under photoperiod stress inducing conditions as described in Figure 3.10 A.

A 1:2:1 ratio of B:R:Fr caused similar levels of photoperiod stress symptoms as white light (Figure 3.12). This is consistent with the previous result showing that white light causes stronger photoperiod stress than monochromatic red and blue light (Figure 3.10). A 1:2:1 ratio of monochromatic lights was selected because it mirrors the ratio of red, blue, and far-red light in the white light of the climate chamber which has been used for these experiments (Table 2.9). The light intensity of monochromatic blue, red, and far-red light was adjusted such that together the PAR of 1:2:1 B:R:Fr was similar to that of white light in the climate chamber.

Natural sunlight generally has an R:Fr ratio of 1.2 (Holmes and Smith, 1975). Also, according to data obtained in April 2020 in Potsdam-Golm at (52°24'55.5"N 12°58'08.9"E) (Supplementary Figure 7, data courtesy of Virginie Mengin, Max Planck Institute, Golm) on a clear as well as cloudy day, the R:Fr ratio was observed to be ~1.4 during the day. Hence, I investigated the impact of a comparable R:Fr ratio (R:Fr set at 1:1 in our experiments) using only monochromatic lights on photoperiod stress. The findings revealed that a 1:1 R:Fr ratio tended to elicit more pronounced photoperiod stress symptoms than exposure to white light (Figure 3.11). Conversely, shade-like conditions with lower R:Fr ratios, known to induce shade avoidance responses in plants (Casal, 2012), did not induce photoperiod stress (Figure 3.13). phyB is widely recognized for its role in detecting the R:Fr ratio in natural settings. In conditions resembling shade, characterized by low R:Fr ratios, the active Pfr form of phyB decreases (Franklin and Whitelam, 2005). Given the demonstrated involvement of phyB in photoperiod stress (Figure 3.14), it is plausible that the diminished concentration of the Pfr form of phyB during the PLP under shade-like conditions might result in plants failing to perceive the PLP, ultimately leading to non-induction of photoperiod stress symptoms. However, the effect of shade-like conditions on photoperiod stress has only been tested once and needs to be repeated for more concrete evidence. Consequently, these results substantiate the proposition that a higher R:Fr ratio is promotive in inducing photoperiod stress.

However, as mentioned earlier, the ratio of 1:2:1 for B:R:Fr light yielded photoperiod stress symptoms similar to those induced by white light, even with a higher R:Fr ratio (Figure 3.12). This observation suggests the possibility of a protective effect against photoperiod stress attributed to blue light. This is corroborated by the fact that PLP under monochromatic blue light led to lower peroxide levels in WT than in monochromatic red light (Figure 3.10 B).

Light quality is known to have an impact on other abiotic stress responses as well. For instance, different light quality can have a direct impact on responses to drought stress in plants. Blue light-induced stomatal opening mediated by CYCLIN H;1 (CYCH;1) via ROS modulation is important for drought stress tolerance (Zhou et al., 2013). Furthermore, Gyugos et al. (2021) observed an augmented accumulation of several free amino acids in wheat under far-red light in response to drought, as

compared to exposure under blue and red light. Additionally, diverse light spectra exert distinct effects on photosynthesis, a process often targeted by abiotic stressors such as cold (Janda et al., 2020). Kameniarová et al. (2022) demonstrated that under cold stress, red light treatment led to higher induction of chloroplast-related genes, which corresponded to higher photosynthetic parameters.

4.2.2 Photoreceptors CRY2 and phyB play a role in sensing photoperiod stress

In light of the insights presented in section 4.2.1, where it was established that monochromatic red and blue light can induce photoperiod stress and the eminent roles that photoreceptors play in many aspects of plant life, an exploration into the function of red and blue light photoreceptors in photoperiod stress was initiated. To delve into this aspect, photoreceptor mutants were subjected to photoperiod stress conditions. The aim was to ascertain whether photoperiod stress persists even when the ability to perceive a specific light wavelength is impaired due to a corresponding photoreceptor mutation. Among the phytochromes, *phyB* showed lower photoperiod stress symptoms than WT, indicating a relevant role of phyB in sensing photoperiod stress (Figure 3.14). The difference in the response of *phyB* and *phyA* might be explained by the fact that phyB is the major photoreceptor responsible for the perception of higher intensity red light (McCormac et al., 1993; Reed et al., 1994; Somers et al., 1998). Nevertheless, the incorporation of the *phyB* mutation into *ahk2 ahk3* did not alleviate the pronounced photoperiod stress phenotype, possibly due to the continued activity of other photoreceptors, such as CRY2, which appears to exert a more significant influence on photoperiod stress (Figure 3.15). Additionally, the CK receptor pathway, recognized for its pivotal role in shielding against photoperiod stress (Nitschke et al., 2016; Frank et al., 2020) is impaired in *phyB ahk2 ahk3*. It is plausible that the *phyB* mutation alone may not suffice to counteract these effects.

Since both *cry2* and *cry2 ahk2 ahk3* showed very low sensitivity to photoperiod stress (Figure 3.15), it can be concluded that CRY2 plays an important role in the sensing of photoperiod stress. Although CRY2 is photolabile and CRY1 is the more light-stable cryptochrome (Lin et al. 1998), *cry1* was as sensitive to photoperiod stress as the WT (Figure 3.15), indicating no important role of CRY1 in photoperiod stress.

The role of CRY2 in sensing photoperiod stress primarily may be attributed to the role of CRY2 in blue light input to the circadian clock (Devlin and Kay, 2000). It was recently shown that CRY2 interacts with three subunits of METTL3/14-type N6-methyladenosine RNA methyltransferase (m^6A writer) that drives methylation of several mRNAs regulated by the circadian clock (Wang et al., 2021). Also, Mo et al. (2022) observed that CRY2 together with TEOSINTE BRANCHED1-CYCLOIDEA-PCF 22

(TCP22) form photobodies in a blue-light dependent manner, whose characteristics are regulated by CRY2 interacting proteins, PHOTOREGULATORY PROTEIN KINASES (PPKs). They proposed that these alongside LIGHT REGULATED WDs (LWDs) might regulate *CCA1* expression (Mo et al., 2022). Mathematical models have suggested that LWD1 interacts with the TFs, TCP20 and TCP22, and associates directly with *CCA1* (Mo et al., 2022). CRY2 interacts with the clock core component PRR9 in a blue-light dependent manner and light dose-dependent CRY2 decay has been proposed as a mechanistic explanation for the impact of light intensity on circadian pace (He et al., 2022). It has been shown previously that the circadian clock plays an important role in photoperiod stress (Nitschke et al., 2016; Nitschke et al., 2017). The potential role of the circadian clock alongside photoreceptors in sensing photoperiod stress will be further discussed.

Under LD conditions, the expression of *CO*, a crucial floral integrator, is observed to be diminished in *cry2* mutants (Guo et al., 1998). Furthermore, CRY2 is recognized for its role in stabilizing CO through its interaction with CIB1 (Liu et al., 2018). Analysis of flowering pathway mutants has shown that CO could be involved in photoperiod stress (Figure 3.22, section 4.3). It is probable that PLP, which is a prerequisite for photoperiod stress, is perceived in plants as an LD stimulus. The stabilization of CO by CRY2 during this perceived LD could be important for the emergence of photoperiod stress symptoms.

The precise mechanism and downstream signaling of CRY2 to cause photoperiod stress needs further investigation. This will be discussed under future perspectives (see section 5.2).

Among the phototropin mutants, *phot2* showed a strong photoperiod stress phenotype indicating a possible role of PHOT2 in protection against photoperiod stress. However, the double mutant *phot1 phot2* showed a similar photoperiod stress phenotype as WT (Figure 3.16). This might be explained by the role of phototropins in chloroplast relocation (Christie, 2007). As reported by Luesse et al. (2010) exposure to 100 µmol m^{-2} s^{-1} of blue light led to an attenuated chloroplast avoidance response in 5-6-week-old *phot2* mutants, while no chloroplast movement was observed in *phot1 phot2* mutants. Luesse et al. (2010) attributed this phenotype to the inhibition of PHOT1-dependent chloroplast accumulation by PHOT2. In our experiments, the absence of chloroplast avoidance response in *phot2* mutants during the PLP could potentially contribute to more pronounced photoperiod stress symptoms. Applying the same reasoning, the introgression of the *phot1* mutation into *phot2* eliminates chloroplast movement, possibly explaining similar photoperiod stress levels in *phot1 phot2* mutants as the WT. However, it remains to be tested whether chloroplast avoidance occurs in response to photoperiod stress.

ztl mutants exhibited similar photoperiod stress symptoms as WT, indicating no direct involvement of ZTL in photoperiod stress (Figure 3.16). Besides being a blue light receptor, ZTL is an

important component of the photoperiodic flowering pathway. ZTL regulates the circadian clock component TOC1 at the protein level (Más et al., 2003). *TOC1* expression was higher in photoperiod stress sensitive CK mutants in response to photoperiod stress, but *toc1* mutants showed a photoperiod stress sensitivity similar to WT (Nitschke, 2015). This indicated an ambiguous role of *TOC1* in photoperiod stress (Nitschke, 2015). Therefore, ZTL and downstream signaling components of ZTL do not seem to play an important role in photoperiod stress.

uvr8 mutants showed much lower photoperiod stress symptoms than WT (Figure 3.18), which could indicate a probable role of UVR8 in sensing photoperiod stress. UVR8 is a UV-B photoreceptor. However, the climate chamber where the plants were exposed to the PLP does not have a source of UV-B radiation. This raised the question of how the UVR8 might be involved in photoperiod stress. It was shown recently that UVR8 monomerized at the wavelength of 300-315 nm and even weakly modulated the gene expression under blue light (Rai et al., 2020). Modulation of blue light signaling by UVR8 in photoperiod stress could possibly explain the low photoperiod stress symptoms in *uvr8* mutants. RUP1 and RUP2 are responsible for the re-dimerization and repression of UVR8 (Tilbrook et al., 2013). The double mutants *rup1 rup2* showed only similar levels of photoperiod stress symptoms as WT rather than higher, indicating that RUP1 and RUP2 are not involved in photoperiod stress (Supplementary Figure 5). Also, the introgression of the *uvr8* mutation in *ahk2 ahk3* did not rescue the strong photoperiod stress phenotype. Thus, the mechanism of photoperiod stress sensing by UVR8 is complex and needs further investigation.

4.2.3 Known downstream light signaling might be relevant in photoperiod stress

Since photoreceptors play a role in sensing photoperiod stress, known downstream light signaling components were tested for their role in photoperiod stress. *cop1, spa1 spa2,* and *spa3 spa4* showed similar photoperiod stress symptoms to WT, which indicates a lack of involvement of the corresponding proteins in photoperiod stress symptom development (Figure 3.19). On the other hand, it is possible that these mutants did not present with lower photoperiod stress symptoms because of the functional redundancy of the corresponding proteins (Fittinghoff et al., 2006).

hy5 showed slightly lower stress symptoms according to stress marker gene expression (Figure 3.18 B-C). However, since COP1 and SPA do not seem to have a role in photoperiod stress, HY5 might be acting in photoperiod stress through other pathways than those known for light signaling. HY5, in response to an unknown retrograde signal, was found to convert from a positive regulator of phANG to a negative regulator (Sun and Guo, 2016). As discussed before, retrograde signaling is important for photoperiod stress. Therefore, HY5 might act through retrograde signaling in

photoperiod stress. However, this possibility remains to be verified through further mutant analysis or retrograde signaling gene expression analysis in *hy5*. Additionally, HY5 binds directly to the promoter of *ELF4* (Li et al., 2011a), one of the critical components assuring the stability of the clock for a proper response to photoperiod stress (Nitschke et al., 2016).

PIF1-OX mutants showed strongly reduced stress marker gene expression in response to photoperiod stress (Figure 3.19 B-C), indicating a probable role of PIF1 in protection against photoperiod stress. It would make one expect that *pifQ* would experience stronger photoperiod stress than WT. However, it should be noted that *pifQ* was only similarly stressed as WT (Figure 3.19). Perhaps, the assumed protective role of PIF1 in photoperiod stress is primarily dose dependent. PIFs also regulate the expression of *GLK1* (Martin et al., 2016), which plays an important role in photoperiod stress through retrograde signaling (see section 4.1.3). It was reported that *GLK1* expression was repressed by PIFs in darkness, an effect that was reversed by light-activated phytochromes. However retrograde signals act antagonistically against this derepression of *GLK1* (Martin et al., 2016). It would be interesting to uncover the interplay between retrograde signaling and light signaling pathways in photoperiod stress.

PIFs play an important role in response to other abiotic stresses as well. Gao et al. (2018) reported an increase in water storage and drought resistance in *ZmPIF1* overexpression transgenic rice. Accumulation of PIFs is regulated in plants at the transcriptional level and by post-translational modifications, which helps plants respond to various abiotic stresses such as high and low temperatures and drought stress (for review: Saud et al., 2022).

Together this result indicates that known light signaling pathway could be relevant in photoperiod stress, however the exact mechanism of action of this pathway in photoperiod stress response is yet to be investigated.

4.2.4 Interaction of photoreceptors and circadian clock could contribute to photoperiod stress

Disturbance of the circadian clock is one of the main causes of photoperiod stress and clock mutant *cca1 lhy* is highly sensitive to photoperiod stress (Nitschke et al., 2016, 2017). It was tested if reducing the light input into the circadian clock of the *cca1 lhy* double mutant by the introgression of photoreceptor mutation would rescue the photoperiod stress symptoms in the *cca1 lhy* (Figure 3.20). None of the photoreceptor mutations were able to rescue the strong photoperiod stress phenotype of *cca1 lhy* (Figure 3.20). Although mutation in *CRY2* was able to rescue the strong photoperiod stress phenotype in *ahk2 ahk3* (Figure 3.15), it could not do so in the *cca1 lhy* clock mutant. Perhaps blocking a single photoreceptor may prove insufficient in impeding the light input to the circadian clock,

considering that both cryptochromes and phytochromes play roles in influencing the circadian clock through light input (Somers et al., 1998). Also, not only photoreceptors influence the clock, but the photoreceptors themselves are transcriptionally regulated by the circadian clock (Devlin, 2002).

CCA1 and *LHY* are morning phased genes (Shim and Imaizumi, 2015). In the context of photoperiod stress, the expression of these genes in both WT plants and the tested mutants was lower than the control levels at the conclusion of the night following PLP (Figure 3.21 A-B). This indicates a significant misregulation of the circadian clock, as corroborated by Nitschke et al. (2016). Intriguingly, a higher expression of *CCA1* was observed in the photoperiod-stressed *ahk2 ahk3* mutant compared to WT, contrary to the expected lower expression as also reported by Nitschke et al. (2016). This difference in the expression of *CCA1* in *ahk2 ahk3* could be due to the different WT controls in both studies, or due to experimental variation. In this study, relative expression was compared to the WT control just before subjective dawn, whereas Nitschke et al. (2016) compared it to the WT control at the beginning of the night (stress-inducing night for PLP-treated plants).

TOC1, an evening gene (Shim and Imaizumi, 2015), exhibited higher expression in all tested genotypes under photoperiod stress compared to their respective controls (Figure 3.21 C). This further underscores the circadian rhythm misregulation in plants experiencing photoperiod stress. Nitschke et al. (2016) also demonstrated increased *TOC1* expression in photoperiod-stressed WT plants. Notably, under photoperiod stress, the expression of *TOC1* in *cry2* was lower than in the WT (Figure 3.21 C). This deviation was absent in the control conditions, suggesting no intrinsic differential regulation of *TOC1* in *cry2* (Figure 3.21 C). While Nitschke (2015) proposed that the heightened *TOC1* expression under photoperiod stress might result from dysregulation of *CCA1* and *LHY*, data from the present study shows similar expression patterns of *CCA1* and *LHY* in *cry2* and WT (Figure 3.21 A-B). Consequently, the correlation between lower *TOC1* expression and reduced photoperiod stress symptoms in PLP treated *cry2* plants remains unclear. Previous studies have indicated that under blue light, plants with silenced *toc1* gene exhibit a free-running period 3-4 hours shorter than WT (Más et al., 2003), while the *cry1 cry2* double mutants show a longer period length than WT (Devlin and Kay, 2000). These opposing effects of *TOC1* and *CRY2* on the period length may contribute to the observed stability of *TOC1* expression in *cry2* under photoperiod stress. However, a comprehensive understanding of the significance of *TOC1* expression in *cry2* during photoperiod stress requires further investigations into period length dynamics.

As *CHE* expression is regulated by CCA1 binding to the *CHE* promoter (Pruneda-Paz et al., 2009), and *CCA1* expression undergoes misregulation in response to photoperiod stress, a misregulation of *CHE* expression was anticipated. Surprisingly, no statistically significant difference in *CHE* expression was observed between control and photoperiod-stressed WT plants, consistent with

the findings of Nitschke (2015). Nevertheless, *CHE* expression exhibited a substantial decrease in photoperiod stress-sensitive *ahk2 ahk3* and *cry1 ahk2 ahk3* plants under photoperiod stress conditions (Figure 3.21 D), a trend also noted by Nitschke (2015) for *ahk2 ahk3*. In contrast, under photoperiod stress conditions *CHE* expression in *cry2* plants was significantly higher than in WT and introducing the *cry2* mutation into *ahk2 ahk3* resulted in WT level *CHE* expression (Figure 3.21 D). Notably, Nitschke (2015) observed that *che-2* mutants demonstrated stronger photoperiod stress symptoms than WT, and thus proposed a protective role of *CHE* in photoperiod stress (Nitschke, 2015). However, the paradoxical scenario of consistently high *CHE* expression in *cca1 lhy* mutants (Pruneda-Paz et al., 2009), which are also sensitive to photoperiod stress (Nitschke et al., 2016; 2017), raises questions about the exact mechanism through which elevated *CHE* expression in *cry2* confers protection against photoperiod stress. This intriguing aspect warrants further in-depth studies to unravel the intricate relationship between *CHE* expression levels and the response to photoperiod stress.

These findings suggest a crucial involvement of CRY2, in conjunction with the circadian clock oscillator, in the sensing of photoperiod stress. However, a comprehensive understanding of the precise action mechanism of CRY2 in photoperiod stress necessitates further exploration into its role within the circadian clock.

4.3 Possible involvement of photoperiodic flowering pathway in sensing photoperiod stress

A prolonged light period causes in SD-entrained plants the activation of the photoperiodic flowering pathway, which is often used experimentally for its controlled induction (Corbesier et al., 1996; Imaizumi et al., 2003; Torti et al., 2012). Photoperiodic flowering works in close concert with the circadian clock as time cues are crucial for observing the changes in the daylength (see section 1.8). Therefore, some photoperiodic flowering pathway mutants were tested under photoperiod stress to investigate if this pathway is also involved in photoperiod stress.

According to ROS level, *co* and *ft tsf* mutants showed lower photoperiod stress symptoms than WT but had similar stress marker gene expression (Figure 3.22). In the other tested mutants, *gi* and *fkf1,* peroxide levels were similar to WT, but *ZAT12* and *BAP1* expression was higher (Figure 3.22). This difference in sensitivity towards different photoperiod stress markers makes the interpretation of the data difficult. However, from this result, it can be stated that *co* and *ft tsf* show generally lower photoperiod stress symptoms compared to WT. However, it should be noted that the *co-1* mutation studied in this experiment, is present in the L*er* background (Putterill et al., 1995), which has not been included here as a control. However, L*er*-0 showed ~27 % lower ROS than Col-0 (Figure 3.26 A) and

co-1 demonstrated nearly negligible ROS levels in response to photoperiod stress (Figure 3.22 A). Consequently, it can be anticipated that if L*er*-0 and *co-1* were compared directly for their response to photoperiod stress in a single experiment, *co* would likely display lower symptoms of photoperiod stress than L*er*-0.

The abundance of *CO* mRNA and protein has been shown to follow an external coincidence model closely tied to the circadian rhythm (Turck et al., 2008). Notably, in extended light periods, CO is known to be stabilized, leading to the activation of downstream genes, particularly of the one encoding the florigen FT (Wigge et al., 2005). Towards the end of an LD, both CRY1 and CRY2 contribute to the stabilization of the CO protein (Turck et al., 2008). The role of CRY2 in photoperiod stress has been emphasized in section 4.2.2 (Figure 3.15). It is plausible that PLP is perceived by plants as an LD, and CRY2-mediated stabilization and thereby activation of CO is important for the manifestation of the photoperiod stress symptoms. Thereby making CO an important factor for the induction of photoperiod stress symptoms. This may explain the reduced photoperiod stress symptoms observed in *co*.

CO functions as a positive regulator of *FT*, allowing for the indirect measurement of CO activity through the quantification of *FT* mRNA (Suárez-López et al., 2001). During the transition from SD to LD conditions, *FT* was upregulated in WT plants, contrasting with the lack of upregulation in *co* mutants (Wigge et al., 2005). Despite *FT* being upregulated in response to photoperiod stress (Cortleven et al., 2022; V. Roeber, personal communication), the strength of photoperiod stress symptoms in *ft* mutants matched that of WT (Figure 3.22). Additionally, the mutation of *TSF*, encoding a close homolog of *FT* regulated by CO similarly as *FT* (Yamaguchi et al., 2005), also did not change the photoperiod stress symptoms as compared to WT (Figure 3.22). However, the *ft tsf* double mutant displayed lower peroxide levels compared to WT in response to photoperiod stress (Figure 3.22). Perhaps, due to their homology, FT and TSF act redundantly in photoperiod stress downstream of CO. The observation that TSF acts redundantly with FT in promoting flowering transition (Yamaguchi et al., 2005), lends support to this argument.

Therefore, from the available data and arguments presented, a rough simplistic model can be proposed where CRY2 positively regulates CO, and CO in turn positively regulates *FT* and *TSF*, which ultimately leads to the development of photoperiod stress symptoms. FT is known to cause accumulation of *FRUITFULL (FUL)*, *SEPALLATA 3 (SEP3)*, and *AP1* transcripts in rosette leaves (Teper-Bamnolker and Samach, 2005). The accumulation of these genes together with the action of FD affects the flowering time (Teper-Bamnolker and Samach, 2005). Perhaps this pathway is also involved in photoperiod stress. Further experimental proofs are necessary for the validation of this model. One of the steps would be to study mutants of the downstream components of the photoperiodic flowering

pathway such as *SOC1, AP1, LFY, FUL, SEP3* and other mutant alleles of *CO* under photoperiod stress conditions.

Furthermore, activation of CO protein under LD conditions contributes to starch accumulation during floral transition through direct induction of *GRANULE BOUND STARCH SYNTHASE* (*GBSS*) gene expression (Ortiz-Marchena et al., 2014). Since starch accumulates in response to photoperiod stress (Figure 3.8), it might be possible that the flowering pathway and the starch metabolism pathway converge to realize the response to photoperiod stress.

The role of the FKF1-GI complex has been well studied in the context of the circadian rhythm (Kim, 2020). In fact, *gi* displayed a reduced expression of *CCA1* and *LHY* (Martin-Tryon et al., 2007) and *CCA1* and *LHY* are also involved in photoperiod stress development (Nitschke et al., 2016; 2017). Since both *gi* and *fkf1* developed a strong stress marker gene expression in response to photoperiod stress compared to WT (Figure 3.22), a role of GI-FKF1 could be proposed in photoperiod stress acting through the regulation of circadian rhythm. However, a detailed understanding of the mechanism requires further investigation.

The flowering pathway appears to be involved in responses to several abiotic and biotic stresses such as drought and freezing stress (Roeber et al., 2021; Chirivì and Betti, 2023). In Arabidopsis, cold induces *GI* expression (Fowler et al., 2005) and GI and CDF regulate several *COLD REGULATED (COR)* genes synergistically or antagonistically (Fornara et al., 2015). Accelerated flowering during drought provides the plants with an adaptive strategy called drought escape, allowing them to finish the life cycle before the severe stress leading eventually to lethality (McKay et al., 2003). During drought escape, *FT* and *TSF* are derepressed in an ABA and GI dependent manner, ultimately leading to flowering initiation (Riboni et al., 2016).

4.4 Photoperiod stress susceptibility is a rare phenotype amongst the ecotypes of *A. thaliana*

As a starting point for testing the effect of photoperiod stress in different ecotypes of *A. thaliana,* different accessions of the Columbia (Col) ecotype, that are genetically quite similar (Somssich, 2019, NASC) were tested under photoperiod stress. Not only Col-0, but other lines with the Col genetic background were equally sensitive to photoperiod stress (Figure 3.23). Col-0 is a direct descendent of Col-1 and was selected for further studies by Redei from a population of non-irradiated Laibach Landsberg population that was particularly responsive to the changes in photoperiod (NASC). This inherent sensitivity to the change in photoperiod could be a possible reason for the high sensitivity of the Col background to the photoperiod stress.

Some of the ecotypes that were genetically similar to Col-0 (similarity index ≥ 0.95) according to the genetic similarity matrix generated by the 1001 Genomes Consortium (2016) through SNP analysis were studied under photoperiod stress-inducing conditions. It was expected that these ecotypes might show a similar photoperiod stress phenotype compared to the Col-0. However, only the ecotype UKSE06-500 showed a similar photoperiod stress phenotype compared to Col-0 for both peroxide levels and stress marker gene expression (Figure 3.24). Most of these ecotypes displayed lower photoperiod stress levels than Col-0. These results are proof that overall sequence similarity to Col-0 is not an important criterion for photoperiod stress sensitivity. Similar results in repetition of these experiments would further strengthen this conclusion.

Ecotypes from the geographical collection curated by Detlef Weigel (Weigel, 2012) were chosen to ensure the representation of regions spanning various latitudes. Regions closer to the equator tend to have more equally divided light and dark periods, while the ones further away from the equator have shorter or longer days depending upon the season. Natural photoperiods can affect the tolerance to abiotic stress; for instance, varying freezing tolerance is observed in geographically distant ecotypes of *A. thaliana*, which can be attributed to their differing natural photoperiod (Alonso-Blanco et al., 2005). It was hypothesized that depending upon the natural photoperiod of ecotypes, a differential response to photoperiod stress may occur. For instance, it was anticipated that Tanz-2 whose natural habitat is near the equator (See Table 2.2), with a 12 h/12 h photoperiod throughout the year might be more sensitive to changes in photoperiod. However, as observed in Figure 3.26, out of all the ecotypes tested including Tanz-2, only Elmonte showed somewhat similar responses as Col-0 to photoperiod stress. Elmonte's natural habitat is 38° N, which is only 10° south of the natural habitat of L*er*-0 (L*er*-0 showed lower photoperiod stress symptoms than Col-0, see Figure 3.26). This small latitudinal difference does not lead to an effective difference in the natural photoperiod and thus does not explain the difference in sensitivity to applied photoperiod stress. Therefore, it can be concluded that the photoperiod in the natural habitat of the investigated ecotypes is not an important factor in photoperiod stress sensitivity.

Ecotypes from the VASC displayed low sensitivity to photoperiod stress according to peroxide levels (Figure 3.25 A, D, G). However, amongst all the ecotypes from the VASC collection, that were also tested for their stress marker gene expression in response to photoperiod stress, only Jea and N-13 showed lower stress marker gene expression than Col-0, while the others had similar *ZAT12* and *BAP1* expression compared to Col-0 (Figure 3.25 B-C, E-F). To grasp the underlying reasons for the stark contrast between peroxide levels and stress marker gene expression in response to photoperiod stress, it is imperative to conduct an analysis of stress marker gene expression for all other members of this

collection along with repetitions. Furthermore, conducting a genomic comparison of this ecotype collection with Col-0 could provide valuable insights.

In a comparison of the photoperiod flowering response of different accessions, the *CRY2* locus was isolated as a relevant gene for the response to photoperiod (El-Din El-Assal et al., 2001) matching the important role of CRY2 in the response to photoperiod stress (Figure 3.15). Exploring the variation in CRY2 loci among diverse ecotypes could provide valuable insights into the role of CRY2 in photoperiod stress across different ecotypes. In general, these results indicate that photoperiod stress sensitivity is not a common trait among the ecotypes of *A. thaliana.*

4.5 Inheritance pattern of photoperiod stress sensitivity

The low photoperiod stress sensitivity of the other ecotypes than Col accessions was intriguing and suggested the possibility of photoperiod stress sensitivity being a recessive trait. To investigate this proposition, Col-0 was crossed with some of the ecotypes that showed very low sensitivity to photoperiod stress, and the individuals of the F1 generation were tested under photoperiod stress inducing conditions. Most of the F1 generation displayed lower photoperiod stress symptoms than Col-0 similar to their latter parent (Figure 3.28 A-C, Figure 3.29, Figure 3.30). This result supports the suggestion that photoperiod stress sensitivity is a recessive trait. Especially, the reduced photoperiod stress symptoms in F1 plants of the reciprocal crosses such as L*er*-0 X Col-0 and Col-0 X L*er*-0, where Col-0 once acted as maternal and once as the paternal donor (Figure 3.30, Figure 3.28 A-C), provides evidence against the role of maternally transferred genes in photoperiod stress.

As an exception to all the tested F1 generations, Tanz-2 X Col-0 displayed photoperiod stress symptoms as strong as Col-0, while Col-0 X Tanz-2 had similar photoperiod stress symptoms as Tanz-2 (Figure 3.28 D-F). Probably the reason for high photoperiod stress symptoms in Tanz-2 X Col-0 can be presumed to be found in the genetic makeup of the Tanz-2, but it is difficult to pinpoint the exact cause within the limits of presently available data.

To further investigate the inheritance pattern of the photoperiod stress sensitivity, the F2 generation of Col-0 X La-1 was studied under photoperiod stress. The level of photoperiod stress symptoms among the F2 generation followed a continuous distribution and lacked any strong bimodal distribution (Figure 3.31). This implied that photoperiod stress is a quantitative trait. However, since the F1 generation had very low sensitivity to photoperiod stress, it is possible that one locus makes a decisive impact on the phenotype. In a repetitive experiment, the population size of the F2 generation would need to be larger than used in this study for a more reliable conclusion.

Most physiological traits are controlled by multiple loci, and therefore even though the parental lines have a huge quantitative difference in the studied trait, the F2 generation often shows a

continuous distribution of the trait (Shindo et al., 2007). The photoperiod stress symptoms in F1 and F2 progenies of the shown ecotype crosses have only been tested once, therefore these results should be considered with some reservation.

5 Future perspectives

5.1 Further investigation of the role of chloroplasts in photoperiod stress

Low photoperiod stress symptoms in *gun4, gun5, glk1 glk2,* and *rcd1* mutants pointed towards a role of retrograde signaling in photoperiod stress (Figure 3.6). For further confirmation, *GUN4, GUN5, GLK1,* and *GLK2* overexpressing transgenic lines can be tested under photoperiod stress. Stronger photoperiod stress symptoms in these lines would further support the argument for their involvement in photoperiod stress.

It was concluded from Figure 3.8 and Figure 3.9 that excess sugar during and at the end of the PLP could be one of the contributors to photoperiod stress. To further confirm this hypothesis, it would be interesting to test some sugar accumulation mutants under photoperiod stress conditions, to investigate if they respond with stronger photoperiod stress symptoms than WT. SUGARS WILL EVENTUALLY BE EXPORTED TRANSPORTER (SWEET) are sugar uniporters and the *sweet11 sweet12* double mutant is known to accumulate sucrose, hexoses, and starch in leaves (Gebauer et al., 2017). SUCROSE TRANSPORTER 2 (SUC2) is a sucrose proton symporter responsible for loading sucrose into the phloem. *pho3* mutant (phosphorus deficient mutant) was shown to carry a defective *SUC2* gene and accumulate glucose, fructose, sucrose, and starch (Lloyd and Zakhleniuk, 2004). Therefore, *sweet11 sweet12* and *pho3* would be interesting candidates for investigation of their sensitivity to photoperiod stress.

Since the redox state of NAD is directly coupled to several metabolic reactions such as those of photosynthesis, starch metabolism, and redox homeostasis (Geigenberger, 2011; Steinbeck et al., 2020), monitoring the ratio of NAD+/NADH during the photoperiod stress could lend further insight into the role of the chloroplasts in photoperiod stress. Similarly, the ATP/ADP ratio is also important for several metabolic reactions of photosynthesis and its measurement could thus shed light on the status of the chloroplast during photoperiod stress.

Lastly, it was interesting to note that the *phot2* mutant showed a stronger photoperiod stress response compared to WT (Figure 3.16). Luesse et al. (2010) observed that *phot2* mutants accumulated chloroplast towards the periclinal cell wall at all light intensities. It would be interesting to investigate whether a similar chloroplast accumulation also occurs in *phot2* mutants during the PLP of the photoperiod stress treatment. This would add to the understanding about the role of chloroplast in photoperiod stress.

5.2 Further investigation of the role of CRY2 in photoperiod stress

A perturbed circadian clock due to PLP is the primary cause of photoperiod stress (Nitschke et al., 2016, 2017). It was observed in this study that circadian clock components such as *TOC1* and *CHE* are differentially regulated in *cry2* mutants (Figure 3.20 C-D). As a next step to comprehend the role of CRY2 in photoperiod stress in reference to the circadian clock, it might be interesting to study the oscillation of the circadian clock in WT and *cry2* mutants during and after the photoperiod stress treatment. This could be done possibly by monitoring *CAB2::LUC* expression during photoperiod stress, similar to the study performed by Devlin & Kay (2000). If there is a difference in variation of period length between WT and *cry2* during photoperiod stress, an important role of CRY2 in photoperiod stress through the circadian clock could be argued.

To further ascertain the importance of light input through CRY2 in photoperiod stress, the *cry2* mutant with the missense mutation D387A could be tested under photoperiod stress. This mutation disturbs a universally conserved site for FAD binding to CRY2 and the mutants lack blue light dependent phosphorylation and degradation (Liu et al., 2008; Liu et al., 2020).

5.3 Influence of photoperiod stress on flowering time

The mutant analysis in this study (Figure 3.22) and flowering pathway gene expression analysis by V. Roeber (Personal communication) indicate a possible involvement of the photoperiodic flowering pathway in photoperiod stress. In sections 4.2.2 and 4.3, it has been argued that plants perceive a PLP treatment as LD, and stabilization of CO by CRY2 via CIB1 interaction could probably be an underlying mechanism for the development of photoperiod stress symptoms. To verify the involvement of this interaction, as a first step, it might be interesting to check if CIB1 and CO interact during photoperiod stress by co-immunoprecipitation as performed by Liu et al. (2018).

Corbesier et al. (1996) observed that in 30-day-old SD-grown non-vernalized Col plants, five consecutive 32 h continuous light period periods could induce flowering in SD grown plants. Furthermore, Torti et al. (2012) showed that a single exposure of 4-weeks-old SD-grown plants to LD (8 h light/ 16 h dark) was enough to induce the meristem of these SD-grown plants to flower. Most of the mutant analysis in this study has been performed on 5-weeks-old (~35-day-old) plants under a strong photoperiod stress treatment with 16 h PLP which in total makes for 32 h continuous light (Figure 3.6 A). Noting the flowering time in plants treated with strong photoperiod stress compared to non-treated plants grown in SD and LD could provide further evidence for a role of the flowering pathway in photoperiod stress.

5.4 Deeper analysis of photoperiod stress phenotype in the ecotypes of *A. thaliana*

More ecotypes of *A. thaliana* need to be tested under photoperiod stress to reveal the loci that are the underlying reason for the plants' response to photoperiod stress. Additionally, RILs (Simon et al., 2008; Schwartz et al., 2009; Matsusaka et al., 2021), near-isogenic lines (NILs) (Keurentjes et al., 2007), and MAGIC lines (Kover et al., 2009) could be studied to identify the loci of interest for photoperiod stress. Furthermore, more than 50 individuals from the F2 generations of more than one cross could be analyzed to map the loci of interest by QTL mapping. This can also be combined with the power of GWAS analysis.

In the last decade, several studies have combined the classical QTL mapping approach with GWAS to find the loci of interest. Brachi et al. (2010) studied flowering time in natural accessions and RILs of *A. thaliana* under an ecologically realistic environment and identified 62 additive QTLs that are involved in regulating flowering time using traditional linkage mapping. They combined this information with GWAS to verify QTLs and list candidate genes. Sanchez-Bermejo et al. (2015) performed GWAS and QTL analysis in RILs to identify *CRY2* as an important gene involved in temperature sensitivity in hypocotyl elongation. Lardon et al. (2020) performed GWAS on 190 ecotypes to explore the genetics of various *in vitro* traits alongside shoot regeneration from root explants. This study pointed towards *WUSCHEL* as the master regulator of this trait and novel genes like *AT3G09925, SUP, EDA40,* and *DOF4.4* were identified in this regard (Lardon et al., 2020).

5.5 Photoperiod stress in plants under non-laboratory conditions

Until now, photoperiod stress has only been conducted under laboratory conditions with light intensities up to 300 µmol m^{-2} s^{-1}. It would be interesting to grow plants for 4 to 5 weeks under simulated light conditions, where light intensities can be gradually increased up to 1000 µmol m^{-2} s^{-1} followed by a gradual decrease like in a typical day. PLPs of different lengths and with different light intensities can be applied to these plants to see if photoperiod stress can occur in nature due to artificial lighting. Plants in cities may experience an unexpected PLP when artificial light levels surge in the night during festivities. Indeed, studies are in progress to decipher the effect of artificial light on roadside trees in urban areas and it has been noted that bud-burst, flowering, leaf coloring, and abscission are often affected in these trees (Bennie et al., 2016).

6 Conclusions

In this study, the effects of light quantity and quality on photoperiod stress have been studied. It has been shown that in order to cause photoperiod stress, a minimum light intensity of 50 µmol m^{-2} s^{-1} is necessary during the PLP. Since photoreceptors respond to much lower light intensities (Li et al., 2011b), this hinted to the involvement of chloroplasts, which are known for sensing changes in light intensities of greater magnitude (Spetea et al., 2014). Low photoperiod stress symptoms in retrograde signaling mutants *gun4, gun5, glk1 glk2*, and *rcd1* supported this hypothesis. Moreover, starch and glucose accumulated in response to photoperiod stress, and starch biosynthesis mutants showed lower photoperiod stress symptoms indicating an important role of starch metabolism in photoperiod stress. This provided further evidence of the role of chloroplast in photoperiod stress.

Both monochromatic blue and red light induced photoperiod stress and the corresponding mutation of blue and red light photoreceptor genes *CRY2* and *PHYB* led to low photoperiod symptoms. Since the circadian clock genes *TOC1* and *CHE* were differentially regulated in *cry2* mutant compared to WT in response to photoperiod stress, it has been postulated that perhaps CRY2 acts in photoperiod stress by giving light input to the circadian clock.

The circadian clock also regulates starch and sugar metabolism and vice versa (Müller et al., 2014), which could be a potential link between plastid and light signaling. These signaling pathways are linked on different levels. For example, retrograde control of phyB levels (Jiang et al., 2019) and the functionality of HY5 (Ruckle et al., 2007). Plastid and phytochrome signaling pathways interact antagonistically to regulate the expression of *GLK1* (Martin et al., 2016).

Taken together, this work has provided evidence that in sensing and responding to photoperiod stress both chloroplasts and photoreceptors are required. It might be assumed that plastid and light signaling are interwoven to generate a complex stress response to photoperiod stress stimulus.

Additionally, this work has indicated that CO, an important photoperiodic flowering pathway integrator, could be involved in photoperiod stress. The photoperiodic flowering pathway is also strongly associated with light signaling and starch metabolism pathways (Kim et al., 2009; Matsoukas et al., 2013).

Lastly, the effect of photoperiod stress was investigated in different ecotypes of *A. thaliana,* and it was concluded that photoperiod stress susceptibility was a rare trait in nature. Furthermore, results from testing of F1 crosses of photoperiod stress sensitive ecotype Col-0 with other non-sensitive ecotypes under photoperiod stress conditions revealed that photoperiod susceptibility is a recessive trait.

7 References

1001 Genomes Consortium (2016) 1,135 Genomes reveal the global pattern of polymorphism in *Arabidopsis thaliana*. Cell **166**: 481–491

Abe M, Kobayashi Y, Yamamoto S, Daimon Y, Yamaguchi A, Ikeda Y, Ichinoki H, Notaguchi M, Goto K, Araki T (2005) FD, a bZIP protein mediating signals from the floral pathway integrator FT at the shoot apex. Science **309**: 1052–1056

Abuelsoud W, Cortleven A, Schmülling T (2020) Photoperiod stress induces an oxidative burst-like response and is associated with increased apoplastic peroxidase and decreased catalase activities. Journal of Plant Physiology **253**: 153-252

Achard P, Herr A, Baulcombe DC, Harberd NP (2004) Modulation of floral development by a gibberellin-regulated microRNA. Development **131**: 3357–3365

Adhikari ND, Froehlich JE, Strand DD, Buck SM, Kramer DM, Larkin RM (2011) GUN4-Porphyrin Complexes Bind the ChlH/GUN5 Subunit of Mg-Chelatase and Promote Chlorophyll Biosynthesis in *Arabidopsis*. The Plant Cell **23**: 1449–1467

Ahmad M, Cashmore AR (1993) HY4 gene of *A. thaliana* encodes a protein with characteristics of a blue-light photoreceptor. Nature **366**: 162–166

Ahmad M, Grancher N, Heil M, Black RC, Giovani B, Galland P, Lardemer D (2002) Action Spectrum for cryptochrome-dependent hypocotyl growth inhibition in Arabidopsis. Plant Physiology **129**: 774–785

Ahmad M, Jarillo JA, Cashmore AR (1998) Chimeric proteins between cry1 and cry2 Arabidopsis blue light photoreceptors indicate overlapping functions and varying protein stability. Plant Cell **10**: 197–207

Akram NA, Shafiq F, Ashraf M (2017) Ascorbic acid-A potential oxidant scavenger and its role in plant development and abiotic stress tolerance. Frontiers in Plant Science **8**: 613

Alabadí D, Oyama T, Yanovsky MJ, Harmon FG, Más P, Kay SA (2001) Reciprocal regulation between *TOC1* and *LHY* / *CCA1* within the Arabidopsis circadian clock. Science **293**: 880–883

Alonso-Blanco C, Gomez-Mena C, Llorente F, Koornneef M, Salinas J, Martínez-Zapater JM (2005) Genetic and molecular analyses of natural variation indicate *CBF2* as a candidate Gene for underlying a freezing tolerance quantitative trait locus in Arabidopsis. Plant Physiology **139**: 1304–1312

Amasino R (2004) Vernalization, competence, and the epigenetic memory of winter. Plant Cell **16**: 2553–2559

Amasino R (2018) A path to a biennial life history. Nature Plants **4**: 752–753

Amasino RM (2005) Vernalization and flowering time. Current Opinion in Biotechnology **16**: 154–158

Amasino RM, Michaels SD (2010) The timing of flowering. Plant Physiology **154**: 516–520

Ankele E, Kindgren P, Pesquet E, Strand Å (2007) In vivo visualization of Mg-protoporphyrin IX, a coordinator of photosynthetic gene expression in the nucleus and the Chloroplast. The Plant Cell **19**: 1964–1979

Baker NR (2008) Chlorophyll fluorescence: A probe of photosynthesis in vivo. Annu Rev Plant Biol **59**: 89–113

Balcerowicz M, Mahjoub M, Nguyen D, Lan H, Stoeckle D, Conde S, Jaeger KE, Wigge PA, Ezer D (2021) An early-morning gene network controlled by phytochromes and cryptochromes regulates photomorphogenesis pathways in Arabidopsis. Molecular Plant **14**: 983–996

Banerjee R, Schleicher E, Meier S, Viana RM, Pokorny R, Ahmad M, Bittl R, Batschauer A (2007) The signaling state of Arabidopsis Cryptochrome 2 contains flavin semiquinone. Journal of Biological Chemistry **282**: 14916–14922

Bennie J, Davies TW, Cruse D, Gaston KJ (2016) Ecological effects of artificial light at night on wild plants. Journal of Ecology **104**: 611–620

Bonnefont-Rousselot D (2002) Glucose and reactive oxygen species. Current Opinion in Clinical Nutrition and Metabolic Care **5**: 561–568

Bouly J-P, Schleicher E, Dionisio-Sese M, Vandenbussche F, Van Der Straeten D, Bakrim N, Meier S, Batschauer A, Galland P, Bittl R, et al (2007) Cryptochrome blue light photoreceptors are activated through interconversion of flavin redox states. Journal of Biological Chemistry **282**: 9383–9391

Brachi B, Faure N, Horton M, Flahauw E, Vazquez A, Nordborg M, Bergelson J, Cuguen J, Roux F (2010) Linkage and association mapping of *Arabidopsis thaliana* flowering time in nature. PLoS Genetics **6**: e1000940

Braun DM, Slewinski TL (2009) Genetic control of carbon partitioning in grasses: Roles of *Sucrose Transporters* and *Tie-dyed* loci in phloem loading. Plant Physiology **149**: 71–81

Briggs WR, Christie JM (2002) Phototropins 1 and 2: versatile plant blue-light receptors. Trends in Plant Science **7**: 204–210

Brudler R, Hitomi K, Daiyasu H, Toh H, Kucho K, Ishiura M, Kanehisa M, Roberts VA, Todo T, Tainer JA, et al (2003) Identification of a new cryptochrome class. Molecular Cell **11**: 59–67

Bruggemann EP, Doan B, Handwerger K, Storz G (1998) Characterization of an unstable allele of the Arabidopsis HY4 locus. Genetics **149**: 1575–1585

Burgie ES, Bussell AN, Walker JM, Dubiel K, Vierstra RD (2014) Crystal structure of the photosensing module from a red/far-red light-absorbing plant phytochrome. Proceedings of the National Academy of Sciences USA **111**: 10179–10184

Bursch K, Toledo-Ortiz G, Pireyre M, Lohr M, Braatz C, Johansson H (2020) Identification of BBX proteins as rate-limiting cofactors of HY5. Nature Plants **6**: 921–928

Casal JJ (2012) Shade Avoidance. The Arabidopsis Book. The American Society of Plant Biologists, BioOne, Rockville, USA **10**: e0157

Casazza AP, Rossini S, Rosso MG, Soave C (2005) Mutational and expression analysis of ELIP1 and ELIP2 in *Arabidopsis thaliana*. Plant Molecular Biology **58**: 41–51

Caspar T, Huber SC, Somerville C (1985) Alterations in growth, photosynthesis, and respiration in a starchless mutant of *Arabidopsis thaliana* (L.) deficient in chloroplast phosphoglucomutase activity. Plant Physiology **79**: 11–17

Celaya RB, Liscum E (2005) Phototropins and associated signaling: Providing the power of movement in higher Plants. Photochemistry and Photobiology **81**: 73

Chatterjee A, Dey T, Galiba G, Kocsy GK, Dey N, Kar RK (2021) Effect of combination of light and drought stress on physiology and oxidative metabolism of rice plants. Plant Science Today **8:** 762-777

Chatterton NJ, John E. Silvius (1981) Photosynthate partitioning into starch in soybean leaves. II. Irradiance level and daily photosynthetic period duration effects. Plant Physiology **67**: 257–260

Chen M, Ji M, Wen B, Liu L, Li S, Chen X, Gao D, Li L (2016) GOLDEN 2-LIKE transcription factors of plants. Frontiers in Plant Science **7:** 1509

Chen M, Tao Y, Lim J, Shaw A, Chory J (2005) Regulation of phytochrome B nuclear localization through light-dependent unmasking of nuclear-localization signals. Current Biology **15**: 637–642

Cheng J, He C-X, Zhang Z-W, Xu F, Zhang D-W, Wang X, Yuan S, Lin H-H Plastid signals confer Arabidopsis tolerance to water stress. Zeitschrift für Naturforschung C **66:** 47-54

Cheval C, Perez M, Leba LJ, Ranty B, Perochon A, Reichelt M, Mithöfer A, Robe E, Mazars C, Galaud JP, et al (2017) PRR2, a pseudo-response regulator, promotes salicylic acid and camalexin accumulation during plant immunity. Scientific Reports **7**: 6979

Chirivì D, Betti C (2023) Molecular links between flowering and abiotic stress response: A Focus on Poaceae. Plants **12**: 331

Christie JM (2007) Phototropin blue-light receptors. Annual Review of Plant Biology **58**: 21–45

Christie JM, Arvai AS, Baxter KJ, Heilmann M, Pratt AJ, O'Hara A, Kelly SM, Hothorn M, Smith BO, Hitomi K, et al (2012) Plant UVR8 photoreceptor senses UV-B by tryptophan-mediated disruption of cross-dimer salt bridges. Science **335**: 1492–1496

Christie JM, Blackwood L, Petersen J, Sullivan S (2015) Plant flavoprotein photoreceptors. Plant and Cell Physiology **56**: 401–413

Christie JM, Swartz TE, Bogomolni RA, Briggs WR (2002) Phototropin LOV domains exhibit distinct roles in regulating photoreceptor function. The Plant Journal **32**: 205–219

Cluis CP, Mouchel CF, Hardtke CS (2004) The Arabidopsis transcription factor HY5 integrates light and hormone signaling pathways. The Plant Journal **38**: 332–347

Colombo M, Tadini L, Peracchio C, Ferrari R, Pesaresi P (2016) GUN1, a jack-of-all-trades in chloroplast protein homeostasis and signaling. Frontiers in Plant Science **7:** 1427

Corbesier L, Coupland G (2006) The quest for florigen: a review of recent progress. Journal of Experimental Botany **57**: 3395–3403

Corbesier L, Gadisseur I, Silvestre G, Jacqmard A, Bernier G (1996) Design in *Arabidopsis thaliana* of a synchronous system of floral induction by one long day. The Plant Journal **9**: 947–952

Cortleven A, Roeber VM, Frank M, Bertels J, Lortzing V, Beemster GTS, Schmülling T (2022) Photoperiod stress in *Arabidopsis thaliana* induces a transcriptional response resembling that of pathogen infection. Frontiers in Plant Science **13**: 838284

Couée I, Sulmon C, Gouesbet G, El Amrani A (2006) Involvement of soluble sugars in reactive oxygen species balance and responses to oxidative stress in plants. Journal of Experimental Botany **57**: 449–459

Crawford T, Lehotai N, Strand Å (2018) The role of retrograde signals during plant stress responses. Journal of Experimental Botany **69**: 2783–2795

Dalchau N, Baek SJ, Briggs HM, Robertson FC, Dodd AN, Gardner MJ, Stancombe MA, Haydon MJ, Stan G-B, Gonçalves JM, et al (2011) The circadian oscillator gene *GIGANTEA* mediates a long-term response of the *Arabidopsis thaliana* circadian clock to sucrose. Proc Natl Acad Sci USA **108**: 5104–5109

Daudi A, O'Brien JA (2012) Detection of Hydrogen Peroxide by DAB Staining in Arabidopsis Leaves. Bio Protocol **2**: e263

Demkura PV, Ballaré CL (2012) UVR8 mediates UV-B-induced Arabidopsis defense responses against *Botrytis cinerea* by controlling sinapate accumulation. Molecular Plant **5**: 642–652

Devlin PF (2002) Signs of the time: environmental input to the circadian clock. Journal of Experimental Botany **53**: 1535–1550

Devlin PF, Kay SA (2000) Cryptochromes are required for phytochrome signaling to the circadian clock but not for rhythmicity. Plant Cell **12**: 2499–2509

Di Wu, Hu Q, Yan Z, Chen W, Yan C, Huang X, Zhang J, Yang P, Deng H, Wang J, et al (2012) Structural basis of ultraviolet-B perception by UVR8. Nature **484**: 214–219

Dong S, Beckles DM (2019) Dynamic changes in the starch-sugar interconversion within plant source and sink tissues promote a better abiotic stress response. Journal of Plant Physiology **234–235**: 80–93

Dou H, Niu G (2020) Plant responses to light. Plant Factory. Elsevier, Academic Press, Cambridge, USA pp 153–166

Egli B, Kölling K, Köhler C, Zeeman SC, Streb S (2010) Loss of cytosolic phosphoglucomutase compromises gametophyte development in Arabidopsis. Plant Physiology **154**: 1659–1671

El-Din El-Assal S, Alonso-Blanco C, Peeters AJM, Raz V, Koornneef M (2001) A QTL for flowering time in Arabidopsis reveals a novel allele of CRY2. Nature Genetics **29**: 435–440

El-Esawi M, Arthaut L-D, Jourdan N, d'Harlingue A, Link J, Martino CF, Ahmad M (2017) Blue-light induced biosynthesis of ROS contributes to the signaling mechanism of Arabidopsis cryptochrome. Scientific Reports **7**: 13875

Eliyahu E, Rog I, Inbal D, Danon A (2015) ACHT4-driven oxidation of APS1 attenuates starch synthesis under low light intensity in Arabidopsis plants. Proceedings of the National Academy of Sciences USA **112**: 12876–12881

Essemine J, Govindachary S, Joly D, Ammar S, Bouzid S, Carpentier R (2012) Effect of moderate and high light on photosystem II function in *Arabidopsis thaliana* depleted in digalactosyl-diacylglycerol. Biochimica et Biophysica Acta (BBA) - Bioenergetics **1817**: 1367–1373

Fackendahl P (2012) Functional analysis of Arabidopsis SPA Proteins in plant Growth Control. Plant Physiology **169:** 2200-2214

Fairchild CD, Schumaker MA, Quail PH (2000) HFR1 encodes an atypical bHLH protein that acts in phytochrome A signal transduction. Genes & Development **14:** 2377-2391

Fanciullino AL, Bidel LPR, Urban L (2014) Carotenoid responses to environmental stimuli: integrating redox and carbon controls into a fruit model. Plant Cell & Environment **37**: 273–289

Farré EM, Harmer SL, Harmon FG, Yanovsky MJ, Kay SA (2005) Overlapping and distinct roles of PRR7 and PRR9 in the Arabidopsis circadian clock. Current Biology **15**: 47–54

Favory J-J, Stec A, Gruber H, Rizzini L, Oravecz A, Funk M, Albert A, Cloix C, Jenkins GI, Oakeley EJ, et al (2009) Interaction of COP1 and UVR8 regulates UV-B-induced photomorphogenesis and stress acclimation in Arabidopsis. EMBO Journal **28**: 591–601

Feng L, Raza MA, Li Z, Chen Y, Khalid MHB, Du J, Liu W, Wu X, Song C, Yu L, et al (2019) The Influence of Light Intensity and Leaf Movement on Photosynthesis Characteristics and Carbon Balance of Soybean. Frontiers in Plant Science **9**: 1952

Fey V, Wagner R, Braütigam K, Wirtz M, Hell R, Dietzmann A, Leister D, Oelmüller R, Pfannschmidt T (2005) Retrograde plastid redox signals in the expression of nuclear genes for chloroplast proteins of *Arabidopsis thaliana*. Journal of Biological Chemistry **280**: 5318–5328

Fitter DW, Martin DJ, Copley MJ, Scotland RW, Langdale JA (2002) *GLK* gene pairs regulate chloroplast development in diverse plant species. The Plant Journal **31**: 713–727

Fittinghoff K, Laubinger S, Nixdorf M, Fackendahl P, Baumgardt R, Batschauer A, Hoecker U (2006) Functional and expression analysis of Arabidopsis *SPA* genes during seedling photomorphogenesis and adult growth. The Plant Journal **47**: 577–590

Floris M, Bassi R, Robaglia C, Alboresi A, Lanet E (2013) Post-transcriptional control of light-harvesting genes expression under light stress. Plant Molecular Biology **82**: 147–154

Fornara F, De Montaigu A, Sánchez-Villarreal A, Takahashi Y, Ver Loren Van Themaat E, Huettel B, Davis SJ, Coupland G (2015) The GI – CDF module of Arabidopsis affects freezing tolerance and growth as well as flowering. The Plant Journal **81**: 695–706

Fornara F, Panigrahi KCS, Gissot L, Sauerbrunn N, Rühl M, Jarillo JA, Coupland G (2009) Arabidopsis DOF transcription factors act redundantly to reduce *CONSTANS* expression and are essential for a photoperiodic flowering response. Developmental Cell **17**: 75–86

Fowler SG, Cook D, Thomashow MF (2005) Low temperature induction of Arabidopsis *CBF1* , *2* , and *3* is Gated by the circadian clock. Plant Physiology **137**: 961–968

Franco-Zorrilla JM, Martín AC, Leyva A, Paz-Ares J (2005) Interaction between phosphate-starvation, sugar, and cytokinin signaling in Arabidopsis and the roles of cytokinin receptors CRE1/AHK4 and AHK3. Plant Physiology **138**: 847–857

Frank A, Matiolli CC, Viana AJC, Hearn TJ, Kusakina J, Belbin FE, Wells Newman D, Yochikawa A, Cano-Ramirez DL, Chembath A, et al (2018) Circadian entrainment in Arabidopsis by the sugar-responsive transcription factor bZIP63. Current Biology **28**: 2597-2606.e6

Frank M (2019) The involvement of phytohormones, tissue and age in the response to photoperiod stress in *Arabidopsis thaliana*. Doctoral Dissertation. Freie Universität Berlin, Berlin

Frank M, Cortleven A, Novák O, Schmülling T (2020) Root-derived *trans* -zeatin cytokinin protects Arabidopsis plants against photoperiod stress. Plant Cell & Environment **43**: 2637–2649

Frank M, Cortleven A, Pěnčík A, Novak O, Schmülling T (2022) The photoperiod stress response in *Arabidopsis thaliana* depends on auxin acting as an antagonist to the protectant cytokinin. International Journal of Molecular Sciences **23**: 2936

Franklin KA, Whitelam GC (2005) Phytochromes and shade-avoidance responses in plants. Annals of Botany **96**: 169–175

Fujibe T, Saji H, Arakawa K, Yabe N, Takeuchi Y, Yamamoto KT (2004) A Methyl Viologen-Resistant Mutant of Arabidopsis, Which Is Allelic to Ozone-Sensitive *rcd1* , Is Tolerant to Supplemental Ultraviolet-B Irradiation. Plant Physiology **134**: 275–285

Gallagher S, Short TW, Ray PM, Pratt LH, Briggs WR (1988) Light-mediated changes in two proteins found associated with plasma membrane fractions from pea stem sections. Proceedings of the National Academy of Sciences USA **85**: 8003–8007

Gao J, Liu Z, Zhao B, Liu P, Zhang J-W (2020) Physiological and comparative proteomic analysis provides new insights into the effects of shade stress in maize (*Zea mays* L.). BMC Plant Biology **20**: 60

Gao Y, Wu M, Zhang M, Jiang W, Ren X, Liang E, Zhang D, Zhang C, Xiao N, Li Y, et al (2018) A maize phytochrome-interacting factors protein ZmPIF1 enhances drought tolerance by inducing stomatal closure and improves grain yield in *Oryza sativa*. Plant Biotechnology Journal **16**: 1375–1387

Gebauer P, Korn M, Engelsdorf T, Sonnewald U, Koch C, Voll LM (2017) Sugar accumulation in leaves of Arabidopsis s*weet11/sweet12* double mutants enhances priming of the salicylic acid-mediated defense response. Frontiers in Plant Science **8**: 1378

Geigenberger P (2011) Regulation of starch biosynthesis in response to a fluctuating environment. Plant Physiology **155**: 1566–1577

Gottlieb LD (1982) Conservation and duplication of isozymes in plants. Science **216**: 373–380

Graf A, Schlereth A, Stitt M, Smith AM (2010) Circadian control of carbohydrate availability for growth in Arabidopsis plants at night. Proceedings of the National Academy of Sciences USA **107**: 9458–9463

Graf A, Smith AM (2011) Starch and the clock: the dark side of plant productivity. Trends in Plant Science **16**: 169–175

Guo H, Yang H, Mockler TC, Lin C (1998) Regulation of flowering time by Arabidopsis photoreceptors. Science **279**: 1360–1363

Gyugos M, Ahres M, Gulyás Z, Szalai G, Darkó É, Mednyánszky Z, Dey N, Kar RK, Simon-Sarkadi L, Kocsy G (2021) Light spectrum modifies the drought-induced changes of glutathione and free amino acid levels in wheat. Acta Physiolgiae Plantarum **43**: 90

Halaban R (1969) Effects of light quality on the circadian rhythm of leaf movement of a short-day-plant. Plant Physiology **44**: 973–977

Haque MS, Kjaer KH, Rosenqvist E, Ottosen C-O (2015) Continuous light increases growth, daily carbon gain, antioxidants, and alters carbohydrate metabolism in a cultivated and a wild tomato species. Frontiers in Plant Science **6:** 522

Haydon MJ, Mielczarek O, Robertson FC, Hubbard KE, Webb AAR (2013) Photosynthetic entrainment of the *Arabidopsis thaliana* circadian clock. Nature **502**: 689–692

He Y, Yu Y, Wang X, Qin Y, Su C, Wang L (2022) Aschoff's rule on circadian rhythms orchestrated by blue light sensor CRY2 and clock component PRR9. Nature Communications **13**: 5869

Henderson IR, Shindo C, Dean C (2003) The need for winter in the switch to flowering. Annual Review of Genetics **37**: 371–392

Hendriks JHM, Kolbe A, Gibon Y, Stitt M, Geigenberger P (2003) ADP-glucose pyrophosphorylase is activated by posttranslational redox-modification in response to light and to sugars in leaves of Arabidopsis and other plant species. Plant Physiology **133**: 838–849

Henzler T, Steudle E (2000) Transport and metabolic degradation of hydrogen peroxide in C*hara corallina*: model calculations and measurements with the pressure probe suggest transport of H_2O_2 across water channels. Journal of Experimental Botany **51**: 2053–2066

Herbert M, Burkhard Ch, Schnarrenberger C (1979) A survey for isoenzymes of glucosephosphate isomerase, phosphoglucomutase, glucose-6-phosphate dehydrogenase and 6-phosphogluconate dehydrogenase in C3-, C4-and crassulacean-acid-metabolism plants, and green algae. Planta **145**: 95–104

Hermanowicz P, Banaś AK, Sztatelman O, Gabryś H, Łabuz J (2019) UV-B induces chloroplast movements in a phototropin-dependent manner. Frontiers in Plant Science **10**: 1279

Hiltbrunner A, Tscheuschler A, Viczián A, Kunkel T, Kircher S, Schäfer E (2006) FHY1 and FHL act together to mediate nuclear accumulation of the phytochrome A photoreceptor. Plant and Cell Physiology **47**: 1023–1034

Hiltbrunner A, Viczián A, Bury E, Tscheuschler A, Kircher S, Tóth R, Honsberger A, Nagy F, Fankhauser C, Schäfer E (2005) Nuclear accumulation of the phytochrome A photoreceptor requires FHY1. Current Biology **15**: 2125–2130

Hoecker U (2017) The activities of the E3 ubiquitin ligase COP1/SPA, a key repressor in light signaling. Current Opinion in Plant Biology **37**: 63–69

Hoffman PD, Batschauer A, Hays JB (1996) PHH1, a novel gene from *Arabidopsis thaliana* that encodes a protein similar to plant blue-light photoreceptors and microbial photolyases. Mol Genetics and Genomics **253**: 259–265

Holm M, Ma L-G, Qu L-J, Deng X-W (2002) Two interacting bZIP proteins are direct targets of COP1-mediated control of light-dependent gene expression in Arabidopsis. Genes & Development **16**: 1247–1259

Holmes MG, Smith H (1975) The function of phytochrome in plants growing in the natural environment. Nature **254**: 512–514

Hou S, Liu Z, Shen H, Wu D (2019) Damage-Associated Molecular Pattern-triggered immunity in plants. Frontiers in Plant Science **10**: 646

Hu C-H, Wang P-Q, Zhang P-P, Nie X-M, Li B-B, Tai L, Liu W-T, Li W-Q, Chen K-M (2020) NADPH Oxidases: The vital performers and center hubs during plant growth and signaling. Cells **9**: 437

Huala E, Oeller PW, Liscum E, Han I-S, Larsen E, Briggs WR (1997) *Arabidopsis* NPH1: A protein kinase with a putative redox-sensing domain. Science **278**: 2120–2123

Huang H, Ullah F, Zhou D-X, Yi M, Zhao Y (2019) Mechanisms of ROS regulation of plant development and stress responses. Frontiers in Plant Science **10**: 800

Hufford KM, Mazer SJ (2003) Plant ecotypes: genetic differentiation in the age of ecological restoration. Trends in Ecology & Evolution **18**: 147–155

Hummel I, Pantin F, Sulpice R, Piques M, Rolland G, Dauzat M, Christophe A, Pervent M, Bouteillé M, Stitt M, et al (2010) Arabidopsis plants acclimate to water deficit at low cost through changes of carbon usage: An integrated perspective using growth, metabolite, enzyme, and gene expression analysis. Plant Physiology **154**: 357–372

Iglesias AA, Preiss J (1992) Bacterial glycogen and plant starch biosynthesis. Biochemical Education **20**: 196–203

Iino M (2001) Phototropism in higher plants. Comprehensive Series in Photosciences. Elsevier, Amsterdam, Netherlands, pp 659–811

Imaizumi T, Schultz TF, Harmon FG, Ho LA, Kay SA (2005) FKF1 F-Box protein mediates cyclic degradation of a repressor of *CONSTANS* in Arabidopsis. Science **309**: 293–297

Imaizumi T, Tran HG, Swartz TE, Briggs WR, Kay SA (2003) FKF1 is essential for photoperiodic-specific light signalling in Arabidopsis. Nature **426**: 302–306

Iñigo S, Alvarez MJ, Strasser B, Califano A, Cerdán PD (2012) PFT1, the MED25 subunit of the plant Mediator complex, promotes flowering through CONSTANS dependent and independent mechanisms in Arabidopsis. The Plant Journal **69**: 601–612

Ito S, Song YH, Imaizumi T (2012) LOV domain-containing F-Box Proteins: Light-dependent protein degradation modules in Arabidopsis. Molecular Plant **5**: 573–582

Janda T, Hideg É, Vanková R (2020) Editorial: The Role of Light in Abiotic Stress Acclimation. Frontiers in Plant Science **11**: 184

Jang I-C, Yang J-Y, Seo HS, Chua N-H (2005) HFR1 is targeted by COP1 E3 ligase for post-translational proteolysis during phytochrome A signaling. Genes & Development **19**: 593–602

Jang S, Marchal V, Panigrahi KCS, Wenkel S, Soppe W, Deng X-W, Valverde F, Coupland G (2008) Arabidopsis COP1 shapes the temporal pattern of CO accumulation conferring a photoperiodic flowering response. EMBO Journal **27**: 1277–1288

Janse Van Rensburg HC, Van Den Ende W (2018) UDP-Glucose: A Potential Signaling Molecule in Plants? Front Plant Sci **8**: 2230

Janse Van Rensburg HC, Van Den Ende W, Signorelli S (2019) Autophagy in plants: Both a puppet and a puppet master of sugars. Frontiers in Plant Science **10**: 14

Jansson S, Pichersky E, Bassi R, Green BR, Ikeuchi M, Melis A, Simpson DJ, Spangfort M, Staehelin LA, Thornber JP (1992) A nomenclature for the genes encoding the chlorophylla/b-binding proteins of higher plants. Plant Mol Biol Rep **10**: 242–253

Jenkins GI (2014) The UV-B Photoreceptor UVR8: From structure to physiology. Plant Cell **26**: 21–37

Jensen PE, Gibson LCD, Henningsen KW, Hunter CN (1996) Expression of the chlI, chlD, and chlH genes from the *Cyanobacterium Synechocystis* PCC6803 in *Escherichia coli* and demonstration that the three cognate proteins are required for Magnesium-protoporphyrin Chelatase activity. Journal of Biological Chemistry **271**: 16662–16667

Jia Y, Kong X, Hu K, Cao M, Liu J, Ma C, Guo S, Yuan X, Zhao S, Robert HS, et al (2020) PIFs coordinate shade avoidance by inhibiting auxin repressor *ARF18* and metabolic regulator *QQS*. New Phytologist **228**: 609–621

Jiang J, Zeng L, Ke H, De La Cruz B, Dehesh K (2019) Orthogonal regulation of phytochrome B abundance by stress-specific plastidial retrograde signaling metabolite. Nature Communications **10**: 2904

Jimeno S, Camarillo R, Mejías-Navarro F, Fernández-Ávila MJ, Soria-Bretones I, Prados-Carvajal R, Huertas P (2018) The helicase PIF1 facilitates resection over sequences prone to forming G4 structures. Cell Reports **24**: 3262-3273.e4

Johanson U, West J, Lister C, Michaels S, Amasino R, Dean C (2000) Molecular analysis of *FRIGIDA*, a major determinant of natural variation in Arabidopsis flowering time. Science **290**: 344–347

Jose J, Bánfalvi Z (2019) The role of GIGANTEA in flowering and abiotic stress adaptation in plants. Columella **6**: 7–18

Kagawa T, Sakai T, Suetsugu N, Oikawa K, Ishiguro S, Kato T, Tabata S, Okada K, Wada M (2001) Arabidopsis NPL1: A phototropin homolog controlling the chloroplast high-light avoidance response. Science **291**: 2138–2141

Kaiser E, Morales A, Harbinson J, Heuvelink E, Prinzenberg AE, Marcelis LFM (2016) Metabolic and diffusional limitations of photosynthesis in fluctuating irradiance in *Arabidopsis thaliana*. Science Reports **6**: 31252

Kameniarová M, Černý M, Novák J, Ondrisková V, Hrušková L, Berka M, Vankova R, Brzobohatý B (2022) Light quality modulates plant cold response and freezing tolerance. Frontiers in Plant Science **13**: 887103

Kathare PK, Xu X, Nguyen A, Huq E (2020) A COP1-PIF-HEC regulatory module fine-tunes photomorphogenesis in Arabidopsis. The Plant Journal **104**: 113–123

Katiyar-Agarwal S, Zhu J, Kim K, Agarwal M, Fu X, Huang A, Zhu J-K (2006) The plasma membrane Na $^{+}$/H $^{+}$ antiporter SOS1 interacts with RCD1 and functions in oxidative stress tolerance in Arabidopsis. Proceedings of the National Academy of Sciences USA **103**: 18816–18821

Keunen E, Peshev D, Vangronsveld J, Van Den Ende W, Cuypers A (2013) Plant sugars are crucial players in the oxidative challenge during abiotic stress: extending the traditional concept. Plant Cell & Environment **36**: 1242–1255

Keurentjes JJB, Bentsink L, Alonso-Blanco C, Hanhart CJ, Blankestijn-De Vries H, Effgen S, Vreugdenhil D, Koornneef M (2007) Development of a near-isogenic line Population of *Arabidopsis thaliana* and comparison of mapping power with a recombinant inbred line population. Genetics **175**: 891–905

Khandelwal A, Elvitigala T, Ghosh B, Quatrano RS (2008) Arabidopsis transcriptome reveals control circuits regulating redox homeostasis and the role of an AP2 transcription factor. Plant Physiology **148**: 2050–2058

Kim D-H (2020) Current understanding of flowering pathways in plants: focusing on the vernalization pathway in Arabidopsis and several vegetable crop plants. Horticulture, Environment, and Biotechnology **61**: 209–227

Kim D-H, Doyle MR, Sung S, Amasino RM (2009) Vernalization: Winter and the timing of flowering in plants. Annual Reviews of Cell and Developmental Biology **25**: 277–299

Kim DH, Yamaguchi S, Lim S, Oh E, Park J, Hanada A, Kamiya Y, Choi G (2008) SOMNUS, a CCCH-type Zinc Finger protein in Arabidopsis, negatively regulates light-dependent seed germination downstream of PIL5. The Plant Cell **20**: 1260–1277

Kindgren P, Dubreuil C, Strand Å (2015) The recovery of plastid function is required for optimal response to low temperatures in Arabidopsis. PLoS ONE **10**: e0138010

Kishida Y (1989) Changes in Light Intensity at Twilight and Estimation of the Biological Photoperiod. JARQ **22**: 247–252

Kliebenstein DJ, Lim JE, Landry LG, Last RL (2002) Arabidopsis *UVR8* Regulates Ultraviolet-B signal transduction and tolerance and contains sequence similarity to human *Regulator of Chromatin Condensation 1*. Plant Physiology **130**: 234–243

Klose C, Nagy F, Schäfer E (2020) Thermal reversion of plant phytochromes. Molecular Plant **13**: 386–397

Koncz C, Chua N-H, Schell JS (1992) Methods in Arabidopsis research. World Scientific Singapore, Singapore

Koussevitzky S, Nott A, Mockler TC, Hong F, Sachetto-Martins G, Surpin M, Lim J, Mittler R, Chory J (2007) Signals from chloroplasts converge to regulate nuclear gene expression. Science **316**: 715–719

Kover PX, Valdar W, Trakalo J, Scarcelli N, Ehrenreich IM, Purugganan MD, Durrant C, Mott R (2009) A multiparent advanced generation inter-cross to fine-map quantitative traits in *Arabidopsis thaliana*. PLoS Genetics **5**: e1000551

Krasensky J, Jonak C (2012) Drought, salt, and temperature stress-induced metabolic rearrangements and regulatory networks. Journal of Experimental Botany **63**: 1593–1608

Krieger-Liszkay A (2004) Singlet oxygen production in photosynthesis. Journal of Experimental Botany **56**: 337–346

Langdale JA, Kidner CA (1994) *bundle sheath defective*, a mutation that disrupts cellular differentiation in maize leaves. Development **120**: 673–681

Lardon R, Wijnker E, Keurentjes J, Geelen D (2020) The genetic framework of shoot regeneration in Arabidopsis comprises master regulators and conditional fine-tuning factors. Communications Biology **3**: 549

Larkin RM, Alonso JM, Ecker JR, Chory J (2003) GUN4, a Regulator of chlorophyll synthesis and intracellular signaling. Science **299**: 902–906

Lascève G, Leymarie J, Olney MA, Liscum E, Christie JM, Vavasseur A, Briggs WR (1999) Arabidopsis contains at least four independent Blue-Light-Activated Signal Transduction Pathways1. Plant Physiology **120**: 605–614

Lau OS, Huang X, Charron J-B, Lee J-H, Li G, Deng XW (2011) Interaction of Arabidopsis DET1 with CCA1 and LHY in Mediating transcriptional repression in the plant circadian clock. Molecular Cell **43**: 703–712

Laubinger S, Fittinghoff K, Hoecker U (2004) The SPA Quartet: A family of WD-repeat proteins with a central role in suppression of photomorphogenesis in Arabidopsis. Plant Cell **16**: 2293–2306

Laubinger S, Hoecker U (2003) The SPA1-like proteins SPA3 and SPA4 repress photomorphogenesis in the light. The Plant Journal **35**: 373–385

Leister D, Kleine T (2016) Definition of a core module for the nuclear retrograde response to altered organellar gene expression identifies GLK overexpressors as *gun* mutants. Physiologia Plantarum **157**: 297–309

Leivar P, Monte E (2014) PIFs: Systems integrators in plant development. Plant Cell **26**: 56–78

Leivar P, Monte E, Oka Y, Liu T, Carle C, Castillon A, Huq E, Quail PH (2008) Multiple phytochrome-interacting bHLH transcription factors repress premature seedling photomorphogenesis in darkness. Current Biology **18**: 1815–1823

Li G, Siddiqui H, Teng Y, Lin R, Wan X, Li J, Lau O-S, Ouyang X, Dai M, Wan J, et al (2011a) Coordinated transcriptional regulation underlying the circadian clock in Arabidopsis. Nature Cell Biology **13**: 616–622

Li J, Li G, Wang H, Wang Deng X (2011b) Phytochrome Signaling Mechanisms. The Arabidopsis Book. The American Society of Plant Biologists, BioOne, Rockville, USA **9**: e0148

Li M, Kim C (2022) Chloroplast ROS and stress signaling. Plant Communications **3**: 100264

Li R-Q, Jiang M, Huang J-Z, Møller IM, Shu Q-Y (2021) Mutations of the Genomes Uncoupled 4 gene cause ROS accumulation and repress expression of peroxidase genes in rice. Frontiers in Plant Science **12**: 682453

Li Y, Liu H, Ma T, Li J, Yuan J, Xu Y-C, Sun R, Zhang X, Jing Y, Guo Y-L, et al (2023) Arabidopsis EXECUTER1 interacts with WRKY transcription factors to mediate plastid-to-nucleus singlet oxygen signaling. The Plant Cell **35**: 827–851

Liang T, Mei S, Shi C, Yang Y, Peng Y, Ma L, Wang F, Li X, Huang X, Yin Y, et al (2018) UVR8 interacts with BES1 and BIM1 to regulate transcription and photomorphogenesis in Arabidopsis. Developmental Cell **44**: 512-523.e5

Lim J, Park J-H, Jung S, Hwang D, Nam HG, Hong S (2018) Antagonistic roles of phyA and phyB in far-red light-dependent leaf senescence in *Arabidopsis thaliana*. Plant and Cell Physiology **59**: 1753–1764

Lin C (2002) Blue light receptors and signal transduction. Plant Cell **14**: S207–S225

Lin C, Robertson DE, Ahmad M, Raibekas AA, Jorns MS, Dutton PL, Cashmore AR (1995) Association of Flavin Adenine Dinucleotide with the Arabidopsis blue light receptor CRY1. Science **269**: 968–970

Lin C, Shalitin D (2003) Cryptochrome structure and signal Transduction. Annual Review of Plant Biology **54**: 469–496

Lin C, Yang H, Guo H, Mockler T, Chen J, Cashmore AR (1998) Enhancement of blue-light sensitivity of Arabidopsis seedlings by a blue light receptor cryptochrome 2. Proceedings of the National Academy of Sciences USA **95**: 2686–2690

Liu H, Liu B, Zhao C, Pepper M, Lin C (2011) The action mechanisms of plant cryptochromes. Trends in Plant Science **16**: 684–691

Liu H, Yu X, Li K, Klejnot J, Yang H, Lisiero D, Lin C (2008) Photoexcited CRY2 interacts with CIB1 to regulate transcription and floral initiation in Arabidopsis. Science **322**: 1535–1539

Liu J, Van Iersel MW (2021) Photosynthetic physiology of blue, green, and red light: Light intensity effects and underlying mechanisms. Frontiers in Plant Science **12**: 619987

Liu Q, Su T, He W, Ren H, Liu S, Chen Y, Gao L, Hu X, Lu H, Cao S, et al (2020) Photooligomerization determines photosensitivity and photoreactivity of plant cryptochromes. Molecular Plant **13**: 398–413

Liu Y, Li X, Ma D, Chen Z, Wang J, Liu H (2018) CIB1 and CO interact to mediate CRY2-dependent regulation of flowering. EMBO Reports **19**: e45762

Lloyd JC, Zakhleniuk OV (2004) Responses of primary and secondary metabolism to sugar accumulation revealed by microarray expression analysis of the Arabidopsis mutant, *pho3*. Journal of Experimental Botany **55**: 1221–1230

Lloyd JR, Kossmann J (2015) Transitory and storage starch metabolism: two sides of the same coin? Current Opinion in Biotechnology **32**: 143–148

Lorberth R, Ritte G, Willmitzer L, Kossmann J (1998) Inhibition of a starch-granule–bound protein leads to modified starch and repression of cold sweetening. Nature Biotechnol **16**: 473–477

Lu Y, Gehan JP, Sharkey TD (2005) Daylength and circadian effects on starch degradation and maltose metabolism. Plant Physiology **138**: 2280–2291

Luesse DR, DeBlasio SL, Hangarter RP (2010) Integration of phot1, phot2, and phyB signalling in light-induced chloroplast movements. Journal of Experimental Botany **61**: 4387–4397

Lukan T, Coll A (2022) Intertwined roles of reactive oxygen species and salicylic acid signaling are crucial for the plant response to biotic stress. International Journal of Molecular Sciences **23**: 5568

Ma P, Bai T, Wang X, Ma F (2015) Effects of light intensity on photosynthesis and photoprotective mechanisms in apple under progressive drought. Journal of Integrative Agriculture **14**: 1755–1766

MacNeill GJ, Mehrpouyan S, Minow MAA, Patterson JA, Tetlow IJ, Emes MJ (2017) Starch as a source, starch as a sink: the bifunctional role of starch in carbon allocation. Journal of Experimental Botany **68**: 4433–4453

Mair A, Pedrotti L, Wurzinger B, Anrather D, Simeunovic A, Weiste C, Valerio C, Dietrich K, Kirchler T, Nägele T, et al (2015) SnRK1-triggered switch of bZIP63 dimerization mediates the low-energy response in plants. eLife **4**: e05828

Malhotra K, Kim S-T, Batschauer A, Dawut L, Sancar A (1995) Putative blue-light photoreceptors from *Arabidopsis thaliana* and *Sinapis alba* with a high degree of sequence homology to DNA photolyase contain the two photolyase cofactors but lack DNA repair activity. Biochemistry **34**: 6892–6899

Martin C, Smith AM (1995) Starch biosynthesis. Plant Cell **7**: 971–985

Martín G, Leivar P, Ludevid D, Tepperman JM, Quail PH, Monte E (2016) Phytochrome and retrograde signalling pathways converge to antagonistically regulate a light-induced transcriptional network. Nature Commununications **7**: 11431

Martin G, Soy J, Monte E (2016) Genomic analysis reveals contrasting PIFq contribution to diurnal rhythmic gene expression in PIF-induced and -repressed genes. Frontiers in Plant Science **7:** 962

Martin-Tryon EL, Kreps JA, Harmer SL (2007) *GIGANTEA* acts in blue light signaling and has biochemically separable roles in circadian clock and flowering time regulation. Plant Physiology **143**: 473–486

Más P, Alabadí D, Yanovsky MJ, Oyama T, Kay SA (2003) Dual role of TOC1 in the control of circadian and photomorphogenic responses in Arabidopsis. The Plant Cell **15**: 223–236

Matsoukas IG, Massiah AJ, Thomas B (2013) Starch metabolism and antiflorigenic signals modulate the juvenile-to-adult phase transition in Arabidopsis. Plant Cell & Environment **36**: 1802–1811

Matsusaka D, Filiault D, Sanchez DH, Botto JF (2021) Ultra-high-density QTL marker mapping for seedling photomorphogenesis mediating Arabidopsis establishment in Southern Patagonia. Frontiers in Plant Science **12**: 677728

McClung CR (2006) Plant circadian rhythms. Plant Cell **18**: 792–803

McCormac AC, Wagner D, Boylan MT, Quail PH, Smith H, Whitelam GC (1993) Photoresponses of transgenic Arabidopsis seedlings expressing introduced phytochrome B-encoding cDNAs:

evidence that phytochrome A and phytochrome B have distinct photoregulatory functions. The Plant Journal **4**: 19–27

McKay JK, Richards JH, Mitchell-Olds T (2003) Genetics of drought adaptation in *Arabidopsis thaliana* : I. Pleiotropy contributes to genetic correlations among ecological traits. Molecular Ecology **12**: 1137–1151

McNellis TW, Von Arnim AG, Araki T, Komeda Y, Miséra S, Deng XW (1994) Genetic and molecular analysis of an allelic series of *cop1* mutants suggests functional roles for the multiple protein domains. Plant Cell **6**: 487–500

Mengel K, Friedrich B, Judel GK (1985) Effect of light intensity on the concentrations of phytohormones in developing wheat grains. Journal of Plant Physiology **120**: 255–266

Metz JG, Pakrasi HB, Seibert M, Arntzer CJ (1986) Evidence for a dual function of the herbicide-binding D1 protein in photosystem II. FEBS Letters **205**: 269–274

Michaels SD, Amasino RM (2001) Loss of *FLOWERING LOCUS C* activity eliminates the late-flowering phenotype of *FRIGIDA* and autonomous pathway mutations but not responsiveness to vernalization. Plant Cell **13**: 935–941

Michaels SD, Himelblau E, Kim SY, Schomburg FM, Amasino RM (2005) Integration of flowering signals in winter-annual Arabidopsis. Plant Physiology **137**: 149–156

Mielecki J, Gawroński P, Karpiński S (2020) Retrograde signaling: Understanding the communication between organelles. IJMS **21**: 6173

Mishra P, Panigrahi KC (2015) GIGANTEA-an emerging story. Frontiers in Plant Sciences **6:** 8

Mishra S, Khurana JP (2017) Emerging roles and new paradigms in signaling mechanisms of plant cryptochromes. Critical Reviews in Plant Sciences **36**: 89–115

Mo W, Zhang J, Zhang L, Yang Z, Yang L, Yao N, Xiao Y, Li T, Li Y, Zhang G, et al (2022) Arabidopsis cryptochrome 2 forms photobodies with TCP22 under blue light and regulates the circadian clock. Nature Communications **13**: 2631

Mochizuki N, Brusslan JA, Larkin R, Nagatani A, Chory J (2001) *Arabidopsis genomes uncoupled 5 (GUN5)* mutant reveals the involvement of Mg-chelatase H subunit in plastid-to-nucleus signal transduction. Proceedings of the National Academy of Sciences USA **98**: 2053–2058

Mochizuki N, Tanaka R, Tanaka A, Masuda T, Nagatani A (2008) The steady-state level of Mg-protoporphyrin IX is not a determinant of plastid-to-nucleus signaling in Arabidopsis. Proceedings of the National Academy of Sciences USA **105**: 15184–15189

Moon J, Suh S, Lee H, Choi K, Hong CB, Paek N, Kim S, Lee I (2003) The *SOC1* MADS-box gene integrates vernalization and gibberellin signals for flowering in Arabidopsis. The Plant Journal **35**: 613–623

Moraes TA, Mengin V, Annunziata MG, Encke B, Krohn N, Höhne M, Stitt M (2019) Response of the circadian clock and diel Starch turnover to one day of low light or ow CO_2. Plant Physiol **179**: 1457–1478

Morgan DC, Smith H (1978) The relationship between phytochrome-photoequilibrium and Development in light grown *Chenopodium album* L. Planta **142**: 187–193

Moulin M, McCormac AC, Terry MJ, Smith AG (2008) Tetrapyrrole profiling in Arabidopsis seedlings reveals that retrograde plastid nuclear signaling is not due to Mg-protoporphyrin IX accumulation. Proceedings of the National Academy of Sciences USA **105**: 15178–15183

Movahedi M, Zoulias N, Casson SA, Sun P, Liang Y-K, Hetherington AM, Gray JE, Chater CCC (2021) Stomatal responses to carbon dioxide and light require abscisic acid catabolism in Arabidopsis. Interface Focus **11**: 20200036

Müller LM, Von Korff M, Davis SJ (2014) Connections between circadian clocks and carbon metabolism reveal species-specific effects on growth control. Journal of Experimental Botany **65**: 2915–2923

Mutasa-Gottgens E, Hedden P (2009) Gibberellin as a factor in floral regulatory networks. Journal of Experimental Botany **60**: 1979–1989

Neill S (2002) Hydrogen peroxide signalling. Current Opinion in Plant Biology **5**: 388–395

Nelson DC, Lasswell J, Rogg LE, Cohen MA, Bartel B (2000) *FKF1*, a clock-controlled gene that regulates the transition to flowering in Arabidopsis. Cell **101**: 331–340

Nitschke S (2015) Novel roles for cytokinin in the responses to high light and circadian stress. Doctoral Dissertation. Freie Universität Berlin, Berlin.

Nitschke S, Cortleven A, Iven T, Feussner I, Havaux M, Riefler M, Schmülling T (2016) Circadian stress regimes affect the circadian clock and cause jasmonic acid-dependent cell death in cytokinin-deficient Arabidopsis plants. Plant Cell **28:** 1616-1639

Nitschke S, Cortleven A, Schmülling T (2017) Novel stress in plants by altering the photoperiod. Trends in Plant Science **22**: 913–916

Oakenfull RJ, Davis SJ (2017) Shining a light on the Arabidopsis circadian clock. Plant Cell & Environment **40**: 2571–2585

Oh E, Kang H, Yamaguchi S, Park J, Lee D, Kamiya Y, Choi G (2009) Genome-wide analysis of genes targeted by PHYTOCHROME INTERACTING FACTOR 3-LIKE5 during seed germination in Arabidopsis. The Plant Cell **21**: 403–419

Ortiz-Marchena MI, Albi T, Lucas-Reina E, Said FE, Romero-Campero FJ, Cano B, Ruiz MT, Romero JM, Valverde F (2014) Photoperiodic control of carbon distribution during the floral transition in Arabidopsis. The Plant Cell **26**: 565–584

Orzechowski S, Sitnicka D, Grabowska A, Compart J, Fettke J, Zdunek-Zastocka E (2021) Effect of short-term cold treatment on carbohydrate metabolism in potato leaves. International Journal of Molecular Sciences **22**: 7203

Overmyer K, Tuominen H, Kettunen R, Betz C, Langebartels C, Sandermann H, Kangasjärvi J (2000) Ozone-sensitive Arabidopsis *rcd1* mutant reveals opposite roles for ethylene and jasmonate signaling pathways in regulating superoxide-dependent cell death. Plant Cell **12**: 1849–1862

Paik I, Huq E (2019) Plant photoreceptors: Multi-functional sensory proteins and their signaling networks. Seminars in Cell & Developmental Biology **92**: 114–121

Pansook S, Incharoensakdi A, Phunpruch S (2019) Effects of the Photosystem II Inhibitors CCCP and DCMU on Hydrogen Production by the Unicellular Halotolerant Cyanobacterium *Aphanothece halophytica*. The Scientific World Journal **2019**: 1–10

Paulišić S, Qin W, Arora Verasztó H, Then C, Alary B, Nogue F, Tsiantis M, Hothorn M, Martínez-García JF (2021) Adjustment of the PIF7-HFR1 transcriptional module activity controls plant shade adaptation. The EMBO Journal **40**: e104273

Peter E, Grimm B (2009) GUN4 is required for posttranslational control of Plant tetrapyrrole biosynthesis. Molecular Plant **2**: 1198–1210

Pezzetta D (2019) The role of cytokinin in light-dependent seed germination in Arabidopsis thaliana. Doctoral Dissertation. Freie Universität Berlin, Berlin

Philippou K, Ronald J, Sánchez-Villarreal A, Davis AM, Davis SJ (2019) Physiological and genetic dissection of sucrose inputs to the *Arabidopsis thaliana* circadian system. Genes **10**: 334

Pierik R, Ballaré CL (2021) Control of plant growth and defense by photoreceptors: From mechanisms to opportunities in agriculture. Molecular Plant **14**: 61–76

Piovene C, Orsini F, Bosi S, Sanoubar R, Bregola V, Dinelli G, Gianquinto G (2015) Optimal red:blue ratio in LED lighting for nutraceutical indoor horticulture. Scientia Horticulturae **193**: 202–208

Pollard DA (2012) Design and construction of recombinant inbred lines. In: Rifkin, S. (eds) Quantitative Trait Loci (QTL). Methods in Molecular Biology. Quantitative Trait Loci (QTL). Humana Press, Totowa, USA, pp 31–39

Ponnu J, Hoecker U (2021) Illuminating the COP1/SPA ubiquitin ligase: Fresh insights into its structure and functions during plant photomorphogenesis. Frontiers in Plant Science **12**: 662793

Proietti S, Moscatello S, Riccio F, Downey P, Battistelli A (2021) Continuous lighting promotes plant growth, light conversion efficiency, and nutritional quality of *Eruca vesicaria* (L.) Cav. in controlled environment with minor effects due to light quality. Frontiers in Plant Science **12**: 730119

Pruneda-Paz JL, Breton G, Para A, Kay SA (2009) A functional genomics approach reveals CHE as a component of the Arabidopsis circadian clock. Science **323**: 1481–1485

Putterill J, Robson F, Lee K, Simon R, Coupland G (1995) The CONSTANS gene of Arabidopsis promotes flowering and encodes a protein showing similarities to zinc finger transcription factors. Cell **80**: 847–857

Qi J, Wang J, Gong Z, Zhou J-M (2017) Apoplastic ROS signaling in plant immunity. Current Opinion in Plant Biology **38**: 92–100

Rai N, O'Hara A, Farkas D, Safronov O, Ratanasopa K, Wang F, Lindfors AV, Jenkins GI, Lehto T, Salojärvi J, et al (2020) The photoreceptor UVR8 mediates the perception of both UV-B and UV-A wavelengths up to 350 nm of sunlight with responsivity moderated by cryptochromes. Plant Cell & Environment **43**: 1513–1527

Rawat R, Takahashi N, Hsu PY, Jones MA, Schwartz J, Salemi MR, Phinney BS, Harmer SL (2011) REVEILLE8 and PSEUDO-REPONSE REGULATOR5 form a negative feedback loop within the Arabidopsis circadian clock. PLoS Genetics **7**: e1001350

Reed JW, Nagatani A, Elich TD, Fagan M, Chory J (1994) Phytochrome A and phytochrome B have overlapping but distinct functions in Arabidopsis development. Plant Physiology **104**: 1139–1149

Ren H, Han J, Yang P, Mao W, Liu X, Qiu L, Qian C, Liu Y, Chen Z, Ouyang X, et al (2019) Two E3 ligases antagonistically regulate the UV-B response in Arabidopsis. Proceedings of the National Academy of Sciences USA **116**: 4722–4731

Ribeiro C, Stitt M, Hotta CT (2022) How stress affects your budget—stress impacts on starch metabolism. Frontiers in Plant Science **13**: 774060

Riboni M, Robustelli Test A, Galbiati M, Tonelli C, Conti L (2016) ABA-dependent control of *GIGANTEA* signalling enables drought escape via up-regulation of *FLOWERING LOCUS T* in *Arabidopsis thaliana*. Journal of Experimental Botany **67**: 6309–6322

Richter AS, Nägele T, Grimm B, Kaufmann K, Schroda M, Leister D, Kleine T (2023) Retrograde signaling in plants: A critical review focusing on the GUN pathway and beyond. Plant Communications **4**: 100511

Riefler M, Novak O, Strnad M, Schmülling T (2005) Arabidopsis cytokinin receptor mutants reveal functions in shoot growth, leaf senescence, seed size, germination, root development, and cytokinin metabolism. The Plant Cell **18**: 40–54

Ritte G, Heydenreich M, Mahlow S, Haebel S, Kötting O, Steup M (2006) Phosphorylation of C6- and C3-positions of glucosyl residues in starch is catalysed by distinct dikinases. FEBS Letters **580**: 4872–4876

Rizzini L, Favory J-J, Cloix C, Faggionato D, O'Hara A, Kaiserli E, Baumeister R, Schäfer E, Nagy F, Jenkins GI, et al (2011) Perception of UV-B by the *Arabidopsis* UVR8 protein. Science **332**: 103–106

Rockwell NC, Su Y-S, Lagarias JC (2006) Phytochrome structure and signaling mechanisms. Annual Review of Plant Biology **57**: 837–858

Roeber VM, Bajaj I, Rohde M, Schmülling T, Cortleven A (2021) Light acts as a stressor and influences abiotic and biotic stress responses in plants. Plant Cell & Environment **44**: 645–664

Ronald J, Davis SJ (2017) Making the clock tick: the transcriptional landscape of the plant circadian clock. F1000Research **6**: 951

Ruckle ME, DeMarco SM, Larkin RM (2007) Plastid signals remodel light signaling networks and are essential for efficient chloroplast biogenesis in Arabidopsis. The Plant Cell **19**: 3944–3960

Rusaczonek A, Czarnocka W, Willems P, Sujkowska-Rybkowska M, Van Breusegem F, Karpiński S (2021) Phototropin 1 and 2 influence photosynthesis, UV-C induced photooxidative stress responses, and cell death. Cells **10**: 200

Sachdev S, Ansari SA, Ansari MI, Fujita M, Hasanuzzaman M (2021) Abiotic stress and reactive oxygen species: Generation, signaling, and defense mechanisms. Antioxidants **10**: 277

Sanchez-Bermejo E, Zhu W, Tasset C, Eimer H, Sureshkumar S, Singh R, Sundaramoorthi V, Colling L, Balasubramanian S (2015) Genetic architecture of natural variation in thermal responses of Arabidopsis. Plant Physiology **169**: 647–659

Saud S, Shi Z, Xiong L, Danish S, Datta R, Ahmad I, Fahad S, Banout J (2022) Recognizing the basics of phytochrome-interacting factors in plants for abiotic stress tolerance. Plant Stress **3**: 100050

Savitch LV, Allard G, Seki M, Robert LS, Tinker NA, Huner NPA, Shinozaki K, Singh J (2005) The effect of overexpression of two Brassica CBF/DREB1-like transcription factors on photosynthetic capacity and freezing tolerance in *Brassica napus*. Plant and Cell Physiology **46**: 1525–1539

Savitch LV, Subramaniam R, Allard GC, Singh J (2007) The GLK1 'regulon' encodes disease defense related proteins and confers resistance to *Fusarium graminearum* in Arabidopsis. Biochemical and Biophysical Research Communications **359**: 234–238

Sawa M, Nusinow DA, Kay SA, Imaizumi T (2007) FKF1 and GIGANTEA complex formation Is required for day-length measurement in Arabidopsis. Science **318**: 261–265

Schmalenbach I, Zhang L, Ryngajllo M, Jiménez-Gómez JM (2014) Functional analysis of the *Landsberg erecta* allele of *FRIGIDA*. BMC Plant Biology **14**: 218

Schwartz C, Balasubramanian S, Warthmann N, Michael TP, Lempe J, Sureshkumar S, Kobayashi Y, Maloof JN, Borevitz JO, Chory J, et al (2009) *Cis* -regulatory changes at *FLOWERING LOCUS T* mediate natural variation in flowering responses of *Arabidopsis thaliana*. Genetics **183**: 723–732

Searle I, He Y, Turck F, Vincent C, Fornara F, Kröber S, Amasino RA, Coupland G (2006) The transcription factor FLC confers a flowering response to vernalization by repressing meristem competence and systemic signaling in Arabidopsis. Genes & Development **20**: 898–912

Seki M, Ohara T, Hearn TJ, Frank A, Da Silva VCH, Caldana C, Webb AAR, Satake A (2017) Adjustment of the Arabidopsis circadian oscillator by sugar signalling dictates the regulation of starch metabolism. Scientific Reports **7**: 8305

Selby CP, Sancar A (2006) A cryptochrome/photolyase class of enzymes with single-stranded DNA-specific photolyase activity. Proceedings of the National Academy of Sciences USA **103**: 17696–17700

Shapiguzov A, Vainonen JP, Hunter K, Tossavainen H, Tiwari A, Järvi S, Hellman M, Aarabi F, Alseekh S, Wybouw B, et al (2019) Arabidopsis RCD1 coordinates chloroplast and mitochondrial functions through interaction with ANAC transcription factors. eLife **8**: e43284

Sharrock RA, Quail PH (1989) Novel phytochrome sequences in *Arabidopsis thaliana*: Structure, evolution, and differential expression of a plant regulatory photoreceptor family. Genes & Development **3**: 1745–1757

Sheldon CC, Burn JE, Perez PP, Metzger J, Edwards JA, Peacock WJ, Dennis ES (1999) The *FLF* MADS Box gene: A repressor of flowering in Arabidopsis regulated by vernalization and methylation. Plant Cell **11**: 445–458

Shen Y-Y, Wang X-F, Wu F-Q, Du S-Y, Cao Z, Shang Y, Wang X-L, Peng C-C, Yu X-C, Zhu S-Y, et al (2006) The Mg-chelatase H subunit is an abscisic acid receptor. Nature **443**: 823–826

Shi Y, Ke X, Yang X, Liu Y, Hou X (2022) Plants response to light stress. Journal of Genetics and Genomics **49**: 735–747

Shim JS, Imaizumi T (2015) Circadian clock and photoperiodic response in Arabidopsis: From seasonal flowering to redox homeostasis. Biochemistry **54**: 157–170

Shimizu T, Masuda T (2021) The role of tetrapyrrole- and GUN1-dependent signaling on chloroplast biogenesis. Plants **10**: 196

Shindo C, Bernasconi G, Hardtke CS (2007) Natural genetic variation in Arabidopsis: Tools, traits and prospects for evolutionary ecology. Annals of Botany **99**: 1043–1054

Shinomura T, Nagatani A, Hanzawa H, Kubota M, Watanabe M, Furuya M (1996) Action spectra for phytochrome A- and B-specific photoinduction of seed germination in *Arabidopsis thaliana*. Proceedings of the National Academy of Sciences USA **93**: 8129–8133

Simon M, Loudet O, Durand S, Bérard A, Brunel D, Sennesal F-X, Durand-Tardif M, Pelletier G, Camilleri C (2008) Quantitative trait loci mapping in five new large recombinant inbred line Populations of *Arabidopsis thaliana* Genotyped With Consensus Single-Nucleotide polymorphism markers. Genetics **178**: 2253–2264

Sipari N, Lihavainen J, Keinänen M (2022) Metabolite profiling of paraquat tolerant *Arabidopsis thaliana radical-induced cell death1 (rcd1)*-A mediator of antioxidant defence mechanisms. Antioxidants **11**: 2034

Skryhan K, Gurrieri L, Sparla F, Trost P, Blennow A (2018) Redox regulation of starch metabolism. Frontiers in Plant Science **9**: 1344

Smith AM, Stitt M (2007) Coordination of carbon supply and plant growth. Plant Cell & Environment **30**: 1126–1149

Smith AM, Zeeman SC (2020) Starch: A flexible, adaptable carbon store coupled to plant growth. Annual Review of Plant Biology **71**: 217–245

Smith AM, Zeeman SC (2006) Quantification of starch in plant tissues. Nature Protocols **1**: 1342–1345

Smith H (1982) Light quality, photoperception, and plant strategy. Annual Review of Plant Physiology **33**: 481–518

Smith H, Whitelam GC (1997) The shade avoidance syndrome: multiple responses mediated by multiple phytochromes. Plant Cell & Environment **20**: 840–844

Somers DE, Devlin PF, Kay SA (1998) Phytochromes and cryptochromes in the entrainment of the Arabidopsis circadian clock. Science **282**: 1488–1490

Somssich M (2019) A short history of *Arabidopsis thaliana* (L.) Heynh. Columbia-0. PeerJ Preprints **6:** 26931v3

Song S-H, Dick B, Penzkofer A, Pokorny R, Batschauer A, Essen L-O (2006) Absorption and fluorescence spectroscopic characterization of cryptochrome 3 from *Arabidopsis thaliana*. Journal of Photochemistry and Photobiology B: Biology **85**: 1–16

Spetea C, Rintamäki E, Schoefs B (2014) Changing the light environment: Chloroplast signalling and response mechanisms. Philosophical Transactions of the Royal Society B **369**: 20130220

Srikanth A, Schmid M (2011) Regulation of flowering time: all roads lead to Rome. Cellular and Molecular Life Sciences **68**: 2013–2037

Stahl W, Sies H (2003) Antioxidant activity of carotenoids. Molecular Aspects of Medicine **24**: 345–351

Steinbeck J, Fuchs P, Negroni YL, Elsässer M, Lichtenauer S, Stockdreher Y, Feitosa-Araujo E, Kroll JB, Niemeier J-O, Humberg C, et al (2020) In vivo NADH/NAD^+ biosensing reveals the dynamics of cytosolic redox metabolism in plants. Plant Cell **32**: 3324–3345

Strand Å, Asami T, Alonso J, Ecker JR, Chory J (2003) Chloroplast to nucleus communication triggered by accumulation of Mg-protoporphyrinIX. Nature **421**: 79–83

Suárez-López P, Wheatley K, Robson F, Onouchi H, Valverde F, Coupland G (2001) CONSTANS mediates between the circadian clock and the control of flowering in Arabidopsis. Nature **410**: 1116–1120

Suetsugu N, Wada M (2013) Evolution of three LOV blue light receptor families in green plants and photosynthetic stramenopiles: Phototropin, ZTL/FKF1/LKP2 and Aureochrome. Plant and Cell Physiology **54**: 8–23

Sulpice R, Pyl E-T, Ishihara H, Trenkamp S, Steinfath M, Witucka-Wall H, Gibon Y, Usadel B, Poree F, Piques MC, et al (2009) Starch as a major integrator in the regulation of plant growth. Proceedings of the National Academy of Sciences USA **106**: 10348–10353

Sun A-Z, Guo F-Q (2016) Chloroplast retrograde regulation of heat stress responses in plants. Frontiers in Plant Science **7:** 398

Susek RE, Ausubel FM, Chory J (1993) Signal transduction mutants of Arabidopsis uncouple nuclear CAB and RBCS gene expression from chloroplast development. Cell **74**: 787–799

Takase T, Nishiyama Y, Tanihigashi H, Ogura Y, Miyazaki Y, Yamada Y, Kiyosue T (2011) *LOV KELCH PROTEIN2* and *ZEITLUPE* repress Arabidopsis photoperiodic flowering under non-inductive conditions, dependent on *FLAVIN-BINDING KELCH REPEAT F-BOX1*. The Plant Journal **67**: 608–621

Teotia S, Tang G (2015) To bloom or not to bloom: Role of microRNAs in plant flowering. Molecular Plant **8**: 359–377

Teper-Bamnolker P, Samach A (2005) The flowering integrator FT regulates *SEPALLATA3* and *FRUITFULL* accumulation in Arabidopsis Leaves. The Plant Cell **17**: 2661–2675

Thalmann M, Santelia D (2017) Starch as a determinant of plant fitness under abiotic stress. New Phytologist **214**: 943–951

Thitisaksakul M, Jiménez RC, Arias MC, Beckles DM (2012) Effects of environmental factors on cereal starch biosynthesis and composition. Journal of Cereal Science **56**: 67–80

Tilbrook K, Arongaus AB, Binkert M, Heijde M, Yin R, Ulm R (2013) The UVR8 UV-B photoreceptor: perception, signaling and response. The Arabidopsis Book. The American Society of Plant Biologists, BioOne, Rockville, USA **11**: e0164

Toldi D, Gyugos M, Darkó É, Szalai G, Gulyás Z, Gierczik K, Székely A, Boldizsár Á, Galiba G, Müller M, et al (2019) Light intensity and spectrum affect metabolism of glutathione and amino acids at transcriptional level. PLoS ONE **14**: e0227271

Tong M, Lee K, Ezer D, Cortijo S, Jung J, Charoensawan V, Box MS, Jaeger KE, Takahashi N, Mas P, et al (2020) The evening complex establishes repressive chromatin domains via H2A.Z deposition. Plant Physiology **182**: 612–625

Torti S, Fornara F, Vincent C, Andrés F, Nordström K, Göbel U, Knoll D, Schoof H, Coupland G (2012) Analysis of the *Arabidopsis* shoot meristem transcriptome during floral transition identifies distinct regulatory patterns and a Leucine-rich repeat protein that promotes flowering. Plant Cell **24**: 444–462

Tóth R, Kevei É, Hall A, Millar AJ, Nagy F, Kozma-Bognár L (2001) Circadian clock-regulated expression of phytochrome and cryptochrome genes in Arabidopsis. Plant Physiology **127**: 1607–1616

Trethewey RN, Ap Rees T (1994) A mutant of *Arabidopsis thaliana* lacking the ability to transport glucose across the chloroplast envelope. Biochemical Journal **301**: 449–454

Turck F, Fornara F, Coupland G (2008) Regulation and Identity of Florigen: FLOWERING LOCUS T moves center stage. Annual Review of Plant Biology **59**: 573–594

Valverde F, Mouradov A, Soppe W, Ravenscroft D, Samach A, Coupland G (2004) Photoreceptor regulation of CONSTANS protein in photoperiodic flowering. Science **303**: 1003–1006

Vandesompele J, De Preter K, Pattyn F, Poppe B, Van Roy N, De Paepe A, Speleman F (2002) Accurate normalization of real-time quantitative RT-PCR data by geometric averaging of multiple internal control genes. Genome Biol **3**: research0034.1

Versluys M, Tarkowski ŁP, Van Den Ende W (2017) Fructans as DAMPs or MAMPs: Evolutionary prospects, cross-tolerance, and multistress resistance potential. Frontiers in Plant Science **7:** 2061

Viana AJC, Matiolli CC, Newman DW, Vieira JGP, Duarte GT, Martins MCM, Gilbault E, Hotta CT, Caldana C, Vincentz M (2021) The sugar-responsive circadian clock regulator bZIP63 modulates plant growth. New Phytologist **231**: 1875–1889

Voigt C, Oster U, Börnke F, Jahns P, Dietz K, Leister D, Kleine T (2010) In-depth analysis of the distinctive effects of norflurazon implies that tetrapyrrole biosynthesis, organellar gene expression and ABA cooperate in the GUN-type of plastid signalling. Physiologia Plantarum **138**: 503–519

Wang H, Gong M, Xin H, Tang L, Dai D, Gao Y, Liu C (2018) Effects of chilling stress on the accumulation of soluble sugars and their key enzymes in *Jatropha curcas* seedlings. Physiology and Molecular Biology of Plants **24**: 857–865

Wang L, Kim J, Somers DE (2013) Transcriptional corepressor TOPLESS complexes with pseudoresponse regulator proteins and histone deacetylases to regulate circadian transcription. Proceedings of the National Academy of Sciences USA **110**: 761–766

Wang Q, Lin C (2020) Mechanisms of cryptochrome-mediated photoresponses in plants. Annual Review of Plant Biology **71**: 103–129

Wang Q, Zuo Z, Wang X, Gu L, Yoshizumi T, Yang Z, Yang L, Liu Q, Liu W, Han Y-J, et al (2016) Photoactivation and inactivation of Arabidopsis cryptochrome 2. Science **354**: 343–347

Wang S, Chu B, Lue W, Yu T, Eimert K, Chen J (1997) *adg2-1* represents a missense mutation in the ADPG pyrophosphorylase large subunit gene of *Arabidopsis thaliana*. The Plant Journal **11**: 1121–1126

Wang S, Lue W, Yu T, Long J, Wang C, Eimert K, Chen J (1998) Characterization of *ADG1*, an Arabidopsis locus encoding for ADPG pyrophosphorylase small subunit, demonstrates that the presence of the small subunit is required for large subunit stability. The Plant Journal **13**: 63–70

Wang X, Jiang B, Gu L, Chen Y, Mora M, Zhu M, Noory E, Wang Q, Lin C (2021) A photoregulatory mechanism of the circadian clock in Arabidopsis. Nature Plants **7**: 1397–1408

Wang Y, Selinski J, Mao C, Zhu Y, Berkowitz O, Whelan J (2020) Linking mitochondrial and chloroplast retrograde signalling in plants. Philosophical Transactions of Royal Society B **375**: 20190410

Wang Z, Zhao S, Liu J, Zhao H, Sun X, Wu T, Pei T, Wang Y, Liu Q, Yang H, et al (2022) Genome-wide identification of tomato Golden 2-Like transcription factors and abiotic stress related members screening. BMC Plant Biology **22**: 82

Ward JM, Cufr CA, Denzel MA, Neff MM (2005) The Dof transcription factor OBP3 modulates phytochrome and cryptochrome signaling in Arabidopsis. The Plant Cell **17**: 475–485

Waters MT, Wang P, Korkaric M, Capper RG, Saunders NJ, Langdale JA (2009) GLK transcription factors coordinate expression of the photosynthetic apparatus in Arabidopsis. The Plant Cell **21**: 1109–1128

Wei Y, Wang S, Yu D (2023) The role of light quality in regulating early seedling development. Plants **12**: 2746

Weigel D (2012) Natural variation in Arabidopsis: From molecular genetics to ecological genomics. Plant Physiology **158**: 2–22

Whitelam GC, Devlin PF (1997) Roles of different phytochromes in Arabidopsis photomorphogenesis. Plant Cell & Environment **20**: 752–758

Wigge PA, Kim MC, Jaeger KE, Busch W, Schmid M, Lohmann JU, Weigel D (2005) Integration of spatial and temporal information during floral induction in Arabidopsis. Science **309**: 1056–1059

Wittmann C, Aschan G, Pfanz H (2001) Leaf and twig photosynthesis of young beech *(Fagus sylvatica)* and aspen *(Populus tremula)* trees grown under different light regime. Basic and Applied Ecology **2**: 145–154

Woodson JD, Perez-Ruiz JM, Chory J (2011) Heme synthesis by plastid Ferrochelatase I regulates nuclear gene expression in plants. Current Biology **21**: 897–903

Wu G-Z, Bock R (2021) GUN control in retrograde signaling: How GENOMES UNCOUPLED proteins adjust nuclear gene expression to plastid biogenesis. The Plant Cell **33**: 457–474

Wu Y, Liao W, Dawuda MM, Hu L, Yu J (2019) 5-Aminolevulinic acid (ALA) biosynthetic and metabolic pathways and its role in higher plants: a review. Plant Growth Regulation **87**: 357–374

Xiao G, Zhou J, Lu X, Huang R, Zhang H (2018) Excessive UDPG resulting from the mutation of *UAP1* causes programmed cell death by triggering reactive oxygen species accumulation and caspase-like activity in rice. New Phytologist **217**: 332–343

Xiao Y, Chu L, Zhang Y, Bian Y, Xiao J, Xu D (2022) HY5: A pivotal regulator of light-dependent development in higher plants. Frontiers in Plant Science **12**: 800989

Xie Q, Wang P, Liu X, Yuan L, Wang L, Zhang C, Li Y, Xing H, Zhi L, Yue Z, et al (2014) LNK1 and LNK2 are transcriptional coactivators in the Arabidopsis circadian oscillator. Plant Cell **26**: 2843–2857

Yadav A, Singh D, Lingwan M, Yadukrishnan P, Masakapalli SK, Datta S (2020) Light signaling and UV-B-mediated plant growth regulation. Journal of Integrative Plant Biology **62**: 1270–1292

Yamaguchi A, Kobayashi Y, Goto K, Abe M, Araki T (2005) TWIN SISTER OF FT (TSF) acts as a floral pathway integrator redundantly with FT. Plant and Cell Physiology **46**: 1175–1189

Yang F, Huang S, Gao R, Liu W, Yong T, Wang X, Wu X, Yang W (2014) Growth of soybean seedlings in relay strip intercropping systems in relation to light quantity and red:far-red ratio. Field Crops Research **155**: 245–253

Yang F, Liao D, Wu X, Gao R, Fan Y, Raza MA, Wang X, Yong T, Liu W, Liu J, et al (2017) Effect of aboveground and belowground interactions on the intercrop yields in maize-soybean relay intercropping systems. Field Crops Research **203**: 16–23

Yang Y, Liang T, Zhang L, Shao K, Gu X, Shang R, Shi N, Li X, Zhang P, Liu H (2018) UVR8 interacts with WRKY36 to regulate HY5 transcription and hypocotyl elongation in Arabidopsis. Nature Plants **4**: 98–107

Yano R, Nakamura M, Yoneyama T, Nishida I (2005) Starch-related α-Glucan/Water Dikinase is involved in the cold-induced development of freezing tolerance in Arabidopsis. Plant Physiology **138**: 837–846

Yavari N, Tripathi R, Wu B-S, MacPherson S, Singh J, Lefsrud M (2021) The effect of light quality on plant physiology, photosynthetic, and stress response in *Arabidopsis thaliana* leaves. PLoS ONE **16**: e0247380

Yeom M, Kim H, Lim J, Shin A-Y, Hong S, Kim J-I, Nam HG (2014) How do phytochromes transmit the light quality information to the circadian clock in Arabidopsis? Molecular Plant **7**: 1701–1704

Yin R, Skvortsova MY, Loubéry S, Ulm R (2016) COP1 is required for UV-B–induced nuclear accumulation of the UVR8 photoreceptor. Proceedings of the National Academy of Sciences USA **113:** E4415-E4422

Yin Y, Yu C, Yu L, Zhao J, Sun C, Ma Y, Zhou G (2015) The influence of light intensity and photoperiod on duckweed biomass and starch accumulation for bioethanol production. Bioresource Technology **187**: 84–90

Yoshiba Y, Kiyosue T, Nakashima K, Yamaguchi-Shinozaki K, Shinozaki K (1997) Regulation of levels of proline as an osmolyte in plants under water stress. Plant and Cell Physiology **38**: 1095–1102

Yu J-W, Rubio V, Lee N-Y, Bai S, Lee S-Y, Kim S-S, Liu L, Zhang Y, Irigoyen ML, Sullivan JA, et al (2008) COP1 and ELF3 control circadian function and photoperiodic flowering by regulating GI stability. Molecular Cell **32**: 617–630

Yu T-S, Kofler H, Häusler RE, Hille D, Flügge U-I, Zeeman SC, Smith AM, Kossmann J, Lloyd J, Ritte G, M Steup, W L Lue, J Chen, A Weber (2001) The Arabidopsis *sex1* mutant is defective in the R1 protein, a general regulator of starch degradation in plants, and not in the chloroplast hexose transporter. The Plant Cell **13:** 1907-1918

Yu X, Liu H, Klejnot J, Lin C (2010) The cryptochrome blue light receptors. The Arabidopsis Book. The American Society of Plant Biologists, BioOne, Rockville, USA **8**: e0135

Zanella M, Borghi GL, Pirone C, Thalmann M, Pazmino D, Costa A, Santelia D, Trost P, Sparla F (2016) β-amylase 1 (BAM1) degrades transitory starch to sustain proline biosynthesis during drought stress. Journal of Experimental Botany **67**: 1819–1826

Zeeman SC, Delatte T, Messerli G, Umhang M, Stettler M, Mettler T, Streb S, Reinhold H, Kötting O (2007a) Starch breakdown: recent discoveries suggest distinct pathways and novel mechanisms. Functional Plant Biology **34**: 465

Zeeman SC, Smith SM, Smith AM (2007b) The diurnal metabolism of leaf starch. Biochemical Journal **401**: 13–28

Zeier J, Pink B, Mueller MartinJ, Berger S (2004) Light conditions influence specific defence responses in incompatible plant-pathogen interactions: uncoupling systemic resistance from salicylic acid and PR-1 accumulation. Planta **219:** 673-683

Zheng L, Van Labeke M-C (2017) Long-term effects of red- and blue-light emitting diodes on leaf anatomy and photosynthetic efficiency of three ornamental pot plants. Frontiers in Plant Science **8**: 917

Zhou XF, Jin YH, Yoo CY, Lin X-L, Kim W-Y, Yun D-J, Bressan RA, Hasegawa PM, Jin JB (2013) CYCLIN H;1 regulates drought stress responses and blue light-induced stomatal opening by inhibiting reactive oxygen species accumulation in Arabidopsis. Plant Physiology **162**: 1030–1041

Zrenner R, Stitt M (1991) Comparison of the effect of rapidly and gradually developing water-stress on carbohydrate metabolism in spinach leaves. Plant Cell & Environment **14**: 939–946

8 Supplementary information

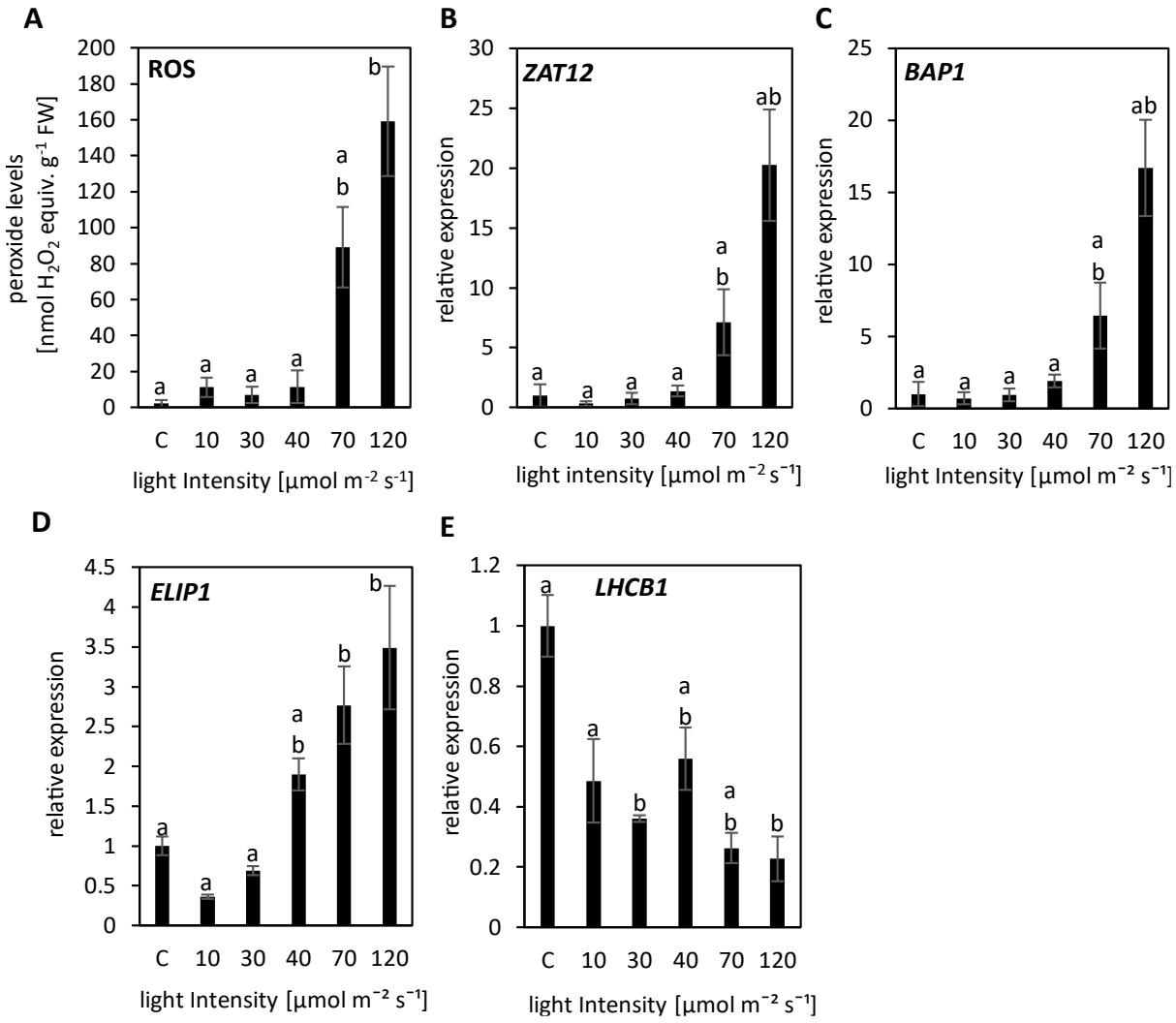

Supplementary Figure 1: The strength of the photoperiod stress symptoms is light intensity dependent. 4-weeks-old SD-grown WT plants were treated with 4 h of PLP with light intensities between 10-120 µmol m^{-2} s^{-1} (see the experimental setup in Figure 3.1 A). (A) ROS equivalents. Error bars represent SE (n ≥ 3). (B-E) Relative expression of *ZAT12*, *BAP1*, *ELIP1* and *LHCB1*. Error bars represent SE (n ≥ 3). Expression was normalized to WT control which was set to 1. Letters indicate significant difference between groups as determined by ANOVA followed by Tukey post-hoc test ($p < 0.05$). C, control; PLP, prolonged light period. This experiment was conducted twice with similar results. A third repetition was performed with light intensity range 30-120 µmol m^{-2} s^{-1} during the PLP and stress response at 70 µmol m^{-2} s^{-1} was not measured in this experiment and 50 µmol m^{-2} s^{-1} was the minimum light intensity at which photoperiod stress was induced (see Figure 3.1).

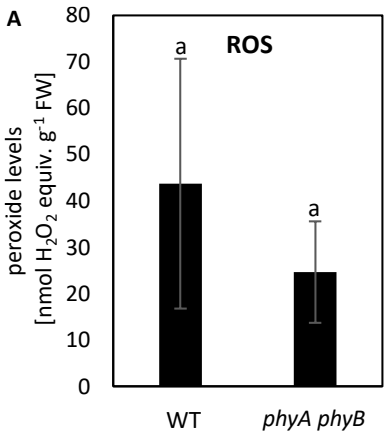

Supplementary Figure 2: The photoperiod stress response in *phyA phyB* double mutants. The experimental setup can be found in Figure 3.6 A. Due to growth defects *phyA phyB* was germinated and cultivated for 3 weeks in LD followed by cultivation under SD for next 2 weeks. WT was grown under SD for 5 weeks. These 5-weeks-old plants were treated with a 16 h PLP. (A) ROS equivalents. Error bars represent SE (n ≥ 3). Letters represent significant differences between groups as determined by Wilcoxon rank-sum test ($p < 0.05$). PLP, prolonged light period. This experiment was conducted twice with similar results.

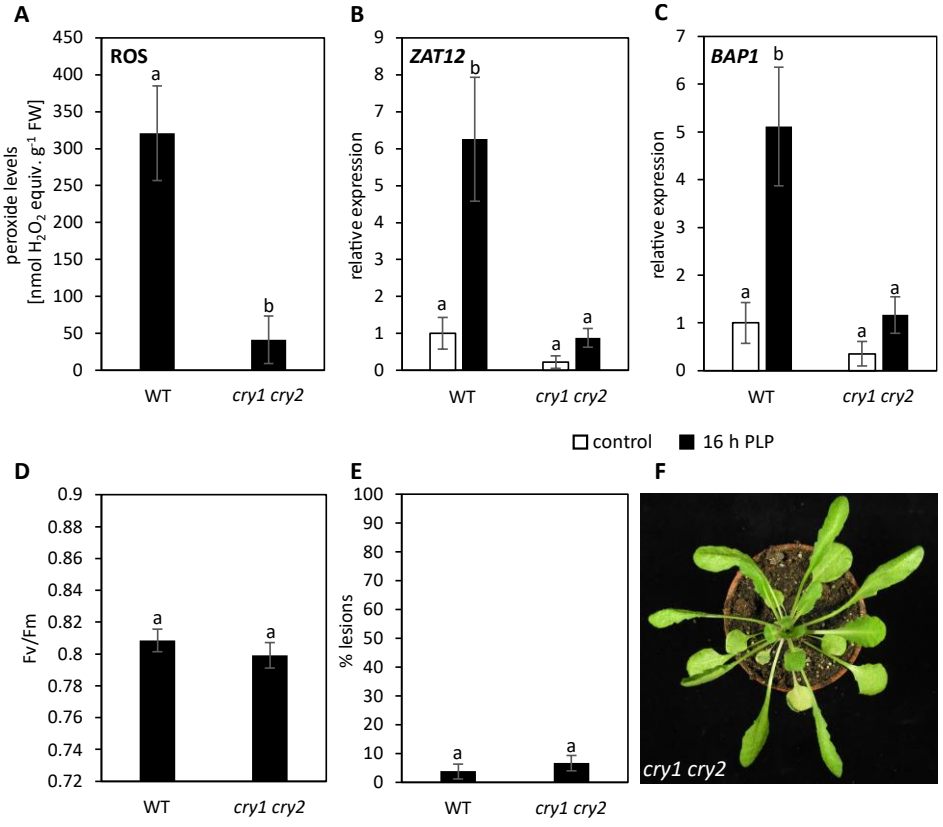

Supplementary Figure 3: The photoperiod stress response in *cry1 cry2* mutants. 5-weeks-old SD-grown plants were treated with a 16 h PLP. Experimental setup can be found in Figure 3.6 A. (A) ROS equivalents. Error bars represent SE (n ≥ 3). (B-C) Relative expression of *ZAT12* and *BAP1*. Error bars represent SE (n ≥ 3). Expression was normalized to WT control which was set to 1. (D) Percent lesions after photoperiod stress (n ≥ 10). (E) Quantum efficiency (Fv/Fm) after photoperiod stress (n ≥ 8). (F) Picture of photoperiod-stressed *cry1 cry2* mutant taken during the day following the stress-inducing night. Letters represent a significant difference between groups as determined by Kruskal-Wallis-Test followed by Wilcoxon rank-sum test ($p < 0.05$). PLP, prolonged light period. (A) was measured twice with similar results and (B-E) was measured once.

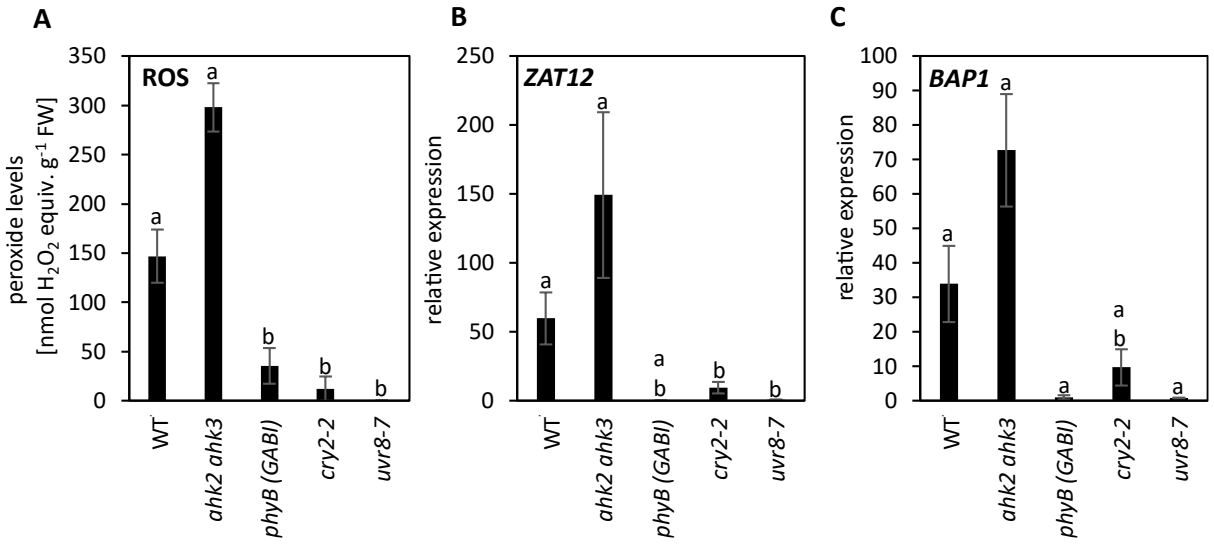

Supplementary Figure 4: The photoperiod stress response in second alleles of photoreceptor mutants. 5-weeks-old SD-grown plants were treated with 16 h PLP. Experimental setup can be found in Figure 3.6 A. (A) ROS equivalents. Error bars represent SE (n ≥ 3). (B-C) Relative expression of *ZAT12* and *BAP1*. Error bars represent SE (n ≥ 3). Expression was normalized to WT control which was set to 1. PLP, prolonged light period. Letters represent significant difference between groups as determined by ANOVA followed by Tukey post-hoc test (A, C) and Kruskal-Wallis-Test followed by Wilcoxon rank-sum test (B) ($p < 0.05$). (A) was conducted twice with similar results (B-C) was conducted once.

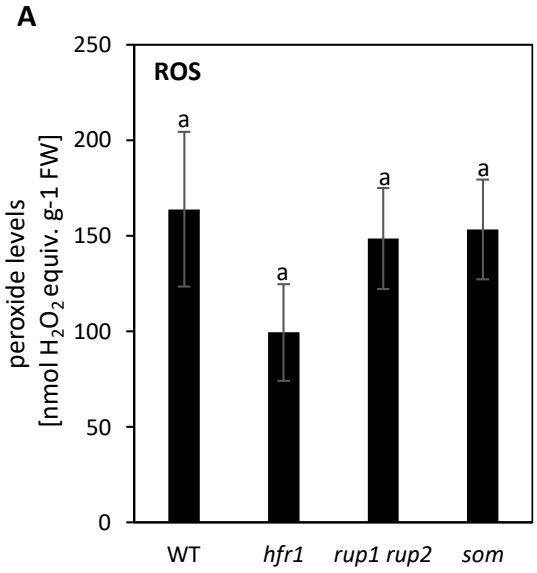

Supplementary Figure 5: The photoperiod stress response in light signaling mutants. 5-weeks-old SD-grown plants were treated with 16 h PLP. Experimental setup can be found in Figure 3.6 A. (A) ROS equivalents. Error bars represent SE (n ≥ 3). Letters represent significant difference between groups as determined by Kruskal-Wallis-Test followed by Wilcoxon rank-sum test ($p < 0.05$). PLP, prolonged light period. This experiment was conducted twice with similar results.

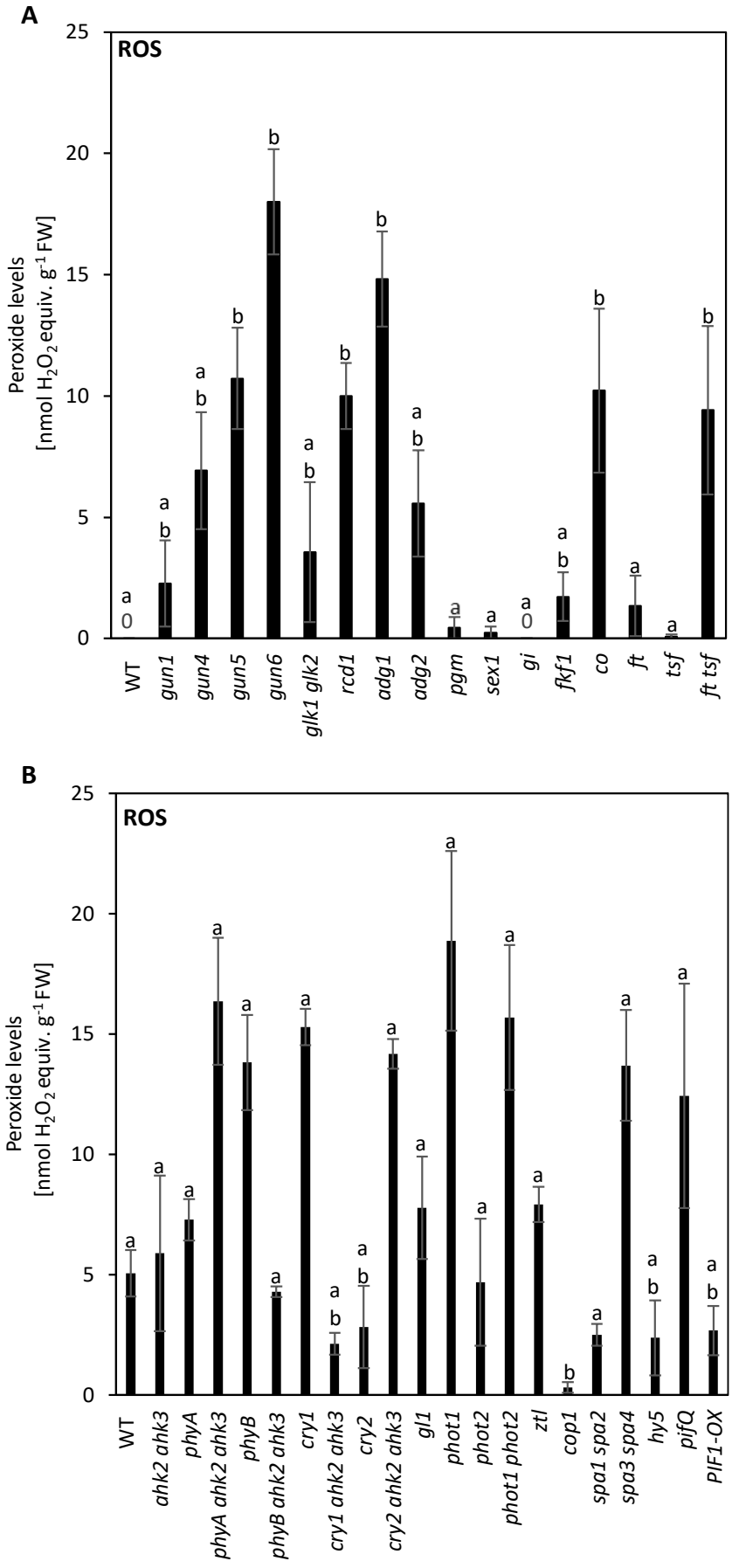
A
ROS
Peroxide levels
[nmol H_2O_2 equiv. g^{-1} FW]
25
20
15
10
5
0
WT
gun1
gun4
gun5
gun6
glk1 glk2
rcd1
adg1
adg2
pgm
sex1
gi
fkf1
co
ft
tsf
ft tsf
B
ROS
Peroxide levels
[nmol H_2O_2 equiv. g^{-1} FW]
25
20
15
10
5
0
WT
ahk2 ahk3
phyA
phyA ahk2 ahk3
phyB
phyB ahk2 ahk3
cry1
cry1 ahk2 ahk3
cry2
cry2 ahk2 ahk3
gl1
phot1
phot2
phot1 phot2
ztl
cop1
spa1 spa2
spa3 spa4
hy5
pifQ
PIF1-OX

Supplementary Figure 6: ROS levels in the tested mutant under control state of SD photoperiod. 5-weeks-old SD-grown non-treated plants were tested for ROS levels under control state. Leaf samples were harvested at time points indicated by arrow heads in the experimental setup in Figure 3.6 A. (A, B) ROS equivalents. Error bars represent SE (n ≥ 3). Letters represent significant difference between groups as determined by ANOVA followed by Tukey post-hoc test ($p < 0.05$). PLP, prolonged light period. This experiment was conducted once.

The peroxide level in some genotypes is higher than in the WT under control state, however upon photoperiod stress, it was less than WT. *phyB, gun4, gun5*, and *co* are examples of such genotypes. In general, the ROS levels under control conditions are lower than 25 nmol H_2O_2 equiv. g^{-1} FW in all genotypes. There is a difference of 5 nmol H_2O_2 equiv. g^{-1} FW between the peroxide levels in WT in Supplementary Figure 6 A and Supplementary Figure 6 B. This could be due to experimental variation.

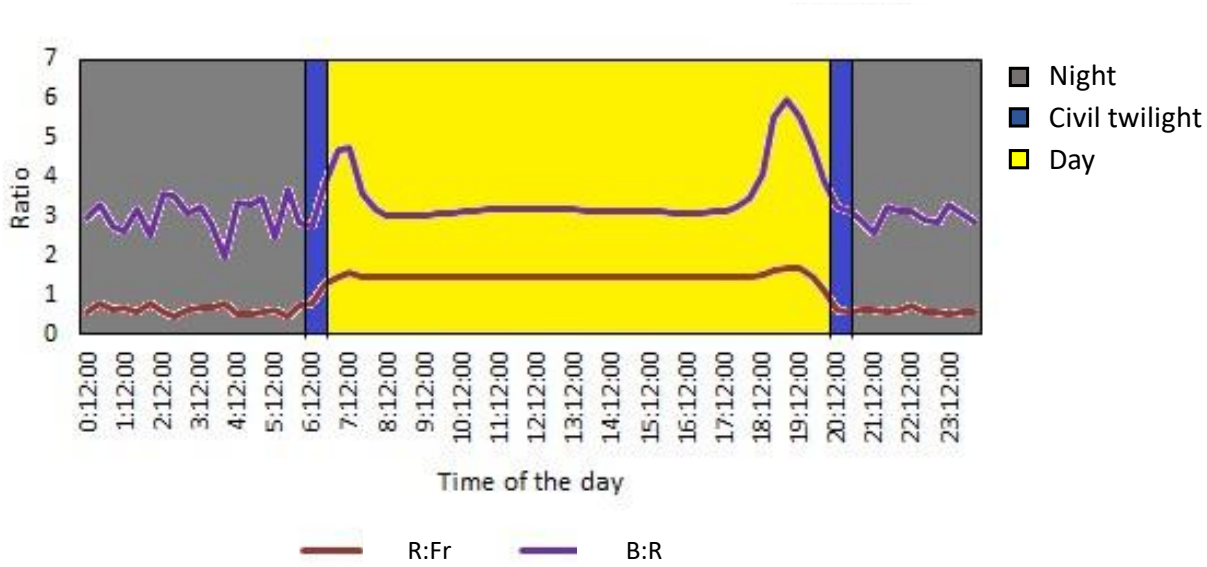

Supplementary Figure 7: Representative graph of the R:Fr and B:R ratio on a cloudless sunny day. This ratio of R:Fr (maroon curve) and B:R (purple curve) in natural light conditions was measured on 06.04.2020 at Max Planck Institute, Golm (52°24'55.5"N 12°58'08.9“ E). Data are courtesy of Virginie Mengin. Night is the dark period (grey colored), civil twilight is the period when sun is 6° below the horizon (Kishida, 1989) (dark blue colored), day is the light period (yellow colored). R:Fr, Red:Far-red; B:R, Blue:Red.

9. Publications

The following publications were published or will be published from this work.

Roeber VM, Bajaj I, Rohde M, Schmülling T, Cortleven A (2021) Light acts as a stressor and influences abiotic and biotic stress responses in plants. Plant Cell & Environment **44**: 645–664

Bajaj I, Cortleven A, Schmülling T (under preparation) Effect of light quantity and quality on photoperiod stress.